The Chemerin Receptor GPR1 Signals Through a RhoA/ROCK Pathway and Contributes to Glucose Homeostasis in Obese Mice

by

Jillian L. Rourke

Submitted in partial fulfillment of the requirements
for the degree of Doctor of Philosophy

at

Dalhousie University
Halifax, Nova Scotia
February 2015

Table of Contents

List of Tables

List of Figures

Abstract

Chemerin is an adipose-derived hormone that regulates adipose tissue development, immunity, metabolism, and glucose homeostasis. To date, all chemerin function has been attributed to activation of the G protein-coupled receptor chemokine-like receptor-1 (CMKLR1). Chemerin is also the only known ligand for a second receptor, G protein-coupled receptor-1 (GPR1). The function of GPR1 is unknown in mammals. This study investigated the *in vitro* signal transduction mechanisms of CMKLR1 and GPR1, and characterized the *in vivo* effects of *Gpr1* loss on adiposity and glucose homeostasis during obesity and diabetes development in mice. Receptor signaling and tissue expression were assessed using a panel of *in vitro* luciferase- reporters and quantitative PCR, respectively. Unlike CMKLR1, chemerin activation of GPR1 does not induce mitogen-activated protein kinase (MAPK) signaling, but does exhibit higher potency for arrestin recruitment. In common, chemerin activation of both CMKLR1 and GPR1 enhances serum-response factor (SRF) – mediated target gene expression and enhances cell migration via a ras homolog gene family member A (RhoA)/rho-associated protein kinase (ROCK) and MAPK/extracellular-signal-regulated kinase (ERK) dependent pathway. *Gpr1* and *Cmklr1* exhibit unique expression profiles, having in common highest levels of each observed in white adipose tissue (WAT). In mice, *Gpr1*, is expressed in metabolically active tissues: skeletal muscle, adipose tissue, and brain. The highest *Gpr1* mRNA levels were detected in the hypothalamus, oxidative soleus muscle and in the non-adipocyte stromal vascular fraction (SVF) of adipose tissue. Consistent with this expression pattern, *Gpr1* loss resulted in reduced food consumption and exacerbated glucose tolerance in mice consuming a high-fat diet. The later was likely a consequence of impaired insulin secretion and insulin resistance as evidenced by low fasting and glucose-stimulated insulin levels and reduced insulin receptor expression in skeletal muscle, respectively. These results demonstrate that GPR1 is an active chemerin receptor and identify RhoA/SRF as a novel chemerin-signaling axis. Differential receptor expression suggests that GPR1 may play a distinct role in chemerin function. This study provides evidence for the first mammalian function of GPR1 as a chemerin receptor implicated in the maintenance of glucose homeostasis during obesity and identifies novel targets for modulating chemerin function through the RhoA/SRF pathway.

List of Abbreviations and Symbols Used

Adp	adipocyte fraction
ADP	adenosine diphosphate
AgRP	agouti-related peptide
AGS	gastric adenocarcinoma
AKT	RAC-alpha serine/threonine-protein kinase
AMPK	AMP-activated protein kinase
APS	adapter protein with Pleckstrin homology and Src homology 2 domains
AS160	AKT substrate of 160 kDa
ATP	adenosine triphosphate
AUC	area under the curve
BAT	brown adipose tissue
BMI	body mass index
BRET	bioluminescence resonance energy transfer
C3G	CRK SH3-binding protein
Ca^{2+}	calcium
CAD	coronary artery disease
cAMP	cyclic adenosine monophosphate
CAP	c-cbl associated protein
CBL	Casitas B-lineage lymphoma
CCRL2	chemokine (CC motif) receptor-like 2
CDC42	cell division control protein 42 homolog
cDNA	complimentary DNA
CDS	coding sequence
CHO	Chinese hamster ovary
CMKLR1	chemokine-like receptor 1
CNS	central nervous system
CREB	cAMP response element-binding protein
CRK	CT10 regulator of kinase II

CRP	C-reactive protein
CYCA	cyclophilin A
DMEM	Dulbecco's modified eagle medium
DPP-4	dipeptidyl peptidase-4
EGF	extracellular growth factor
EGFP	enhanced green fluorescent protein
ELISA	enzyme-linked immuno- sorbent assay
ER	endoplasmic reticulum
ERK	extracellular regulated kinase
ETS	E26 transformation-specific
FBS	fetal bovine serum
FOXO	forkhead box protein class O
G-actin	monomeric globular actin
G6PC	glucose-6 phosphatase
GA	gastrocnemius muscle
GAP	GTPase activating protein
GEF	guanine nucleotide exchange factor
GIP	glucose-dependent insulinotropic peptide
GLP-1	glucagon-like peptide-1
GLUT	glucose transporter
GPCR	G protein-coupled receptor
GPR1	G protein-coupled receptor 1
GRB2	growth factor receptor-bound protein 2
GS	glycogen synthase
GSIS	glucose-stimulated insulin secretion
GSK	glycogen synthase kinase
GTT	glucose tolerance test
HEK	human embryonic kidney
HET	heterozygous
HFD	high fat diet
HRP	horseradish peroxidase

IL	interleukin
INSR	insulin receptor
IRS	insulin receptor substrate
IST	insulin sensitivity test
JNK	janus kinase
K^+	potassium ions
KO	knockout
LDL	low-density lipoprotein
LDLRKO	low-density lipoprotein receptor knockout
LFD	low-fat diet
LPA	lysophosphatidic acid
LPS	lipopolysaccharide
LTR	long terminal repeats
MAC1	macrophage antigen-1
MAPK	mitogen-activated protein kinase
MetS	metabolic syndrome
mTOR	mammalian target of rapamycin
MYH1	myosin heavy polypeptide 1
NFκB	nuclear factor κ B protein
NK	natural killer
NPY	neuropeptide Y
OA	osteoarthritis
p70s6K	ribosomal protein S6 kinase
pA	polyadenylation signal
PAI-1	plasminogen activator inhibitor-1
PDK1	phosphoinositide-dependent kinase 1
PDX1	pancreatic and duodenal homeobox 1
PEPCK	phosphoenolpyruvte carboxylase
PGC1	proliferator-activated receptor-gamma coactivator 1
PH	pleckstrin homology
PI3K	phosphoinositide-3-kinase

PIP3	phosphatidylinositol (3,4,5)-triphosphate
POMC	proopiomelanocortin
PR3	proteinase 3
PTP	protein tyrosine phosphatase
PTT	pyruvate tolerance test
PTX	pertussis toxin
qPCR	quantitative real-time PCR
Rac	ras-related C3 botulinum toxin substrate
RalA	V-ral simian leukemia viral oncogene homolog A (ras related)
RBP4	retinol-binding protein 4
RhoA	ras homolog gene family member A
ROCK	rho-associated protein kinase
ROS	reactive oxygen species
RPMI	Roswell Park Memorial Institute
SA	splice acceptor
SDS	Sodium dodecyl sulphate
SH2	Src-homology 2
SHC	Src-homology/collagen
SNARE	soluble NSF attachment protein receptor
SNP	single nucleotide polymorphism
SOCS	suppressor of cytokine signaling
SOL	soleus
SOS	son of sevenless
SREBP	sterol regulatory element-binding protein 1
SRF	serum response factor
SVF	stromal vascular fraction
T2D	type 2 diabetes
TA	tibialis anterior muscle
TBST	tris-buffers saline 0.1% Tween
TC10	small GTP-binding protein TC10
TCF	ternary complex factor

TIGM	Texas Institute of Genomic Medicine
TNF	tumour necrosis factor
WAT	white adipose tissue
WT	wild-type
α	alpha
β	beta
βgal	β-galactosidase
βGeo	β-galactosidase neomycin resistance

Acknowledgements

To my supervisor Dr. Chris Sinal who, through a wise combination of guidance, and unwavering support helped me to pursue my own interests and to find independence from dependence on external validation. Thank you for creating the space that I needed to learn to be an effective, confident and independent student, scientist, and person. The skills I have gained through your patient mentorship will be invaluable as I continue on this journey.

Secondly, I would like to thank my lab mates, Matt, Helen, Murugan, and Nicky for your immeasurable help and friendship. Your technical expertise and companionship helped to make this a productive experience and made both the highs and lows of research life more enjoyable.

Additionally, I could not have asked for a more welcoming and supportive department. Thank you to Eileen Denovan-Wright and the members of my advisory committee, Dr. Susan Howlett and Dr. Denis Dupré, for your advice and guidance. To Sandi, Luisa, and Cheryl, thank you for helping me to navigate the graduate school maze and for providing a place where I always knew I could find a supportive face. Also, thank you to Kay Murphy, Tom Toguri, and Dr. Sebastian Parlee, for your technical support.

Lastly, I would like to thank my friends and family. Thank you to my parents for recognizing and encouraging my inquisitive nature and for instilling in me a commitment to quality work and the dedication and perseverance required for success. To those friends who endured this rollercoaster at my side, Natalie, Jon, Nicole, Helen, and most of all my dedicated husband Geoff, thank you for laughter, for teaching me to be more than a scientist, and for always giving me a soft place to land. You deserve to be "Dr" for a week too: I could not have done it without you.

Chapter 1: Introduction

1.1 Thesis Overview

Under conditions where energy intake persistently exceeds energy expenditure, excess white adipose tissue (WAT) accumulates throughout the body and ultimately leads to the development of obesity. The prevalence of obesity is increasing worldwide, affecting approximately 1.9 billion people globally (1). Obesity is characterized by numerous pathologic disruptions in inflammation and metabolism that ultimately contribute to increased risk for secondary disorders including the metabolic syndrome, cardiovascular disease and type 2 diabetes (T2D).

As a highly active endocrine organ, adipose tissue synthesizes and secretes a diverse collection of hormone-like proteins termed adipokines. Adipokines are produced from adipocytes themselves, or from other adipose tissue-resident cells, such as stem cells, immunocytes, endothelial cells, and fibroblasts. Most of these are proteins with hormone-like actions, but also include some well-established cytokines, and even enzymes (2,3). Several biologically active lipids are also widely considered to act as adipokines including non-esterified fatty acids, and free fatty acids. Following secretion, adipokines influence the development and metabolic function of nearby adipose tissue cells. Additionally, adipokines contribute to metabolic regulation through hormone-like actions on the brain, liver, pancreas, and skeletal muscle. To function as indicators of energy status and adipose tissue mass the secretion of adipokines must be dynamic and modifiable. Consistent with this, clinical studies demonstrate that the circulating levels of numerous adipokines are dramatically altered with obesity. It is believed that this adipokine dysregulation in obesity contributes to pathologic changes in energy homeostasis, inflammation, glucose handling, and food intake, and ultimately drives increased risk for obesity comorbidities.

Chemerin is a hormone-like protein that has recently been added to the rapidly expanding list of adipokines (4) and is the focus of this thesis. Herein, the first chapter of this thesis introduces the mechanisms regulating glucose homeostasis both normally and

in the context of obesity and T2D. Particular emphasis is placed on the adipokine-based mechanisms that contribute to insulin resistance and pancreatic β-cell failure during T2D development. The second chapter explores the extent of our knowledge on the role of chemerin in metabolic and inflammatory diseases. These introductory chapters set the stage for the third, fourth and fifth chapters, which describe original research concerning the elucidation of chemerin signaling through chemokine-like receptor 1 (CMKLR1) and G protein-coupled receptor 1 (GPR1) as well as an investigation into the impact of GPR1 loss on metabolic function and glucose homeostasis. The final chapter discusses the implications of these results and suggests future avenues of research for exploring chemerin biology in obesity and diabetes.

1. 2 T2D Overview

1.2.1 T2D Prevalence and Impact

In 2013 the International Diabetes Federation declared that the diabetes pandemic now affects 387 million people worldwide, with a predicted rise to 592 million (or 1 in 10) adults by 2030 (5). In Canada, diabetes prevalence increased by 230% between 1998 and 2009 (6). Individuals with T2D are at increased risk of cardiovascular disease, renal disease, and amputation, and are twice as likely to require physician and specialist care (7). In the US alone the impact of T2D is predicted to cost upwards of US$600 million per day in combined direct (health care) and indirect (loss or productivity, premature death) costs (8). The impact of T2D therefore is significant not only for individuals and families but also for society and Canada's publically funded healthcare system. As such, preventative and long-term strategies for improved diabetes care could have a tremendous impact on individuals and the health care system.

1.2.2 T2D Diagnosis, Symptoms, and Complications

T2D is a chronic, progressive metabolic disorder that is best characterized by the presence of elevated blood glucose (hyperglycemia). Glucose is the primary nutrient for

cellular energy production in the brain and other organs. The main source of glucose is ingestion of glucose-containing and carbohydrate-rich foods from the diet. To a lesser extent, the liver uses amino acids and other metabolic precursors for *de novo* glucose synthesis through gluconeogenesis (9). Normally, a highly coordinated endocrine system maintains blood glucose levels between 4 -8 mM throughout daily periods of fasting and feeding (6). Loss of this endocrine control results in a rise of blood glucose levels. The earliest clinically recognized stage of T2D is referred to as prediabetes. Prediabetes is characterized by elevated fasting glucose, impaired oral glucose tolerance, or elevated glycated hemoglobin A1C (a by-product of hyperglycemia) (6). Individuals with prediabetes are at considerably increased risk for T2D manifestation (10). T2D is diagnosed when fasting blood glucose levels are greater than 7 mM, oral glucose tolerance levels exceed 11.2 mM, or when glycated hemoglobin A1C levels are greater than 6.5% (6).

The clinical parameters used to diagnose T2D were determined based on the increased risk for glucose toxicity, tissue damage, and chronic complications that occur above the indicated blood glucose levels (6). Acutely elevated blood glucose levels are associated with feelings of hunger, fatigue, and frequent urination, owing to impaired glucose uptake for use in cells and increased urinary output for glucose excretion. Most cells of the body can maintain intracellular glucose levels despite elevated blood glucose levels, protecting them from hyperglycemia. Blood vessels, neurons, and cells of the eyes and kidneys do not have this capacity and are particularly sensitive to damage in chronic hyperglycemia (11,12). In these susceptible cells, increased intracellular glucose metabolism results in overproduction of reactive oxygen species and glycated proteins, activation of oxidative stress, inflammatory signaling, and abnormal PKC activation, ultimately leading to dramatic changes in gene expression and loss of cellular function (13,14). As such, microvascular, macrovascular, and nerve dysfunction are prominent features of chronic hyperglycemia (15). This damage increases risk for reduced peripheral circulation and sensitivity, retinopathy/blindness, atherosclerosis, and kidney failure in diabetes (16-18).

1.2.3 T2D Etiology

T2D is caused by a combination of genetics, lifestyle, and environmental factors. More than 40 genes associated with increased risk for T2D have been identified (19). In most cases, these genes contribute to the function of insulin-producing pancreatic β-cells; however, the precise mechanisms by which they predispose individuals to T2D remain poorly understood. Most diabetes-associated genes have been inferred from single nucleotide polymorphisms (SNPs). T2D disease risk correlates with an increase in the number of predisposing SNPs (19,20). Developmental causes, sleeping disorders, depression, environmental toxins, and use of certain medications have also been linked to a small proportion of T2D risk (21-25). Overall these factors have been estimated to contribute to no more than 10% of T2D risk.

An estimated 90% of T2D disease risk derives from lifestyle factors including: poor diet, sedentary lifestyle, overweight, and obesity (26,27). The 2012 Canadian Community Health Survey estimates that 18.4% of Canadian adults are obese (body mass index (BMI) > 30 kg/m^2), while 41.3% of men and 26.9% of women are overweight (BMI 25-30 kg/m^2). Taken together, self-reported estimates of Canadian obesity demonstrate that 59.9% of men and 45% of women are currently at increased risk (28) for diseases such as cardiovascular disease, cancer, and dementia, as well as considerably high risk for T2D development (29-31). Given the tight degree of association between obesity and T2D, it is not surprising that these rising obesity rates are mirrored by a substantial rise in T2D diagnoses (32).

The increased risk for T2D with obesity is attributed to an accumulation in functional deficits in the key organs and hormones responsible for maintaining glucose homeostasis (33). The brain, liver, pancreas, gastrointestinal tract, skeletal muscle, and adipose tissue normally cooperate to maintain daily fluctuations in blood glucose within narrow limits through balanced glucose uptake, utilization, storage, and synthesis. The pancreatic hormones insulin, glucagon, and somatostatin, as well as numerous adipokines, facilitate dynamic communication between these organ systems in order to coordinate glucose homeostasis. The following sections outline our current understanding of glucose homeostasis both normally and in the context of the dysfunction that occurs in

obesity and T2D development. For the purpose of this thesis, particular emphasis is placed on the role of the pancreas, insulin, and adipokines.

1.3 Normal and Impaired Glucose Homeostasis

To ensure adequate glucose supply to tissues and to prevent the tissue damage and dysfunction that occurs with hyperglycemia, a tight balance of glucose absorption from the intestines, glucose uptake/storage/utilization by peripheral tissues, and glucose production by the liver is required (Fig 1.1). Central to glucose homeostasis is the pancreatic islet, which produces the insulin required for glucose uptake and inhibition of liver glucose production. Gut-derived incretin hormones contribute to glucose homeostasis by modulating the insulin sensitivity of peripheral tissues, and β-cell insulin secretion. Peripheral tissues, including skeletal muscle, adipose tissue, and liver express receptors for numerous glucose homeostasis mediators and play critical roles in glucose uptake, storage, and utilization. Moreover, adipose tissue itself secretes a variety of endocrine factors, adipokines, which contribute to insulin secretion, sensitivity and metabolic function. As such, the endocrine regulation of glucose homeostasis requires the cooperation of numerous organ systems to maintain tight blood glucose control.

In obesity the normal endocrine regulation of glucose homeostasis often becomes disrupted through a variety of complex mechanisms. Nutrient overload contributes to cellular stress in the pancreas, liver, adipose tissue and skeletal muscle (34). This in combination with excess lipid deposition in non-adipose tissue sites and adipocyte hypertrophy contribute to immune cell activation and a chronic state of low-grade, systemic inflammation (35). Adipokine secretion from adipose tissue is altered such that there is an increase in pro-inflammatory adipokines and a decrease in insulinotropic and insulin sensitizing adipokines (36,37). Accumulation of these pathological changes in cellular and organ function contributes to the development of peripheral tissue insulin resistance and impaired pancreatic insulin secretion, both of which are key driving forces for the development of T2D.

An understanding of the normal and pathological processes involved in glucose homeostasis and T2D is necessary in order to identify novel methods for disease

prevention and improvement. The following sections will: outline normal mechanisms of glucose homeostasis, including regulation by insulin, incretin hormones and adipokines; discuss the pathological stages of diabetes development in obesity; and describe mechanisms by which adipokines contribute to diabetes pathogenesis in obesity.

1.4 Insulin Regulates Glucose Homeostasis

Insulin is a potent anabolic hormone that serves as the primary messenger used to regulate blood glucose concentration. Insulin is exclusively produced and secreted by pancreatic β-cells in response to rising blood glucose levels. Following secretion, insulin activates adipose tissue and skeletal muscle glucose uptake and thereby promotes a lowering of blood glucose levels. In these tissues, the facilitative glucose transporter 4 (GLUT4) is required for glucose uptake across the cell plasma membrane. In the absence of insulin, the endocytic rate of GLUT4-containing vesicle transport to the plasma membrane exceeds the exocytic rate resulting in less than 5% of total GLUT4 localizing to the plasma membrane and minimal glucose uptake (38). Insulin receptor signaling stimulates glucose uptake by increasing the translocation of GLUT4 from intracellular sites to the plasma membrane where it facilitates glucose entry into the cell (39,40). Additionally, insulin stimulates metabolism of the incoming glucose for energy production or storage as glycogen or lipid by promoting glycogenesis and lipogenesis, respectively (41,42). In the liver, insulin prevents hyperglycemia by inhibiting the production of new glucose (gluconeogenesis) and promoting glucose storage as glycogen (glycogenesis). Additionally, insulin stimulates cell growth and differentiation by promoting protein synthesis and inhibiting protein breakdown (43,44). Insulin is also required to inhibit secretion of the catabolic hormone glucagon (45,46), which promotes liver glycogenolysis and gluconeogenesis to increase glucose mobilization and counteract the actions of insulin. Collectively, insulin action serves to promote glucose uptake and storage for use in times of caloric deficit, and ultimately lowers blood glucose levels. Consequently, β-cells must integrate multiple metabolic signals, including glucose, lipids, cytokines, and adipokines, to facilitate tightly controlled insulin secretion.

1.4.1 Mechanisms of Insulin Secretion: Glucose Stimulated Insulin Secretion

Insulin secretion is tightly coupled to blood glucose levels through the process of glucose-stimulated insulin secretion (GSIS). The best characterized mechanism for GSIS is the glucose-dependent ATP-sensitive potassium (K^+)-channel pathway (Fig. 1.2). Pancreatic β-cells are excitable cells expressing numerous ion channels (47). The ATP-sensitive K^+-channel in β-cells is open under low glucose conditions, allowing K^+ to flow freely out of the cell. In this state, insulin is stored in cytosolic vesicles that are docked at the plasma membrane in preparation for release (48). As blood glucose levels rise, there is increased glucose uptake into the β-cells via passive facilitated diffusion through GLUTs (1, 2, and 3) located in the β-cell plasma membrane (49). Glucose metabolism through glycolysis and the mitochondrial tricarboxylic acid cycle increases the intracellular ATP: ADP ratio. This triggers closure of the ATP-sensitive K^+-channel and the ensuing increase in intracellular K^+ depolarizes the cell. Depolarization-mediated activation of voltage-sensitive calcium (Ca^{2+}) channels on the plasma membrane causes an influx of Ca^{2+} and initiates fusion of membrane-docked, insulin-rich vesicles with the plasma membrane and release of insulin from the β-cell (8). This is called first phase insulin secretion, which is terminated when stored insulin granules are depleted. Second phase insulin secretion, a prolonged insulin release, proceeds subsequent to the rapid release of first phase and requires insulin transcription, translation, processing and packaging to generate new insulin for both release and replenishment of stored vesicles (48).

Given the glucose lowering capacity of insulin and the potentially life threatening consequences of hypoglycemia, it is critical that control of insulin action also incorporates mechanisms for the termination of insulin secretion to prevent blood glucose levels from dropping too low. Once in the blood stream, insulin is rapidly degraded by renal and hepatic insulinase, resulting in an insulin half-life of only 6 minutes (50). In the pancreas, a decline in blood glucose results in a reduction in the ATP: ADP ratio, opening of the K^+ ATP channel, repolarization of the cell and closure of the voltage-sensitive Ca^{2+} channel. A rich vascular network surrounding the islets ensures both access to blood glucose, and the rapid diffusion of insulin into the blood for circulation (51). This tight

coupling of glucose levels and insulin secretion enables the pancreatic β-cells to act as key glucose-sensing effectors capable of rapid and dynamic responses to continuously changing blood glucose levels and positions the β-cells as a central hub for the coordination of glucose homeostasis.

1.4.2 Mechanisms of Insulin Secretion: The Incretin Effect

In addition to blood glucose levels, endocrine signals triggered by nutrient ingestion also contribute to the regulation of insulin secretion. The incretin hormones glucagon-like-peptide-1 (GLP-1) and glucose-dependent insulinotropic polypeptide (GIP) are gut-derived hormones that potentiate GSIS immediately following a meal (52-54). GIP and GLP-1 are produced in the proximal small intestine and bowel, respectively and rise within minutes of a meal (54). The best-established target of these incretin hormones is the islet β-cells, which abundantly express the GLP-1 and GIP receptors (55). Pharmacological inhibition of the GIP or GLP-1 receptors results in increased postprandial blood glucose levels (56-58). The precise mechanisms of incretin-mediated enhancement of GSIS remain unclear but appear to involve increases in intracellular cyclic adenosine monophosphate (cAMP), phosphoinositide-3-kinase (PI3K) activity, and increased intracellular Ca^{2+}, which increase K^{+}-ATP channel closure and enhance insulin vesicle exocytosis (59). Moreover, GLP-1 activation of the transcription factor Pdx-1 also increases insulin production by promoting insulin gene expression and enhancing insulin mRNA stability (60). Incretin activity is short-lived because the enzyme dipeptidyl peptidase-4 (DPP-4) rapidly cleaves and inactivates both GLP-1 and GIP (61), limiting the incretin effect to within minutes of meal ingestion. These studies support a role for extra-pancreatic incretin actions in regulation of glucose homeostasis through modulation of insulin secretion.

1.4.3 Mechanisms of Insulin Signaling and Action

Following secretion, insulin signaling in peripheral tissues directly influences glucose uptake through GLUT4 mobilization, energy storage through metabolic enzyme

modulation, and cellular growth through support of survival and proliferation gene expression. These actions are achieved through binding and activation of insulin receptors. The insulin receptor is a tetrameric ($\alpha_2\beta_2$) tyrosine kinase receptor comprised of two α and two β subunits and expressed on the plasma membrane of insulin responsive cells including myocytes, adipocytes, hepatocytes, and β-cells (62). Following insulin binding to the α subunits a conformational change in the receptor results in β subunit autophosphorylation (63). Phosphorylated β subunits exhibit increased kinase activity, stimulating phosphorylation of numerous second messengers and several distinct signaling pathways.

Notably, insulin receptor signaling activates two distinct pathways, the insulin receptor substrate (IRS) pathway and the IRS-independent lipid raft pathway, to mediate glucose uptake in adipose tissue and skeletal muscle (Fig. 1.3). The IRS pathway activates PI3K and AKT signaling to increase GLUT4 levels on the plasma membrane through activation of GTPase proteins (Rab5, Rab8, Rab10, and Rab14 and RalA), the motor protein MYO1C, calmodulin, the SNARE proteins Synip and CDP138, and rearrangement of the actin/microtubule cytoskeleton (38,39,64-67). This PI3K and AKT pathway signaling facilitates GLUT4-containing vesicle release from the cytosol, movement along cytoskeletal scaffolds, and delivery to the plasma membrane. The IRS-independent pathway involves activation of an APS/CAP/CBL/CRKII signaling complex, which localizes insulin signaling to lipid rafts through association with the lipid raft bound protein flotillin (68,69). This signaling activates the guanine nucleotide exchange factor (GEF) C3G and the Rho-family GTPase TC10. TC10 target proteins are involved in GLUT4 vesicle tethering in the cytosol or vesicle targeting to the plasma membrane (70-72). Together, these molecular targets of insulin signaling link APS activation to repression of vesicle tethering and membrane targeting resulting in a second signal for increased GLUT4 at the plasma membrane and glucose uptake.

In addition to glucose uptake, insulin receptor signaling pathways also contribute to cell growth and metabolic regulation through activation of the PI3K/AKT and GRB2 growth factor pathways in liver, skeletal muscle, and adipose tissue. In the liver the primary functions of insulin are to promote glucose utilization and storage as well as repress glucose synthesis and release (73). Specifically, insulin activation of AKT

signaling in hepatocytes increases glycogen synthase and glycogen synthase kinase mRNA expression in support of glucose metabolism and glycogen synthesis (74). Insulin signaling in hepatocytes also inhibits the mRNA expression of gluconeogenic enzymes such as glucose-6-phosphatase (G6PC), fructose-1-6-bisphosphatase, and phosphoenolpyruvate carboxykinase via modulation of the transcription factors PGC1α, hepatic nuclear factor-4, and the forkhead protein family member O (74). Similarly, insulin signaling through PI3K/AKT in adipose tissue activates the transcription factor sterol regulatory element binding protein to increase mRNA expression of fatty-acid synthesizing enzymes such as acetyl-coA carboxylase, and fatty acid synthase to promote lipid synthesis and storage (42). In multiple cell types, IRS activation of the growth factor GRB2 contributes to the growth-promoting actions of insulin by activating a Ras/MAPK signaling cascade that leads to a proliferation/survival gene expression program (74,75). Together these pathways couple insulin activation of the insulin receptor and IRS proteins to changes in mRNA and protein expression, which collectively support glucose utilization and storage, as well as cell growth, survival and proliferation.

Altogether the IRS-dependent and independent mechanisms of insulin signaling in skeletal muscle, adipose tissue, and liver promote a decline in blood glucose levels through glucose uptake and inhibition of glucose production. When insulin levels subsequently decline in sync with the falling blood glucose levels, this signaling must be terminated to prevent excess glucose uptake and low blood glucose (hypoglycemia). In the tissues, protein tyrosine phosphatases (e.g. PTP1B) contribute to insulin receptor signaling termination by dephosphorylating the insulin receptor and insulin signaling effectors (76,77). Additionally, a number of insulin-induced kinases, including PI3K, mTOR, and AKT, participate in a feedback signal whereby phosphorylation of serine residues within the insulin receptor and/or the IRS proteins decreases insulin-stimulated tyrosine phosphorylation. Insulin-bound insulin receptors are also internalized into endosomal compartments, resulting in signal transduction that is spatially distinct from that which occurs at the plasma membrane (78-80). In time, insulin receptor inactivation and endosomal acidic insulinase-mediated insulin degradation within lysosomes terminates the insulin signal (78). The suppressors of cytokine signaling (SOCS) family

and the insulin receptor-binding protein Grb-IR, also contribute to termination of insulin signaling through a physical blockade of substrate interactions as well as phosphorylation and degradation of the insulin receptor or IRS proteins (37,81,82). Together these pathways for the termination of insulin signaling create a cellular environment that favours GLUT4 endocytosis, reducing plasma membrane GLUT4 levels and terminating glucose uptake.

1.5 Obesity and T2D

Adipose tissue is an insulin-responsive tissue that plays an important role in glucose uptake and storage as lipid. The endocrine function of adipose tissue contributes to the metabolic fine-tuning required for tight glucose control. The excess adipose tissue characteristic of overweight and obesity has been implicated in pathological changes in glucose and energy homeostasis that contribute to the development of T2D. The following sections discuss the roles and mechanisms of adipose tissue-mediated regulation of normal and pathological glucose handling.

1.5.1 The Adipo-Insular Axis

A two-way physiological connection between β-cell insulin secretion, peripheral tissue energy status, and insulin sensitivity ensures a balance between insulin supply and demand and the maintenance of nutrient homeostasis (83). As an insulin-regulated energy store, white adipocytes have a tremendous capacity for lipid storage and growth, both of which contribute to modulation of adipokine secretion and position adipose tissue as a key energy-sensing organ. The adipo-insular axis comprises the network of endocrine signals linking adipose tissue to pancreatic function and peripheral insulin sensitivity (84) (Fig. 1.4). The adipo-insular axis model was originally based on the endocrine function of the adipokine leptin. In this role, leptin acts as an energy status signal supporting: hypothalamic regulation of food consumption; energy utilization by brown adipose tissue (BAT); and glucose homeostasis in skeletal muscle, adipose tissue, and pancreas (85,86).

Subsequently, numerous adipokines have been shown to regulate glucose homeostasis through actions on β-cell function and peripheral tissue insulin sensitivity (36,84).

1.5.2 Adipokines Modulate Insulin Sensitivity in Peripheral Tissues

Obesity-induced insulin resistance is a significant driving force behind the obesity-diabetes link. Insulin resistance is an insensitivity of insulin target tissues to the actions of insulin. Exquisitely complex networks of metabolic derangements in endocrine, and inflammatory pathways are implicated in the etiology of insulin resistance (Fig. 1.3). In obesity the secretion of numerous adipokines becomes disrupted such that there is an increase in pro-inflammatory and insulin-resistance adipokines and a decline in protective insulin sensitizing adipokines (36). This shift in adipokine profile contributes to the pathological changes coupling obesity with the development and maintenance of insulin resistance.

Obesity is characterized by chronic low-grade inflammation, which is a dominant pathological catalyst for the development of insulin resistance (35,87). In obesity, the adipose tissue storage capacity cannot completely compensate for nutrient overload, resulting in increased circulating free fatty acids, and ectopic lipid deposition in non-adipose tissues such as liver, skeletal muscle, and pancreas (88,89). The ectopic lipid deposition in peripheral tissues results in immune cell recruitment and activation, increased cytokine production, and a chronic low-grade systemic inflammation (90). An increase in pro-inflammatory adipokines, including tumor necrosis factor alpha (TNFα), interleukin (IL)-6, and chronically elevated circulating free fatty acids, activate ERK, JNK, NFkB, and SOCS inflammatory signaling in myocytes, hepatocytes, and β-cells, resulting in insulin resistance (37). Several mechanisms for inflammation-induced insulin resistance have been identified and include: increased inhibitory serine phosphorylation of insulin receptors and IRS, decreased GLUT4 vesicle exocytosis, increased pro-gluconeogenic gene mRNA expression, increased reactive oxygen species, mitochondrial dysfunction, and endoplasmic reticulum (ER) and oxidative stress (37,88,89) (Fig. 1.5). Ultimately, adipokine dysregulation in obesity, including increased circulating free fatty acids and pro-inflammatory adipokines, contributes to tissue inflammation, inhibition of

insulin signaling pathways and the development of insulin resistance in skeletal muscle, adipose tissue, liver, and pancreas.

Anti-inflammatory, insulin-sensitizing adipokines, whose expression is decreased in obesity, have also been implicated in insulin resistance. In healthy individuals adiponectin increases beneficial processes including insulin sensitivity, glucose uptake, and fatty acid oxidation through activation of the key energy homeostasis AMPK pathway (91). In the inflammatory milieu of obesity, TNFα and IL-6 suppress adiponectin mRNA expression in adipocytes (92). Adiponectin knockout decreases insulin sensitivity in mice, while adiponectin overexpression in obese mice results in improved insulin sensitivity (93,94), suggesting that the loss of adiponectin in obesity contributes to a detrimental decline of insulin sensitivity. Consistent with this, elevated circulating adiponectin predicts increased insulin sensitivity, and loss of adiponectin in obese humans is correlated with increased insulin resistance (95,96). Omentin-1 also shows great promise as an insulin-sensitizing adipokine. The stromal vascular cells of omental (located near the stomach and spleen) WAT produce omentin-1 (97). In addition to activating insulin-sensitizing AKT signaling in adipocytes, omentin-1 has been shown to decrease C-reactive protein (CRP) and TNFα mediated NFκB activation in endothelial cells, suggesting that it may also play a role in decreasing inflammation-induced insulin resistance, (98,99). Elevated glucose and insulin in obesity and diabetes contribute to a decline in omentin-1 levels, reducing its beneficial effects on glucose and inflammatory homeostasis (100). These studies demonstrate mechanisms by which a decline in anti-inflammatory, insulin sensitizing adipokines can contribute to insulin resistance in obesity.

1.5.3 β-cell Compensation, Dysfunction, and Failure Occurs in Obesity

In the context of insulin resistance, more insulin than normal is required to maintain blood glucose levels within the normal range. In the earliest stages of prediabetes, β-cells can sufficiently compensate for increased insulin demand by increasing insulin secretion (101,102). Consequently, individuals may have no discernable impairments in glucose homeostasis for years despite the presence of insulin

resistance. The degree to which β-cells can maintain insulin compensation determines whether an individual ultimately ends up with impaired glucose homeostasis or T2D. Many obese people do not get T2D because their β-cells are able to compensate by increasing insulin secretion (8). Insulin resistance and prediabetes are believed to progress to T2D as a consequence of a failure in functional insulin compensation and ultimately β-cell failure. The progression from prediabetes to T2D involves four pathophysiological stages, which can proceed linearly from one to the next, but can also revert to earlier stages (103).

With insulin resistance, the first stage of prediabetes involves a compensatory increase in basal and GSIS (102,104). An increase in β-cell mass has been measured in humans and is believed to play a role in this increased insulin secretory capacity (105-108). Additionally, in the context of increasing insulin demand β-cell sensitivity to glucose and GLP-1 is enhanced resulting in increased insulin gene and protein expression as well as GSIS (109). At this stage increased circulating free fatty acids enhance compensation via a beneficial amplification of GSIS through activation of the G protein-coupled receptor (GPCR) GPR40 (110). As such, increased β-cell mass, insulin biosynthesis, and sensitivity to nutrient-secretion coupling are believed to contribute to compensatory insulin secretion.

Progression through the proposed phases involves changes in β-cell phenotype, decreased insulin compensation, and β-cell failure leading ultimately to β-cell death. Functional β-cell deficits have been noted in T2D susceptible individuals well before the onset of abnormal glycaemia (111). The earliest clinically recognized deficit is a characteristic failure in first phase insulin secretion (112). This stage results in slightly elevated blood glucose levels and can persist for years, especially in individuals who maintain a healthy diet and active lifestyle. At some critical point the combination of insulin resistance and an accumulation of β-cell deficits contributes to failure in β-cell compensation. Much like insulin resistance, dysfunctional adipokine secretion and inflammation contribute to a complex network of deficits in mitochondrial function, oxidative and ER stress, and lipid cycling that ultimately result in islet inflammation, impaired insulin secretion, and the progressive demise of β-cells. The search for

molecular mechanisms contributing to the maintenance of β-cell compensation that can be employed as novel therapeutic targets to prevent diabetes progression is at the forefront of diabetes research.

1.5.4 Adipokines Contribute to β-Cell Failure and T2D

In addition to responding to glucose, β-cells are tasked with integrating a diversity of metabolic signals in order to maintain metabolic homeostasis. Islet β-cells express numerous adipokine receptors facilitating both insulinotropic or counter regulatory effects on β-cell function and insulin secretion (Fig. 1.6) (36). Circulating leptin levels rise in direct proportion to increasing adipose mass (113). Leptin has been described as having dual actions on β-cell insulin secretion. Through activation of β-cell-expressed leptin receptors, low-dose leptin can inhibit insulin secretion (114,115), while higher leptin levels can stimulate insulin secretion from isolated islets (116). Mouse studies demonstrate differential effects on β-cell survival and insulin secretion with leptin receptor loss in obese animals when compared with lean. This has lead to the prevailing hypothesis that in lean animals leptin restrains β-cell function and growth, but in obese animals this restriction is required to prevent β-cell death, thereby supporting insulin secretion (117,118). These findings support a role for leptin in communicating dynamic changes in adipose tissue energy status and demonstrate the capacity for adipokines to play key roles in the energy sensing required for glucoregulation by the pancreas. Consistent with this, numerous adipokines have been shown to increase GSIS, including adiponectin, visfatin, and nesfatin-1, while others like resistin and TNFα inhibit insulin secretion (119). Ultimately, an imbalance in these adipokines contributes to β-cell dysfunction in T2D through modulation of β-cell proliferation and survival, insulin mRNA and protein expression, and insulin secretion pathways (119).

1.5.5 Adipokines Influence β-Cell Insulin Secretion

Several adipokines have been shown to increase insulin secretion and support β-cell viability. Adiponectin is an adipokine whose circulating levels decrease with increasing adiposity (120,121). Human and rodent β-cells express adiponectin receptors (122). Winzell *et al*. (123) demonstrated that adiponectin potentiates GSIS in obese, but not lean, animals. The role of adiponectin in human islet insulin secretion remains unclear; human islet insulin secretion was unaffected by adiponectin treatment despite adiponectin receptor expression (124). Conversely, an increase in adiposity correlates with increased levels of the adipokines visfatin, and nesfatin-1. These adipokines enhance compensatory insulin secretion and support β-cell gene expression and metabolic function (36,125-129). As such, there is hope that these adipokines will have utility as a tool for increasing insulin secretion in obesity; however, this remains to be investigated more directly *in vivo* and in humans.

Circulating levels of the adipokines resistin and TNFα increase with obesity and are associated with suppression of GSIS in mice or humans. Hotamisligil and Spiegelman demonstrated that adipose tissue-derived TNFα increases in obesity (130,131). Specifically, increased macrophage infiltration in obese adipose tissue results in increased local and systemic TNFα, and IL-6 overproduction (130,132,133). TNFα receptor activation on β-cells results in pro-inflammatory nitric oxide signaling cascades that contribute to increased cytokine expression, β-cell inflammation, and impaired β-cell function, including decreased GSIS (37,134,135). Similarly, circulating resistin levels increase with adiposity (136,137). In mice, resistin induces insulin resistance in peripheral tissues and β-cells, the latter of which results in elevated basal insulin expression and impaired GSIS (138). In humans, resistin is expressed in islets (139) and by immune cells, including those located within obese, inflamed adipose tissue (140). Elevated circulating resistin levels are positively correlated with obesity and increased T2D risk (141). The precise role of resistin in human islet function remains to be elucidated. These inhibitory actions of adipokines demonstrate the potential for adipose-mediated negative regulation of islet insulin secretion.

Like leptin, some adipokines have dual action on insulin secretion. Circulating apelin levels increase with adiposity, and insulin enhances apelin expression (142). Apelin reduces blood glucose concentration by increasing glucose uptake and utilization

in muscle (143). Through activation of the apelin receptor (APJ) on β-cells, apelin also modulates insulin secretion (144,145). Isolated islet experiments suggest that β-cells demonstrate a biphasic response to apelin whereby low apelin doses inhibit GSIS while high doses potentiate GSIS (146). As such, apelin may serve as a metabolic sensor, which participates in the fine-tuning of insulin secretion under various metabolic states. Similarly, non-esterified fatty acids decrease insulin transcription and exhibit dose- and context-dependent effects on insulin secretion. For example, low/acute treatments result in enhanced islet GSIS while the high/chronic levels occurring with obesity inhibit GSIS (119).

1.5.6 Adipokines Influence β-cell Survival

Proliferation and apoptosis pathways are an important component regulating both the increased β-cell mass in compensatory stages of diabetes development and β-cell loss later in disease progression. Elevated expression of the pro-inflammatory adipokines IL1β, TNFα, and chronically elevated non-esterified fatty acids, for example, have established cytotoxic actions inducing β-cell apoptosis. In the case of TNFα, apoptosis induction occurs via activation of the NFκB pathway (147,148). On the other side of the balance, adiponectin and leptin have established actions increasing β-cell mass through increased proliferation and or protection from apoptosis (149-151). Using both adiponectin expression and knockout in mice, it was demonstrated that adiponectin protects against caspase-8-mediated β-cell apoptosis (152). Collectively, increased apoptosis, decreased proliferation, and inhibition of GSIS occur with adipokine dysregulation and contribute to β-cell failure in obesity.

1.6 Concluding Statements

Through the adipo-insular axis, adipokines contribute to insulin sensitivity, β-cell compensation, inflammation, and β-cell survival. The function of multiple adipokines is dose- and context-specific. It is important to note that the majority of studies

investigating the impact of adipokines on β-cell function and insulin resistance have focused on the changes and actions of an individual adipokine. In obesity, the circulating and local levels of most adipokines identified to date become dysregulated. One study examining the interplay between leptin and adiponectin in rat β-cells demonstrated that co-treatment with leptin abolished the pro-survival actions of adiponectin (153). Moreover, there is considerable overlap amongst adipokine-activated signal transduction pathways, including MAPK/ERK, PI3K, AMPK, JNK, and NFκB, in β-cells (119). This provides mechanisms for functional adipokine crosstalk. These observations stress the importance of future studies examining the net effect of multiple adipokine signals on β-cell function and insulin secretion to more clearly delineate the role of adipokine dysregulation in obesity and T2D. Nonetheless, modulation of adipokine function in diabetes and obesity represents a huge area for potential identification of novel therapeutic strategies for these diseases. This potential propels an ever-expanding research effort to discover novel adipokines and elucidate adipokine function in normal health and disease.

1.7 Figures

Figure 1.1: Endocrine regulation of glucose homeostasis

Glucose homeostasis requires the cooperation of numerous organ systems and hormones. Ingested sugars and carbohydrates are absorbed from the gastrointestinal (G.I.) tract as glucose and contribute to a central blood glucose pool. The brain requires blood glucose for energy production. The pancreas senses elevated blood glucose levels, triggering insulin secretion. Incretin hormones secreted from the G.I. tract in response to ingested nutrients also promote glucose-stimulated insulin secretion (GSIS) from the pancreas. Insulin promotes glucose uptake, utilization and storage in the peripheral tissues (liver, skeletal muscle, adipose tissue). Insulin is also required to inhibit glucose production in the liver. Adipokines are secreted from adipose tissue and have numerous actions on adipose tissue itself, skeletal muscle, and pancreas. Glucagon secretion occurs when blood glucose levels fall and serves to increase glucose release from the liver to promote a rise in blood glucose levels.

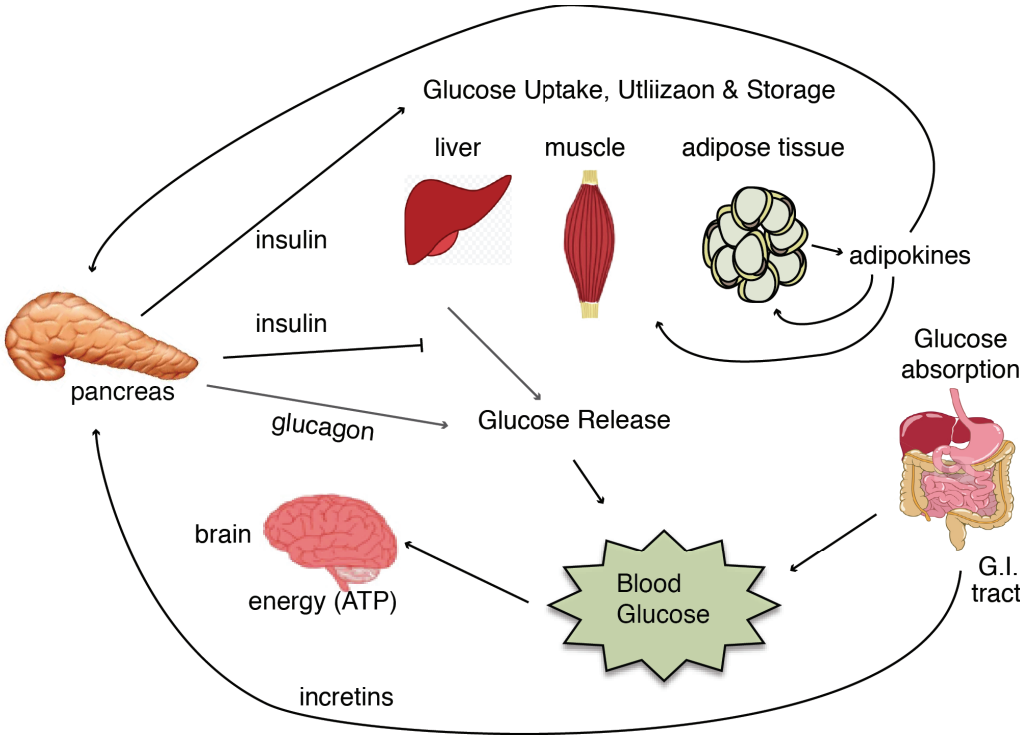
Glucose Uptake, Utliizaon & Storage
liver
muscle
adipose tissue
insulin
adipokines
insulin
Glucose
absorption
pancreas
glucagon
Glucose Release
brain
energy (ATP)
Blood
Glucose
G.I.
tract
incretins

Fig. 1.1

Figure 1:2: Glucose-stimulated insulin secretion (GSIS) from the pancreatic β-cell

Glucose entry and mitochondrial metabolism in the pancreatic β-cell will result in an increased ATP: ADP ratio and closure of the ATP-sensitive K^+ channel. Increased intracellular K^+ accumulation results in membrane depolarization, activation of the voltage-dependent Ca^{2+} channel, and Ca^{2+} entry into the cell. Ca^{2+} stimulates fusion of membrane-docked insulin-containing vesicles with the membrane and insulin release. Second-phase insulin secretion requires insulin gene transcription, translation, and processing of insulin proteins into vesicles for transmigration along actin cytoskeletal networks and eventual membrane fusion and release. The incretin hormone GLP-1 enhances glucose-stimulated insulin secretion (GSIS) through activation of AKT, PKA, and ERK signaling pathways that support β-cell survival and proliferation, insulin production, and insulin release. **Abbreviations**: Adenosine diphosphate: ADP, adenosine triphosphate: ATP, calcium: Ca^{2+}, GLUT: glucose transporter potassium ion: K+, extracellular-regulated kinase: ERK, protein kinase A:PKA, RAC-alpha serine/threonine-protein kinase: AKT, glucose-6-phosphate: glucose-6-p.

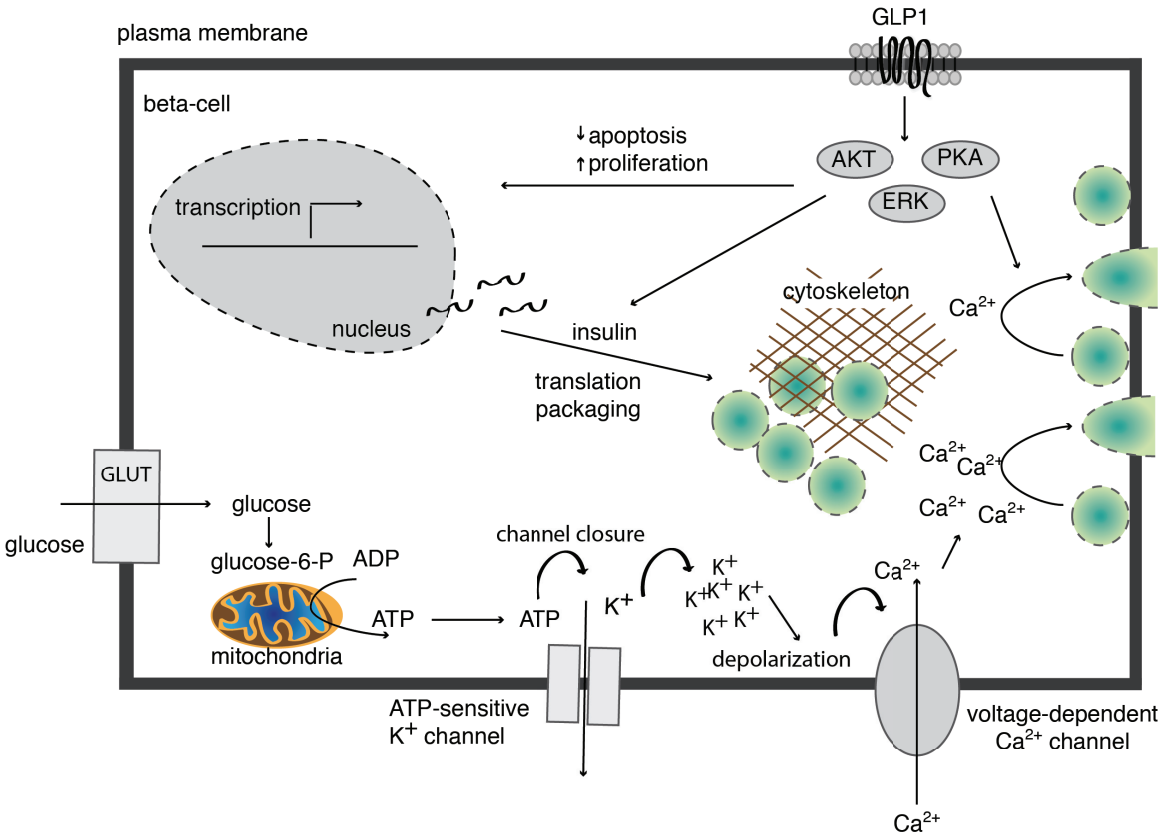
plasma membrane
GLP1
beta-cell
↓apoptosis
↑proliferation
AKT
PKA
ERK
transcription
nucleus
cytoskeleton
Ca2+
insulin
translation
packaging
GLUT
glucose
glucose
glucose-6-P
ADP
ATP
mitochondria
channel closure
ATP
K+
K+
depolarization
Ca2+
Ca2+
Ca2+
Ca2+
Ca2+
ATP-sensitive
K+ channel
voltage-dependent
Ca2+ channel
Ca2+

Fig. 1.2

Figure 1.3: Insulin receptor signal transduction and glucose uptake in skeletal muscle, liver and white adipose tissue

Insulin receptor signaling activates two distinct signal transduction pathways for the regulation of glucose uptake through GLUT4 and metabolism. Activation of IRS proteins results in both PI3K-mediated conversion of membrane lipids to PIP_3, activation of PDK1 and AKT. AKT inhibits the GAP activity of AS160 permitting rab-mediated GLUT4 vesicle translocation and membrane binding. AKT also influences gene expression programs required for regulation of glycogen synthesis, gluconeogenesis, and protein synthesis to support energy storage and cell growth. IRS activation also activates MAPK/ERK signaling through the adaptor proteins GRB2, SHC, and SOS, as well as Ras activation. The second insulin receptor pathway involves activation and lipid raft-association of an APS/CAP/CBL/CRK complex, which activates C3G and the ral-GEF TC10. RalA activation and association with MYO1C promotes GLUT4 vesicle movement along the actin cytoskeleton for directed translocation of vesicles to the plasma membrane. Insulin signaling is terminated through PTP-mediated de-phosphorylation of insulin receptor and IRS proteins or *via* internalization of the insulin receptor to endosomal compartments where initial spatially distinct signaling is terminated by insulin degradation by the enzyme EAI and insulin receptor dephosphorylation.

Abbreviations: RAC-alpha serine/threonine-protein kinase: AKT, adapter protein with Pleckstrin homology and Src homology 2 domains: APS, AKT substrate of 160 kDa: AS160, CRK SH3-binding protein: C3G, c-cbl associated protein: CAP, Casitas B-lineage lymphoma: CBL, CT10 regulator of kinase II: CRK, extracellular-regulated kinase: ERK, forkhead box protein class O: FOXO, GTPase activating protein: GAP, guanine nucleotide exchange factor: GEF, glucose transporter 4:GLUT4, Growth factor receptor-bound protein 2: GRB2, Glycogen synthase (GS), glycogen synthase kinase: GSK, insulin receptor substrate: IRS, mammalian target of rapamycin mTOR, ribosomal protein S6 kinase: p70s6K, phosphoinositide-dependent kinase 1:PDK1, phosphoenolpyruvte carboxylase: PEPCK, phosphoinositide-3-kinase:PI3K, phosphatidyl-inositol (3,4,5)-triphosphate: PIP3, protein tyrosine phosphatase: PTP, V-ral simian leukemia viral oncogene homolog A (ras related):RAL, Src-homology/collagen protein: SHC, soluble NSF attachment protein receptor: SNARE, son of sevenless: SOS, small GTP-binding protein TC10: TC10.

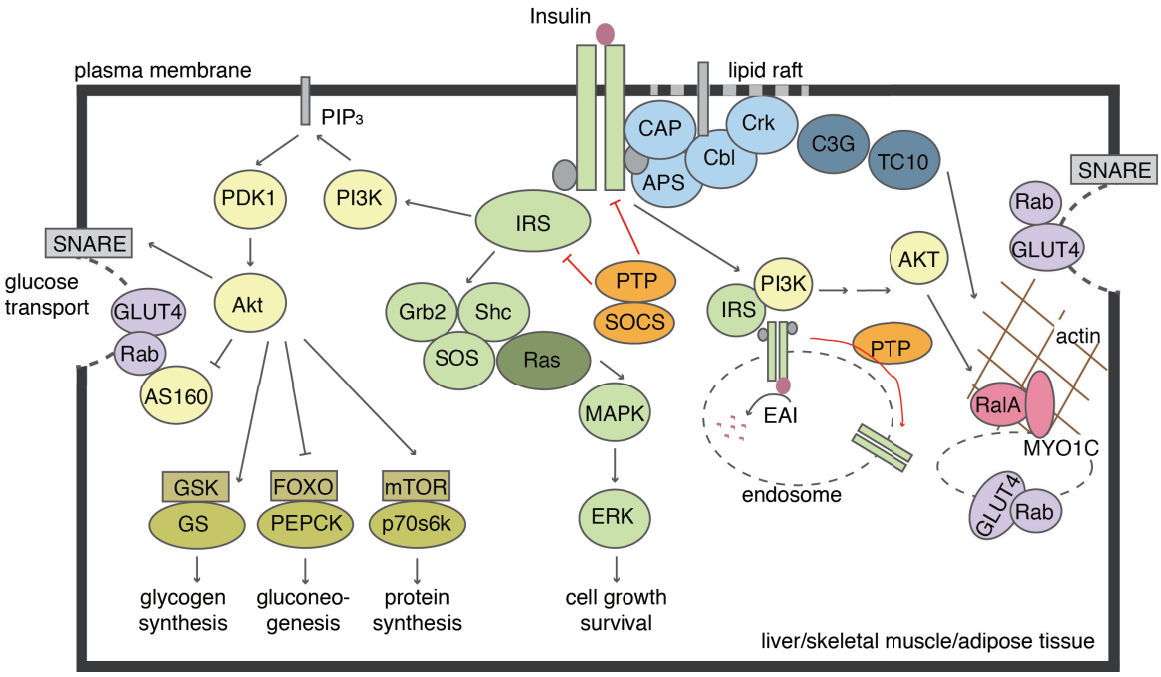
Insulin
plasma membrane
lipid raft
PIP3
PDK1
PI3K
IRS
CAP
Cbl
APS
Crk
C3G
TC10
SNARE
Rab
GLUT4
SNARE
glucose
transport
GLUT4
Rab
AS160
Akt
Grb2
Shc
SOS
Ras
PTP
SOCS
MAPK
ERK
PI3K
IRS
AKT
PTP
EAI
endosome
actin
RalA
MYO1C
GLUT4
Rab
GSK
GS
FOXO
PEPCK
mTOR
p70s6k
glycogen
synthesis
gluconeo-
genesis
protein
synthesis
cell growth
survival
liver/skeletal muscle/adipose tissue

Fig. 1.3

Figure 1.4: The adipo-insular axis

The brain, pancreas, and adipose tissue cooperate to regulate glucose homeostasis through secretion of a variety of hormones. Insulin secreted from the pancreas stimulates glucose uptake, and lipid synthesis in adipose tissue. Adipose tissue synthesizes and secretes a variety of glucose-modulating proteins that exert positive and negative regulation on insulin secretion. Adiponectin, visfatin, and acute release of free fatty acids increase insulin secretion from pancreatic β-cells. Tumor necrosis factor-α (TNFα), interleukin-6 (IL6), and chronic overstimulation with free fatty acids impairs insulin secretion from the pancreas. Leptin released from adipose tissue can influence sympathetic and parasympathetic signals from the hypothalamus to the pancreas, which restrain insulin secretion and β-cell proliferation.

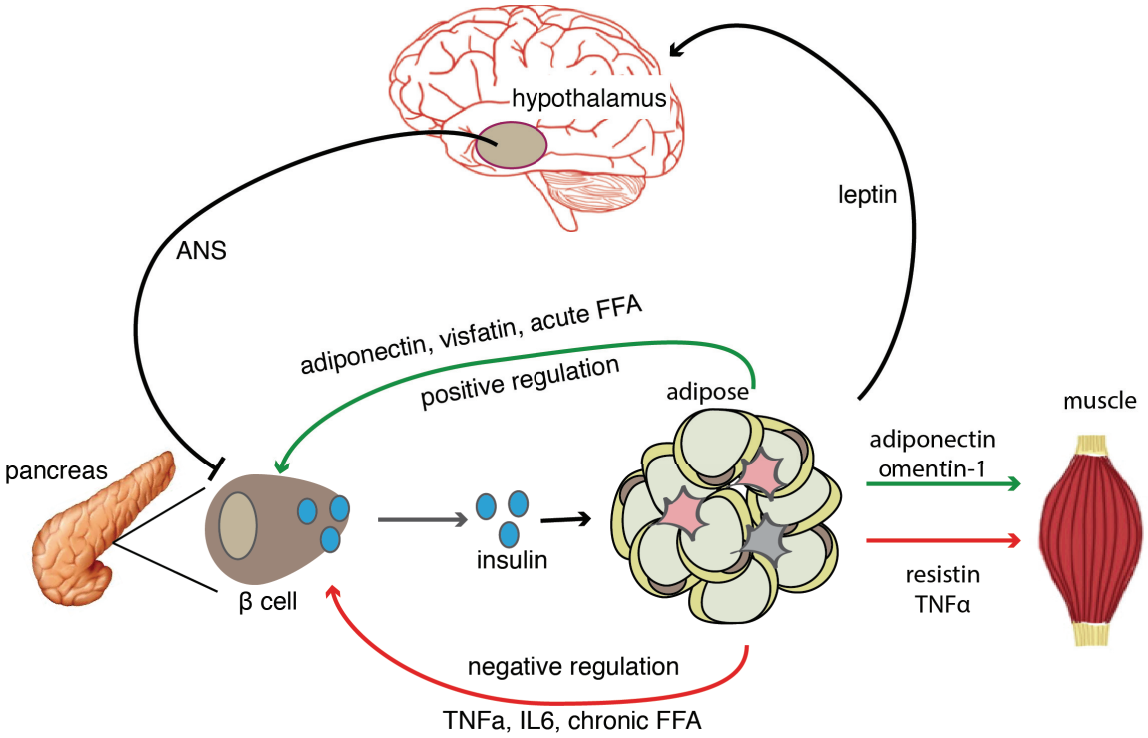
hypothalamus
leptin
ANS
adiponectin, visfatin, acute FFA
positive regulation
adipose
muscle
pancreas
adiponectin
omentin-1
insulin
resistin
TNFα
β cell
negative regulation
TNFa, IL6, chronic FFA

Fig. 1.4

Figure 1.5: Mechanisms of obesity-associated insulin resistance

An increase in free fatty acids, and the pro-inflammatory cytokines and adipokines TNFα, IL-6, RBP4, and leptin during obesity results in insulin receptor and IRS protein inhibition through PTP, SOCS, ERK, and JNK signal activation as well as induction of cytokine mRNA expression by the transcription factor NFκB. Moreover, these inflammatory mediators decrease GLUT4 translocation or mRNA expression and increase oxidative and ER stress. A loss of the insulin sensitizing adipokines adiponectin and omentin-1 in obesity results in a loss of protective AKT signaling and support of glucose transport and pro-growth gene expression. **Abbreviations**: suppressor of cytokine signaling: SOCS, janus kinase: JNK, reactive oxygen species: ROS, endoplasmic reticulum: ER, tumor necrosis factor alpha: TNFα, interleukin-6:IL-6, retinol-binding protein 4: RBP4, free fatty acids: FFA. See Fig. 1.3 for insulin signaling abbreviations.

Fig. 1.5

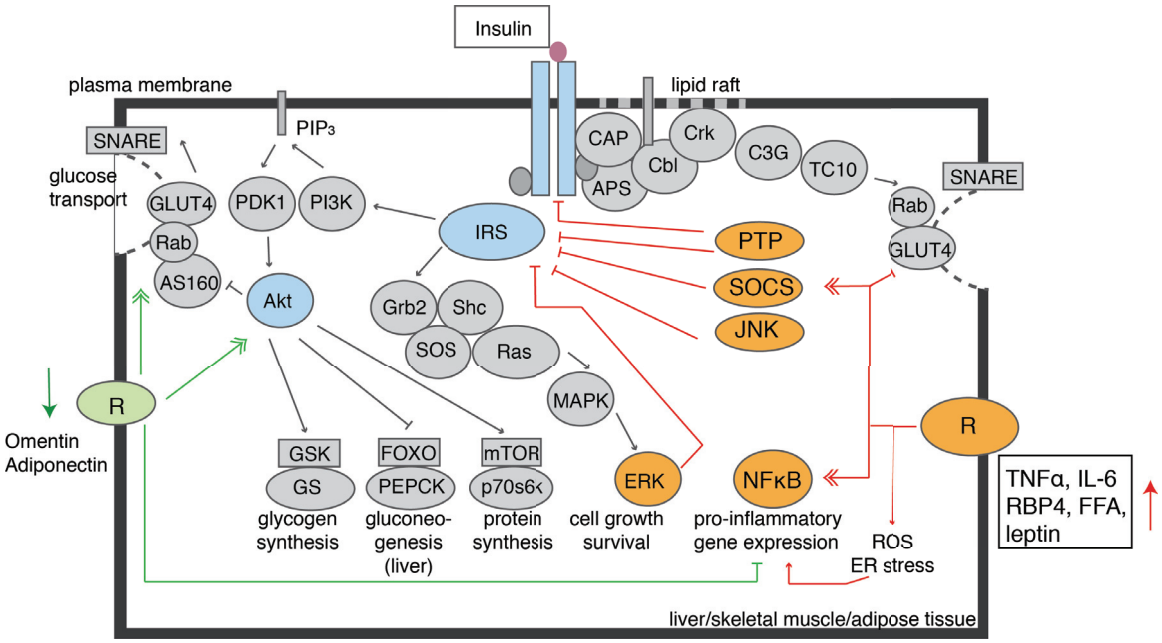
Insulin
plasma membrane
lipid raft
SNARE
PIP3
glucose transport
GLUT4
PDK1
PI3K
CAP
Crk
Cbl
APS
C3G
TC10
SNARE
Rab
GLUT4
IRS
PTP
SOCS
JNK
Rab
AS160
Akt
Grb2
Shc
SOS
Ras
MAPK
R
Omentin
Adiponectin
GSK
GS
glycogen synthesis
FOXO
PEPCK
gluconeo-genesis (liver)
mTOR
p70s6k
protein synthesis
ERK
cell growth survival
NFκB
pro-inflammatory gene expression
ROS
ER stress
R
TNFα, IL-6
RBP4, FFA,
leptin
liver/skeletal muscle/adipose tissue

Fig. 1.5

Figure 1.6: Adipokines modulate β-cell function and insulin secretion

β-cells express numerous adipokine receptors whose signaling profiles exhibit tremendous overlap with those regulating β-cell function, survival, and insulin secretion. Chronic overstimulation with free fatty acids results in oxidative stress and ROS generation, which decrease the intracellular ATP: ADP ratio. TNFα activation of JNK and NFκB signaling decreases insulin mRNA expression and increases the expression of pro-inflammatory cytokines. Resistin inhibits insulin receptor activation. DPP-4 degrades GLP1, thereby reducing the stimulatory effects of GLP1 on insulin secretion. Apelin inhibits GLUT4 vesicle translocation and modulates β-cell apoptosis, proliferation and insulin production through activation of multiple intracellular messengers including AMPK. Adiponectin activation of AMPK supports β-cell proliferation and insulin gene expression. Visfatin supports insulin receptor phosphorylation. High leptin levels promote insulin release, while low levels inhibit insulin production. **Abbreviations**: AMP-activated protein kinase: AMPK, RAC-alpha serine/threonine-protein kinase: AKT, adenosine triphosphate: ATP, adenosine diphosphate: ADP, dipeptidyl peptidase-4: DPP-4, extracellular-regulated kinase: ERK, free fatty acids: FFA, glucagon-like peptide-1: GLP1, janus kinase: JNK, nuclear factor κ B protein: NFκB, phosphoinositide-3-kinase: PI3K, pancreatic and duodenal homeobox 1: PDX1, protein kinase A: PKA, reactive oxygen species: ROS.

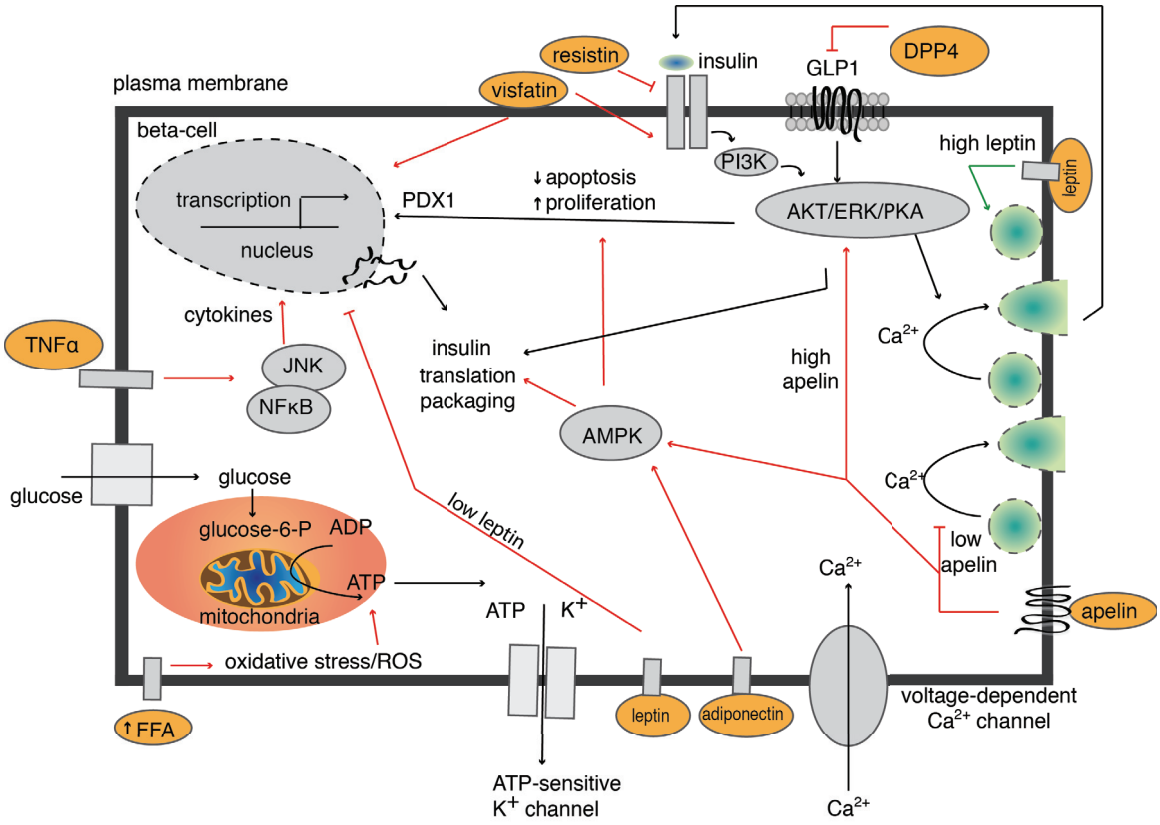
plasma membrane
beta-cell
resistin
visfatin
insulin
GLP1
DPP4
PI3K
high leptin
leptin
transcription
nucleus
PDX1
↓apoptosis
↑proliferation
AKT/ERK/PKA
cytokines
TNFα
JNK
NFκB
insulin
translation
packaging
high
apelin
Ca2+
AMPK
glucose
glucose
glucose-6-P
ADP
ATP
mitochondria
low leptin
low
apelin
apelin
oxidative stress/ROS
↑FFA
ATP
K+
leptin
adiponectin
voltage-dependent
Ca2+ channel
ATP-sensitive
K+ channel

Fig. 1.6

Chapter 2: Towards an Integrative Approach to Understanding the Role of Chemerin in Human Health and Disease

2.1 Rationale and Objectives

Chemerin is a secreted protein that has been identified as a novel adipokine with autocrine/paracrine roles in adipose development and function as well as endocrine roles in metabolism, glucose homeostasis, and immunity. Following prochemerin secretion, protease-mediated generation of chemerin isoforms with a range of biological activities is a key regulatory mechanism controlling local, context-specific chemerin bioactivity. Together, experimental and clinical data suggest that localized and/or circulating chemerin expression and activation are elevated in numerous metabolic and inflammatory diseases including psoriasis, obesity, T2D, metabolic syndrome, and cardiovascular disease. These elevations are positively correlated with deleterious changes in glucose, lipid, and cytokine homeostasis and may serve as a link between obesity, inflammation, and other metabolic disorders. This chapter highlights the current state of knowledge regarding chemerin expression, processing, biological function, and relevance to human disease. Furthermore, it discusses study variability, deficiencies in current measurement, and questions concerning chemerin function in disease, with a special emphasis on techniques and tools used to properly assess chemerin biology. An integration of basic and clinical research is key to understanding how chemerin influences disease pathobiology, and whether modulation of chemerin levels and/or activity may serve as a potential method to prevent and treat metabolic diseases.

The figures and text presented in this chapter are reproduced with copyright permission (Appendix I) from the review article (154). This review article was written in equal partnership with Helen Dranse. For clarity of the thesis minor editorial changes were made from the original: some text was omitted, some was included in chapter 6.

2.2 Regulation of Chemerin Activity

Chemerin, also known as tazarotene-induced gene 2, or retinoic acid receptor responder 2, is structurally related to the cathelicidin/cystatin family of proteins and was originally identified as a gene up-regulated in psoriatic skin by the synthetic retinoid tazarotene (155). Chemerin signaling is tightly regulated through a number of mechanisms including expression, secretion, processing and signaling events. The precise coordination of these regulatory mechanisms is essential for establishing chemerin levels, localization and, ultimately, activity.

2.2.1 Expression and Secretion

Chemerin is expressed at the highest levels in placenta, liver, and WAT, and to a lesser extent in many other tissues such as lung, BAT, heart, ovary, kidney, skeletal muscle and pancreas (4,156-158). Within WAT, chemerin expression is enriched in adipocytes as compared to the stromal vascular fraction (SVF) (4,156) and, in addition to the liver, WAT is believed to be the main source of circulating chemerin. Similar to other adipokines such as leptin and adiponectin, serum levels of chemerin in mice oscillate in a diurnal-like fashion with peak and trough periods, corresponding to the day–night cycle (159); however, in humans these oscillations may be minimal (160). In healthy, lean populations, the concentration of total circulating chemerin ranges from 90 to 200 ng/mL in both serum and plasma (161-163). In general, females and older adults have higher total circulating chemerin than males and younger adults, respectively (156,161,164,165), although not all studies have reported these trends (166-169). Chemerin is initially synthesized as preprochemerin, a 163 amino acid protein with an N-terminal signal sequence (20 amino acids) that is cleaved prior to secretion of the inactive 18-kDa precursor, prochemerin (Chem-163) (170). The majority of circulating chemerin is believed to exist in the relatively inactive prochemerin form and requires proteolytic processing to bioactive chemerin isoforms in order to exert local biological actions.

2.2.2 Processing

Following secretion, prochemerin can be processed by a variety of extracellular proteases of the coagulation, fibrinolytic and inflammatory cascades, which are differentially expressed in a wide range of tissues and cell populations. These enzymes, through cleavage at distinct sites in the C-terminus, convert prochemerin into a number of bioactive isoforms that vary in length and biological activity (Table 2.1). For example, the removal of six amino acids results in Chem-157, which exhibits the highest activity (approximately 100-fold higher than prochemerin (170)), while Chem-156 has slightly less activity, Chem-155 and -158 low activity, and Chem-152 and -154 are relatively inactive (170-175). Importantly, some proteases are able to process prochemerin at more than one cleavage site (e.g. elastase, tryptase (174)) and various chemerin isoforms may also be further processed. For example, carboxypeptidases B and N process relatively low active chemerin isoforms into more active forms (171), while other proteases such as proteinase 3 (PR3) or mast cell chymase are able to process pro- or bioactive chemerin, respectively, into relatively inactive forms (176). This multi-step processing of chemerin provides a mechanism for local and systemic chemerin activation as well as inactivation, both directly and by limiting available precursors. Furthermore, Chem-155, which has low bioactivity, might act as a weak antagonist in the presence of highly active chemerin isoforms (173), suggesting that the ratio between active and inactive isoforms is an important determinant of chemerin bioactivity. It is important to note that the majority of studies report chemerin bioactivity relative to one particular function or signaling pathway, and thus it remains unclear whether individual chemerin isoforms have differential bioactivity on multiple pathways or functions.

The bulk of knowledge regarding chemerin processing and bioactivity derives from *ex vivo* studies; however, several endogenous chemerin isoforms have also been isolated from human samples. Differential patterns of chemerin isoform production in human blood (Chem-155, 157, 158), ascites (Chem-157), synovial fluid (Chem-158), cerebrospinal fluid (Chem-158) and hemofiltrate (Chem- 154) indicate that complex prochemerin processing occurs *in vivo* (170,172-175) (Table 2.2). At present, all proteases that modulate chemerin activity do so through processing of the C-terminus,

illustrating the importance of this region of the protein for chemerin bioactivity. Currently, no information is available regarding the effect of this C-terminal processing on the tertiary/quaternary structure of chemerin or the functional relevance of particular amino acids or amino acid motifs within the remainder of the protein. Thus, further characterization of chemerin isoform generation is necessary in order to fully understand local chemerin bioactivity and the biological functions of chemerin.

2.2.3 Receptors and Signaling

Chemerin was initially described as the natural ligand and chemotactic signal for cells expressing the GPCR CMKLR1 (170,172). Chemerin has also been shown to bind and activate another GPCR, GPR1, which is closely structurally related to CMKLR1. GPR1 has an established role in nutrient sensing in yeast (177,178); however, little is known regarding the function of this receptor in mammals. While chemerin has been shown to bind and activate GPR1 with similar affinity to CMKLR1 (179), essentially nothing is known regarding the signal transduction pathways coupled to GPR1, and to date, all of the known biological (signaling) activities of chemerin have been ascribed to activation of CMKLR1. Thus, an important area of future research is to delineate the contribution of CMKLR1 and GPR1 in mediating the biological actions of chemerin and whether the receptors have complementary and/or distinct roles. In addition to CMKLR1 and GPR1, chemerin is a ligand for a third receptor, chemokine (CC motif) receptor-like 2 (CCRL2), which has phylogenetic homology with members of the CC chemokine receptor subfamily. CCRL2-bound chemerin is not internalized and it is not believed to be a signaling receptor (180). Rather, CCRL2 is believed to focus chemerin localization *in vivo,* increasing local chemerin concentrations, presenting it to nearby cells and thereby contributing to CMKLR1 and potentially GPR1-mediated processes (180,181). The three chemerin receptors have both overlapping and distinct tissue distributions. CMKLR1 is expressed at high levels in leukocyte populations, particularly macrophages and dendritic cells, adipose tissue, bone, lung, brain, heart and placenta (4,170). Similar to CMKLR1, GPR1 is expressed in adipose tissue; however, GPR1 is also expressed in the central nervous system (CNS) and skeletal muscle, and has limited expression in

leukocytes (182). CCRL2 is largely absent in adipose tissue, but is detected in lung, heart, spleen and leukocytes (180). This diversity in receptor localization may contribute to both common and independent signaling mechanisms for bio- active chemerin and consequent biological functions.

Very little is known regarding the signal transduction pathways coupled to CMKLR1 and GPR1 activation. Early studies demonstrated that CMKLR1 activation resulted in intracellular Ca^{2+} release and a reduction in cAMP accumulation. These effects were inhibited by pertussis toxin (PTX) treatment, demonstrating the involvement of a $G\alpha_{i/o}$ family member (170). Chemerin treatment of various cell types, including Chinese hamster ovary (CHO), primary human adipocytes and primary human chondrocytes, has been reported to promote ERK1/2 phosphorylation (4,170,183-186). Notably, some studies report that in human adipocytes and endothelial cells, chemerin treatment at low doses stimulates ERK1/2 phosphorylation, but not at higher doses (4,185), indicating that inhibition of signaling or desensitization may occur at higher concentrations. Chemerin has also been reported to influence several other signaling cascades including p38 MAPK phosphorylation, AKT phosphorylation, and PI3K in mouse and human cells (183-185,187,188). Further elucidation of the signaling pathways associated with chemerin activity, including verification by independent groups, will require targeted focus on chemerin receptors. Specifically, future studies should examine overlapping and differential CMKLR1/GPR1 signaling pathways, unique pathway activation by chemerin isoforms, and the relative contribution of these signaling mechanisms to specific biological actions elicited by chemerin.

2.3 Role of Chemerin in Inflammation

2.3.1 Systemic vs. Local Elevations in Chemerin Levels and Activity

Circulating chemerin levels are elevated in numerous diseases associated with chronic inflammation. For example, serum chemerin levels are significantly elevated in patients with Crohn's disease, ulcerative colitis (167), chronic kidney disease

(168,189,190), chronic pancreatitis (191), preeclampsia (192), polycystic ovary syndrome (160) and liver disease (193-196). This increase in circulating chemerin levels is positively correlated with circulating inflammatory markers such as CRP (164,197-199), IL-6 and TNFα, as well as the pro-inflammatory adipokines leptin and resistin (164,167,189,194,198). Unfortunately, the correlative nature of these studies offers little insight into the mechanisms or impact of these associations as the origin, bioactivity, and/or site of action of the circulating chemerin remains unclear. However, consistent with the observed elevation in circulating chemerin, *in vitro* studies demonstrate enhanced secretion of pro-inflammatory cytokines such as IL-6, IL-8, TNFα, CCL2 and IL-1β (183,184) with chemerin treatment in cultured human chondrocytes and synoviocytes. Likewise, TNFα treatment increases chemerin secretion in cultured human intestinal epithelial cells, murine adipocytes and murine serum (159,200,201). As such, chemerin produced in response to inflammation may actively contribute to the inflammatory response by altering the expression and secretion of inflammatory mediators, potentially creating a positive feedback loop for sustained chronic inflammation.

Consistent with a role for chemerin in the modulation of local inflammatory responses, chemerin levels are often elevated in diseased tissues in both mice and humans, such as psoriasis, cancer, arthritis, lupus and multiple sclerosis (170,180,201-209). It is important to note that increased chemerin expression and bioactivation is often unique to the localized region of inflamed tissue and may or may not correspond to a similar change in circulating chemerin levels. For example, human studies show that in the inflammatory milieu of rheumatoid arthritis, osteoarthritis and psoriatic arthritis, localized synovial fluid chemerin concentrations are elevated up to 2-fold (166,170,175,184,210). However, despite the observed increase in synovial fluid chemerin with osteoarthritis severity, serum chemerin levels remain unchanged (166). Moreover, within diseased joints the ratio of cleaved to total chemerin is dramatically increased and is often associated with unique isoform profiles that differ considerably from the distribution of isoforms in circulation (175). Consistent with localized chemerin isoform production at sites of active tissue injury or inflammation, neutrophil release of chemerin-activating proteases, blood coagulation and human pathogen-derived proteases

may contribute to the increased chemerin activity (174,211,212). However, the tissue source or cell type that contributes to the increase in chemerin levels is largely unknown. Taken together, these studies demonstrate that total circulating chemerin levels may not necessarily reflect the extent of changes occurring in the disease state, whereas the localized expression and activation of chemerin is an important determinant of the influence of chemerin signaling on inflammatory responses.

2.3.2 Chemerin, Pro- or Anti-Inflammatory?

In addition to increasing the expression and secretion of pro-inflammatory mediators, elevation of chemerin levels within inflamed or diseased tissues may contribute directly to inflammation through the modulation of immune cell recruitment. Chemerin has been shown to promote chemotaxis of CMKLR1-expressing leukocyte populations such as human macrophages, immature dendritic cells and natural killer cells to localized sites of inflammation, tissue damage or bleeding, suggesting a pro-inflammatory role (170,180,201-209). In addition, chemerin promotes the adhesion of murine macrophages to extracellular matrix proteins and endothelial cells, supporting a role in both the recruitment and retention of leukocytes at sites of infiltration (187). Animal models have demonstrated a requirement for chemerin signaling in the development of optimal tissue swelling and leukocyte infiltration in various mouse inflammation models such as IgE-mediated anaphylaxis and lipopolysaccharide (LPS)-induced pulmonary inflammation (180,205,207). Similarly, CNS inflammation is reduced in the absence of CMKLR1 expression in mouse experimental autoimmune encephalomyelitis, a model of autoimmune demyelinating disease (213). Thus, clinical and experimental data support a role for chemerin in the promotion of local inflammatory processes.

Conversely, some animal studies have demonstrated that inhibition of endogenous chemerin activity or a loss of CMKLR1 expression exacerbated inflammation and decreased leukocyte infiltration in various inflammation models such as peritoneal inflammation (214), LPS-induced lung injury (215) and acute viral pneumonia (216). Consistent with this, experimental data have shown that under certain experimental

conditions chemerin inhibits the production of pro-inflammatory mediators such as TNFα, IL-1β, IL-6, IL-12 and RANTES by classically activated murine macrophages *in vitro* (214). However, an independent group has failed to reproduce these anti-inflammatory effects (217), suggesting that other mechanisms might contribute to the anti-inflammatory effects of chemerin. These might include activity on non-leukocyte cells such as endothelial cells where chemerin stimulation has been shown to prevent monocyte adhesion (188). Alternatively, these effects might involve a group of anti-inflammatory mediators termed resolvins, including resolvin E1, which has been proposed to bind and activate CMKLR1 resulting in anti-inflammatory function (218). However, this finding has yet to be confirmed by independent groups and it has been shown that Resolvin E1 interacts with other receptors in addition to CMKLR1 (219). Thus, independent confirmation and future studies are necessary to elucidate the existence and/or mechanisms of anti-inflammatory chemerin signaling.

As current experimental data support both a pro- and anti-inflammatory role for chemerin, it is possible that the primary role of chemerin could be to indicate local conditions and rapidly establish the appropriate pro-inflammatory or suppressive response. Alternatively, different chemerin isoforms may play contrasting roles in various stages of inflammation, with serine proteases secreted early in the immune response (e.g. by neutrophils (212)) generating more active chemerin peptides, and later secreted cysteine proteases (e.g. by macrophages (214)) generating relatively inactive peptides, thus controlling the severity of inflammatory responses. Moreover, chemerin likely plays different roles depending on which populations of cells are activated in a particular condition. Consequently, while chemerin is known to be involved in immune cell recruitment and pathogenic processes, it remains to be determined if chemerin plays a more important role in inflammation initiation, maintenance or resolution, particularly with respect to whether increased chemerin activity is playing a protective or pathologic role in these inflammatory disease states.

2.4 Role of Chemerin in Metabolism

A fundamental shift in our understanding of chemerin biology in human

pathology occurred in 2007 when it was first reported that chemerin and CMKLR1 were expressed in WAT (4) and that circulating total chemerin levels were elevated in obese rodents and humans (4,156). Subsequently, *in vitro*, animal, and human studies have firmly established chemerin as an adipokine with significant relevance to obesity, metabolic disorders and cardiovascular disease.

2.4.1 Chemerin Levels Increase with Obesity

Fluctuations in circulating chemerin levels are closely related to the degree of overall adiposity. Serum chemerin concentrations are higher in obese animal models including leptin- (ob/ob) and leptin receptor (db/db)-deficient mice, obese sand rats and diet-induced obesity (156,159,220,221). In young and adult obese patients, elevated serum or plasma chemerin levels positively correlate with BMI, and measures of central adiposity such as waist to hip ratio, waist circumference (156,162,197,222) and visceral adipose tissue mass (198,223). In obese mice, dysregulation of chemerin levels is associated with an exaggerated oscillatory pattern with a greater frequency and magnitude of change between minimum and maximum serum chemerin levels (159). Consistent with a positive correlation between chemerin levels and adiposity measures, obese patients who underwent weight loss through either bariatric surgery (194,224) or exercise-nutrition-based methods exhibited a significant decline of circulating serum chemerin (162,225,226). Thus, although chemerin is also synthesized and secreted by the liver (162,225,226) as well as some immune and vascular cells, the obesity-associated increase in chemerin levels appears to be primarily adipose tissue derived. This is further supported by reports that adipose tissue explants from obese individuals secrete significantly more chemerin than those isolated from lean individuals, and this secretion correlates with increased BMI, waist-to-hip ratio and fat cell volume (162,225,226). Moreover, chemerin mRNA expression in adipose tissue increases significantly in obese patients, with expression in omental but not subcutaneous adipose tissue correlating positively with circulating concentrations (162). Taken together, both experimental and clinical studies indicate that WAT is a dynamic and modifiable source of chemerin. Importantly, WAT secretes various proteases such as cathepsin G and tryptase that are

able to generate bioactive chemerin isoforms (reviewed in (227)). Consistent with this, one study reported a correlation between the elevations of total and bioactive serum chemerin levels in a murine model of obesity (221). However, while total chemerin levels have been reported in numerous studies, levels of bioactive chemerin in humans and how these are affected by obesity remain to be examined.

In obesity, adipose tissue expansion involves a number of remodeling processes that include the enlargement of existing adipocytes (hypertrophy) and an increase in adipocyte number (hyperplasia). One mechanism that contributes to adipocyte hyperplasia is the increased proliferation and differentiation of preadipocytes into adipocytes. Chemerin signaling is essential during the early clonal expansion phase of adipocyte differentiation, where peroxisome proliferator-activated receptor gamma, the master regulator of adipogenesis, directly increases chemerin expression (221). Reduction of chemerin or CMKLR1 signaling through knockdown or neutralization approaches results in severe impairment of both 3T3-L1 and murine mesenchymal stem cell differentiation into mature adipocytes *in vitro* (4,181,228). Consistent with this, a loss of CMKLR1 *in vivo* is associated with reduced body mass and adiposity, and a resistance to diet-induced obesity (220), demonstrating that chemerin signaling promotes adipogenesis *in vivo.* Coincident with hyperplasia and hypertrophy, dilation of existing capillary networks and formation of new blood vessels via angiogenesis is required to increase blood supply to the expanding adipose tissue mass. As chemerin treatment has been shown to activate key angiogenic signaling cascades, to induce proliferation and migration of human endothelial cells, and to promote capillary tube formation (185,229), this adipokine may also support adipose tissue expansion by inducing angiogenesis and promoting vascularization. Moreover, CMKLR1 knockout (KO) mice eat less food, suggesting an endocrine role for adipose-derived chemerin to regulate energy intake and adipose tissue expansion (220).

Increased adiposity also induces chronic low-grade inflammation in adipose tissue, which is causally linked to obesity itself as well as many obesity-associated comorbidities (230). Increased secretion of adipokines such as TNFα and IL-6, and the recruitment and infiltration of macrophages, T cells, natural killer cells, and immature dendritic cells are characteristic of WAT inflammation. Consistent with the established

role of chemerin as a chemoattractant, adipocyte-derived chemerin acts as a paracrine regulator for the recruitment of CMKLR1-expressing cells to WAT, with a lower percentage of CD3+ T cells and a greater percentage of natural killer cells observed in WAT and a reduction in macrophage infiltration observed in CMKLR1 and chemerin KO mice, respectively (158,220). Moreover, the elevation in chemerin levels that occurs in moderate and severe obesity correlates with increased adipose tissue macrophage infiltration and expression of inflammatory mediators such as CRP, IL-6 and TNFα (164,167). These may rise as a consequence of increased expression of pro-inflammatory cytokines such as TNFα, LPS and IL-1β (159,231,232), which have an established role in up-regulating chemerin expression and bioactivation in adipocytes. As chemerin levels appear to be closely linked to adipose tissue mass and CRP expression, adipose tissue expansion and inflammation may likely serve as an early signal for increased chemerin production. Furthermore, as adipose tissue contains the proteases required for chemerin activation and inactivation, context-specific regulation of the ratio of active to total chemerin within adipose tissue likely contributes to the modulation of immune cell recruitment.

Together these studies suggest that chemerin expression is dynamic and is substantially elevated in obese individuals. This dysregulation is closely associated with changes in central adiposity and adipose tissue inflammation lending support to the potential role of chemerin as a molecular link between obesity, obesity-associated inflammation, and the development of comorbidities. However, the nature and impact of this relationship remains to be elucidated as it is unclear which factors drive these substantial increases, which chemerin isoforms are increased in obese adipose tissue, and what effect chronically elevated chemerin has on adipose tissue and systemic metabolism.

2.4.2 Chemerin is Associated With Obesity Comorbidities: Metabolic syndrome

Among the most prevalent obesity comorbidities that place individuals at an increased risk for cardiovascular disease and T2D is the metabolic syndrome, which is characterized by a cluster of metabolic disturbances including impaired glucose

homeostasis, high blood pressure and central adiposity. One study has suggested that elevated circulating chemerin is a significant risk factor for metabolic syndrome (233). Consistent with this, levels of circulating and adipose-expressed chemerin are significantly elevated in individuals with metabolic syndrome when compared to healthy controls (163,234,235), are predictive for metabolic syndrome severity (165), and are often positively correlated with elevations in many individual metabolic syndrome markers, including circulating triglycerides, low-density lipoprotein (LDL) cholesterol, waist circumference, insulin resistance, fasting insulin/glucose and systolic as well as diastolic blood pressure (156,161,165,169,222,233,235,236). Conversely, with exercise-induced weight loss, decreased serum chemerin levels correlate with an improvement in metabolic syndrome markers including visceral fat volume, insulin resistance, fasting glucose and waist circumference (226). It will be interesting through future studies to determine (i) the regulatory mechanisms supporting the temporal relationship between chemerin and metabolic syndrome development; (ii) how these changes relate to inflammation and adipose tissue mass in metabolic syndrome; and (iii) whether chemerin acts as a molecular link between the presence of these metabolic perturbations and increased risk for cardiovascular disease and T2D.

2.4.3 Chemerin is Associated With Obesity Comorbidities: Glucose Homeostasis and T2D

T2D is characterized by deleterious elevations in fasting glucose (impaired fasting glucose) as well as reduced insulin-stimulated glucose uptake (impaired glucose tolerance), which derive from sustained hepatic, muscle and adipose insensitivity to the actions of insulin (insulin resistance). On a regular chow diet, CMKLR1 (220) and chemerin (158) KO mice exhibit similar fasting glucose levels as wild-type counterparts. However, when fed a high-fat diet, CMKLR1 KO mice exhibit less adiposity and weight gain and are protected from the elevation in fasting glucose characteristic of diabetes development (220). Despite exhibiting normal basal glucose regulation, both lean and obese CMKLR1 and chemerin KO mice have impaired glucose tolerance. Paradoxically, acute treatment of obese db/db mice with recombinant chemerin (221), chronic

overexpression of chemerin in low- density lipoprotein receptor knockout (LDLRKO) mice (237), and the loss of chemerin signaling in CMKLR1 (220) or chemerin (158) KO mice are all associated with the induction or exacerbation of impaired glucose tolerance. In contrast, chronic overexpression of chemerin in mice on a normal genetic background increases glucose tolerance (158). As such, while there is ample evidence that chemerin influences glucose tolerance in mice, the precise physiological/pathophysiological role is at present unclear.

Numerous factors contribute to successful regulation of glucose tolerance, notably GSIS, and insulin-stimulated glucose uptake in peripheral tissues (insulin sensitivity). Disruption of this regulation has been investigated as a potential source for chemerin-mediated impaired glucose tolerance. Consistent with the observed impaired glucose tolerance, pancreatic β-cells isolated from chemerin KO mice have impaired insulin secretion, as does the pancreatic Min6 cell line following chemerin knockdown (158). Notably, loss of either chemerin or CMKLR1 in lean mice, and chemerin injection in obese db/db mice *in vivo* results in impaired GSIS (158,220). In contrast, circulating insulin levels are comparable in LDLRKO mice with and without chemerin over-expression (237). Together, these data suggest that both reduction and augmentation of chemerin signaling may cause impaired glucose tolerance, at least in part, through impaired GSIS, supporting a potential role for chemerin signaling in regulation of pancreatic β-cell function and insulin secretion (158,220).

Chemerin may play a direct role in insulin sensitivity and glucose uptake, although investigations to this effect have also provided conflicting results. For example, studies have shown both increased (238) and decreased (232) insulin- stimulated glucose uptake in 3T3-L1 adipocytes following chemerin treatment. Of note, these studies were fundamentally different in both the dose and duration of chemerin treatment, with shorter, low nanomolar chemerin (6 nM) (238) resulting in increased glucose uptake, and longer, high-dose chemerin contributing to impaired insulin-stimulated glucose uptake (232). This suggests that the dose and duration of chemerin treatment potentially contribute to the nature of chemerin activity, and further studies with equivalent methodologies will help to clarify the role of chemerin in glucose uptake. Chemerin action may also exhibit tissue selectivity with respect to glucose homeostasis. For example, decreased total tissue

and liver glucose uptake was observed with acute chemerin treatment *in vivo* (221) and reduced total tissue, adipose and skeletal muscle glucose uptake was observed in obese CMKLR1-null mice (220). In euglycemic hyperinsulinaemic clamp studies, chemerin KO mice show normal whole-body insulin sensitivity. This result is similar to the observation that neither lean nor obese CMKLR1-null mice exhibit any impairment in insulin sensitivity tests (220). While net insulin sensitivity is spared, chemerin KO mice exhibit impaired insulin signaling in fat tissue and enhanced insulin signaling in the liver (158). Experiments with primary human or C2C12 skeletal muscle cells, and chemerin KO mice, are consistent with a role for chemerin signaling in inducing insulin resistance and negatively modulating glucose uptake in skeletal muscle (157,158,220,239). Interestingly, no changes in glucose uptake are seen in response to chemerin injection or loss of CMKLR1 in normoglycaemic, lean mice (221). Together, these experiments indicate that the role of chemerin signaling in glucose uptake may be modifiable, depending on the duration of chemerin action, the tissue examined, and the nutritional and pathological status of the model. Thus, *in vitro* and *in vivo* studies demonstrate that chemerin plays a role in insulin and glucose homeostasis, likely as a modulatory factor for insulin secretion and sensitivity, although further studies are required to fully elucidate the mechanisms and clarify contradictory results.

Given the associations between chemerin, obesity, inflammation, and glucose homeostasis established with tissue culture and animal models, numerous studies have examined these relationships in humans. A collection of these studies report that elevated circulating and adipose tissue-expressed chemerin is significantly exacerbated in obese individuals when insulin resistance (221) or T2D is also present (161,162,194). This is often independent of patient weight status (161,162,167,199), although a subset of smaller studies have reported no increase in chemerin levels in T2D (167,193,194). However, consistent with a role for chemerin in glucose homeostasis, serum chemerin concentration is strongly associated with insulin sensitivity. For example, in normoglycaemic, insulin-sensitive patients, impaired fasting glucose, impaired glucose tolerance or T2D individuals, serum or plasma chemerin is independently associated with fasting glucose and serum insulin (161) as well as homeostasis model assessment of insulin resistance and deleterious declines in hyperinsulinaemic euglycemic clamp-

derived insulin sensitivity (199,240). Paradoxically, despite having reduced adiposity, CMKLR1 KO mice exhibit signs of impaired glucose homeostasis (197), suggesting that normal chemerin signaling is required to support glucose regulation. Thus, an increase in circulating chemerin levels during insulin resistance might act as a compensatory mechanism to restore glucose handling. Interestingly, unlike patients with impaired glucose tolerance and T2D, serum chemerin levels were unchanged in patients with only impaired fasting glucose (199). Because impaired glucose tolerance and T2D are indicative of insulin resistance in peripheral skeletal muscle and adipose tissue, but impaired fasting glucose typically indicates liver-derived insulin resistance, these results, together with the tissue- specific insulin resistance observed in mice, suggest that changes in chemerin levels may be most relevant to glucose handling in adipose tissue and skeletal muscle, rather than in the liver.

Consistent with a role for chemerin in insulin sensitivity, decreased chemerin concentrations subsequent to surgical or diet-induced weight loss in obese patients were significantly correlated with reduced levels of inflammatory markers as well as improved insulin resistance (162). In the same study, after 4 weeks of exercise training and before any appreciable changes in body weight, improvements in insulin sensitivity and circulating CRP in impaired glucose tolerance or T2D individuals were observed, coincident with a decrease in circulating chemerin levels. This indicates that chemerin and inflammation may be associated independently of BMI. Given the established relationship between dysregulation of adipokine secretion, inflammation and insulin resistance (for review see (241)), these studies support a role for chemerin in the deleterious changes in inflammation, glucose handling and insulin sensitivity that occur in diabetes and obesity. It is unclear whether chemerin is altered in diabetes in a causative or consequential manner as results from adipose tissue explants (160) and human skeletal muscle cell cultures (239) suggest that increases in chemerin secretion might be both driven by and directly contribute to deleterious alterations in circulating insulin levels.

2.4.4 Chemerin is Associated With Obesity Comorbidities: Cardiovascular Disease

The metabolic perturbations that occur with obesity and metabolic syndrome

contribute to cardiovascular disease development in approximately one-third of cases (242). Given the alterations in chemerin levels in both of these conditions, a limited number of studies have investigated whether chemerin plays a role in cardiovascular pathology. Preliminary work suggests that chemerin may induce expression of vascular pathology markers such as E-selectin and ICAM in children and adults, and may also contribute to arterial wall defects (188,198,243). Consistent with this, individuals diagnosed with coronary artery disease (CAD) have significantly elevated circulating chemerin levels; however, it is unclear whether the magnitude of this elevation predicts CAD severity (235,236,244) or atherosclerotic plaque morphology (164). Conversely, a smaller study of Chinese patients failed to show any elevation in circulating chemerin with CAD, although chemerin and TNFα expression, which were elevated in epicardial adipose tissue, did correlate with the Gensini score of cardiovascular disease severity independent of BMI, waist circumference and glucose (245). A study examining the differential expression of multiple adipokines in human peri-aortic and peri-coronary adipose tissue reported that chemerin expression in both of these adipose depots is significantly elevated with age and highly correlated with atherosclerosis in their respective vessels (246). Moreover, chemerin is expressed in both the foam cells and vascular smooth muscle cells of these atherosclerotic lesions and correlates with overall disease burden. Not only does this support a role for chemerin in the pathogenesis of atherosclerosis and provide a potential mechanistic link between aging and increased atherosclerosis risk, but it lends support to the importance of localized autocrine/ paracrine functions of chemerin within the heart.

Hyperlipidaemia, generally classified as elevated circulating triglycerides and an increased LDL/HDL (high-density lipoprotein) cholesterol ratio, occurs in obesity in part as a consequence of altered lipolysis and is associated with an increased risk for the development of cardiovascular disease. The majority of studies report significant positive correlations with chemerin and circulating triglycerides, LDL cholesterol and blood pressure (156,160,162,163,165,222,233,235,244,247), and negative correlations with HDL cholesterol (194,233,247,248). Given the number of human studies reporting associations between elevated chemerin and altered lipid profiles, surprisingly few studies comment on or seek to investigate a relationship between chemerin and

hyperlipidaemia. While one study has demonstrated that differentiation of 3T3-L1 preadipocytes in the presence of free fatty acids increased chemerin expression (231), very few studies have directly examined the effect of chemerin signaling on the regulation of lipolysis. As with glucose uptake, conflicting results have arisen. Some studies with 3T3-L1 and murine primary adipocytes support a role for chemerin in stimulating lipolysis (4,186) while another reported decreased basal lipolysis following chemerin treatment (249). Notably, in the latter study, effects were blunted in CMKLR1 KO mice, indicating that CMKLR1 does affect lipolysis in some manner. To date, only one study has examined the influence of chemerin on lipid homeostasis *in vivo,* with no change in triglyceride and cholesterol levels following chronic overexpression of chemerin in LDLRKO mice (237). Thus, future studies are necessary to elucidate the involvement of chemerin signaling in lipid homeostasis. Considering the well-established relationship between chemerin, obesity, inflammation and metabolic syndrome, it is not unreasonable to postulate that chemerin will also show associations with cardiovascular risk factors in large, well-controlled clinical studies that examine both circulating and localized chemerin expression.

2.5 Contextualizing Chemerin Function in Health and Disease

Taken together, persistent elevations in total circulating chemerin levels with obesity and positive correlations with an abundance of metabolic and inflammatory perturbations unify the majority of human studies conducted to date. BMI, insulin sensitivity and CRP levels are the most predictive of changes in circulating chemerin levels during weight loss, and likewise insulin sensitivity and circulating CRP predict increased chemerin levels in obesity and diabetes independent of BMI (162). This suggests that any disease associated with inflammation, insulin resistance and/or increased adipose tissue mass as a substantial component of the pathology will also display elevations in circulating or localized chemerin levels. Collectively, human and animal studies suggest dynamic and context- specific regulation of chemerin activity and/or function, dependent on numerous factors, including: location, duration and severity of disease, interactions with other adipokines, genetic and environmental

variation, and the signaling events that occur in response to the activation of chemerin receptors on responding cells. Considering the reported pro- and anti-inflammatory functions, as well as enhancement and inhibition of glucose uptake, chemerin may act as both a pathogenic and protective adipokine depending upon the physiologic context. Similar to most cytokines, chemerin activity appears highly regulated and likely plays essential roles in normal healthy adipose and immune function. In obesity, the development of a chronic state of elevated chemerin levels in the expanding adipose mass and systemic circulation may interact with multiple cell types to serve several functions, including (i) recruitment of CMKLR1-expressing immune cells to promote inflammation; (ii) alteration of adipokine/cytokine secretion from adipocytes and immune cells; (iii) activation of vascular endothelial cells for the promotion of angiogenesis; (iv) alteration of adipose tissue structure and function; and (v) modulation of systemic glucose and lipid handling. Early chemerin elevations are likely adaptive during initial adipose tissue expansion, while chronically elevated chemerin levels may reach inappropriate levels and result in pathologic signaling. This may lead to inappropriate immune responses and disrupted glucose homeostasis. Conversely, similar to leptin, persistently elevated chemerin levels may result in desensitization and a loss of any beneficial chemerin activity; however, chemerin resistance has yet to be directly examined in experimental and clinical studies. Therapeutics targeted to restore this disruption may therefore be of interest for obesity and diabetes management.

2.6 Integrative Methods to Study Chemerin in Human Disease

With the complexity of chemerin regulation in mind, it is not surprising that considerable variation exists in reported chemerin concentrations in healthy populations, ranging from 3 to 250 ng/mL (160,243), and in the magnitude of pathology-related elevations (Table 2.3). Inconsistency also exists in the detection of significant changes and correlations between chemerin and age, gender, BMI, insulin resistance, blood pressure, circulating lipids, T2D and metabolic syndrome. It is important to note that these studies differ in several respects, including (i) chemerin dosage and duration of treatment in cell and animal models; (ii) chemerin sampling location, time and detection

methodology; (iii) genetic, cultural and environmental population variance (161); and (iv) health-related confounders such as disease status, duration and concomitant medication. These factors are frequently omitted and likely have a significant impact on circulating chemerin levels and activity. For example, few studies have investigated the potential impact of medications with established effects on chemerin expression and activation, such as metformin, insulin, rosiglitazone and angiotensin-converting enzyme inhibitors (160,190,228,250,251). In addition, considering the involvement of chemerin in metabolism and inflammation, drugs that reduce levels of circulating lipids (statins, fibrates), glucose (biguanides, insulin) and inflammatory mediators such as CRP (glitazones, non-steroidal anti-inflammatory drugs), will be an important consideration as we move forward into more integrative chemerin studies. Moreover, despite the evidence that supports a relationship between chemerin and inflammation, in particular the importance of enzymes released in the inflammatory cascade that modulate chemerin bioactivity, most studies measure total circulating chemerin and give no consideration to actual bioactive chemerin levels. Furthermore, few studies include inflammatory markers such as CRP and/or IL-6 in multivariate analysis. Considerations of chemerin biology of this nature are indispensable in the investigation to determine a precise role for chemerin in disease pathogenesis and pathobiology.

While many reports recognize that standard enzyme- linked immunosorbent assay (ELISA) methodologies for detecting chemerin fail to differentiate between active and inactive isoforms, only a few have taken measures to address this deficiency. Multiple tools exist for assessing apparent chemerin activity in biological fluids, including (i) *in vitro* cell migration assays using dendritic cells (174) and CMKLR1-expressing pre-B lymphocytes L1.2 (4,171,252); (ii) aequorin-based Ca^{2+} activation of CMKLR1 or GPR1-expressing CHO cells (170); and (iii) the CMKLR1- or GPR1-Tango assay (159,179). These *in vitro* cell-based systems allow screening of small volumes (1–10 μL) of biological fluids such as serum, plasma, and ascites fluid, and are amenable to high-throughput screening of multiple samples. Standard, commercially available ELISAs can be used to determine total levels of chemerin, and recently, a new and very promising ELISA system has been developed, which utilizes novel isoform-specific chemerin antibodies to quantify levels of specific chemerin isoforms (175). Although only used for

the detection of fluid-based isoforms to date, it is conceivable that similar approaches could be adopted for tissue biopsies or explants, permitting measurement of chemerin isoform expression in combination with total chemerin and chemerin receptor expression. In combination, these measurements (outlined in Fig.2.1) will allow detection of dynamic fluctuations in active and total chemerin levels, generation of active to inactive chemerin ratios, and will provide invaluable insight into the temporal and spatial dynamics of chemerin production and activity throughout multiple disease processes.

While identifying associations between specific chemerin isoforms and pathogenic states will further our understanding of the function of chemerin in disease, the relative contribution of various isoforms to different biological functions of chemerin remains a critical gap in our understanding of chemerin biology. For example, an isoform classified as having low activity for one function (e.g. chemotaxis) might have substantial activity for another function (e.g. antibacterial action). This was exemplified in a recent study where cleavage of prochemerin by cathepsin K or L results in the generation of Chem-157 and Chem- 125 isoforms, both of which exhibit antibacterial function, although only Chem-157 acts as a chemoattractant (211). Thus, current studies that examine a single functional end point for determination of isoform activity may not reflect the diversity of isoform-specific signaling. Mechanistically, receptor selectivity or the activation of distinct signaling pathways may contribute to differential isoform functions. The notion that functional selectivity occurs through small changes in chemerin structure highlights the importance of further isoform characterization, which focuses not only on the C-terminus, but also on the functional relevance of the remaining protein. For example, undiscovered functions may lie in regions closer to the N-terminus. Moreover, the presence of amino acids in one isoform vs. another might also modulate chemerin structure and/or stability. This raises the possibility that function-specific regions of the chemerin peptide exist and might be exploited in order to modulate or mimic chemerin function. In support of this notion, short C-terminal chemerin peptides have been generated, which are proposed to have anti-inflammatory function, although this has been disputed in the literature (214,215). Furthermore, the simultaneous presence of multiple isoforms may influence ultimate chemerin function through competition for receptor binding. By integrating knowledge regarding the expression of different

chemerin isoforms in disease states and regulation through processing, receptor binding and signaling events, the possibility exists for identifying novel, function-specific chemerin targets for the treatment of inflammatory and metabolic disorders.

2.7 Thesis Hypothesis and Objectives

As detailed above, the expanding basic science and clinical literature supports extensive regulation of chemerin function in metabolism and immunity. The demonstration that GPR1 may be a second chemerin signaling receptor suggests the possibility for additional regulation of chemerin function through this receptor. I hypothesize that GPR1 is an active chemerin receptor that may have overlapping or distinct signaling properties and functions compared to the established chemerin receptor CMKLR1. The following chapters in this thesis contain studies that investigate this hypothesis by way of the following objectives:

1. Determine if GPR1 is an active chemerin receptor and identify the signal transduction mechanisms that contribute to GPR1 and CMKLR1 activity.
2. Examine the role of GPR1 and CMKLR1 signal transduction in chemerin-mediated cellular responses.
3. Determine where GPR1 is expressed *in vivo* and investigate how the absence of GPR1 alters metabolic function normally and throughout the development of obesity and diabetes.

2.8 Figures

Figure 2.1: Schematic representation of methods and considerations for the integrative assessment of chemerin biology in patients.

Chemerin regulation is dynamic and varies with patient gender, ethnicity, age, health status and medication use. Chemerin is secreted as a biologically inactive precursor, prochemerin, within sites of tissue damage and inflammation, and is elevated in the serum and plasma of patients with obesity, diabetes, inflammation, and numerous other diseases. C-terminal chemerin processing by a variety of locally expressed proteases generates a diversity of chemerin isoforms, which exhibit a range of biological activities, tissue distributions, and potential functions. Overlapping and complimentary techniques are available for measuring levels and expression patterns of total chemerin, isoforms, receptors and bioactivity in patient samples, including biological fluids and tissue biopsies. Future studies that employ methodologies of this nature and incorporate numerous disease parameters into data analysis will permit accurate determination of the nature of fluctuations and dysregulation of chemerin levels in physiology/pathobiology. TNF, tumor necrosis factor; CRP, C-reactive protein; IL, interleukin; BMI, body mass index; WHR, waist to hip ratio; WC, waist circumference.

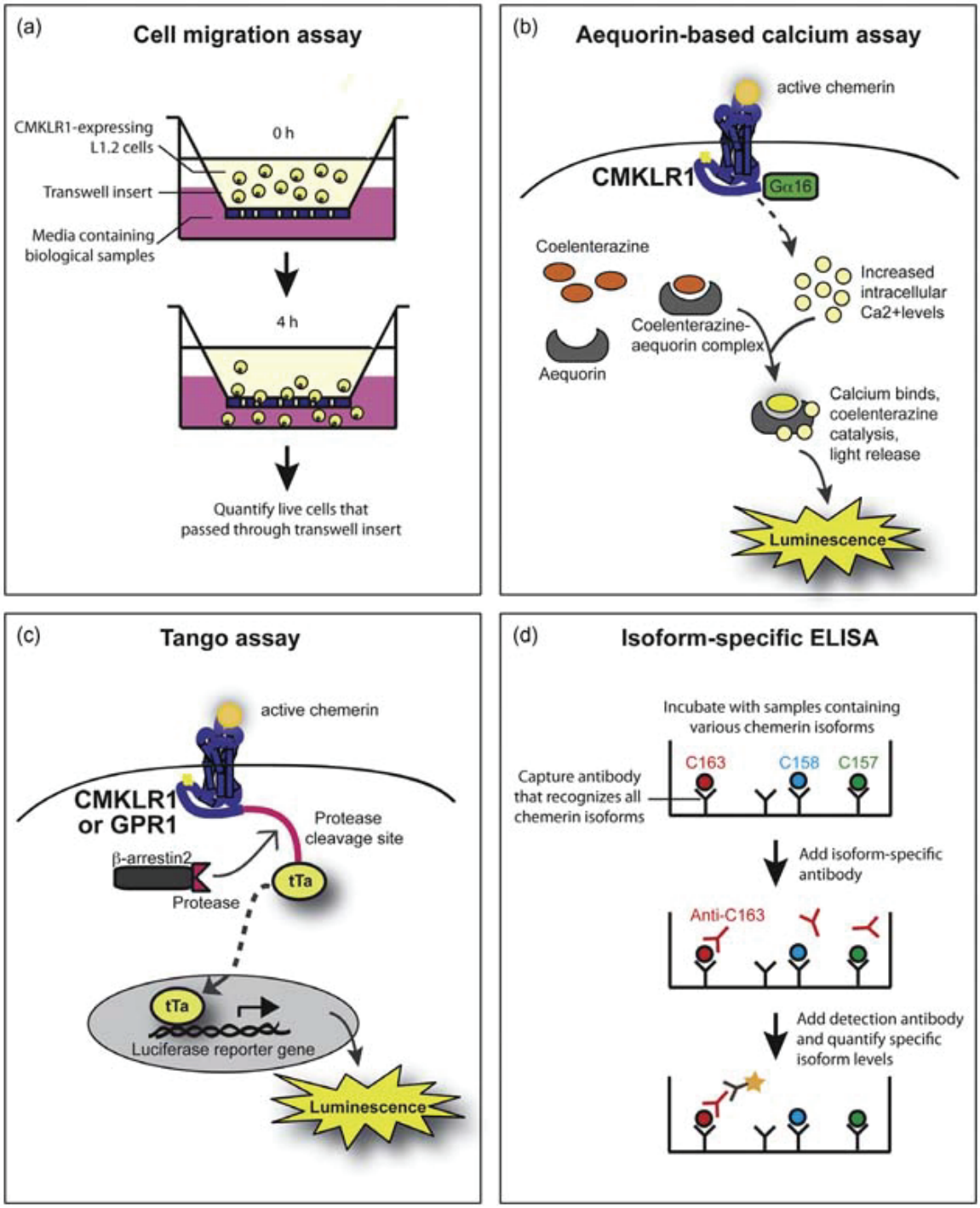
(a)
Cell migration assay
CMKLR1-expressing L1.2 cells
0 h
Transwell insert
Media containing biological samples
4 h
Quantify live cells that passed through transwell insert
(b)
Aequorin-based calcium assay
active chemerin
CMKLR1
Gα16
Coelenterazine
Coelenterazine-aequorin complex
Aequorin
Increased intracellular Ca2+levels
Calcium binds, coelenterazine catalysis, light release
Luminescence
(c)
Tango assay
active chemerin
CMKLR1 or GPR1
Protease cleavage site
β-arrestin2
tTa
Protease
tTa
Luciferase reporter gene
Luminescence
(d)
Isoform-specific ELISA
Incubate with samples containing various chemerin isoforms
C163
C158
C157
Capture antibody that recognizes all chemerin isoforms
Add isoform-specific antibody
Anti-C163
Add detection antibody and quantify specific isoform levels

Figure 2.1

2.9 Tables

Table 2.1: Prochemerin processing

Chemerin is secreted in an inactive precursor form, prochemerin, which is proteolytically processed by a variety of extracellular proteases to generate chemerin isoforms with differing levels of bioactivity. Some proteases are able to cleave chemerin at more than one site, and chemerin isoforms may be sequentially processed by different enzymes to modulate activity levels. The coordinated expression and activity of chemerin-modifying enzymes is essential for regulating chemerin bioactivation, inactivation, and consequently, biological function. Activity is in reference to functional assays for chemotaxis or intracellular Ca^{2+} release.

Protease	Cleaves	Generates	C-terminal sequence	Resulting Activity*
PROCHEMERIN ($Chem_{21-163}$)			…PGQFAFSKALPRS	Inactive
Carboxypeptidase N or B (171)	Chem-158	Chem-157	…PGQFAFS	Converts high to highest
Cathepsin G (212)	Chem-163	Chem-156	…PGQFAF	High
Cathepsins K, L* (211)	Chem-163	Chem-157	…PGQFAFS	Highest
Human leukocyte elastase (212)	Chem-163	Chem-157 Chem-155 Chem-152	…PGQFAFS …PGQFA …PG	Highest Low Inactive
Mast cell chymase (176)	Chem-156 Chem-157	Chem-154	…PGQF	Converts high/highest to inactive
Mast cell tryptase (174)	Chem-163	Chem-158 Chem-155	…PGQFAFSK …PGQFA	Low Low
Plasmin (174)	Chem-163	Chem-158	…PGQFAFSK	Low
Proteinase 3 (176)	Chem-163	Chem-155	…PGQFA	Low
Staphopain B (211)	Chem-163	Chem-157	…PGQFAFS	Highest
Factors XIIa, VIIa, plasmin, plasminogen activators (uPA, tPA) (174)	Described as activators of chemerin, but precise cleavage sites not yet determined			
*Also generates Chem-125, which has no chemotactic activity but demonstrates antibacterial activity (211)				

Table 2.2: Sources of chemerin isoforms

Distinct chemerin isoforms have been identified in several different biological fluids, indicating that chemerin undergoes complex processing *in vivo*. Future studies that investigate the presence of particular isoforms in disease states will contribute to this rapidly growing list.

Biological Source	Identified isoforms
Ascites (170)	Chem-157
Cerebrospinal fluid (173,253)	Chem-158
Hemofiltrate (172)	Chem-154
Plasma (174,253)	Chem-155, -157, -158, -163
Synovial fluid (253)	Chem-158

Table 2.3: Dysregulation of chemerin levels in multiple disease states

As an adipokine with roles in adipose tissue and immunity, chemerin is of interest in inflammatory and metabolic disease. Although the absolute concentration of circulating chemerin varies among populations and studies, elevations in total plasma and serum chemerin occur in inflammatory skin disease, diabetes, and numerous other chronic and acute conditions. CAD, coronary artery disease; NAFLD, non-alcoholic fatty liver disease, T1D, type 1 diabetes; T2D, type 2 diabetes, MetS, metabolic syndrome; NGT, normal glucose tolerance.

Reported chemerin levels (ng/ml)				Sample	Reference
Healthy		**Disease**			
INFLAMMATION					
~125	Healthy	~200 [a]	Psoriasis	Serum	(254)
		~50 [a]	Chronic Dermatitis		
METABOLISM					
Metabolic Syndrome					
186	Healthy	230 [a]	Obese	Serum	(165)
		266 [a, b]	Obese + MetS		
95	Lean	111[a]	MetS with no CAD	Serum	(163)
		133[ab]	MetS + CAD		
Diabetes					
180	Healthy	191[a]	T2D	Plasma	(161)
94	Healthy	144 [a]	T2D	Serum	(167)
197.4	NGT	193.3	Impaired fasting glucose	Serum	(199)
		227.3 [a]	Impaired glucose tolerance		
		237.9 [a]	T2D		
190	NGT	~230 [a]	T2D	Serum	(162)
266	Lean	265	T2D	Plasma	(243)
		546.3 [a]	T2D + perivascular disease		
62.1	Healthy	68.6	T2D	Plasma	(169)
		74.6 [a, b]	T2D + Hypertension		
102.4	Healthy	101.77	T2D	Serum	(255)
		104.6	T2D + microalbuminuria		
		132.06[ab]	T2D + macroalbuminuria		
217.6	Pregnancy	230.3	Pregnancy + gestational diabetes	Serum	(256)
98	Childhood	220 [a]	onset T1D	Plasma	(257)
		255 [a]	long standing T1D		
OTHER					
107.5	Adult	120.9 [a]	sleep apnea	Serum	(197)
25.9	Men	30.3	chronic hepatitis C	Serum	(258)
37.3	Women				
210.8	Pregnancy	258.9 [a]	preeclampsia	Serum	(259)

Reported chemerin levels (ng/ml)				Sample	Reference
Healthy		**Disease**			
OTHER cntd…					
151	Healthy	235 [a]	NAFLD	Serum	(195)
204.8	Pregnancy	249.5 [a]	preeclampsia	Serum	(192)
79.5	One vessel occlusion	86.6 [a]	Multiple vessel occlusion CAD	Serum	(236)
50	Healthy	97 34.4 [a]	Chronic Pancreatitis Acute Pancreatitis	Serum	(191)
45	Healthy	65 [a] 47 [b]	Renal failure Renal failure + kidney transplant	Serum	(190)
2.62	Women	6.02 [a]	Polycystic ovarian syndrome	Serum	(160)
89	Healthy	140 [a, b] 124 [a, b]	Crohn's Ulcerative Colitis	Serum	(260)
254.3	Healthy	542.2 [a]	Chronic hemodialysis	Serum	(189)

[a] $p<0.05$ vs. control population. [b] $p<0.05$ vs. comparator condition.

Chapter 3: Investigating Differential Signaling Through Chemerin Receptors

3.1 Rationale and Objectives

As highlighted in Chapter 2, little is known about the signaling pathways that couple to chemerin activation of CMKLR1 and GPR1. Early studies with CMKLR1 showed chemerin-induced phosphorylation of MAPK/ERK and p38 proteins. Two studies have also suggested that chemerin activation of CMKLR1 reduced intracellular cAMP levels (170,261). Chemerin binding to GPR1 has been shown and suggested to induce little, if any, signal transduction despite increased potency for arrestin recruitment (179). Nothing has been published on the activation of signal transduction pathways downstream of GPR1. The first objective of this thesis was to examine the signal transduction properties of both chemerin receptors CMKLR1 and GPR1 and determine the extent of GPR1 activation by chemerin. Given that CMKLR1 and GPR1 are both GPCRs, this was examined using a variety of luciferase reporter assays for generalized GPCR activation and established GPCR signaling pathways.

Components of this chapter will be included with Chapter 4 for manuscript submission. Nichole McMullen performed the BRET experiments.

3.2 Introduction

The seven transmembrane spanning serpentine GPCRs couple a wide range of extracellular stimuli including hormones, lipid messengers, and adhesion proteins to intracellular effectors and function in a vast diversity of physiological and pathological processes. In 2013, 26% of approved drugs were believed to target GPCR activity (262). Atherosclerosis, pain, bone loss, cancer, inflammation, obesity, and diabetes have all been linked with aberrant GPCR function; however, the currently targeted GPCRs represent only about 10% of total GPCRs, leaving tremendous potential for drug discovery and disease modulation. The importance of understanding GPCR signal

transduction was recently acknowledged when Robert Lefkowitz and Brian Kobilka were awarded the 2012 Nobel Prize in Chemistry for studies of GPCRs. Despite this recognition, poor understanding of endogenous GPCR ligand function remains one of the key factors attributed to the relative scarcity of GPCR-targeting drugs.

Members of the GPCR family are identified based on the presence of 7 transmembrane spanning alpha helical regions, connected by 3 extracellular and 3 intracellular loop regions, an extracellular N–terminus, and an intracellular C-terminus. Based on sequence homology, the GPCR superfamily is subdivided into 5 major families: family A/rhodopsin (~284 GPCRs), family B/secretin (~15), family C/glutamate (~22), family F/frizzled (~11), family/adhesion (~33) (262). Although members of these families differ with respect to the size of their N- and C-terminal regions, as well as the presence of conserved residues and motifs, they have in common their ability to signal through activation of heterotrimeric guanine nucleotide proteins, or G proteins.

Many ligands induce coupling of more than one G protein to a GPCR, often with differing signal strength. As such, GPCR signal transduction offers a complex diversity of signaling options permitting their function as sensors linking extracellular stimuli to key changes in gene expression and cellular function. There are 4 major classes of Gα proteins ($G\alpha_s$, $G\alpha_{q/11}$, $G\alpha_{i/o}$, and $G\alpha_{12/13}$) that facilitate the diversity of observed GPCR signaling. Each class of Gα proteins activates characteristic signal transduction cascades culminating in modulation of transcription factor activity and initiation or repression of specific gene expression patterns (263).

The signaling properties of each Gα class are summarized below and in Fig. 3.1. $G\alpha_s$ characteristically activates adenylyl cyclase resulting in increased cAMP, PKA and MEK/ERK activation. By contrast, $G\alpha_{i/o}$ protein activation inhibits adenylyl cyclase, thereby decreasing cAMP. $G\alpha_{i/o}$ has also been reported to activate the small Rho family G proteins CDC42, RhoA, and Rac. Classically $G\alpha_{q/11}$ activation is associated with activation of phospholipase C β and the induction of increased intracellular Ca^{2+}, protein kinase C activation and the subsequent activation of RAF/MEK/ERK and GEF/RHO/ROCK pathways. Additionally, $G\alpha_{q/11}$ signaling can activate an AKT/MEK cascade that terminates with mTOR, NFκB, and p70s6k activation. A vast number of

GPCRs couple to the $G\alpha_{12/13}$ pathway to some extent, often in addition to $G\alpha_s$, $G\alpha_{q/11}$, or $G\alpha_{i/o}$ coupling (264). $G\alpha_{12/13}$ activates a variety of GEFs that in turn activate RhoA, ROCK, actin cytoskeletal reorganization and possibly also p38 activation (265). G protein-independent signaling through $G\beta\gamma$ has also been identified through PI3K/AKT, which inhibits PKA, reduces downstream MAPK/ERK signaling and activates MEK-dependent mTOR signaling. Together, $G\alpha$ protein signaling activates a diversity of signals that culminate with activation of a network of transcription factors permitting dynamic and highly coordinated modulation of gene expression and cell function in response to extracellular stimuli.

GPCR activation and inactivation is tightly regulated. The GPCR signaling lifecycle involves 3 characteristic stages: receptor activation, effector activation cascades, and signal termination. In the plasma membrane, GPCRs exist in equilibrium between inactive (R) and active states (R*). In the absence of ligand binding, intramolecular interactions promote an inactive receptor conformation. Ligand binding disrupts these interactions and stabilizes the receptor active conformation. Mutation-based studies in multiple receptors support a role for the E/DRY motif, a highly conserved amino acid motif in Type A receptors in maintaining an inactive conformation (266). Mutations of the E/D moiety commonly result in constitutive receptor activity (267), while mutations of the conserved R can result in G protein uncoupling and receptor inactivation (268,269). Signal transduction occurs when the R* active conformation initiates guanine nucleotide exchange on the $G\alpha$ subunit of a receptor-associated G protein from the inactive GDP to the active GTP form. This activation leads to dissociation of the $G\beta\gamma$ subunit from the $G\alpha$ subunit. Both $G\alpha$ and $G\beta\gamma$ subunits can then interact with intracellular effector proteins to mediate a defined biological response. Subsequent to activation and G protein dissociation, GPCRs are phosphorylated by a group of regulatory proteins known as GPCR kinases, a process that initiates recruitment of an arrestin protein. In some cases arrestin recruitment also contributes to signal transduction through activation of a distinct G protein-independent signal transduction cascade. Arrestin recruitment promotes receptor internalization into endosomes for recycling or degradation thereby promoting signal termination. This mechanism also plays an important role in GPCR desensitization in the presence of prolonged stimuli. This

dynamic GPCR activation and inactivation cycling permits the sensitive regulation of the intensity, duration, and function of extracellular stimuli signaling.

Like many other hormones, chemerin signaling is governed by signaling through its GPCR receptors CMKLR1 and GPR1, both family A GPCRs. Chemerin signaling through a $G\alpha_{i/o}$ protein has been demonstrated using the $G\alpha_{i/o}$ inhibitor PTX, which blocks chemerin-mediated chemotaxis of macrophages, dendritic cells, and synoviocytes (170,184). Chemerin activation of Ca^{2+} release, AKT, p38, PI3K, decreased cAMP, and ERK1/2 have all been implicated in the function of chemerin in a diversity of cell types, including adipocytes, human embryonic kidney (HEK)-293A, leukocytes, endothelial cells, chondrocytes, synoviocytes and gastric cancer cells (4,170,183-186,188,261). The above signaling was directly or indirectly attributed to CMKLR1 activation. With respect to GPR1 signaling, Barnea *et al*. found a small increase in intracellular Ca^{2+} with a very high dose of chemerin (1 μM) in HEK293T cells in the presence of the promiscuous $G\alpha_{q/11}$ family member $G\alpha_{15}$ but not with endogenous Gα proteins. Although Barnea *et al*. identified chemerin as the ligand for GPR1 in 2008, the International Union of Basic and Clinical Pharmacology (IUPHAR) and The British Pharmacological Society (IUPHAR/BPS) Guide to Pharmacology still classifies GPR1 as an orphan receptor likely as a consequence of the absence of clear activation of intracellular signaling by chemerin. By contrast, based on sequence similarity with other receptors, CMKLR1 has been classified as a lipid receptor and highlighted for its potential as a drug target in inflammation, bone loss, viral pneumonia, and obesity (262). In both cases, a better understanding of chemerin activation and signaling via these receptors will be necessary prior to targeting these receptors for drug development and disease applications.

3.3 Materials and Methods

3.3.1 Reagents Used

For all reporter assays, cells transfected with human or mouse receptors were treated with recombinant human (MyBioSource; San Diego, CA, USA, cat# MBSK13851) or mouse

(R&D Systems; Minneapolis, ME, USA, cat# 2325-CM-025/CF) chemerin-157, respectively. PTX (Sigma Aldrich; Oakville, Ontario, cat# P7208).

3.3.2 Plasmids

Chemerin receptor complementary DNA (cDNA) was amplified by PCR using platinum Pfx DNA polymerase (Life Technologies; Burlington, ON Canada, cat# 11708013) from existing plasmid templates for human (h) and mouse (m) CMKLR1 and GPR1 using primers designed to insert restriction sites as indicated (Table 3.1). PCR products were restriction enzyme digested and inserted into pCDNA3.1/myc-his (-) B (for myc/his and untagged receptors) or pEGFP-N1 (for C-terminally-enhanced green fluorescent protein (EGFP)-tagged receptors) using standard cloning procedures. Human receptor constructs contain an in-frame stop codon 5' to the myc/his tag, generating untagged receptors. All plasmids were verified by sequencing. Human arrestin-2, arrestin-3 and CDC42-Rluc plasmids were a generous gift from Dr. Denis Dupré. Chemerin receptor tl-ta fusion constructs were generated as described previously (179). Human and mouse GPR1-tl-ta site directed mutagenesis was completed using the Quickchange II Site Directed Mutagenesis Kit (Agilent; Santa Clara, CA, USA, cat #200523) according to the manufacturer's instructions using the primers shown in Table 3.1. pGL4.34[*luc*2P/SRF-RE/Hygro] was purchased from Promega (Promega; Madison, WI, USA, cat# E1350). pCMV-beta-galactosidase (βgal) was used as a control vector.

3.3.3 CMKLR1 and GPR1 Receptor Tango Bioassay

As outlined in Chapter 2 (Fig. 2.1c), the Tango assay couples recruitment of arrestin2 to an activated GPCR to transcription/translation of the luciferase enzyme and a luminescent signal. Chemerin receptor activity was estimated using the Tango assay system with both human and mouse CMKLR1- and GPR1-transcriptional transactivator fusion proteins and recombinant human or mouse chemerin-157 in HTLA cells (HEK293 cells stably transfected with tTA-dependent luciferase reporter and an arrestin2-TEV fusion gene) as described previously (159).

3.3.4 Aequorin-based Ca^{2+}Assay

As described in Chapter 2 (Fig. 2.1b), the aequorin assay is a cell-based assay permitting detection of changes in intracellular Ca^{2+} that occur through activation of $G\alpha_{16}$ (a promiscuous G protein that signals through a Ca^{2+} pathway), or endogenous Ca^{2+}-coupled G protein pathways using the Ca^{2+} sensitive aequorin enzyme and the luminescent substrate coelantrazine. CHO-A2 cells stably transfected with mitochondrial aequorin and human $G\alpha_{16}$ (a Ca^{2+}-coupled member of the $G_{q/11}$ family) (Euroscreen, Belgium) were maintained in Ham's F-12 medium supplemented with 10% fetal bovine serum (FBS), 100 IU/mL penicillin, 100 μg/ml streptomycin, and 250 μg/ ml Zeocin. Cells were seeded in a white 96-well tissue culture plate at a density of 20,000 cells/well and allowed to adhere overnight. Cells were transfected with 50 ng either pCDNA control vector, or one of the human or mouse chemerin receptors (CMKLR1 or GPR1) using 0.2 μg of polyethylenimine transfection reagent (Sigma Aldrich; Oakville, ON, Canada, cat# 408727) in antibiotic medium for 24 hours. Medium was replaced with fresh antibiotic-free medium for an additional 18 to 20 hours prior to assay. Cells were incubated in 5 μM coelantrazine h for 3 hours at 37^{o}C and allowed to come to room temperature prior to treatment. Cells were treated with 25 μM of the Ca^{2+} ionophore digitonin to assess maximal Ca^{2+} response or with the indicated vehicle and chemerin treatments. Luminescence was measured immediately following treatment using a Luminoskan Ascent luminometer with 469 nm filter and 20-second integration time. Signal intensity for vehicle and chemerin treated cells was normalized to the digitonin-induced signal and expressed as percent maximal digitonin response.

3.3.5 Luciferase Signaling Reporters

Stable reporters: HEK293A cells stably transfected with an inducible response element – dependent firefly luciferase reporter were generated using the Cignal Lenti SRE Reporter (luc) kit (SABiosciences; Mississauga, ON, Canada cat# CLS-010L) according to the manufacturer's instructions. The resulting stable cells contain response element

promoters as outlined in Table 3.2. Signal transduction pathways leading to activation of the individual reporter promoters are outlined in Fig. 3.2. Cells used in experiments were derived from a single clone following selection with 2 μg/ml puromycin and functional testing. HEK293A-reporter cells (17,500 cells/well) were plated in 48-well tissue culture plates in Dulbecco's modified eagle medium (DMEM)/10% FBS and allowed to adhere overnight. Cells were transfected with chemerin receptor as indicated (100 ng), a βgal control vector (75 ng), and pCDNA (75 ng) using 0.4 μg of polyethylenimine transfection reagent (Sigma Aldrich; Oakville, ON, Canada, cat# 408727) in Opti-MEM/1% FBS for 18 hours. Following transfection, medium was replaced with serum-free Opti-MEM for 2 hours prior to addition of concentrated treatments. Treatment times for each reporter are indicated in Table 3.2. All incubations were done under standard culture conditions (37^{o}C in 95% air, 5% CO2). At the end of the treatment time, culture medium was removed and cells were lysed in 100 μl reporter lysis buffer (Promega; Madison, WI, USA, cat# E4030). βgal activity was determined by incubating 1:1 of cell lysate with βgal assay buffer (200 mM sodium phosphate buffer, 2 mM $MgCl_2$, 100 mM β-mercaptoethanol, 1.33 mg/ml ortho-nitrophenyl-β-galactoside) for 5 minutes prior to reading absorbance at 420 nm. Luminescence was determined by mixing 10 μl of cell lysate with 80 μl of luciferase assay substrate (Promega; Madison, WI, USA, cat# E151A) in a white 96-well plate and immediately measuring total luminescence using a Luminoskan Ascent luminometer with 10-second integration time. Fold change luminescence was calculated by dividing luminescence by βgal for each sample and was expressed relative to the indicated control.

Serum response factor (SRF) reporter (Fig. 3.1a): Signal transduction assays with HEK293A cells were conducted essentially as described for stable reporters, with the notable exception that pCDNA was replaced with the SRF reporter pGL4.34[*luc*2P/SRF-RE/Hygro] (75 ng). Following transfection, medium was replaced with serum-free Opti-MEM for 4 hours prior to addition of concentrated treatments.

3.3.6 Bioluminescence Resonance Energy Transfer (BRET) Assay

Direct interactions between chemerin receptors and arrestin2 or arrestin3 were quantified via BRET1. HEK293A cells (20000 cells/well) were grown overnight in a white 96-well plate and transfected with the indicated EGFP and Rluc constructs (25 ng Rluc BRET donor arrestin, 100 ng EGFP BRET acceptor chemerin receptor). Twenty-four hours post-transfection, the cell culture medium was replaced with PBS. Total EGFP was determined with 480 nm excitation and 520 emission filters for all wells. Coelantrazine h (5 μM) was added, incubated for 55 seconds prior to determination of total luminescence with 1 second integration time. Treatments, as indicated, were added to all wells, incubated for 5 minutes prior to BRET measurement of donor (460 nm) and acceptor (520 nm) emission for 5 consecutive runs. The BRET ratio was calculated as follows:

$$BRET_{ratio} = \frac{\text{Emission 520 (donor + acceptor pair)}}{\text{Emission 460 (donor + acceptor pair)}} - \frac{\text{Emission 520 (donor only)}}{\text{Emission 460 (donor only)}}$$

3.3.7 Statistical Analyses

All data are expressed as mean ± SEM. Comparisons were performed using a repeated measures, one- or two-way ANOVA, or two-tailed t-test, as indicated with Holm-Sidak multiple comparisons test.

3.4 Results

3.4.1 CMKLR1 and GPR1 Share Similar Structural Properties and Predicted G protein Binding

CMKLR1 recruits arrestin and activates signal transduction that depends upon $G\alpha_{i/o}$, while some have suggested that GPR1 signal transduction may be weak or absent (170,179). Since relatively little is known about GPR1 we sought to determine structural motifs that may play a role in regulation of GPR1 signaling through comparison with CMKLR1 and the prototypical family A GPCR beta-2 adrenergic receptor (β_2AR) using a ClustalW alignment (Fig. 3.3a). Human CMKLR1 and GPR1 shared 39% amino acid

identity with one another and were 80% conserved in mouse. The amino acid location and orientation of 7 putative transmembrane domains was predicted using the online GTPred prediction algorithm (Fig. 3.3b) and highlighted in bold-type in the alignment. Numerous conserved characteristic transmembrane residues of Type A G protein coupled receptors (highlighted in grey) were found in both CMKLR1 and GPR1. Notably, neither GPR1 nor CMKLR1 contained a perfect E/DRY motif. The conserved E/DRY motif, located at the end of transmembrane domain III was DRC for CMKLR1 and DHY for GPR1. This diversion from the consensus motif was also present in the mouse CMKLR1 sequence; however, the mouse GPR1 sequence contains a consensus matching DRY. Both CMKLR1 and GPR1 also had a shorter transmembrane domain IV, extracellular loop III, and C-terminal tail than the β_2AR. Using the PRED-COUPLE 2.0 (270,271) to predict the G protein coupling specificity of CMKLR1 and GPR1, we showed that both CMKLR1 and GPR1 are predicted to couple with $G\alpha_{q/11}$, and $G\alpha_{i/o}$. Human CMKLR1 alone was predicted to couple to $G\alpha_{12/13}$, while none of the receptor sequences examined were predicted to couple to $G\alpha_s$ (Fig.3.3c).

3.4.2 Species Differences in CMKLR1 and GPR1 Arrestin Recruitment

Given the close association between receptor activation and the recruitment of arrestin, arrestin recruitment is frequently used as a surrogate marker for receptor activation. Chemerin receptor activation was examined using the Tango bioassay, a proximity-based assay that couples recruitment of arrestin-2 to the activated receptor to a luminescent readout. Treatment with increasing doses of chemerin in HTLA cells resulted in a significant increase in luminescence at 3, 10, and 30 nM or 30 nM only, for hCMKLR1 or mCMKLR1, respectively (Fig. 3.4a). Chemerin treatment of cells transfected with hCMKLR1 resulted in a much greater fold-change (600-fold) than mCMKLR1 (7-fold) when compared with vehicle treated cells. Similarly, treatment of HTLA cells transfected with either hGPR1 or mGPR1 resulted in a significant increase in receptor activation at as low as 1 nM for mGPR1 or 10 nM for hGPR1 (Fig. 3.4b). Notably, basal receptor activity for mGPR1 was significantly higher than for hGPR1. Accordingly, while hGPR1 activation reached levels more than 200-fold higher than

vehicle with 30 nM chemerin treatment, mGPR1 fold change from baseline was only 3-fold.

3.4.3 The "DRY" Ionic Lock in CMKLR1 and GPR1 Regulates Receptor Activity

The E/DRY motif has a well-established role in regulation of receptor activity, in particular transitions between active and inactive conformations. Alignment of the human and mouse GPR1 sequences within this region demonstrates that the human receptor contains an atypical DHY sequence while mGPR1 contains the highly conserved DRY (Fig. 3.5a). Given the observed differences between mouse and human GPR1 basal activity and sensitivity to chemerin activation, we used site-directed mutagenesis to examine the impact of E/DRY motif differences on GPR1 activation in the Tango assay (Fig. 3.5b). As shown before, HTLA cells transfected with a GPR1 construct containing the endogenous DRY sequence demonstrated that mGPR1 exhibits significantly higher basal activation than hGPR1 and that both receptors were sensitive to activation by chemerin. Mutation of arginine (R) at position 135 to a histidine in the mouse GPR1 receptor, to match what is seen in the human receptor, resulted in an upward shift in the basal activity and a loss of chemerin sensitivity. Mutation of the human GPR1 histidine at position 135 to an arginine, to mimic the mGPR1 sequence, resulted in a downward shift in basal activity and a rightward shift in the chemerin-induced activation curve, suggesting a decrease in chemerin potency.

Numerous GPCRs exhibit a preference for recruitment of specific arrestin family members (272). To further examine arrestin recruitment to the chemerin receptors, we employed a BRET assay system where different luciferase-tagged arrestin isoforms are transfected into HEK293A cells combination with EGFP-tagged chemerin receptors. In this system, recruitment of luciferase-tagged arrestin to the activated receptor results in EGFP excitation (Fig. 3.6a). To ensure that each EGFP-tagged chemerin receptor was well expressed and that levels of the receptors were not altered by co-transfection of the arrestin proteins or chemerin treatment, we examined total EGFP in HEK293A cells transfected with the indicated combinations of either arrestin-3 or arrestin-2 with each of the chemerin receptors (Fig. 3.6b). Chemerin receptor EGFP levels were similar under

both basal and chemerin treated conditions and were unchanged with transfection of either arrestin-3 or arrestin-2. Similarly, it was also necessary to ensure that chemerin receptor transfection did not significantly alter levels of the luciferase-tagged arrestin proteins (Fig. 3.6c). Luciferase activity was similar between arrestin-2 and arrestin-3 basally, following chemerin treatment, and in the presence of each of the chemerin receptors.

To determine the extent of arrestin recruitment to the chemerin receptors, we performed BRET in HEK293A cells transfected with EGFP-tagged hCMKLR1, hGPR1, mCMKLR1, or mGPR1 in combination with either arrestin-3 or arrstin-2 luciferase (Fig. 3.7) Under basal conditions, BRET ratios were significantly higher in cells transfected with human or mouse GPR1 when compared with cells transfected with CMKLR1 for both arrestin-3 and arrestin-2 recruitment (Fig. 3.7a). To ensure that arrestin recruitment to the receptors was a specific event and not a product of random proximity of the luciferase and EGFP components of the BRET system, BRET using arrestin-3 was compared with a membrane-targeted CD4-luciferase protein, which was not expected to interact with the chemerin receptors (Fig. 3.7b). Chemerin treatment of cells transfected with arrestin-3 luciferase in combination with either hCMKLR1 or hGPR1 resulted in a significant increase in the BRET ratio; however, no activation was seen when arrestin-3 was replaced with CD4.

To further examine the ability of chemerin to induce arrestin recruitment to the activated receptors, each EGFP-tagged receptor was transfected in combination with either arrestin-3 or arrestin-2 (Fig. 3.7c). These cells were treated with vehicle or 30 nM chemerin and the BRET ratio was determined for 5 successive measurements spanning approximately 25-30 minutes total. Chemerin treatment significantly increased the BRET ratio with both arrestin-3 and arrestin-2 in cells transfected with hCMKLR1 or mGPR1 at all time points examined. By contrast, chemerin treatment of cells transfected with hGPR1 resulted in a significant increase in BRET only in the 4^{th} and 5^{th} measurements in cells transfected with arrestin-3, and the 3^{rd} measurement in the presence of arrestin-2. Similarly, activation of mCMKLR1 BRET was significantly increased at the 1^{st} and 3^{rd} time point for arrestin-3 and only the 3^{rd} time point for arrestin-2. Overall, transfection with CMKLR1 resulted in a larger fold-change induction in BRET than GPR1, reaching

levels of 15-fold (hCMKLR1) and 80-fold (mCMKLR1) compared to the 10-fold (hGPR1) and 2-fold (mGPR1) of GPR1.

3.4.4 Both CMKLR1 and GPR1 Require $G\alpha_{i/o}$ for Arrestin Recruitment

We predicted that the chemerin receptors could couple to $G\alpha_{i/o}$ and the literature reports CMKLR1 $G\alpha_{i/o}$ coupling (170,184). To examine the $G\alpha_{i/o}$ dependence of CMKLR1 and GPR1, we used the Tango assay to assess arrestin recruitment in the presence of the $G\alpha_{i/o}$ inhibitor PTX (Fig. 3.8). In the presence of PTX, 30 nM chemerin was no longer able to significantly increase hCMKLR1 activation. PTX had less effect on hGPR1 activity, where 30 nM chemerin was still able to significantly increase arrestin recruitment; however, this induction was significantly reduced when compared with vehicle treated cells. These data suggest that both CMKLR1 and GPR1 couple to $G\alpha_{i/o}$.

3.4.5 CMKLR1 But Not GPR1 Activates Ca^{2+} Signaling

Given the $G\alpha_{i/o}$ coupling of CMKLR1 and GPR1 and the prediction that both chemerin receptors could also couple to $G\alpha_{q/11}$, we examined activation of these pathways using Ca^{2+} and cAMP reporter assays (Fig. 3.9). Both human and mouse CMKLR1 were able to significantly increase intracellular Ca^{2+} concentrations when treated with chemerin in CHO-A2 cells stably transfected with the Ca^{2+}-coupled $G\alpha_{q/11}$ family member $G\alpha_{16}$ (Fig. 3.8a). Neither transfection with mouse nor human GPR1 was sufficient to support chemerin activation of Ca^{2+} signaling, suggesting that GPR1 does not couple to $G\alpha_{16}$ or other Ca^{2+}-coupled $G\alpha_{q/11}$ family members. Despite coupling to $G\alpha_{i/o}$ and literature reports suggesting that CMKLR1 activation decreases cAMP (170,261), we observed no significant changes in cAMP signaling with chemerin treatment alone or in combination with the adenylyl cyclase activator forskolin with any of the chemerin receptors tested (Fig. 3.9b).

3.4.6 CMKLR1 Activates MAPK/ERK While Both CMKLR1 and GPR1 Activate RhoA Signaling

It is now well-established that most GPCRs couple to more than one type of Gα protein (273). To get a more complete picture of the potential G-protein coupling of the chemerin receptors, we also examined activation of the MAPK/ERK and RhoA pathway reporter assays, which are typically activated downstream of $G\alpha_s$ and $G\alpha_{12/13}$ proteins, respectively (Fig. 3.10). Treatment of the MAPK/ERK reporter with increasing doses of chemerin resulted in significant pathway activation in the presence of mCMKLR1 receptors but not with hCMKLR1, hGPR1, or mGPR1 (Fig. 3.10a). By contrast, treatment with 100 nM chemerin resulted in significant activation of RhoA pathway signaling for both human and mouse CMKLR1 and GPR1 (Fig. 3.10b).

3.4.7 CMKLR1 and GPR1 Co-Transfection Does Not Alter Arrestin, cAMP, or MAPK Signaling Reporter Activation

Research over the past 10 years has increasingly supported the importance of GPCR homo- and hetero-dimerization for regulation of ligand sensitivity and pathway selectivity of GPCRs (274). Additionally, CMKLR1 dimerization with the chemokine receptors CXCR4 and CCR7 influences the function the ligand binding of receptor pairs (275). We examined the potential for CMKLR1 and GPR1 heterodimerization using the Tango assay. In this system the luminescent signal is linked to activation of only the -tl-ta fusion receptor, CMKLR1 for example, therefore permitting co-transfection of un-tagged GPR1 receptor or, vice versa, to examine the impact of one receptor on the arrestin recruitment of the other. Chemerin significantly activated CMKLR1-tl-ta when co-transfected with either the empty vector control or untagged hGPR1 (Fig. 3.11a). Similarly, chemerin treatment significantly increased hGPR1-tl-ta activation when co-transfected with either pCDNA or untagged hCMKLR1 (Fig. 3.11b). There was no significant difference between the activation levels of tango receptors in cells where they were co-transfected with pCDNA or with an untagged chemerin receptor. Likewise, co-transfection of CMKLR1 and GPR1 resulted in a similar absence of chemerin-induced

activation in the cAMP reporter when compared with transfection of the receptors alone for both mouse and human receptors (Fig. 3.11c). As demonstrated previously, chemerin activates MAPK/ERK pathway signaling through mCMKLR1. This activation was still present when mGPR1 was co-transfected with mCMKLR1 but was not significantly different from transfection of mCMKLR1 alone (Fig.3.11e). Human GPR1 and CMKLR1 co-transfection did not result in MAPK/ERK pathway activation.

3.5 Discussion

The goal of this study was to determine if chemerin activation of GPR1 induces intracellular signal transduction and to what extent the signal transduction profiles of CMKLR1 and GPR1 differ or overlap. I showed that both CMKLR1 and GPR1 recruit arrestin following chemerin activation. Arrestin recruitment to CMKRL1 displayed different kinetics and efficacy when compared with GPR1. Species-specific differences in arrestin recruitment were also found. Notably, recruitment of arrestin-2 and arrestin-3 to unstimulated mGPR1 was significantly higher than hGPR1, hCMKLR1 and mCMKLR1. Consistent with literature reports, CMKLR1 but not GPR1 signaling increased intracellular Ca^{2+} and MAPK/ERK pathway activation. In contrast, neither CMKLR1 nor GPR1 signaling resulted in changes in cAMP signal transduction. Moreover, I reported the novel finding that both CMKLR1 and GPR1 activated signal transduction through a Rho-GTPase pathway. As such, this study provides evidence that GPR1 is a chemerin receptor capable of activating signal transduction beyond arrestin recruitment, and that chemerin activates both distinct and overlapping signaling pathways through CMKLR1 and GPR1.

Human and mouse receptor isoforms displayed different basal activities and sensitivity to chemerin activation. In the tango, BRET, Ca^{2+}, MAPK, and Rho assays chemerin activation of mCMKLR1 was significantly greater than hCMKLR1. Reliable CMKLR1 and GPR1 antibodies were not available to determine the total or membrane localized chemerin receptor expression; however, the similar extent and localization of transfected EGFP-tagged receptor expression in the BRET assay suggests that the observed differences in signaling were not solely a consequence of protein expression or membrane targeting. These findings suggest that chemerin activation of the mouse

receptor may be more efficacious than for human. Similarly, despite elevated basal arrestin-2 coupling and minimal fold-change induction, chemerin activation of mGPR1 occurred with higher potency than hGPR1 in the Tango assay. We investigated the possibility that these species-specific differences in GPR1 arise as a consequence of a difference in the sequence of the DRY motif, a well-established regulator of receptor basal activity and ligand-responsiveness (266). Our findings that chemerin sensitivity was reduced (hGPR1) or completely lost (mGPR1) with DRY motif mutation and that neither produced a species-like switch in receptor activation profiles demonstrate that the endogenous sequence of each receptor is best suited for chemerin sensitivity and not the sole cause of the observed species differences in arrestin coupling. Moreover, the apparent constitutive activity of mGPR1 was limited to arrestin recruitment, and was not observed to any great extent in the absolute RLU values in the Ca^{2+}, cAMP, MAPK, or Rho assays (data not shown) suggesting that GPR1 second messenger pathway activation may be conserved between mouse and human receptors.

There are four known arrestin isoforms: arrestin-1 and -4 (restricted to visual systems) and arrestin-2 and -3 (ubiquitously expressed). Most non-visual GPCRs can recruit both arrestin-2 and arrestin-3 (272,276). The Tango assay and BRET assay both demonstrated that arrestin-2 recruitment was significant and dose dependent with chemerin activation of CMKLR1 and GPR1. The BRET assay provided further evidence that arrestin-3 recruitment may be greater than arrestin-2 with respect to hGPR1, mCMKLR1, and possibly also hCMKLR1. This arrestin preference may have implications for chemerin receptor lifecycle regulation. Oakley *et al*. proposed that GPCRs could be classified into two subclasses based on their arrestin recruitment (272). In this model one class of receptors exhibits equivalent affinity for both arrestins and displays stable arrestin-receptor complexes that remain intact upon receptor internalization. These receptors, including the Angiotensin AT_{1A} and Vasopressin V_2 receptors, recycle slowly to the membrane and are frequently degraded following internalization, resulting in receptor desensitization. By contrast, the second class of receptors in this model exhibits higher arrestin-3 affinity; however, both arrestin-3 and arrestin-2 coupling to these receptors is more transient than the first class and rapidly dissociates. In this case, receptors such as the β_2 and α_{1b} adrenergic receptors are rapidly

resensitized for ligand activation. The BRET data presented herein suggest that hGPR1, mCMKLR1, and hCMKLR1 may fall into the second class of receptors while mGPR1 appears more likely to belong to the first. Consistent with the transient nature of the second class of arrestin coupling, both human and mouse CMKLR1 had oscillatory coupling with arrestin-3 throughout the time course following chemerin treatment. While dedicated experiments examining receptor lifecycle are required to determine the mechanisms and impact of this coupling affinity on chemerin receptor cycling and activity, these findings suggest that differences in mGPR1 arrestin preference and cycling could contribute to the observed difference in mGPR1 basal and chemerin-stimulated activity in the Tango assay.

While arrestin-based assays permit examination of general receptor activation and arrestin coupling, they do not provide any indication of the second messenger pathways downstream of receptor activation. It is widely accepted that most GPCRs couple to more than one G protein and activate multiple signal transduction cascades (273). Given our prediction that CMKLR1 and GPR1 could couple to $G\alpha_{i/o}$, $G\alpha_{q/11}$, and $G\alpha_{12/13,}$ and the array of reports demonstrating $G\alpha_{i/o}$, MAPK, cAMP, and Ca^{2+} signaling through CMKLR1, we examined the receptor-specific and species differences for CMKLR1 and GPR1 mediated activation of these pathways. We predicted that both CMKLR1 and GPR1 couple to $G\alpha_{q/11}$ and would therefore have the potential to activate Ca^{2+} signaling. In this chapter we showed that CMKLR1 but not GPR1 activation resulted in an increase in intracellular Ca^{2+} in CHO-A2 cells. Although the stable transfection of the $G\alpha_{q/11}$ family member $G\alpha_{16}$ in these cells prohibits distinguishing CMKLR1-mediated activation of endogenous Ca^{2+}-coupled signaling, this finding is consistent with those of others (179) and with the observation that endogenously expressed CMKLR1 activates Ca^{2+} signaling in human macrophages and dendritic cells (170). Consistent with the observations of Barnea *et al*., the first group to identify chemerin as a GPR1 ligand (179), we showed no detectible endogenous or $G\alpha_{16}$ mediated activation of Ca^{2+} signaling through GPR1.

MAPK pathway activation has been reported downstream of $G\alpha_{q/11}$ and Ca^{2+} signaling. We saw MAPK pathway activation only with mCMKLR1 and observed no effect on this pathway with hCMKLR1 or GPR1, suggesting that $G\alpha_{q/11}$ coupling to

mCMKLR1 may also contribute to chemerin activation of MAPK cascades. Previous reports have shown MAPK signaling by both h-and mCMKLR1. Several factors could contribute to differences in our findings from those of others including our use of the SRE reporter, which differs from the protein phosphorylation endpoint of previous studies. Previous studies also show that chemerin activation of MAPK/ERK pathways is desensitized in both a time and dose-dependent manner, suggesting that the timing for detection of this pathway requires optimization. Chapter 4 elaborates on treatment and dose consideration for chemerin signaling. Together these data suggest that, counter to our prediction, CMKLR1 but not GPR1 couples to $G\alpha_{q/11}$. We cannot; however, rule out the possibility that GPR1 coupling to $G\alpha_{q/11}$ occurs and activates Ca^{2+}-independent signaling, through AKT for example. Lastly, we predicted that CMKLR1 and GPR1 could couple to $G\alpha_{i/o}$ but not $G\alpha_{s}$, suggesting that chemerin signaling could result in a decrease in cAMP. In contrast to previous reports showing decreased cAMP with CMKLR1 activation (261), we found no evidence of CMKLR1 or GPR1 mediated changes in cAMP under either basal conditions or following stimulation with the adenylyl cyclase activator forskolin. As such, it is unclear to what extent the chemerin receptors couple to $G\alpha_{i/o}$ and adenylyl cyclase inhibition. Although CMKRL1 and GPR1 G protein coupling were similar in our prediction, these findings support unique coupling and signaling profiles for CMKRL1 and GPR1.

Activation of Rho-GTPase pathways is a common downstream target of $G\alpha_{i/o}$, $G\alpha_{q/11}$, and $G\alpha_{12/13}$ signaling (277). GPCR signaling through these pathways have been implicated in cellular migration, transformation, and differentiation (278,279). Herein we present the novel finding that chemerin activates signaling through a Rho-dependent pathway via both CMKLR1 and GPR1. To our knowledge this is the first report of chemerin-mediated activation of Rho-GTPase signaling. Based on our prediction of G protein coupling to CMKLR1 and GPR1, this signaling could be occurring through $G\alpha_{i/o}$, and/or $G\alpha_{q/11}$ coupling. hCMKLR1 was also predicted to couple with $G\alpha_{12/13}$ providing additional potential for Rho-GTPase pathway activation with this receptor. While there is some evidence that Rho-GTPase pathways can contribute to p38 activation (280) and may therefore represent an upstream event in the previously identified chemerin signaling cascades, it is likely that this pathway represents an unexplored mechanism for chemerin

function that could have implications for the role of chemerin in immune cell chemotaxis, differentiation, proliferation and survival. Chapter 4 explores this potential in detail.

Relative to other GPCRs, whose signaling biology has been extensively studied, little is known about the signaling pathways that couple to chemerin activation of CMKLR1 and GPR1. The experiments presented in this chapter suggest that, while some overlap may exist in signaling though the chemerin receptors (Rho-GTPase), differential signaling may also occur (MAPK, arrestin). These distinctions are of interest because they may contribute to regulation of chemerin function through redundant and unique functions of CMKLR1 and GPR1. Further investigation of chemerin signal transduction may ultimately provide insight into the mechanisms of chemerin function in numerous systems.

3.6 Figures

Figure 3.1: G protein-coupled receptor signal transduction

Schematic representation of GPCR signaling through the four families of G proteins: $G\alpha_{q/11}$ ($G\alpha_q$), $G\alpha_s$, $G\alpha_{i/o}$ ($G\alpha_i$), $G\alpha_{12/13}$ ($G\alpha_{12}$). **Abbreviations**: AC: adenylate cyclase, AKT: RAC-alpha serine/threonine-protein kinase, AMPK: AMP-activated protein kinase, $Ca^{2+:}$ calcium, cAMP: cyclic adenosine monophosphate, CDC42: cell division control protein 42 homolog, CREB: cAMP response element-binding protein, ERK: extracellular-regulated kinase, GEF: guanine nucleotide exchange factor, JNK: janus kinase, IKKs: I kappa B kinase, MEK: mitogen activated protein kinase kinase, mTOR: mammalian target of rapamycin, NFκB: nuclear factor κ B protein, p38: p38 mitogen-activated protein kinases, p70s6K: ribosomal protein S6 kinase,
PAK: Serine/threonine-protein kinase, PI3K: phosphoinositide-3-kinase, PIP3: phosphatidyl-inositol (3,4,5)-triphosphate, PKA: protein kinase A,
PKC: protein kinase C, PLCβ: phospholipase C beta, RAC: ras-related C3 botulinum toxin substrate, RAF: Rapidly Accelerated Fibrosarcoma, RHO: ras homolog gene family member GTPase, ROCK: rho-associated protein kinase, SRC: Proto-oncogene tyrosine-protein kinase

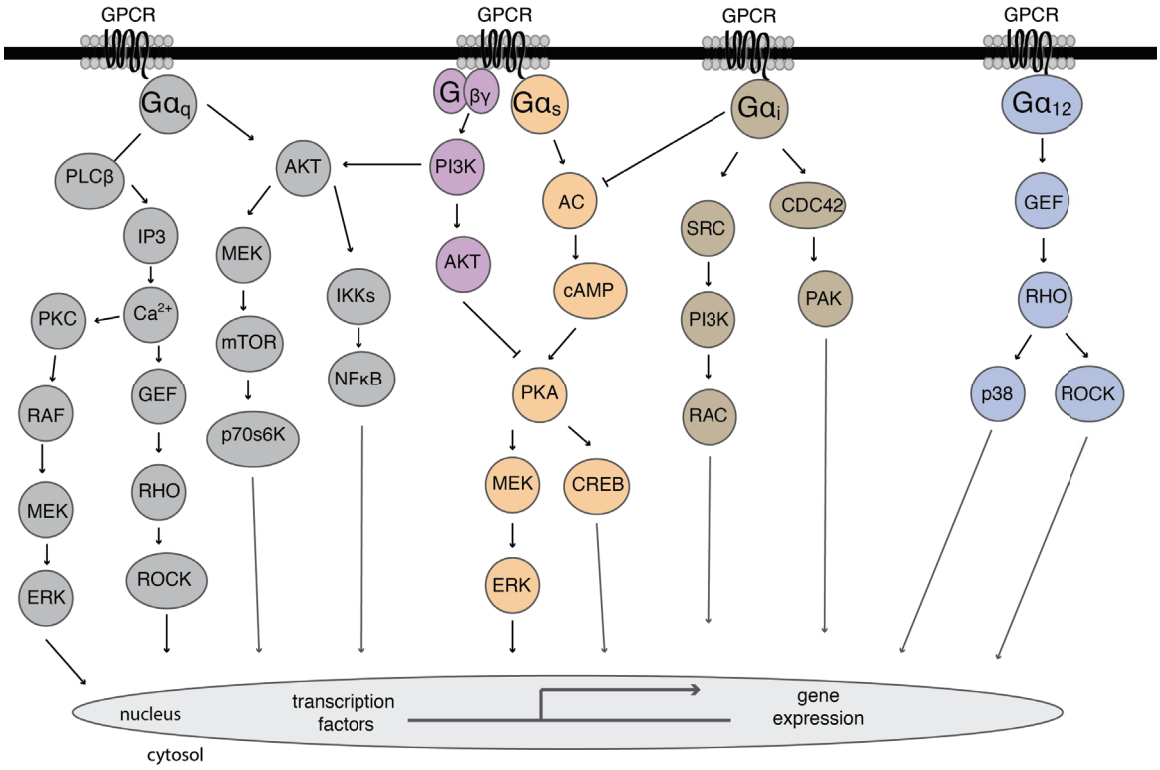
GPCR
GPCR
GPCR
GPCR
Gαq
Gβγ
Gαs
Gαi
Gα12
PLCβ
AKT
PI3K
AC
SRC
CDC42
GEF
IP3
MEK
AKT
cAMP
PI3K
PAK
RHO
PKC
Ca2+
IKKs
mTOR
NFκB
PKA
RAC
p38
ROCK
RAF
GEF
p70s6K
MEK
CREB
RHO
MEK
ROCK
ERK
ERK
nucleus
transcription factors
gene expression
cytosol

Figure 3.1

Figure 3.2: Schematic representation of luciferase signaling reporters

HEK293A cells transfected with a CRE, SRE, or SRFRE-driven luciferase reporter gene were used for assessment of the cAMP, ERK, and RHOA pathways, respectively. Extracellular stimuli producing activation of cAMP and PKA lead to activation of the transcription factor CREB and transcription of the CRE-controlled luciferase reporter. Extracellular stimuli producing activation of the MEK/ERK pathway leads to activation of the TCF family of transcription factors, which complex with SRF in the nucleus and activate transcription of the SRE-controlled luciferase reporter. Extracellular stimuli producing activation of RHOA/ROCK signaling results in LIMK activation, cofilin inhibition and initiation of G-actin polymerization into F-actin. G-actin depletion liberates the cytosolic restraint on the MRTF family of transcriptional co-activators permitting complex formation with SRF in the nucleus and activation of SRFRE-controlled luciferase reporter expression. **Abbreviations**: cAMP: cyclic adenosine monophosphate, CREB: cAMP response element-binding protein, ERK: extracellular-regulated kinase, F-actin: filamentous actin, G-actin: globular actin, LIMK: LIM kinase, MRTF: myocardin-related transcription factor, MEK: mitogen activated protein kinase kinase, PKA: protein kinase A, RE: response element, RHOA: ras homolog gene family member A, ROCK: rho-associated protein kinase, SRF: serum response factor, TCF: ternary complex factor

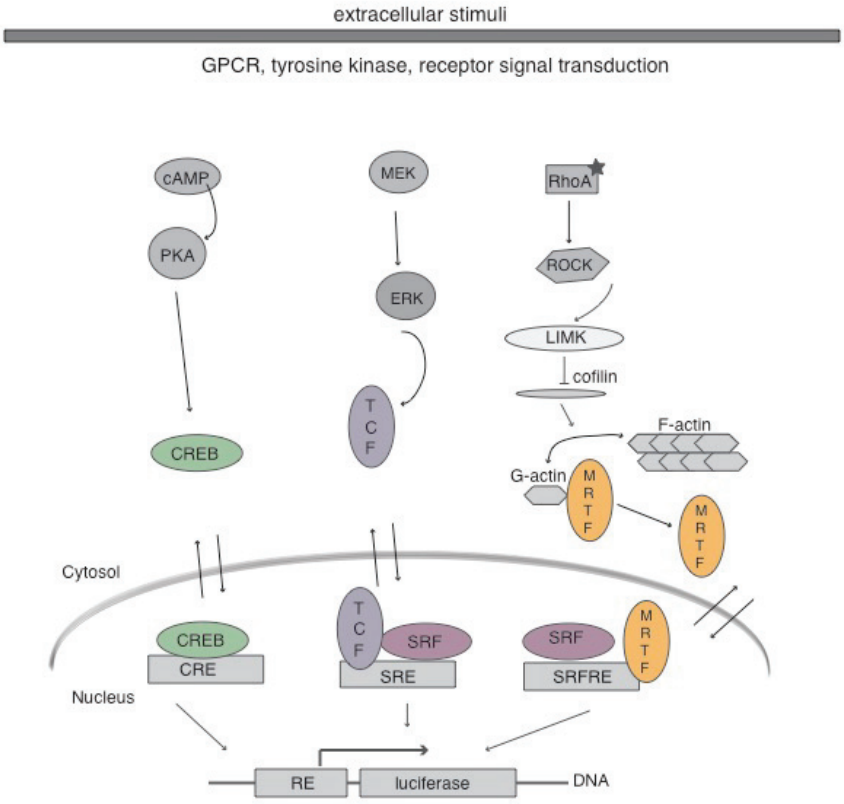
extracellular stimuli
GPCR, tyrosine kinase, receptor signal transduction
cAMP
PKA
CREB
MEK
ERK
TCF
RhoA
ROCK
LIMK
cofilin
F-actin
G-actin
MRTF
MRTF
Cytosol
Nucleus
CREB
CRE
TCF
SRF
SRE
SRF
MRTF
SRFRE
RE
luciferase
DNA

Figure 3.2

Figure 3.3: Predicted CMKLR1 and GPR1 transmembrane domain alignment and G protein binding

The human CMKLR1 and GPR1 amino acid sequences were compared using a ClustalW alignment. Since both GPR1 and CMKLR1 belong to the Type A GPCR family, the β_2AR, a prototypical member of this family, was chosen for comparison within the alignment. The GTPred prediction tool, which predicts transmembrane domain regions based on a "structure-conscious" hidden Markov model was used to estimate the location of CMKLR1 and GPR1 transmembrane domains, which are in bold-type. Amino acids highlighted in grey represent conserved characteristic transmembrane residues of Type A G protein coupled receptors (a). Location, length and orientation (outside (o) to inside (i) or inside to outside) of predicted transmembrane domains (b). PRED-COUPLE 2.0 was used to predict the coupling specificity of human (h) and mouse (m) CMKLR1 and GPR1 to the G proteins $G\alpha_{q/11}$, $G\alpha_{i/o}$, $G\alpha_{s}$, and $G\alpha_{12/13}$ (c). Positive predictions are in bold type.

a.

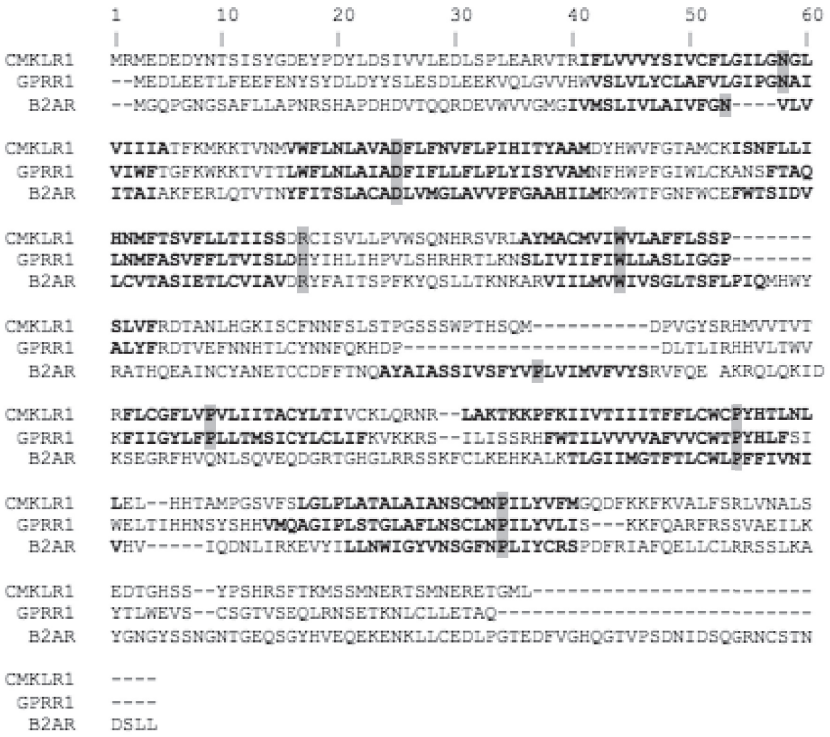

b.

GPR1

TM	LOCATION	ORIENTATION
I	40-62	o-i
II	74-99	i-o
III	115-133	o-i
IV	154-175	i-o
V	211-231	o-i
VI	245-265	i-o
VII	281-307	o-i

CMKLR1

TM	LOCATION	ORIENTATION
I	41-65	o-i
II	76-101	i-o
III	114-135	o-i
IV	156-177	i-o
V	225-243	o-i
VI	261-282	i-o
VII	296-319	o-i

c.

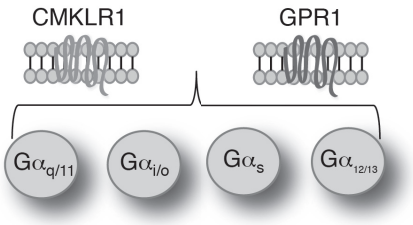

Normalized posterior probablity score

	$G\alpha_{q/11}$	$G\alpha_{i/o}$	$G\alpha_{s}$	$G\alpha_{12/13}$
hCMKLR1	**0.93**	**0.99**	0.11	**0.50**
hGPR1	**0.90**	**0.88**	0.10	0.02
mCMKLR1	**0.53**	**0.99**	0.00	0.00
mGPR1	**0.90**	**0.89**	0.01	0.01

Score: < 0.3 negative
> 0.3 positive

Figure 3.3

Figure 3.4: Receptor and species-specific variation in chemerin-mediated arrestin recruitment

Human (h) or mouse (m) CMKLR1 (a)- or GPR1-tTA fusion receptors (b) were transfected in HTLA cells to assess receptor activation following treatment with increasing doses of chemerin. The resulting luminescent signal was expressed relative to β-galactosidase activity (RLU) or as fold change luminescence relative to 0 nM chemerin treatment, N= 3. One-way ANOVA *$p<0.05$ vs. 0 nM chemerin within receptor (# $p<0.05$ vs. 0 nM chemerin for mGPR1).

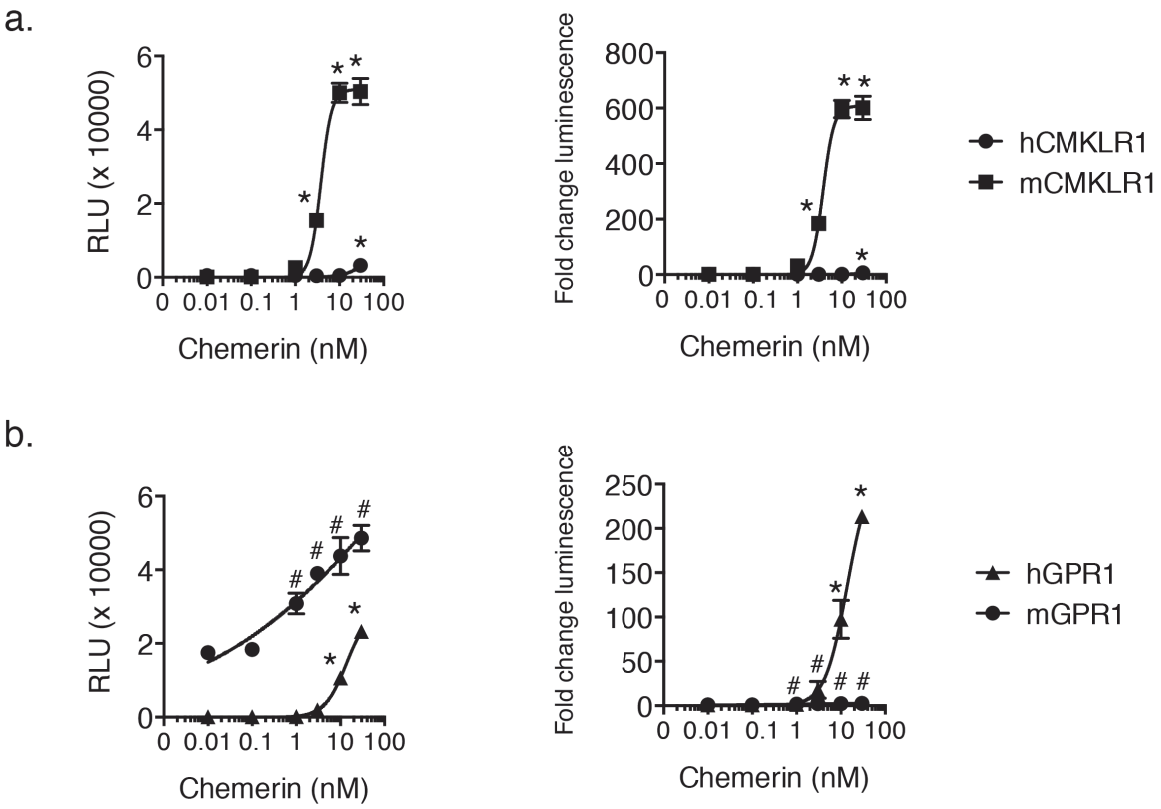
a.
RLU (x 10000)
Chemerin (nM)
Fold change luminescence
Chemerin (nM)
hCMKLR1
mCMKLR1
b.
RLU (x 10000)
Chemerin (nM)
Fold change luminescence
Chemerin (nM)
hGPR1
mGPR1

Figure 3.4

Figure 3.5: The DRY/DHY domain in GPR1 is required for basal receptor activity and chemerin sensitivity

Schematic representation of the amino acid sequence of human (h) and mouse (m) GPR1 within the 2nd intracellular loop. The DRY motif is highlighted with a blue box and denoted R when in the conserved DRY form or R* for the DHY form typically associated with constitutive activity. Numbers at the top represent amino acid location within the full protein (a). Site-directed mutagenesis was used to mutate the hGPR1 endogenous DHY to DRY (hGPR1 H135R) and the mGPR1 endogenous DRY to DHY (mGPR1 R135H) (b). These constructs were transfected into HTLA cells to assess receptor activation following treatment with increasing doses of chemerin. The resulting luminescent signal was expressed relative to β-galactosidase activity (RLU) N= 3. One-way ANOVA *$p<0.05$ vs. 0 nM chemerin within receptor. Two-way ANOVA # $p<0.05$ vs. endogenous receptor.

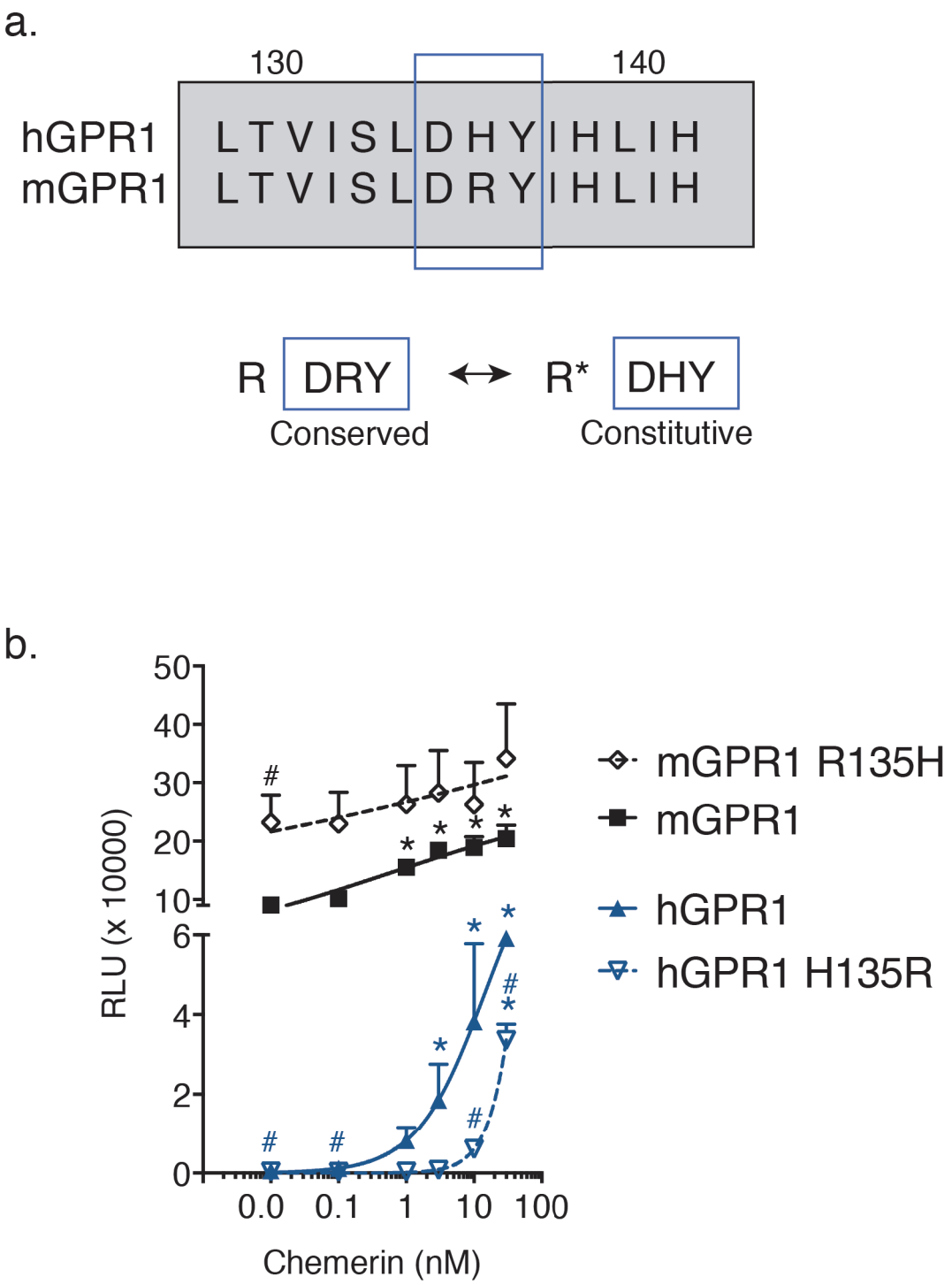
a.
130
140
hGPR1 L T V I S L D H Y I H L I H
mGPR1 L T V I S L D R Y I H L I H
R DRY ↔ R* DHY
Conserved
Constitutive
b.
RLU (x 10000)
50
40
30
20
10
6
4
2
0
0.0
0.1
1
10
100
Chemerin (nM)
mGPR1 R135H
mGPR1
hGPR1
hGPR1 H135R

Figure 3.5

Figure 3.6: Bioluminescence resonance energy transfer (BRET) with chemerin receptors

Schematic representation of the chemerin receptor BRET assay where CMKLR1 or GPR1 receptors that are tagged on their C-terminus with an EGFP protein (Excitation 460 nm, emission (Em) 520 nm) are transfected in combination with a renilla luciferase (luc) tagged arrestin protein (Em 460 nm) (a). When receptors are in the inactive (R) conformation, the arrestin-luc (donor) is too far away from the EGFP-receptor (acceptor) for the 460 nm luc emission to excite EGFP. Upon chemerin binding and conformational change to the R* active receptor confirmation, arrestin is recruited to the active receptor and is in close enough proximity to the receptor-bound EGFP to excite the EGFP, resulting in emission at 520 nm. To determine if the EGFP-tagged chemerin receptors were expressed at similar levels and whether transfection of either arrestin-2 (Arr2) or arrestin-3 (Arr3) luciferase fusion proteins altered chemerin receptor expression, total EGFP was examined in HEK293A cells transfected with the indicated combinations of arrestin and chemerin receptors under basal conditions (veh) or in the presence of 30 nM chemerin (che) by exciting the cells at 460 nm and measuring emission at 520 nm in the absence of luciferase substrate (b). To determine if chemerin receptor transfection alters the expression of arrestin-luciferase proteins, HEK293A cells transfected with the indicated combinations of receptors and arrestin were treated with luciferase substrate prior to measurement of total luminescence with and without chemerin treatment (c). N=3. Two-way ANOVA *$p<0.05$ compared across all possible combinations.

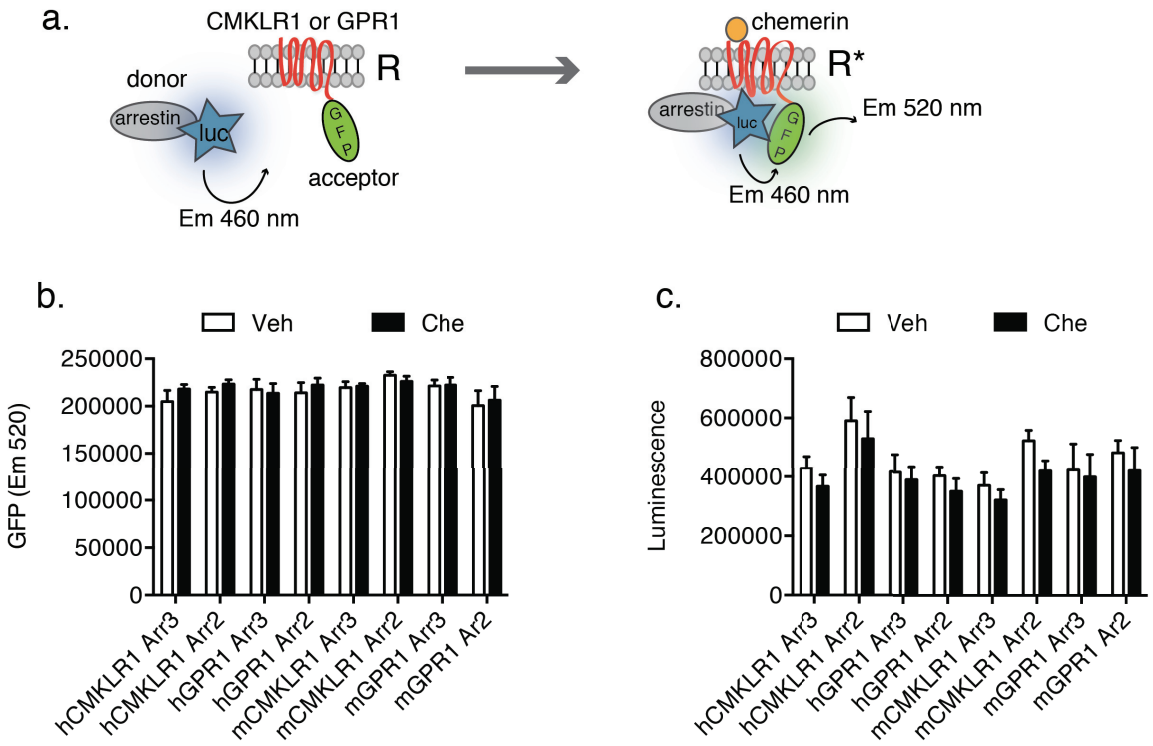
a.
CMKLR1 or GPR1
R
donor
arrestin
luc
G F P
acceptor
Em 460 nm
chemerin
R*
Em 520 nm
Em 460 nm
b.
Veh
Che
GFP (Em 520)
250000
200000
150000
100000
50000
0
hCMKLR1 Arr3
hCMKLR1 Arr2
hGPR1 Arr3
hGPR1 Arr2
mCMKLR1 Arr3
mCMKLR1 Arr2
mGPR1 Arr3
mGPR1 Ar2
c.
Veh
Che
Luminescence
800000
600000
400000
200000
0
hCMKLR1 Arr3
hCMKLR1 Arr2
hGPR1 Arr3
hGPR1 Arr2
mCMKLR1 Arr3
mCMKLR1 Arr2
mGPR1 Arr3
mGPR1 Ar2

Figure 3.6

Figure 3.7: Chemerin activation of hCMKLR1, hGPR1, and mCMKLR1 recruits both arrestin-2 and arrestin-3

To determine the extent of arrestin recruitment to unstimulated receptors, HEK293A cells were transfected with one of the EGFP-tagged chemerin receptors in combination with either luciferase-tagged arrestin-3 (Arr3) or arrestin-2 (Arr2) and the BRET ratio was determined under basal conditions 15 minutes (run 3) following luciferase substrate addition. N=3 (a). To examine the specificity of the measured BRET interaction, HEK293A cells were transfected with EGFP-tagged hCMKLR1 (hCMK-EGFP) or hGPR1 (hGPR1-EGFP) in combination with either luciferase-tagged arrestin-3 (Arr3-Rluc) or luciferase-tagged CD4 (CD4-Rluc), a membrane-associated protein with no known GPCR interaction (b). N=2 replicates from a single experiment. BRET ratio was determined 15 minutes following luciferase substrate addition. To examine chemerin receptor activation, HEK293A cells were transfected with one of the four indicated chemerin-EGFP receptors in combination with either Arr3 or Arr2. The BRET ratio was determined in cells treated with vehicle (veh) or 30 nM chemerin (che) over 5 successive measurements (1, 2, 3, 4, 5) and expressed as fold change relative to veh (V). N=3. Two-way ANOVA *$p<0.05$ as indicated (a) vs. veh (b) vs. veh within arr3/arr2 (c).

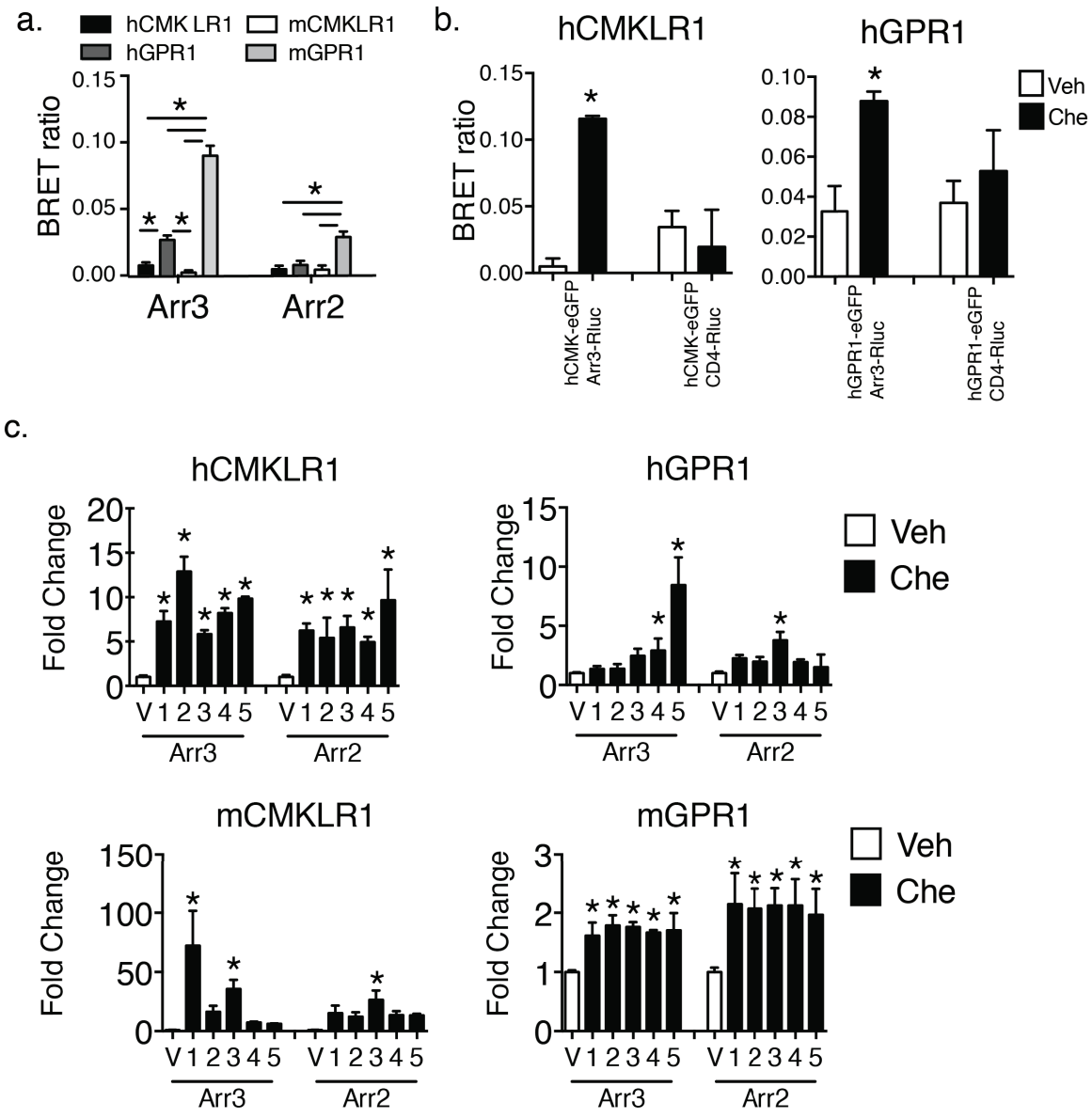
a.
hCMK LR1
hGPR1
mCMKLR1
mGPR1
BRET ratio
0.15
0.10
0.05
0.00
Arr3
Arr2
b.
hCMKLR1
hGPR1
BRET ratio
Veh
Che
hCMK-eGFP Arr3-Rluc
hCMK-eGFP CD4-Rluc
hGPR1-eGFP Arr3-Rluc
hGPR1-eGFP CD4-Rluc
c.
hCMKLR1
hGPR1
mCMKLR1
mGPR1
Fold Change
V 1 2 3 4 5
Arr3
Arr2
Veh
Che

Figure 3.7

Figure 3.8: $G\alpha_{i/o}$ is required for arrestin recruitment to both CMKLR1 and GPR1

Human (h) CMKLR1 or GPR1-tl-TA fusion receptors were transfected in HTLA cells to assess receptor activation following treatment with increasing doses of chemerin (Che) with or without 1 hour pre-treatment with the $G\alpha_{i/o}$ inhibitor pertussis toxin (PTX). The resulting luminescent signal was expressed relative to β-galactosidase activity as fold change luminescence relative to 0 nM chemerin treatment N= 3. Two-way ANOVA *$p<0.05$ vs. veh no PTX unless otherwise indicated.

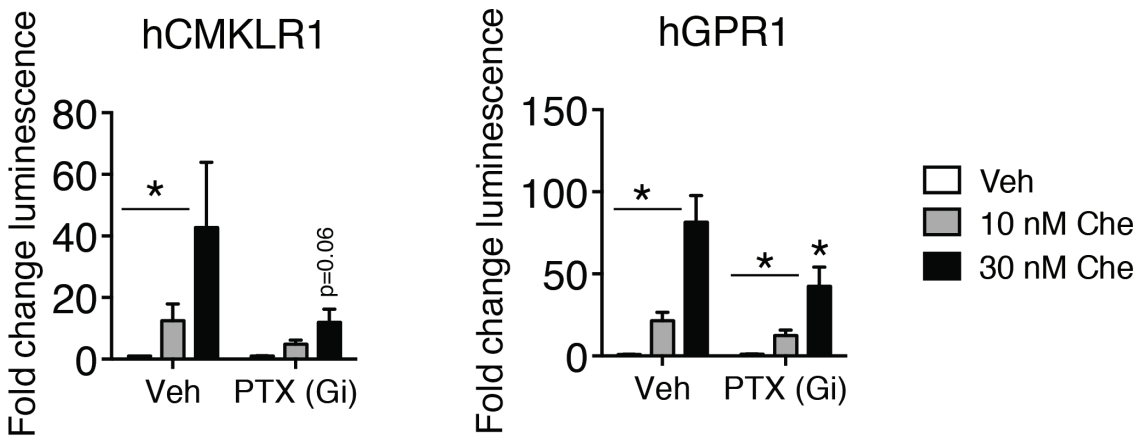
hCMKLR1
Fold change luminescence
80
60
40
20
0
*
p=0.06
Veh
PTX (Gi)
hGPR1
Fold change luminescence
150
100
50
0
*
*
*
Veh
PTX (Gi)
Veh
10 nM Che
30 nM Che

Figure 3.8

Figure 3.9: Chemerin activation of Ca^{2+} and cAMP signaling

CHO-A2 cells stably transfected with aequorin and $G\alpha_{16}$ were transfected with the indicated receptors and treated with either vehicle (veh) or 30 nM chemerin (Che) prior to detection of calcium (Ca^{2+})-dependent luminescence (a). Cells were treated with digitonin to induce maximal induction of Ca^{2+} release and data are presented as percent maximal digitonin response. HEK293A cells stably transfected with a luciferase reporter for the cAMP (b), pathway were transfected with either the pCDNA control or one of the four chemerin receptors (h: human, m: mouse) and treated with vehicle (veh) or with increasing doses of chemerin (che). Reporter cells were also treated with the adenylyl cyclase activator forskolin (5 μM) (FOR) alone or in combination with chemerin. Luciferase/β-galactosidase activity is expressed as fold change relative to veh. N=2 (a), N=3 (b). One-way ANOVA *$p<0.05$ vs. veh within receptor.

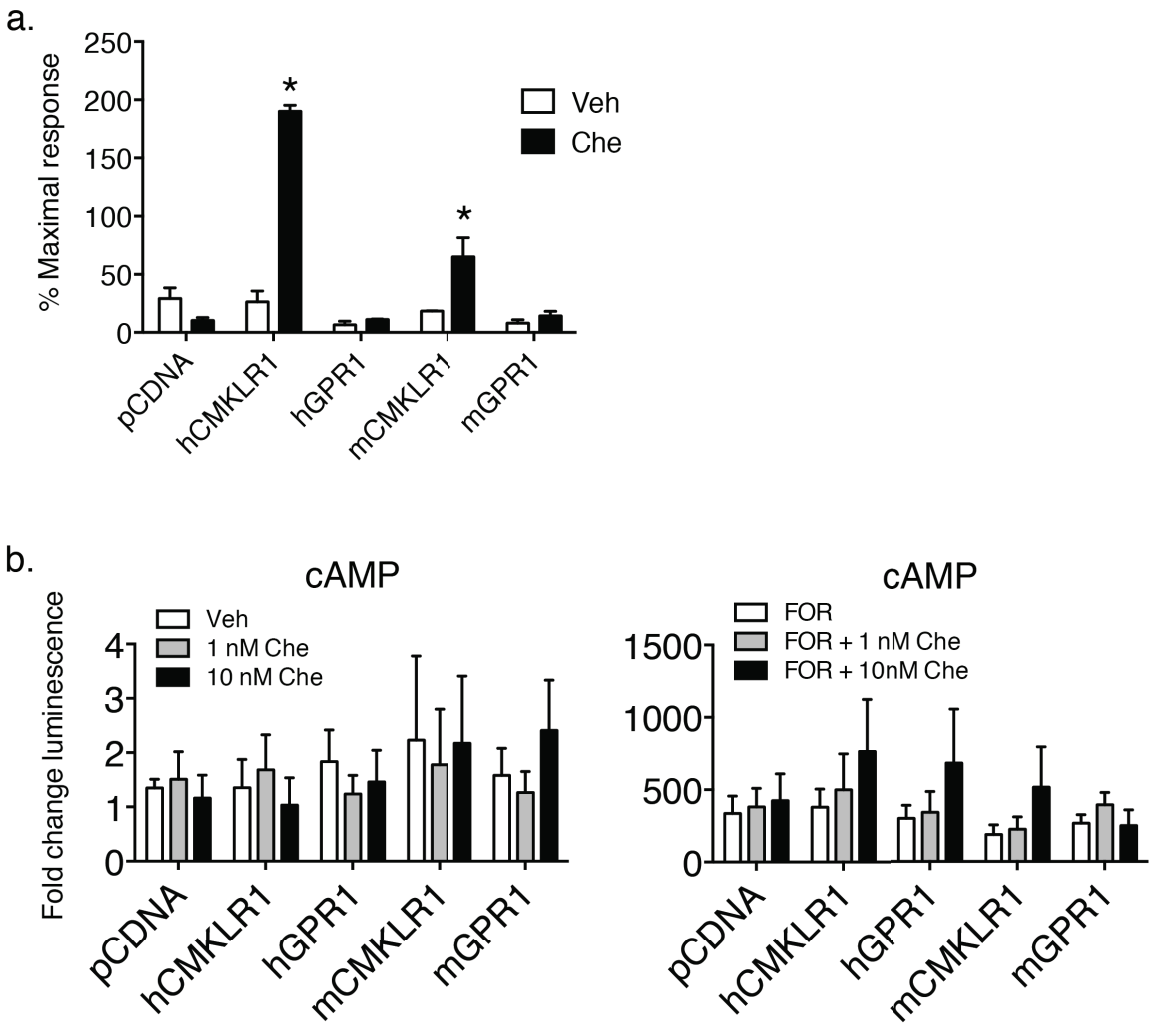
a.
% Maximal response
250
200
150
100
50
0
*
*
Veh
Che
pCDNA
hCMKLR1
hGPR1
mCMKLR1
mGPR1
b.
cAMP
Fold change luminescence
Veh
1 nM Che
10 nM Che
4
3
2
1
0
pCDNA
hCMKLR1
hGPR1
mCMKLR1
mGPR1
cAMP
FOR
FOR + 1 nM Che
FOR + 10nM Che
1500
1000
500
0
pCDNA
hCMKLR1
hGPR1
mCMKLR1
mGPR1

Figure 3.9

Figure 3.10: Chemerin activates MAPK/ERK and RhoA pathways

HEK293A cells stably transfected with the luciferase reporter for MAPK/ERK (a) or transiently transfected with the luciferase reporter for RhoA signal transduction (b) were transfected with either the pCDNA control or one of the four chemerin receptors (h: human, m: mouse) and treated with vehicle (veh) or with increasing doses of chemerin (che). Luciferase/β-galactosidase activity is expressed as fold change relative to veh. N=2 (a), N=3 (b). One-way ANOVA *$p<0.05$ vs. veh within receptor.

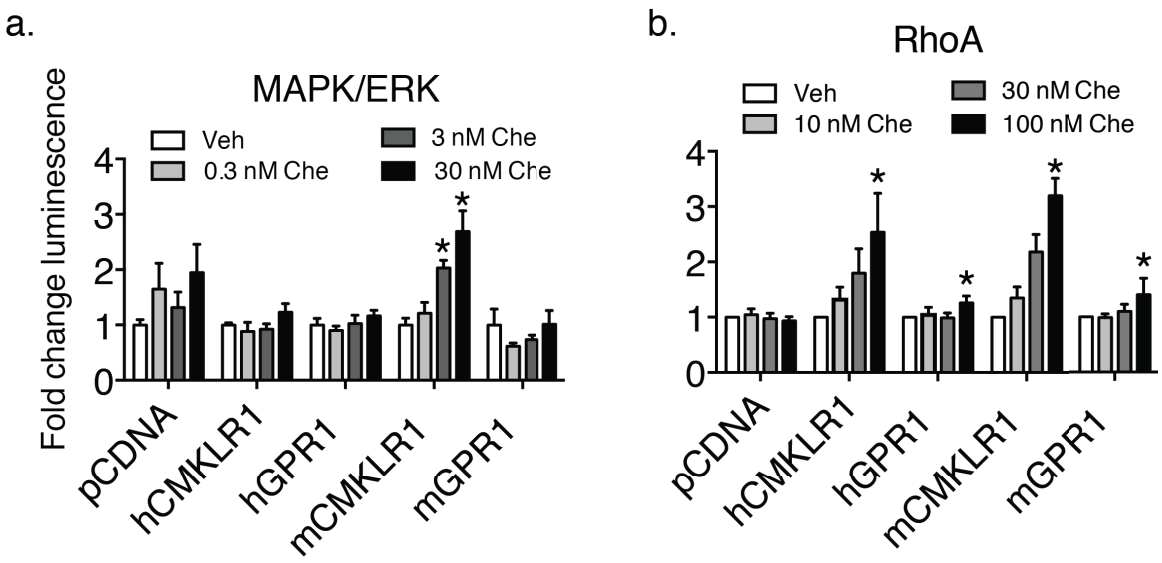
a.
MAPK/ERK
Fold change luminescence
Veh
0.3 nM Che
3 nM Che
30 nM Che
0
1
2
3
4
*
*
pCDNA
hCMKLR1
hGPR1
mCMKLR1
mGPR1
b.
RhoA
Veh
10 nM Che
30 nM Che
100 nM Che
0
1
2
3
4
*
*
*
pCDNA
hCMKLR1
hGPR1
mCMKLR1
mGPR1

Figure 3.10

Figure 3.11: CMKLR1 and GPR1 co-transfection does not alter receptor activation or chemerin sensitivity

To determine if chemerin receptor oligomerization could influence chemerin signaling CMKLR1 and GPR1 were co-transfected in HTLA cells (a & b), HEK293A-cAMP (c), or HEK293A-MAPK/ERK cells (d). To determine the impact of GPR1 co-transfection on CMKLR1 signaling, human (h) CMKLR1-tl-ta was co-transfected with pCDNA or untagged GPR1 (a) To determine the impact of CMKLR1 co-transfection on GPR1 signaling, hGPR1-tl-ta was co-transfected with pCDNA or untagged CMKLR1 (b). N=3 (a and b), N=2 (c, d). One-way ANOVA *p <0.05 vs. veh.

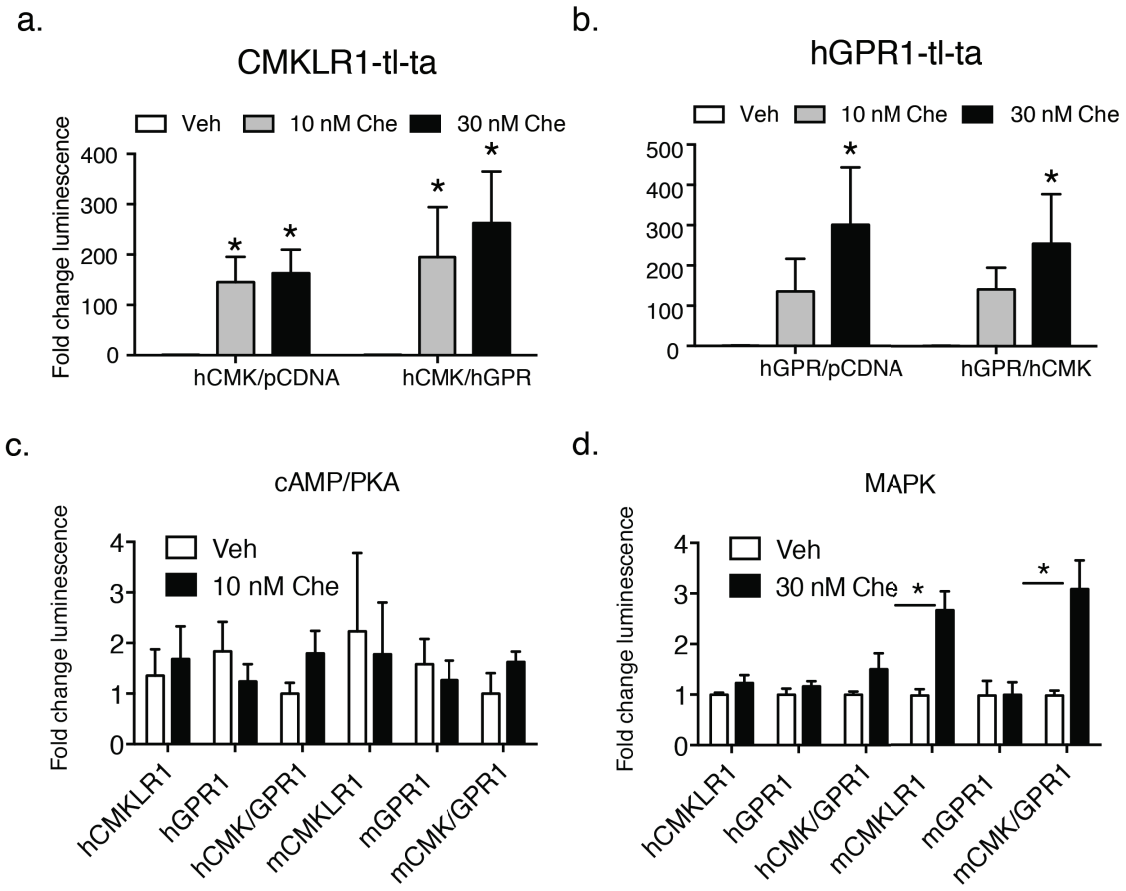
a.
CMKLR1-tl-ta
Veh
10 nM Che
30 nM Che
Fold change luminescence
400
300
200
100
0
hCMK/pCDNA
hCMK/hGPR
b.
hGPR1-tl-ta
Veh
10 nM Che
30 nM Che
500
400
300
200
100
0
hGPR/pCDNA
hGPR/hCMK
c.
cAMP/PKA
Veh
10 nM Che
Fold change luminescence
4
3
2
1
0
hCMKLR1
hGPR1
hCMK/GPR1
mCMKLR1
mGPR1
mCMK/GPR1
d.
MAPK
Veh
30 nM Che
Fold change luminescence
4
3
2
1
0
hCMKLR1
hGPR1
hCMK/GPR1
mCMKLR1
mGPR1
mCMK/GPR1

Figure 3.11

3.7 Tables

Table 3.1: Cloning and mutagenesis primers

Plasmid	Primer	Sequence
pCDNA4.3(B)-hCMKLR1-no tag	hCMKLR1-*Eco*RV Fw hCMKLR1-*Sac*II Rv	AAAAGATATCACGGAGAATGAGAATGGAGGATGA AAAACCGCGGTCAAAGCATGCCGGTCTCCCTCT
pCDNA4.3(B)-mCMKLR1-myc/his	mCMKLR1-*Eco*RI Fw mCMKLR1-*Sac*II Rv	AAAAGAATTCACGGTCTCCAAAGAGATGGAGTAC AAAACCGCGGGAGGGTACTGGTCTCCTTCTCATT
pCDNA4.3(B)-hGPR1- notag	hGPR1-*Eco*RV Fw hGPR1-*Sac*II- Rv	AAAAGATATCGCAAGATCATGGAAGATTTGGAGGAA AAAACCGCGGTTAATTGAGCTGTTTCCAGGAGACAC
pCDNA4.3(B)-mGPR1 – myc/his	mGPR1-*Eco*R1 Fw mGPR1- *Sac*II Rv	AAAAGAATTCCATGATCGAAGTCTCAAAGGAAATGTT AAAACCGCGGCTGGGCAGTTTCTAGGAGAGAGAG
pEGFP-N1-hCMKLR1	hCMKLR1-*Xho*I-Fw hCMKLR1-*Bam*HI-Rv	GCCGCTCGAGCCGCCACCATGAGAATGGAGGATGAAGATTACAACA GCCGGGATCCCCAAGCATGCCGGTCTCCCTCTCATTCATA
pEGFP-N1-mCMKLR1	mCMKLR1-EcoRI Fw mCMKLR1-SacII Rv	AAAAGAATTCACGGTCTCCAAAGAGATGGAGTAC AAAACCGCGGGAGGGTACTGGTCTCCTTCTCATT
pEGFP-N1-hGPR1	hGPR1-*Xho*I-Fw hGPR1-*Bam*HI-Rv	GCCGCTCGAGCCGCCACCATGGAAGATTTGGAGGAAACATTATTTGAAGAA GCCGGGATCCCCTTGAGCTGTTTCCAGGAGACACAGATT
pEGFP-N1-mGPR1	mGPR1-*Xho*I-Fw mGPR1-*Bam*HI-Rv	GGGCCCTCGAGACCATGGAAGTCTCAAAGGAAATGTTATTTGAGGAG GGGCCCGGATCCCCCTGGGCAGTTTCTAGGAGAGACAGGCT

Plasmid	Primer	Sequence
hGPR1 SDM	H135R Fw H135R Rv	GTGATCAGCCTGGACCGCTATATCCACTTGA TCAAGTGGATATAGCGGTCCAGGCTGATCAC
mGPR1 SDM	R135H Fw R135H Rv	TGATCAGCCTGGACCACTACATCCACTTGCTCC GGAGCAAGTGGATGTAGTGGTCCAGGCTGATCA

Table 3.2: Luciferase signaling reporters

Pathway	Transcr-iption Factor	Response Element	Response element sequence	Treat-ment Time (hr)
cAMP/PKA	CREB	CRE	TGACGTCA	6
MAPK/ERK	TCF/SRF	SRE	GGATGTCCATATTAGGA	6
RhoA	SRF	SRFRE	CCATATTAGGACATCTACCATGT	18

Chapter 4: Chemerin Activation of RhoA/ROCK Signaling is Required for CMKLR1- and GPR1-Mediated Chemotaxis

4.1 Rationale and Objectives

The results presented thus far demonstrate both distinct and overlapping signaling properties of the chemerin receptors CMKLR1 and GPR1. Specifically, neither receptor appears to activate cAMP-mediated signaling, while CMKLR1 but not GPR1 activates MAPK pathway signaling. Of particular interest from this work is the observation that both CMKLR1 and GPR1 receptors appear to activate signal transduction in the RhoA/SRF pathway. These pathways play a critical role in actin cytoskeleton reorganization, cell motility, proliferation and survival in numerous cell types. As such, the second objective of this thesis was to investigate how and to what extent chemerin signaling activates MAPK and SRF and the impact of this signal transduction on the well-established ability of chemerin to promote cell migration. To investigate this we used pharmacological inhibitors of RhoA, MAPK, and $G\alpha_{i/o}$ pathway signaling in combination with the SRF-RE luciferase reporter, and models of chemerin-mediated chemotaxis.

Components of this chapter will be included with chapter 3 for manuscript submission.

4.2 Introduction

SRF is a versatile homodimeric transcription factor expressed in numerous cell types. Serum, bioactive lipids and the ligands of numerous GPCRs activate signal transduction cascades that activate SRF and the expression of a variety of SRF target genes, including signaling effector proteins, transcription factors, and components of the cytoskeleton (281-283). SRF regulation of gene expression contributes to multiple cellular functions including cell survival, apoptosis, muscle differentiation, and regulation of actin cytoskeletal dynamics (284-288). Dysfunction in SRF-mediated transcriptional

regulation is associated with human diseases in almost all organ systems, including cardiovascular, integumentary, hematopoietic, pancreatic, skeletal muscle, and CNS (289). Moreover, increased SRF function is associated with tumorigenesis and cancer cell motility in multiple cancer types (290-293). Thus, a better understanding of the extracellular stimuli that modulate SRF transcriptional activity could have application in numerous biological settings.

By complexing with other transcriptional regulators in the nucleus, SRF couples upstream signaling cascades to the coordinated expression of distinct target gene subsets (281) (Fig 4.1). SRF is localized within the nucleus where it binds with high affinity to a conserved DNA sequence, known as the CArG box, which is located within the promoter of hundreds of SRF target genes (294-298). SRF binding to the CArG box serves as a scaffold for the recruitment of various cofactors and transcription factors (299). Two major classes of SRF cofactors couple distinct signal transduction cascades to specific subsets of SRF target gene expression. Signaling through a MAPK pathway activates the ternary complex factor (TCF) transcriptional coactivators and subsequent activation of a TCF-dependent subclass of SRF target genes (300). RhoA pathways and actin cytoskeleton changes activate the myocardin-related transcription factors (MRTFs) and expression of a different subset of SRF target genes (287). In this way SRF, TCFs, and MRTFs couple extracellular stimuli to the expression of specific target genes essential for cell survival, apoptosis, and regulation of the actin cytoskeleton.

Extracellular stimuli that result in Rho-GTPase signaling and/or rearrangement of the actin cytoskeleton are coupled to the expression of genes required for supporting cytoskeletal reorganization and motility through the MRTF family of transcription factors (287). Normal physical changes in cell shape, cell-cell contact, motility, differentiation, and adhesion require dynamic cytoskeletal reorganization and expression of numerous SRF-MRTF target genes. In the unstimulated state, MRTFs are restrained in the cytoplasm by G-actin (301). Through $G\alpha_{12/13}$, $G\alpha_{i/o}$, and $G\alpha_{q/11}$-coupled GPCRS, extracellular stimuli such as serum, growth factors, and cytokines activate the Rho family of GTPases, including CDC42, Rac, and RhoA, which serve as molecular switches to modulate actin polymerization and MRTF release (Fig. 3.1) (302,303). RhoA activation of rho-associated kinase (ROCK), for example, stimulates G-actin polymerization into

filamentous actin (F-actin) fibers and the subsequent release and translocation of MRTFs from the cytoplasm to the nucleus (301,304). Once in the nucleus MRTFs interact with SRF and induce expression of required structural and regulatory genes, including components of the cytoskeleton (actin itself), actin regulators (vinculin), and several regulatory micro-RNAs (288). As such, the Rho- actin- MRTF-SRF pathway links extracellular signaling through Rho-GTPases and changes in the actin cytoskeleton to required changes in the cytoskeleton and gene expression to ultimately support dynamic changes in cellular shape, differentiation, and motility.

In addition to cytoskeletal maintenance through MRTF-dependent gene expression, SRF interaction with TCFs couples extracellular growth signals and MAPK signaling to changes in survival and apoptosis gene expression (300). Mitogenic stimuli such as serum, lysophosphatidic acid (LPA), and platelet-derived growth factor activate Ras-Raf-MEK-ERK kinase cascades that ultimately result in TCF phosphorylation and activation (305). Activated TCFs are targeted to the nucleus where they bind to SRF and a specific DNA sequence known as the E26 transformation-specific (ETS) domain, which adjoins the SRF-bound CArG box. This combination of CArG and ETS domains in gene promoters is called the serum-response element (SRE) and is found in the promoters of growth-related immediate early genes, including numerous transcription factors (*FOS*, *EGR1, JUNB),* and cell cycle/apoptosis, genes (*MCL-1 and NUR77)* for regulation of cell growth and differentiation (284,285,306).

Several mechanisms exist to integrate the input from multiple simultaneous signals for control of SRF target gene expression. This is particularly relevant for extracellular stimuli, such as LPA, that activate both Rho-GTPase and MAPK pathways. In some cases, cell-type specific expression of either TCF or MRTF determines the pattern of gene expression. This is the case with the MRTF myocardin whose selective expression in muscle cells favours the induction of muscle specific gene expression programs required for differentiation and contractility (307-309). In other cell types where the TCF and MRTF families are co-expressed, these coactivators must compete for a common SRF binding site allowing activation of one pathway to antagonize the other (285,310). An example of this is the inhibition of MRTF-regulated smooth-muscle gene expression by the TCF cofactor ELK-1 (285). Additionally, the presence or absence of an

ETS domain adjacent to the CArG box contributes to the selectivity of gene expression and the dependence on MAPK or RHO pathway activation demonstrating the importance of the promoter sequence itself for pathway sensitivity (311). Given the diversity of mechanisms regulating the selectivity of SRF target gene activation, the outcome of a particular stimulus is often cell-type and context-specific limiting prediction of TCF/MRTF selectivity.

We predicted that CMKLR1 and GPR1 activation of $G\alpha_{i/o}$, $G\alpha_{q/11}$, and $G\alpha_{12/13}$ could activate MAPK or Rho-GTPases suggesting the potential for chemerin mediated signaling to SRF. Although no studies have examined chemerin activation of SRF, many established chemerin functions require cytoskeletal reorganization, proliferation/differentiation-specific gene expression programs, and changes in cellular morphology/motility suggesting a possible requirement for SRF. In this regard, immune cell chemotaxis, one of the best-characterized chemerin functions, has a well-established dependence on Rho-GTPases and SRF (288,312). SRF is also a critical regulator of muscle cell differentiation (286). Likewise, chemerin has been shown to play a role in myoblast proliferation and differentiation both *in vitro* and *in vivo* (157,313). Moreover, CMKLR1 and chemerin are required for coordinating the differentiation programs for mesenchymal and hematopoietic stem cells, pathways for which RhoA/SRF regulation is known to be important (181,228,314-316). Consistent with this, Fig 3.1b shows that chemerin treatment of HEK293 cells expressing either CMKLR1 or GPR1 activates the RhoA-dependent SRF-RE reporter. Despite the extensive overlap between known chemerin signaling/function and the established roles of the SRF pathway, Rho-GTPases and SRF have not been examined with respect to any known chemerin function.

4.3 Materials and Methods

4.3.1 Cell Lines and Culture

All cells were maintained under standard growth conditions (37^{o}C in 95% air, 5% CO_2). HEK293A cell line (Life Technologies; Burlington, ON Canada, cat# R70507) was maintained in DMEM (Life Technologies; Burlington, ON Canada, cat# 11965-092).

Murine pre-B lymphoma L1.2 cells were generated previously (174). L1.2 and human gastric adenocarcinoma cells (AGS) (ATCC; Manassas, VA, USA, cat# CRL-1739) were maintained in Roswell Park Memorial Institute (RPMI) 1640 (Life Technologies; Burlington, ON Canada, cat# 11875093. All media were supplemented with 10% fetal FBS and penicillin (100 units/ml) streptomycin (100 μg/ml) (Life Technologies; Burlington, ON Canada, cat# 15140-122), unless otherwise indicated.

4.3.2 Reagents and Inhibitors Used

Cells were treated for the indicated times with: 10 μM LPA (Sigma Aldrich; Oakville, Ontario, Canada, cat# L7260); 0.005- 100 nM recombinant human (MyBioSource; San Diego, CA, USA, cat# MBSK13851) or mouse (R&D Systems; Minneapolis, ME, USA, cat# 2325-CM-025/CF) chemerin-157; 10 μM ROCK inhibitor Y27632 (Cayman Chemical; Ann Arbor, MI, USA, cat#10005583); 10 μM p38 inhibitor SB203580 (Cell Signaling; Danvers, MA, USA, cat # 5633); 10 μM MEK1/2 inhibitor U0126 (Cell Signaling; Danvers, MA, USA, cat # 5633); 1.0 μg/ml Rho inhibitor cell-permeable C3 transferase (Cytoskeleton; Denver, CO, USA, cat # CT04); 100 ng/ml PTX (Sigma Aldrich; Oakville, Ontario , cat# P7208).

4.3.3 Plasmids and Stable Cell Generation

Chemerin receptor-expressing constructs were generated as described in section 3.3.2. HEK293A cells were transiently transfected with pEGFP-N1-hCMKLR1 and selected with 0.4 mg/ml G418 for two weeks prior to individual clone selection for generation of stable HEK293A-hCMKLR1 cells. Human RhoA shRNA pGIPZ vectors (GE Dharmacon): RA1 V2LHS_132702 (target sequence: AAGAAATTCCTTGAATTAG), RA2 V3LHS_646048 (target sequence: TACACAGTAACTATAAGGT), and RA3 V3LHS_642222 (target sequence: ATAACATCGGTATCTGGGT) or the non-silencing shRNA control RHS4346 were transiently transfected into HEK239A cells and stably selected using 5 μg/ml puromycin.

3.3.4 RNA Isolation and Quantitative PCR

Cells were lysed in RLTplus buffer and RNA was isolated using the RNeasy mini plus kit (Qiagen; Germantown, MD, USA, cat #74134) according to the manufacturers instructions. Reverse transcription was used to generate cDNA from 0.5 μg of isolated RNA using RNA to cDNA EcoDry premix (Clontech; Mountain View, CA, cat# 639549). Exon- spanning quantitative real-time PCR (qPCR) primers were designed using the NCBI primer BLAST (Table 4.1). Gene expression was measured using the Roche FastStart SYBR green Master (Roche; Laval, QC, cat# 04673484001) on a Light Cycler 96 instrument according to the manufacturers instructions. Relative gene expression was calculated using the ΔΔCt method (317) with glyceraldehyde 3-phosphate dehydrogenase (*GAPDH*) as the reference gene.

4.3.5 Signaling Luciferase Reporter Assays

SRF-RE and MAPK/ERK reporter assays were performed essentially as described in section 3.3.5 with the following modifications. Following transfection, medium was replaced with serum-free Opti-MEM for 24 hours (4 hour chemerin treatments) or 4 hours (18 hour chemerin treatments) prior to addition of concentrated treatments. Inhibitors were pre-incubated for 2 hours prior to treatment. Cells were pretreated with PTX for 24 hours prior to chemerin treatment. Luminescence measurements were done using a FluoStar Omega plate reader.

4.3.6 CMKLR1 and GPR1 Receptor Tango Bioassay

See section 3.3.3.

4.3.7 Immunoblotting

HEK293A cells stably expressing either the control shRNA, RA1, RA2, or RA3 were trypsinized, collected by centrifugation, and lysed in cell lysis buffer (Cytoskeleton;

Denver, CO, USA, cat#BKO36) containing 1x protease/phosphatase inhibitor (Pierce; Rockford, IL, USA, cat# 78443) for 1 hour at 4^{o}C with constant neutation. Lysate was cleared by centrifugation for 2 minutes at 10,000 x g and stored at -80^{o}C prior to use. Sodium dodecyl sulphate (SDS) loading buffer was added to 100 μg of protein, and boiled for 5 minutes prior to separation on a 15% polyacrylamide gel and transferred for 45 minutes at 75 V to a PVDF membrane. Membranes were dried for 30 minutes, rehydrated in methanol, rinsed in Tris-buffered saline containing 0.1% Tween (TBST), blocked for 30 minutes with 5% milk in TBST, and then incubated with a monoclonal mouse anti-RhoA antibody (1:300) in TBST (Cytoskeleton; Denver, CO, USA, cat# ARH03) overnight at 4^{o}C with constant neutation. Membranes were gently washed in TBST prior to incubation with a goat anti mouse IgG horseradish peroxidase (HRP) conjugated secondary antibody (1:5000) in TBST (Biorad; Mississauga, ON, Canada, cat# 172-1011) for 1 hour at room temperature. Immunoreactivity was detected by incubation with fluorescent ECL-plus western blotting substrate (Pierce; Rockford, IL, USA, cat# 32132) and visualized using a Kodak Image Station. Goat anti-beta-actin (Abcam; Toronto, ON, Canada, cat# AB8229) (1:1000) in TBST/1% milk and rabbit anti-goat IgG HRP (SantaCruz; Dallas, TX, USA cat# SC2768) were used for the protein loading control.

4.3.8 Chemotaxis Assays

L1.2 lymphocyte cells: L1.2 pre-B lymphocytes were maintained in logarithmic growth between 1.5 and 2.0 x 10^6 cells/ml with complete medium (RPMI 1640 +10% FBS) replacement every day. Cells were split at 1.0 x 10^6 cells/ml the day before migration and incubated overnight in 5 nM butyric acid. Cells were collected by centrifugation, resuspended in chemotaxis medium (RPMI 1640 + 1% FBS) containing 2.5 μM calcein AM (Life Technologies; Burlington, ON Canada, cat# C3100MP) and incubated for 90 minutes at 37^{o}C under normal growth conditions to label live cells. Labeled cells (25,000 per well) were placed in the upper chamber of a transwell permeable support migration insert (Corning; Corning, NY, USA, Cat# 3421). Treatments (600 μl) in chemotaxis medium were placed in the lower chamber as indicated. Cells were allowed to migrate

under normal growth conditions for 4 hour prior to collection by centrifugation, resuspension in PBS and measurement of calcein Am fluorescence with excitation/emission filters 485/520 nm on a Fluostar Omega plate reader and expressed as fold change over 0 nM chemerin vehicle control. Where indicated, cells were pretreated with inhibitors for 1 hour prior to migration.

AGS cells: AGS gastric carcinoma cells were maintained in logarithmic growth at 40 to 70% confluence with complete medium (RPMI 1640 + 10% FBS) replacement every 2 – 3 days. Cells were trypsinized, collected by centrifugation and resuspended in serum-free RPMI medium. Cells (1.0×10^5 per well) were added to the upper chamber of 8 μm pore ThinCert tissue culture inserts (Greiner Bio One; Monroe, NC, USA, cat# 662638). Treatments (600 μl) in serum-free medium were placed in the lower chamber as indicated. Cells were treated with inhibitors for 15 minutes prior to migration, as indicated, and allowed to migrate under normal growth conditions for 24 hours. Non-adherent cells were removed from the upper chamber prior to adherent cell fixation in 100% methanol at -20^{o}C for 15 minutes. Cells adhered to the upper side of the membrane were removed using a cotton swab and the insert was washed 2x in ice-cold PBS. Migrated cells adhered to the lower side of the insert were labeled for 15 minutes in 1 mg/ml HOESCHT 33258 for 15 minutes. Inserts were washed in PBS, carefully removed and mounted on glass slides using aqueous mounting medium (Sigma Aldrich; Oakville, Ontario, Canada, cat# F4680). Five random-field images per insert were obtained at 40X magnification using a Zeiss Axiovert 200 with a Hamamatsu Orca R2 camera. Stained cells on the underside of each membrane were counted visually and expressed as fold change over vehicle control.

4.3.9 Thymidine Incorporation Cell Proliferation Assay

Log phase cells were plated at 30,000 (HEK293A-hCMKLR1-EGFP) or 15, 000 (AGS) cells/ml in 24-well plates and allowed to adhere for 18 hours. Cells were serum-starved for 24 hours and then treated as indicated. Replicating DNA was labeled by incubating cells for 1 hour at 37^{o}C with 1 μCi/ml [methyl-^{3}H] thymidine (Perkin Elmer;

Woodbridge, ON, Canada, cat# NET027L001MC). Following culture medium removal, cells were washed 2x in ice-cold PBS, prior to fixation and precipitation in 10% tri-chloroacetic acid for a minimum of 1 hour at 4^{o}C. Tri-chloroacetic acid was removed, rinsed away with 100% ethanol and plates were allowed to dry at room temperature. The adhered monolayer was dissolved in 700 µl 0.1N NaOH/1% SDS and neutralized with 13 µl of 1.0 M HCl. 100 µl of the resulting suspension was added to 6 ml of EcoLite liquid scintillation fluid (MP Biomedicals; Santa Ana, CA, USA, cat# 0188247501) and radioactivity measured using a LS 6500 liquid scintillation counter (Beckman Coulter; Brea, CA, USA).

4.3.10 Statistical Analyses

All data are expressed as mean ± SEM. Comparisons were performed using a repeated measures, one- or two-way ANOVA, or two-tailed t-test, as indicated with Holm-Sidak multiple comparisons test.

4.4 Results

4.4.1 SRF-RE Activation by Rho Family GTPases and LPA

To examine the potential for chemerin activation of Rho-GTPase signaling and SRF we used an SRF luciferase reporter system. This reporter was developed for specific detection of RHOA-mediated SRF activation; however, sensitivity of the reporter to other RHO GTPases was unclear in the manufacturer's specifications. Therefore, specificity of the SRF-RE for RHO pathway activation was established by co-transfecting HEK293A cells with SRF-RE in combination with constitutively active members of the rho family GTPases (Rac, CDC42, or RhoA) or by treating with various doses of the RhoA (C3T) and ROCK (Y27632) inhibitors (Fig. 4.2). Constitutively active CDC42 expression and to a much greater extent RhoA expression resulted in significant activation of the SRF-RE reporter (Fig. 4.2a). Constitutively active Rac did not activate SRF-RE. To determine the responsiveness of the SRF-RE system to activation by extracellular stimuli, SRF-RE-expressing cells were treated with vehicle, or the bioactive lipid LPA, a known activator of the SRF pathway (318) (Fig. 4.2b). LPA treatment resulted in significant activation of the SRF pathway with all treatment times. LPA treatment (4 hours) produced the largest SRF activation, reaching levels approximately 70-fold higher than those observed with vehicle treatment and declining rapidly with increasing treatment time. To determine the dependence of this observed activation on RhoA pathway signaling, cells were treated with LPA for 4 hours in combination with increasing doses of the RhoA inhibitor C3T (Fig. 4.2c) or Y27632, an inhibitor of the RhoA target protein ROCK (Fig. 4.2d). Significant dose-dependent SRF inhibition occurred with both C3T and Y27632. Neither high dose C3T (2 μg/ml) nor Y27632 (50 μM) were sufficient to reduce SRF activation to those observed in the absence of LPA treatment.

4.4.2 Chemerin Activates SRF-RE

To determine if chemerin can activate SRF-dependent transcriptional regulation, HEK293A cells were transfected with the luciferase reporter SRF-RE alone or in

combination with either an empty vector (pCDNA) control or one of the chemerin receptors: human (h) CMKLR1, hGPR1, mouse (m) CMKLR1, or mGPR1 (Fig. 4.3). Treatment of these cells with increasing doses of chemerin for 4 hours resulted in a significant and dose-dependent increase in SRF reporter activation for all 4 chemerin receptors tested (Fig. 4.3a). No activation was seen in cells transfected with the empty vector pCDNA control. SRF-reporter activation was highest for h- and mCMKLR1 reaching 20- to 30-fold activation relative to no chemerin treatment. GPR1-mediated activation of SRF transcriptional activity achieved with 100 nM chemerin was 2- to 5-fold higher than vehicle treatment.

4.4.3 CMKLR1 and GPR1 Activation of SRF-RE is Dependent Upon $G\alpha_{i/o,}$ RhoA, and ROCK

CMKLR1 has been reported to couple to a PTX- sensitive $G\alpha_{i/o}$ protein (170,184), while no G protein dependence has been reported for GPR1. To determine if the observed activation of SRF-mediated transcription was $G\alpha_{i/o,}$ dependent, HEK293A cells were transfected with SRF-RE and treated with 30 nM chemerin in combination with either PTX or vehicle control (Fig. 4.3b). Cells transfected with empty vector pCDNA control were not activated by chemerin and were not sensitive to PTX. Chemerin significantly increased SRF activation in cells transfected with CMKRL1 or GPR1. This SRF activation was significantly reduced in the presence of PTX with all four chemerin receptors. PTX treatment was sufficient to reduce chemerin-mediated SRF activation to a level similar to that observed in untreated cells for hGPR1 and mGPR1 but not hCMKLR1 or mCMKLR1.

GPCR-mediated activation of RhoA plays a well-established role in SRF activation (279,283). To determine if chemerin receptor activation of SRF was mediated through a RhoA-dependent pathway, cells transfected with the SRF-RE and pCDNA control or a chemerin receptor, were treated with 30 nM chemerin in combination with either C3T (RhoA inhibitor), Y27632 (ROCK inhibitor), or vehicle control (Fig. 4.3c). Cells transfected with the empty vector pCDNA control were not activated by chemerin and were not sensitive to C3T or Y27632. Both C3T and Y27632 significantly reduced

chemerin activation of SRF through all four receptors tested. C3T and Y27632 were sufficient to reduce chemerin-mediated SRF activation to a level similar to that observed in untreated cells for hGPR1, mCMKLR1, and mGPR1. C3T treatment of cells transfected with hCMKLR1 significantly reduced chemerin-mediated SRF activation; however, under these conditions SRF activation remained significantly higher than the no chemerin control. SRF activation of chemerin treated cells transfected with hCMKLR1 was reduced to levels similar to the no chemerin control with Y27632.

GPCR signal transduction is rapidly inactivated following arrestin recruitment to the activated receptor (276). Given that the chemerin receptors recruit arrestin following activation, we looked at SRF activation following a longer 18-hour treatment to determine the impact of treatment length on activation of this pathway (Fig. 4.4). Both FBS and LPA treatment resulted in significantly reduced activation of the SRF pathway when compared with the 4-hour treatment (Fig 4.2 vs. Fig. 4.4) with maximal levels for LPA and FBS treatments reaching 4-fold and 10-fold activation when compared with vehicle (Fig. 4.4a). A low dose of C3T (0.5 μg/ml) or Y27632 (10 μM) was sufficient to completely inhibit 18-hour LPA activation (Fig. 4.4b, c). Accordingly, when HEK293A cells transfected with the SRF-RE in combination with pCDNA or one of the chemerin receptors (Fig. 4.5) were treated with increasing doses of chemerin for 18 hours (Fig. 4.5a), SRF activation was reduced when compared with 4-hour treatments (Fig. 4.3a). Maximal SRF activation was observed for cells transfected with hCMKLR1 and mCMKLR1 at approximately 2- to 3-fold higher than vehicle and no activation was present in cells transfected with either hGPR1 or mGPR1. Y27632 reduced SRF activation below those observed with vehicle in chemerin treated cells transfected with pCDNA (Fig. 4.5b). The activation of SRF observed with chemerin treatment in cells transfected with hCMKLR1or mCMKLR1 was completely lost with both C3T and Y27632 treatment.

Given the sensitivity of the SRF-RE to both RhoA and CDC42, we further investigated the RhoA dependence of chemerin signaling by knocking down RhoA using three shRNA-expressing constructs: RA1, RA2, and RA3 (Fig. 4.6). Following transfection with and stable selection of HEK293A cells transfected with RA1, RA2, RA3, or a control non-targeting shRNA expressing a sequence with no homology to any

known human gene, RhoA mRNA levels were measured by qPCR to determine the extent of RhoA knockdown (Fig. 4.6a). Transfection with RA1, RA2, or RA3 resulted in greater than 50 % reduction in RhoA mRNA. RhoA protein was reduced in cells transfected with RA1, RA2, and RA3 when compared with control, with almost complete RhoA loss in cells transfected with RA3 (Fig. 4.6b). Cntrl, RA2, and RA3 transfected cells were used to determine the impact of RhoA loss on chemerin-mediated SRF activation (Fig. 4.6c). Activation of SRF was unchanged with RhoA knockdown when compared with control shRNA in cells transfected with pCDNA, as well as in vehicle treated cells transfected with the chemerin receptors. RhoA knockdown using the RA2 shRNA significantly, but not completely, reduced chemerin activation of SRF through hCMKLR1. RA2 shRNA was sufficient to completely abrogate chemerin activation of SRF through hGPR1, mCMKLR1 and mGPR1. Similarly, RhoA knockdown with the RA3 sequence completely blocked chemerin activation of SRF through hCMKLR1, hGPR1, mCMKLR1, and mGPR1.

4.4.4 Chemerin Enhances LPA-mediated SRF-RE Activation

The signaling lipid LPA is a well-established and potent activator of RhoA and SRF (318). To determine if chemerin receptor signaling could influence LPA-mediated SRF activation, HEK293A cells, which endogenously express several LPA receptor isoforms (319), were transfected with SRF-RE and either empty vector pCDNA control or a chemerin receptor. These cells were treated with chemerin or LPA alone or in combination (Fig. 4.7). Consistent with activation of the endogenously expressed LPA receptors, LPA induced a 30-fold increase in SRF activation in cells transfected with the empty vector pCDNA control. Addition of 30 nM chemerin, either alone or in combination with LPA had no effect on pCDNA-transfected cells (Fig. 4.7a). Addition of 30 nM chemerin in combination with LPA resulted in SRF activation that was significantly greater than with LPA alone in the presence of hCMKLR1, mCMKLR1, and mGPR1 but not with either hGPR1 or pCDNA.

4.4.5 Chemerin Enhancement of LPA-mediated SRF-RE Activation Requires $G\alpha_{i/o}$, RhoA, and ROCK

PTX was used to determine if the observed enhancement of LPA-mediated SRF activation was $G\alpha_{i/o}$-dependent in HEK293A cells transfected with SRF-RE in combination with one of the chemerin receptors. SRF activation was measured in response to LPA alone or a combination of LPA with 30 nM chemerin in the presence of either PTX or vehicle control (Fig. 4.7b). LPA-mediated activation of SRF was unaffected by PTX regardless of chemerin receptor transfection. The chemerin-mediated enhancement of LPA-induced SRF activation observed with hCMKLR1 and mCMKLR1 was unchanged with PTX treatment. In contrast, chemerin-mediated enhancement of LPA-induced SRF activation was lost with PTX treatment in cells transfected with mGPR1. C3T and Y27632 inhibitors were used to determine if RhoA and ROCK also play a role in mediating chemerin receptor enhancement of LPA signaling to SRF (Fig. 4.7c). C3T and Y27632 significantly reduced SRF activation with LPA alone in cells transfected with pCDNA, hCMKLR1, hGPR1, or mGPR1. Co-treatment with chemerin and LPA was similar to treatment with LPA alone when cells transfected with hCMKLR1, or mGPR1 were treated with either the RhoA or ROCK inhibitors. In contrast, RhoA and ROCK inhibition were insufficient to reduce LPA alone activation of SRF in cells transfected with mCMKLR1. Moreover, while SRF activation in response to the combined LPA chemerin treatment was significantly lower with C3T and Y27632 when compared with no inhibitor treatment, the inhibitors were not sufficient to completely block the enhancing effects of chemerin through mCMKLR1.

There are six known LPA receptors: LPAR1-6 (320). We measured the mRNA expression of LPAR1-6 to determine which LPA receptors are expressed endogenously in HEK293A cells (Fig. 4.8a). We were unable to generate reliable primers for the detection of LPAR4 in these cells. LPAR1 and 2 were most abundant and were significantly higher than LPAR3, LPAR5, and LPAR6. To determine the dependence of chemerin-mediated SRF activation on LPA-receptor activation, HEK293A cells transfected with SRF-RE in combination with the chemerin receptors were treated with LPA alone, or in combination with 30 nM chemerin in the presence of Ki16425, an LPAR1 and LPAR3 antagonist (Fig.

4.8b). Ki16425 significantly reduced LPA-mediated SRF activation in cells transfected with pCDNA, and mGPR1. Cells transfected with hCMKLR1, mCMKLR1, or hGPR1 were protected from this loss of LPA-induced SRF activation. In cells transfected with hCMKLR1, mCMKLR1, or mGPR1 chemerin significantly increased LPA-mediated SRF activation in the presence of vehicle. With the exception of mCMKLR1, this chemerin-enhanced effect was lost with Ki16425 treatment.

To investigate the possibility that LPA could modify chemerin receptor activation we used the Tango bioassay to measure CMKLR1 or GPR1 activation in HTLA cells (Fig. 4.8c). The Tango bioassay specifically links activation of transiently transfected chemerin receptor fusion proteins to a luminescent readout (179,321). By contrast, activity of the endogenous LPA receptors is not coupled to the luminescent readout. As such, the Tango bioassay permits determination of chemerin receptor activation independently of LPA receptor signaling. Chemerin alone activates all four of the chemerin receptors tested. LPA alone did not activate the chemerin receptors. LPA addition to cells treated with chemerin did not enhance activation of pCDNA or any of the tested chemerin receptors, suggesting that LPA does not increase CMKLR1 or GPR1 sensitivity to chemerin.

4.4.6 Chemerin Activates MAPK/ERK Signaling But Does Not Enhance LPA-Mediated Signaling Through This Pathway

Numerous endogenous promoters are cooperatively regulated by SRF and the TCF family of transcription factors, which become activated downstream of MAPK/ERK signaling pathways (300). We used HEK293A cells stably transfected with an SRF/TCF-dependent SRE promoter to determine if chemerin could activate MAPK/ERK signaling (Fig. 4.9). To determine optimal treatment time for MAPK/ERK-mediated SRE activation by extracellular stimuli, we treated cells with established activators of this pathway, 10% FBS in combination with 100 ng/ml extracellular growth factor for 4-24 hours. Maximal SRE activation was achieved with 4-hour treatment reaching levels 80-fold higher than vehicle treated cells (Fig. 4.9a). This activation was dramatically reduced at longer treatment times and was not significantly different from vehicle at 18- or 24-

hour treatment times. 4-hour treatments were used for all subsequent MAPK/ERK experiments. The rho family of small GTPases should not activate the SRE reporter. To examine the specificity of the reporter, HEK293A-SRE cells were transfected with constitutively active Rac, CDC42, or RhoA (Fig. 4.9b). Cells transfected with constitutively active Rac or CDC42 had similar levels of MAPK/ERK activation when compared with vehicle treated cells. Transfection of constitutively active RhoA resulted in a slight but significant 1.7-fold increase in MAPK/ERK activation that was considerably smaller than the 180-fold activation observed following treatment with FBS/EGF. Chemerin treatment resulted in significant activation of MAPK/ERK signaling in HEK293A-SRE cells transfected with hCMKLR1, and mCMKLR1 (Fig. 4.9c). MAPK/ERK activation in HEK293A-SRE cells transfected with hGPR1 and mGPR1 was insufficiently consistent to result in an overall significant result. Chemerin treatment had no effect on SRE activation in HEK293A-SRE transfected with pCDNA. LPA treatment resulted in a significant activation of MAPK/ERK signaling when compared with vehicle in HEK293A-SRE cells transfected with pCDNA or one of the chemerin receptors (Fig. 4.9d). Co-treatment with LPA and chemerin did not significantly increase MAPK/ERK activation when compared with treatment using LPA alone in cells transfected with pCDNA, CMKLR1, or GPR1.

4.4.7 ERK1/2 and p38 are Required for Chemerin Activation of SRF and Play a Role in Chemerin Enhancement of LPA Signaling

Given that chemerin activates RhoA and MAPK/ERK/p38 pathways and that these pathways can converge at SRF, we treated HEK293A cells transfected with the SRF-RE with an inhibitor of either ERK1/2 (U0126) or the MAPK p38 (SB203580) to determine the impact of MAPK signaling on chemerin-mediated SRF activation (Fig. 4.10). U0126 significantly decreased SRF activation when compared with vehicle in cells transfected with pCDNA (Fig. 4.10a). As shown before, chemerin treatment in cells transfected with hCMKLR1, hGPR1, mCMKLR1, or mGPR1 resulted in significant activation of SRF when compared with vehicle. This activation was lost with U0126 or SB203580 treatment in cells transfected with mGPR1 and was significantly reduced with

SB203580, but not U0126, treatment in cells transfected with hCMKLR1. Chemerin-mediated SRF activation in cells transfected with hGPR1, and mCMKLR1 was unaffected by either inhibitor. SRF activation by LPA and LPA/chemerin co-treatment was significantly reduced with U0126 and SB203580 in cells transfected with pCDNA (Fig. 4.10b). Treatment with either MAPK inhibitor abolished the significant enhancement of LPA-mediated SRF activation observed with chemerin co-treatment in cells transfected with hCMKLR1, and mGPR1, but not mCMKLR1. No chemerin enhancement of LPA-mediated SRF activation was observed for hGPR1 with vehicle or inhibitor treatment. Table 4.2 provides a summary of SRF-RE results for chemerin and LPA treatments for all receptors.

4.4.8 Chemerin Signaling Regulates SRF-target Gene Expression

SRF regulates transcription of a diversity of immediate early genes that can broadly be subdivided into TCF- and MRTF-dependent subfamilies. The nature of the genes expressed depends upon the balance of activated TCF and MRTF transcription factors downstream of the extracellular stimuli. Given that chemerin signals through both MAPK and RhoA-dependent pathways, we examined the mRNA expression of a few well-established TCF dependent (EGR1, JUNB, FOS) or MRTF-dependent (VCL, TPM1, SRF), SRF-target genes (282,296,306) (Fig. 4.11). To determine an optimal treatment time, HEK293A cells stably transfected with hCMKLR1-EGFP (HEK293A-CMKLR1) were treated with LPA for 0.5, 1, 2, or 4 hours prior to lysis and gene expression analysis (Fig. 4.11a). LPA treatment significantly increased expression of the genes examined when compared to vehicle treated control with treatment times that varied by gene. Maximal induction of the transcription factors early growth response protein-1 (*EGR1*), and jun- B (*JUNB*), and the oncogene *FOS* occurred following 0.5 hours of treatment whereas, SRF, vinculin (*VCL*) and tropomyosin 1 alpha isoform (*TPM1*) were maximally induced with 4 hours of LPA treatment. These times were used for subsequent analysis using chemerin. Expression of the TCF-dependent transcription factor *JUNB* was unaffected by chemerin treatment (Fig. 4.11b). By contrast, chemerin significantly increased expression of *EGR1* and *FOS* mRNA. Expression of the MRTF-

dependent genes *SRF*, *VCL* and *TPM1* were unaffected by chemerin treatment. Co-treatment with LPA and chemerin significantly increased *FOS* expression when compared with LPA alone but not *EGR1 JUNB, SRF, VCL,* or *TPM1* (Fig. 4.11c).

We used AGS cells to examine the impact of GPR1 signaling on SRF target gene expression (Fig, 4.12). These cells endogenously express minimal chemerin mRNA, and no detectible *CMKR1* mRNA expression; however, *GPR1* mRNA expression was similar to that observed in adipocytes (Fig. 4.12a). Additionally, these cells express LPAR2 and LPAR5 most abundantly and low levels of LPAR1, LPAR3, and LPAR6 (Fig. 4.12b). To determine optimal treatment times for SRF-dependent gene expression, AGS cells were treated for 0.5, 4, or 24 hours with LPA prior to lysis and gene expression analysis (Fig. 4.12c). Similar to the HEK293A-CMKLR1 cells, maximal *EGR1*, *JUNB*, and *FOS* induction occurred with 0.5-hour treatment while *SRF*, *VCL*, and *TPM1* were maximally induced at 4 hours (Fig. 4.12c). AGS cells are sensitive to chemerin doses in the low nanomolar to picomolar range (322). As such, the GPR1-expressing AGS cells were treated with a wide chemerin dose range from 0.005 nM to 100 nM (Fig. 4.13a). There was a slight but not significant trend toward increased expression of *EGR1*, *SRF*, and *TPM1* with increasing doses of chemerin, and no change in *JUNB* or *FOS* expression. *VCL* was slightly but significantly increased with 100 nM chemerin treatment when compared with vehicle treatment. LPA treatment of these cells resulted in a significant increase in the expression of all of the genes examined (Fig. 4.13b). This increase was not significantly different with chemerin co-treatment.

4.4.9 HEK293A-CMKLR1 and AGS Cell Proliferation is Unchanged with Chemerin Treatment

Modulation of proliferation is a well-established function of SRF and SRF target genes, in particular MAPK/TCF-dependent genes (300). To determine the impact of chemerin signaling on proliferation, we performed a thymidine incorporation assay using the HEK293A-CMKLR1 or AGS cells (Fig. 4.14). LPA induced a significant increase in HEK293A-CMKLR1 cell proliferation (Fig. 4.14a). The proliferation of HEK293A-

CMKLR1 cells treated with chemerin was similar to those receiving no chemerin. AGS cell proliferation was unchanged by either chemerin or LPA treatments (Fig. 4.14b).

4.4.10 Chemerin-Mediated Chemotaxis Requires RhoA/ROCK, MAPK, and $G\alpha_{i/o}$

The first and best-established chemerin function is as a chemokine, promoting migration of a variety of cell types (170,209,252,323,324). Moreover, RhoA and SRF activation are key cellular events leading to chemotaxis (287). To determine the involvement of the identified chemerin-activated signal transduction pathways, L1.2 pre-B lymphocytes stably transfected with hCMKLR1 (L1.2-CMKLR1), the gold standard model of chemerin-mediated chemotaxis, were allowed to migrate to chemerin in the presence of Y27632, PTX, U0126, or SB203580 (Fig. 4.15). Increasing doses of chemerin activated L1.2-CMKLR1 migration with as little as 0.1 nM chemerin, reaching a maximum increase of 10-fold with 3 nM chemerin when compared to no chemerin treatment and an EC50 of 0.051 nM (Fig. 4.15a). Chemotaxis to 1 nM chemerin was significantly reduced when the L1.2-CMKLR1 cells were treated with the ROCK inhibitor Y27632 (Fig. 4.15b), the $G\alpha_{i/o}$ inhibitor PTX (Fig. 4.15c), the MEK1/2 inhibitor U0126 (Fig. 4.15d), or the p38 inhibitor SB203580 (Fig. 4.15e). Migration in the presence of any of the inhibitors was similar to those seen with no chemerin treatment.

GPR1-mediated chemotaxis has never been reported in the literature. Given that the AGS cells, which migrate to a variety of extracellular stimuli (325-327), express no detectable CMKLR1 and an abundance of GPR1, we sought to determine if migration of these cells to chemerin required the identified RhoA/ROCK and MAPK signaling pathways (Fig. 4.16). Stimulation of AGS cells with increasing doses of chemerin in the lower well of a transwell chamber resulted in a significant increase in cell migration. Quantification of AGS cell migration to increasing doses of chemerin revealed a maximal 2- to 3-fold induction in migration with an EC50 of 0.41 pM (Fig. 4.16a). Treatment of the AGS cells with Y27632, PTX, or SB203580 completely inhibited migration of these cells to 0.005 nM chemerin but was unaffected by the MEK1/2 inhibitor U0126 (Fig. 4.16b). AGS migration to LPA was significantly greater than vehicle and was not enhanced by co-treatment with chemerin (Fig. 4.16c)

4.5 Discussion

The goal of this study was to investigate the species- and receptor-specific mechanisms and function of chemerin-mediated Rho-GTPase/SRF pathway activation through CMKLR1 and GPR1. We have shown that chemerin signaling activates a RhoA and ROCK-dependent pathway that is required for chemotaxis. Like CMKLR1, GPR1 signaling is largely $G\alpha_{i/o}$-dependent. While many components of CMKLR1 and GPR1 signal transduction through these pathways appear to overlap, we find that CMKLR1 and GPR1 also display both receptor specific and species-selective dependencies on MAPK and Rho-GTPase signals (Fig. 4.17). Chemerin treatment increased TCF target gene expression (*FOS, EGR1*) in HEK293A cells and MRTF-dependent gene expression (*VCL*) in AGS cells. Despite the established role for the MAPK pathway and SRF in proliferation and cell growth chemerin treatment had no effect on cell proliferation. Taken together, this study provides evidence for a novel RhoA-dependent mechanism essential for chemerin-mediated chemotaxis of leukocytes and cancer cells and provides the first report of GPR1-mediated signal transduction and chemotaxis.

MRTF transcription factor activation and complexing with SRF in the nucleus activates the SRF-RE reporter assay system. Consistent with the established role of Rho-GTPases in SRF/MRTF activation, herein we showed that both mouse and human chemerin receptors, CMKLR1 and GPR1, activated SRF through a RhoA and ROCK-dependent signal transduction cascade. In all cases, inhibition of ROCK, a downstream effector of RhoA, completely abrogated chemerin activation of SRF. C3T and RhoA knockdown demonstrated that RhoA function was required for mouse and human CMKLR1 and GPR1 activation of SRF. SRF activation by hCMKLR1 was sensitive to RhoA abundance, with the partial and complete knockdown of RhoA using RA2 and RA3 shRNA sequences producing partial and complete loss of SRF activation, respectively suggesting that h/mGPR1 and h/mCMKLR1 signaling to SRF depends on RhoA. Confirmation of RhoA, ROCK, and SRF activation by western blotting and immunocytochemistry would further help to establish the role these proteins play in chemerin signaling. Moreover, identification of the mechanisms of RhoA and ROCK

activation, in particular CMKLR1- and GPR1-activated GEFs, will be an important step in understanding this chemerin signaling pathway, which represents a novel chemerin signaling cascade.

It is clear; however, that activation of a ROCK-dependent signaling cascade is essential for chemerin-mediated chemotaxis. While studies have previously shown dependence on ERK1/2 and p38 for chemerin-mediated chemotaxis, these findings demonstrate for the first time the importance of RhoA and ROCK activation in this well-established chemerin function. These findings are consistent with extensive literature reports demonstrating that RhoA and ROCK serve as critical mediators relaying extracellular stimuli to changes in actin dynamics, gene, and protein expression for the support of cellular motility (288,312). Consistent with a role for chemerin in actin dynamics, Hart *et al*. reported that studies using peritoneal exudate cells and the inhibitor of actin polymerization cytochalasin D supported a role for chemerin in release of cytoskeleton restraints on the adhesion molecules VLA-4 and VLA-5 and subsequent cell adhesion to fibronectin and VCAM-1 (187). As such our findings may represent a novel pathway for chemerin regulation of the actin cytoskeleton, cell shape, and cell motility. Examination of the impact of chemerin signaling on the actin cytoskeleton will be an important future direction that could expand our understanding of chemerin function, not only in chemotaxis and immunity but also in vascular function, development, and differentiation where these processes play key roles (328-330).

Previous studies had shown $G\alpha_{i/o}$ dependence for chemerin/CMKLR1 mediated macrophage, dendritic cell, and synoviocyte migration (170,184) and we predicted that all four chemerin receptors examined could couple to $G\alpha_{i/o}$. Herein we demonstrated that hCMKLR1 mediated $G\alpha_{i/o}$ activation is essential for chemotaxis of L1.2 lymphocytes and contributed to part, but not all of hCMKLR1 and mCMKLR1 SRF activation. This later finding suggests that coupling to an as of yet unidentified G protein is required to achieve maximal CMKLR1-mediated SRF activation. While specific inhibitors of different $G\alpha$ protein types are not readily available, future experiments using knockdown approaches or G protein-specific BRET could help to identify other CMKLR1 G protein partners and provide further evidence for the role of $G\alpha_{i/o}$ in these pathways. Our finding that SRF activation by mouse and human GPR1 was completely lost with PTX treatment

suggests that the GPR1 receptors rely entirely on $G\alpha_{i/o}$ for SRF-pathway activation and that activation of this pathway was sufficient to support GPR1-mediated chemotaxis in AGS cells. Altogether, these findings provide further support for the importance of $G\alpha_{i/o}$ in chemerin signal transduction and function and provide the first evidence of GPR1 G protein-coupling.

The number of studies reporting chemerin activation of MAPK signaling continue to increase (4,170,183-185,187,239,322,331,332). We found that the ERK1/2 and p38 dependence of CMKRL1 and GPR1 signaling differed with respect to receptor type, species, and functional outcome. Mouse GPR1 activation of SRF was dependent on both ERK1/2 and p38, while hGPR1 required neither. By contrast, p38 was not required for hGPR1 SRF activation but was an important component of hGPR1 chemotaxis in AGS cells. Consistent with this, Wang *et al*. have previously shown ERK1/2 and p38-dependent AGS cell migration to chemerin and inflammatory cytokine expression (322); however, this function was not attributed to any particular chemerin receptor. We showed mCMKLR1 mediated activation of the MAPK/ERK SRE reporter but did not observe any dependence on ERK1/2 for SRF activation. hCMKLR1 displayed the most complex MAPK signaling profile with p38 contributing only partially to SRF activation suggesting that it is either upstream of RhoA and synergizes with other signals for complete activation of RhoA or alternatively that it contributes to modulation of SRF transcription complex formation through actions on other cofactors. Use of combination inhibitor treatments for RhoA/ROCK, MAPK/ERK, PI3K, Ca^{2+}, actin, and AKT will be required to further elucidate to what extent these findings represent a single or multiple pathways for chemerin-mediated SRF activation. Much like RhoA and ROCK, the mechanisms upstream of MAPK signaling by chemerin also remain to be elucidated. It is not uncommon for GPCRs to couple to multiple signaling pathways and for these pathways to display different relative contributions depending on the cellular outcome examined. To this end, a study by Hart *et al*. in 2010 clearly demonstrated that activation of two distinct pathways contribute to different aspects (fibronectin vs. VCAM) of chemerin-mediated cell adhesion (187), suggesting that the variations we observed in chemerin receptor signaling may contribute to the molecular fine-tuning of chemerin function. Overall, these studies demonstrate the complexity of chemerin signaling

through its receptors and the importance that studies in novel systems and cell types examine which chemerin receptors are present and may be contributing to chemerin function.

The MRTF genes downstream of Rho pathway activation are typically involved in cell motility while the TCF target genes downstream of MAPK are typically involved in cell growth, proliferation and survival. We showed that both pathways impact chemerin-mediated chemotaxis. Given that these pathways can antagonize one another, providing a mechanism for the regulation of distinct subsets of SRF target genes (285,310) we also sought to determine how the signaling balance ultimately affects gene expression and cellular proliferation. Chemerin treatment increases C2C12 myocyte but not melanoma proliferation, while both CMKLR1 and chemerin are required for bone marrow-derived mesenchymal stem cell proliferation during the clonal expansion phase of adipocyte differentiation (181,206,313). Chemerin had no effect on HEK293A or AGS cell proliferation, suggesting that the observed ERK signaling does not contribute to a classical MAPK/ERK mediated pathway for cellular proliferation in these cells, and that a role for chemerin in proliferation is likely cell-type specific. With respect to SRF target gene expression, we saw modest increases in gene expression of classical SRF-target genes. In HEK293A-hCMKLR1 cells chemerin increases the TCF targets *FOS*, and *EGR1*, suggesting CMKLR1 signaling favoured TCF-dependent genes. Consistent with this, chemerin and the chemerin-derived peptide C-20 have been shown previously to increase FOS mRNA and protein expression in a small subset of CMKLR1-transfected HEK293 cells (261). In contrast, the observed increase in AGS cell *VCL* expression, an MRTF target gene, suggests that the balance of GPR1 signaling may favour MRTF genes in AGS cells. Given that SRF target genes have been estimated to number in the hundreds, a more comprehensive examination of the impact of chemerin signaling through multiple pathways is warranted and could ultimately reveal novel mechanisms for chemerin function in multiple cell types and systems.

GPCR coupling to multiple signaling events contributes to synergy among extracellular stimuli. Signaling cross-talk has been extensively demonstrated for cytokines, whereby the signaling of one cytokine synergistically amplifies the actions of other cytokines (333,334). Chemerin signaling has been shown to synergize with the

chemokine CCL7 in the promotion of immature monocyte-derived dendritic cell migration (335). This, in combination with the findings of negative cooperativity between chemerin and the chemokines CXCL12 and CCL19, suggests that the function of chemerin may also depend upon the chemokine milieu (275). Herein we demonstrated that chemerin signaling synergizes with the bioactive lipid LPA, producing enhanced SRF activation beyond the additive response obtained with either chemerin or LPA alone through human and mouse CMKLR1 and mouse GPR1. This synergistic effect was $G\alpha_{i/o}$-independent for CMKLR1 but not mGPR1. Chemerin/LPA synergy via hCMKLR1 required both p38 and ERK1/2 for enhanced SRF activation while neither was absolutely required for SRF activation with chemerin alone. These results suggest that the observed synergy requires different pathways for SRF activation than chemerin alone and that an alternate G protein or possibly even Gβγ signaling could contribute to chemerin and LPA signaling crosstalk. Moreover, while the LPAR1/3 receptor antagonist Ki16425 completely blocked LPA-induced SRF activation in cells transfected with pCDNA it was ineffective or only partially effective at blocking LPA alone in cells transfected with hCMKLR1, hGPR1, or mCMKLR1 suggesting that the presence of the chemerin receptors alone could influence LPA signaling. Given that HEK293A cells also express LPAR2 and 5, it is possible that chemerin receptor transfection results in a shift in LPAR expression or dependence. Consistent with this, Gouwy *et al.* demonstrated that cytokine synergy in immature monocyte-derived dendritic cell migration was mediated by changes in the relative abundance of multiple cytokine receptors (335); however, this remains to be investigated for chemerin specifically. It does not appear from the Tango assay results that LPA directly influences chemerin receptor function; however, the converse remains to be tested. Despite remaining uncertainty about the mechanisms that regulate chemerin and LPA synergy, it is clear that chemerin signaling has the potential to modulate the extent of SRF activation by other extracellular stimuli. Given the plethora of cytokines, lipids, and other hormones that become altered in disease states such as inflammation and obesity, these findings supporting chemerin synergism have important implications that may ultimately help to explain the context-specific roles chemerin plays in health and disease.

In summary, we report for the first time a novel pathway for chemerin signaling through a RhoA and ROCK-dependent pathway for activation of the transcriptional regulator SRF. We also demonstrate the importance of $G\alpha_{i/o}$, ERK1/2, and p38 signaling in chemerin function. Additionally, our findings that GPR1 can activate $G\alpha_{i/o}$, ERK1/2, p38, and RHOA/ROCK-dependent signaling and that these pathways are required for AGS cell chemotaxis represent the first characterization of GPR1-mediated signal transduction. As such this study also provides further support for the importance of GPR1 as a chemerin receptor and reiterates the need that future studies examine multiple signaling pathways through both CMKLR1 and GPR1 when investigating the mechanisms of chemerin function.

4.6 Figures

Figure 4.1: MAPK, RhoA, and SRF regulate two cohorts of gene expression

Activation of a Ras/Raf/MEK/ERK MAPK signaling cascade by extracellular stimuli results in phosphorylation and activation of the TCF family of transcription cofactors. These bind to SRF and conserved DNA sequences (ETS domain) within the promoters of a subset of SRF target genes for regulation of cell growth, survival, and apoptosis. Activation of the Rho family of small GTPases, in particular RhoA, results in activation of the kinase ROCK, formation of F-actin polymers from G-actin monomers and release of the cytosolic restraint on the MRTF family of transcription cofactors. Translocation of MRTFs into the nucleus and complexing with SRF modulates the expression of SRF target genes responsible for regulating the actin cytoskeleton, cell motility, and differentiation. **Abbreviations**: ERK: extracellular-regulated kinase, ETS: E26 transformation-specific, F-actin: filamentous actin, G-actin: globular actin, GPCR: G protein-coupled receptor, LIMK: LIM kinase, MRTF: myocardin-related transcription factor, MEK: mitogen activated protein kinase kinase, RHOA: ras homolog gene family member A, ROCK: rho-associated protein kinase, RTK: receptor tyrosine kinase, SRF: serum response factor, TCF: ternary complex factor.

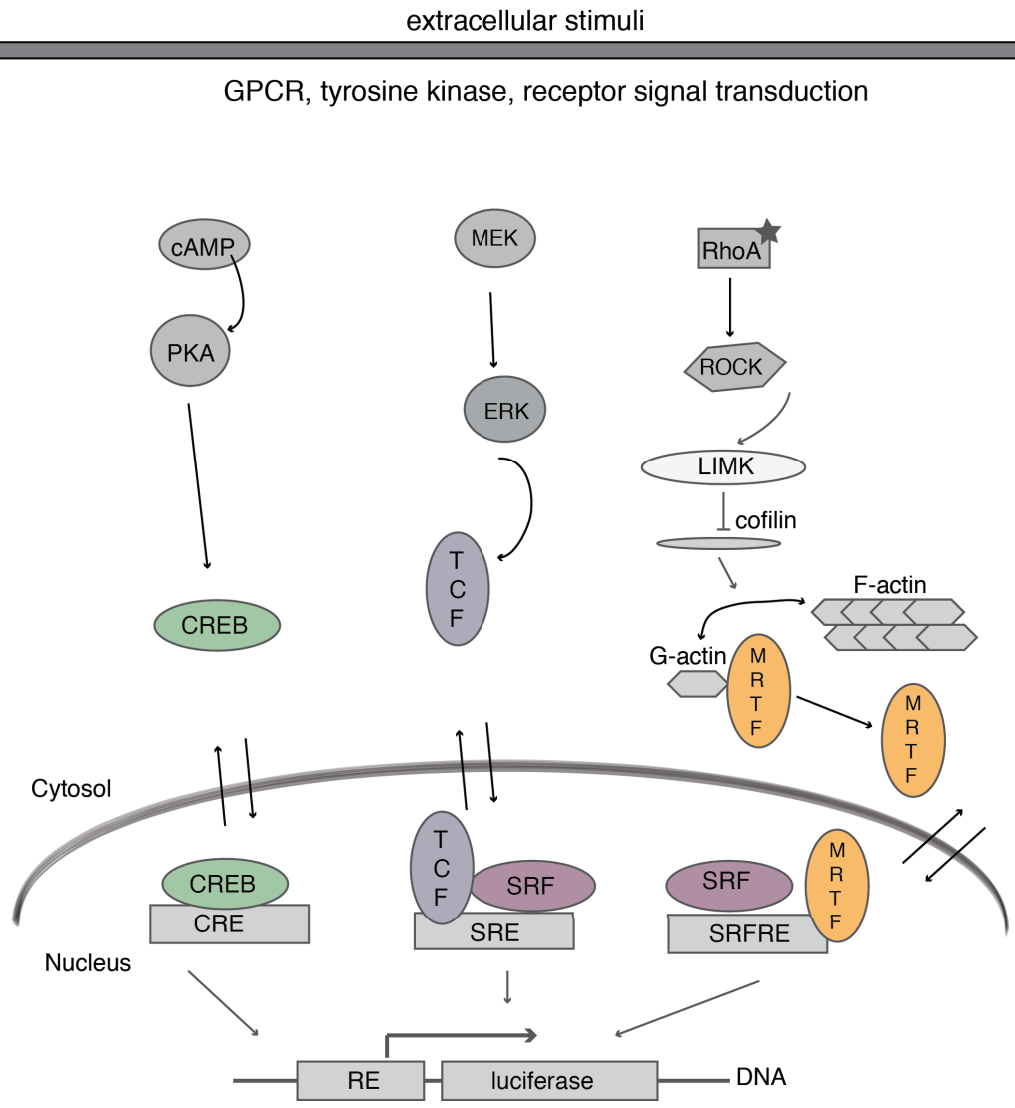
extracellular stimuli
GPCR, tyrosine kinase, receptor signal transduction
cAMP
PKA
CREB
MEK
ERK
TCF
RhoA
ROCK
LIMK
cofilin
F-actin
G-actin
MRTF
MRTF
Cytosol
CREB
CRE
TCF
SRF
SRE
SRF
MRTF
SRFRE
Nucleus
RE
luciferase
DNA

Figure 4.1

Figure 4.2: SRF-RE activation by Rho family GTPases and treatment with LPA

HEK293A cells were transfected with SRF-RE and either the control vector pCDNA, or one of the constitutively active Rho GTPases: Rac, CDC42, RhoA. Cells were lysed 48-hours following transfection. (a). HEK293A cells transfected with SRF-RE and pCDNA were treated with either vehicle (veh), or 10 μM lysophosphatidic acid (LPA) for the indicated times (b). Following 2 hours pre-treatment with the indicated doses of the RhoA inhibitor C3 transferase (C3T) (c) or the ROCK inhibitor Y27632 (d) cells were treated for 4 hours with 10 μM LPA. Luminescence/β-galactosidase activity was determined and expressed relative to pCDNA (a), veh (b), no LPA (c, d). N=2 replicates from a single experiment. One-way ANOVA *$p<0.05$ vs. pCDNA (a), veh (b), LPA (c & d).

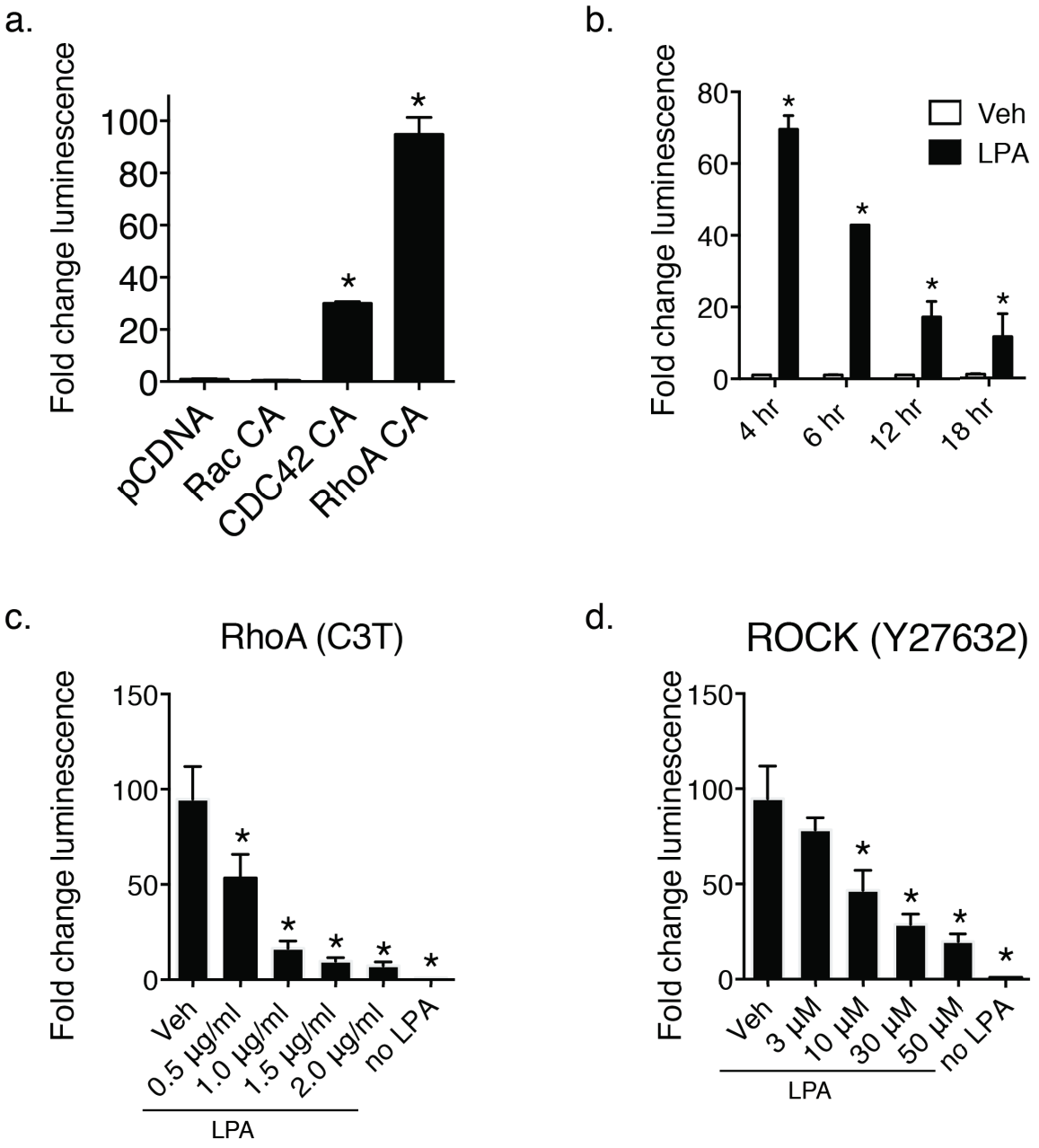
a.
Fold change luminescence
100
80
60
40
20
0
*
*
pCDNA
Rac CA
CDC42 CA
RhoA CA
b.
Fold change luminescence
80
60
40
20
0
Veh
LPA
*
*
*
*
4 hr
6 hr
12 hr
18 hr
c.
RhoA (C3T)
Fold change luminescence
150
100
50
0
*
*
*
*
*
Veh
0.5 µg/ml
1.0 µg/ml
1.5 µg/ml
2.0 µg/ml
no LPA
LPA
d.
ROCK (Y27632)
Fold change luminescence
150
100
50
0
*
*
*
*
Veh
3 µM
10 µM
30 µM
50 µM
no LPA
LPA

Figure 4.2

Figure 4.3: Chemerin activation of SRF-RE via CMKLR1 and GPR1 is reduced with $G\alpha_{i/o}$, RhoA, and ROCK inhibition (4 hour treatments)

HEK293A cells were transfected with SRF-RE and either the control vector pCDNA, or one of the chemerin receptors human (h) or mouse (m) CMKLR1 or GPR1. Cells were treated with chemerin (Che) as indicated for 4 hours. N=5 (a) or pre-treated for 2 hours with 50 ng/ml pertussis toxin (PTX, $G\alpha_{i/o}$ inhibitor) N=3 (b), 1.5 μg/ml C3 transferase (C3T, RhoA inhibitor), or 30 μM Y27632 (Y27, ROCK inhibitor) (c) prior to treatment with 30 nM che. Luminescence/β-galactosidase activity was determined and expressed relative to no che. One-way ANOVA *$p<0.05$ vs. 0 che (a), veh + che (b & c).

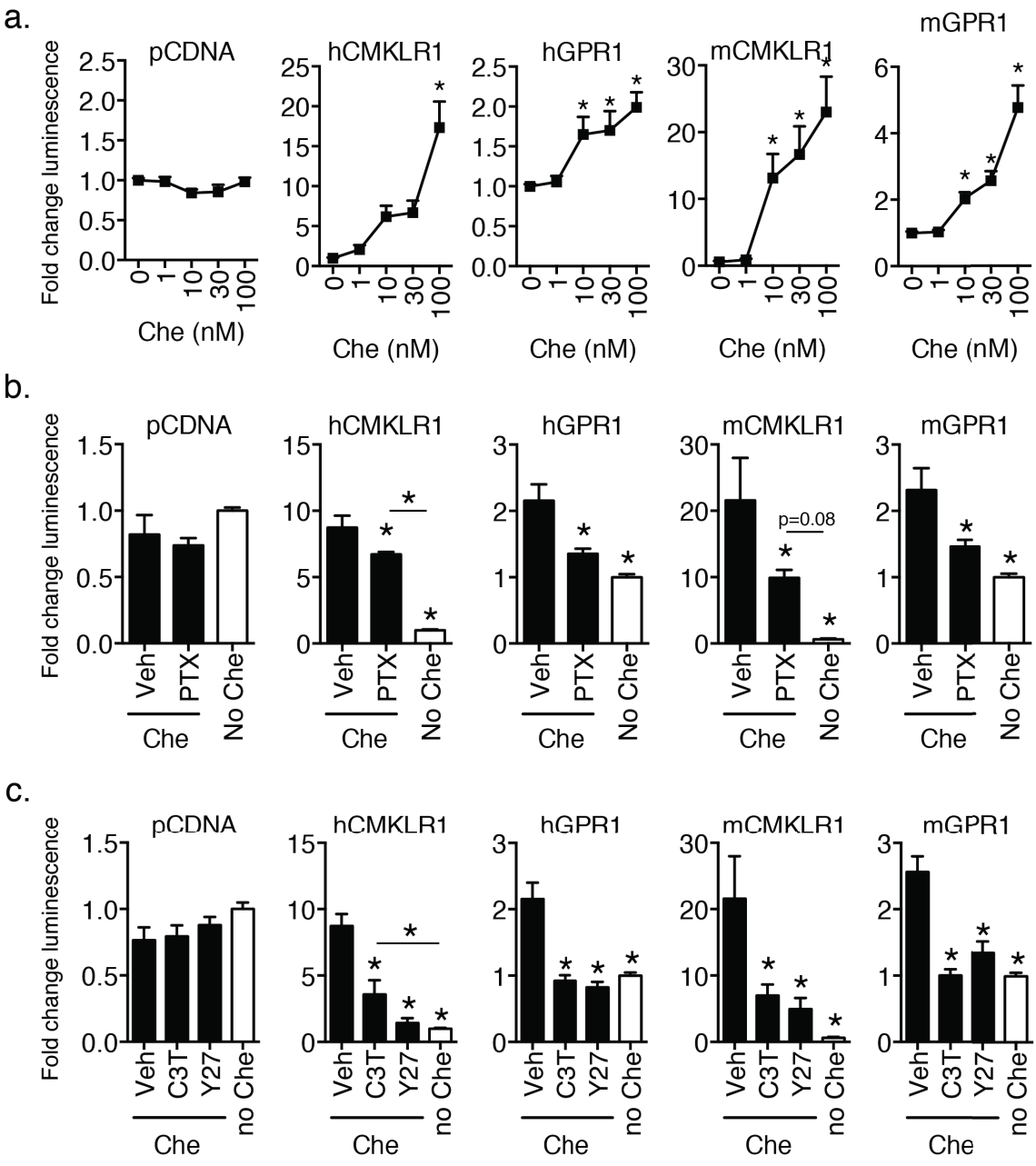
a.
pCDNA
hCMKLR1
hGPR1
mCMKLR1
mGPR1
Fold change luminescence
Che (nM)
0
1
10
30
100
b.
Veh
PTX
No Che
Che
p=0.08
c.
C3T
Y27
no Che

Figure 4.3

Figure 4.4: SRF-RE activation and inhibition with 18 hour treatments

HEK293A cells transfected with SRF-RE and the control vector pCDNA were treated with either vehicle (veh), 10% FBS or 10 μM lysophosphatidic acid (LPA) for 24 hours. N=3 (a). Following 2 hour pre-treatment with the indicated doses of the RhoA inhibitor C3 transferase (C3T) (b) or the ROCK inhibitor Y27632 (c) cells were treated for 18 hours with 10 μM LPA. N=2. Luminescence/β-galactosidase activity was determined and expressed relative to veh (a), no LPA (b, c). One-way ANOVA *$p<0.05$ vs. veh (a), or LPA (b & c).

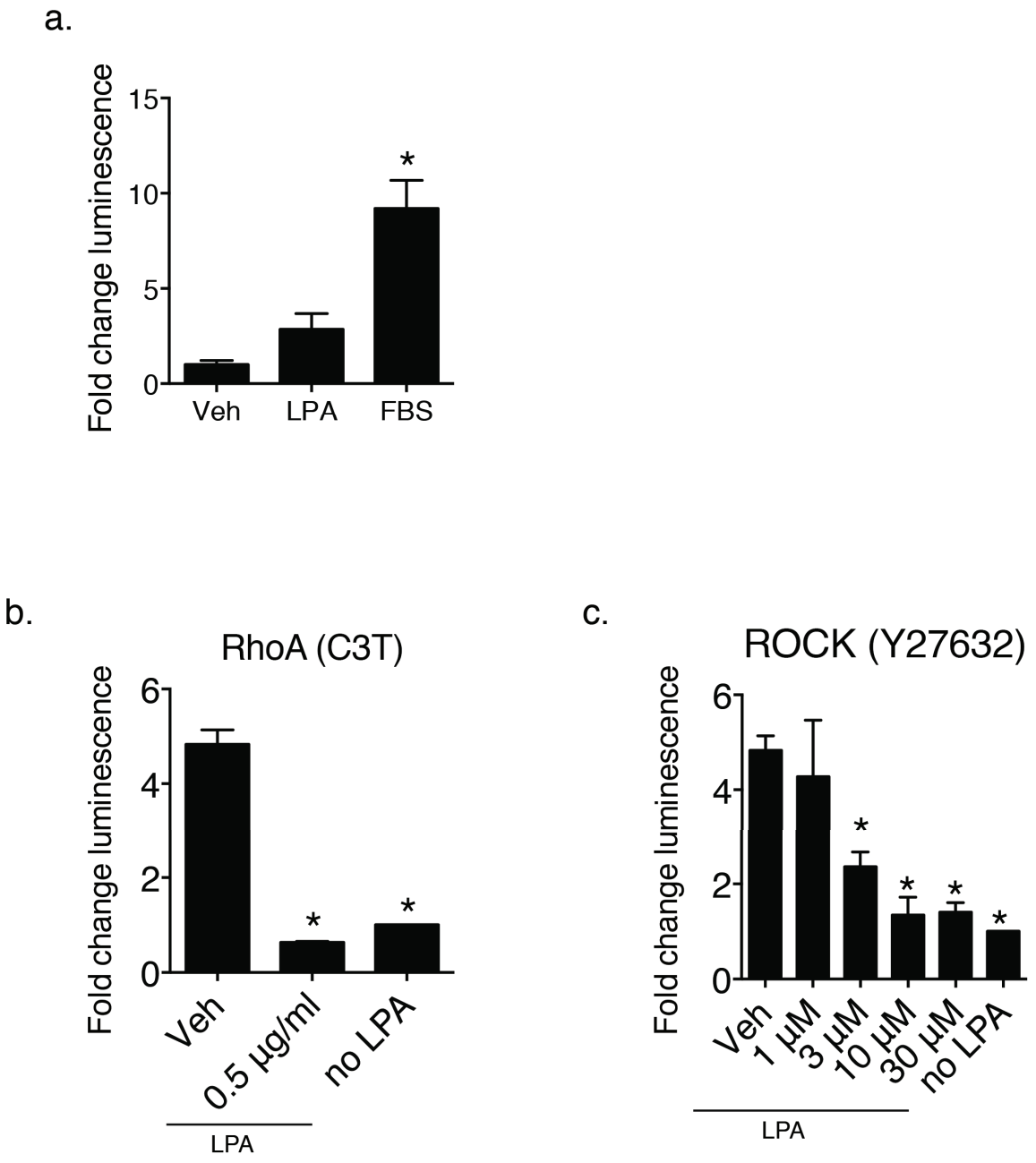
a.
Fold change luminescence
15
10
5
0
*
Veh
LPA
FBS
b.
RhoA (C3T)
Fold change luminescence
6
4
2
0
*
*
Veh
0.5 µg/ml
no LPA
LPA
c.
ROCK (Y27632)
Fold change luminescence
6
4
2
0
*
*
*
*
Veh
1 µM
3 µM
10 µM
30 µM
no LPA
LPA

Figure 4.4

Figure 4.5: Chemerin activation of SRF-RE via CMKLR1 and GPR1 is reduced with RhoA/ROCK inhibition (18 hour treatments)

HEK293A cells were transfected with SRF-RE and either the control vector pCDNA, or one of the chemerin receptors human (h) or mouse (m) CMKLR1 or GPR1. Cells were treated with chemerin (Che) as indicated for 18 hours (a) or pre-treated for 2 hours with 1 μg/ml C3 transferase (C3T, RhoA inhibitor), or 10 μM Y27632 (Y27, ROCK inhibitor) (b) prior to treatment with 30 nM chemerin (Che). Luminescence/β-galactosidase activity was determined and expressed relative to no che. N=3-4. One-way ANOVA *$p<0.05$ vs. 0 nM Che (a). Two-way ANOVA *$p<0.05$ vs. veh or as indicated.

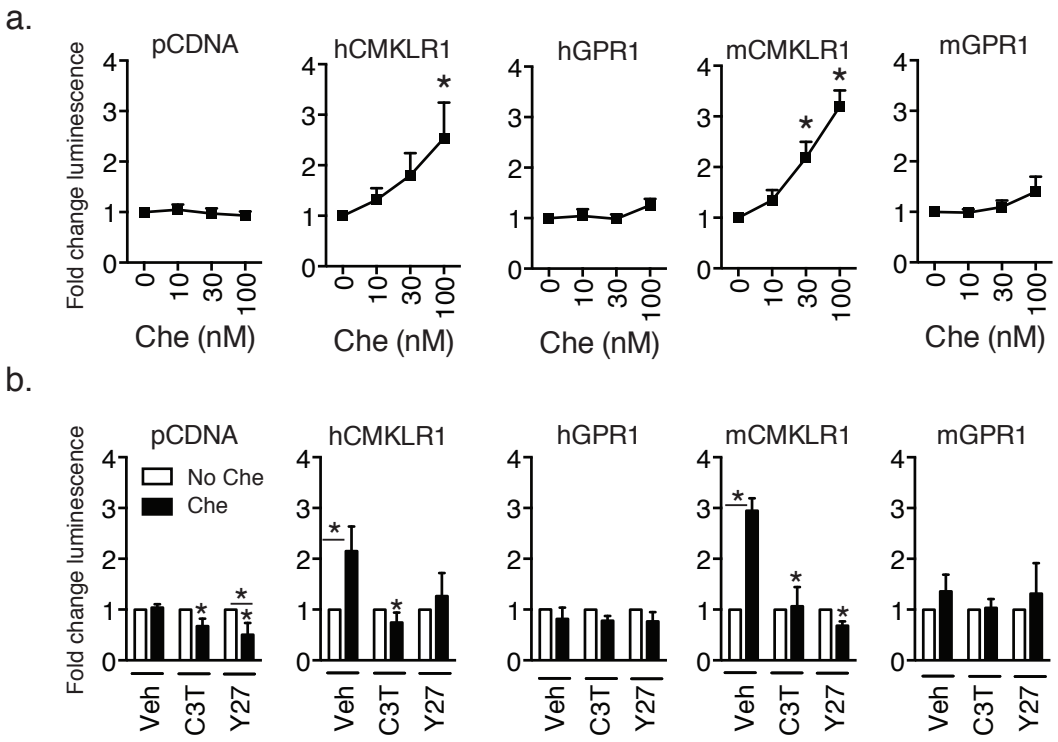
a.
pCDNA
hCMKLR1
hGPR1
mCMKLR1
mGPR1
Fold change luminescence
Che (nM)
0
10
30
100
b.
No Che
Che
Veh
C3T
Y27

Figure 4.5

Figure 4.6: RhoA knockdown inhibits chemerin activation of SRF-RE

RhoA mRNA (qPCR) (a) and protein (immunoblot) (b) levels were examined in HEK293A cells stably transfected with either a non-targeting control shRNA (cntrl) or one of 3 independent sequences targeting RhoA (RA1-702, RA2-408, RA3-222). RhoA mRNA levels were normalized to GAPDH and expressed relative to cntrl. β-actin was used as a loading control for immunoblotting (b). HEK293A cells stably transfected with cntrl, RA2, or RA3 were transfected with SRF-RE in combination with pCDNA or one of the chemerin receptors human (h) or mouse (m) CMKLR1 or GPR1 and treated with vehicle (veh) or 30 nM chemerin for 4 hours. N=3 (N=2 mGPR1). One-way ANOVA *$p<0.05$ vs. cntrl (a). Two-way ANOVA vs. veh or as indicated (c).

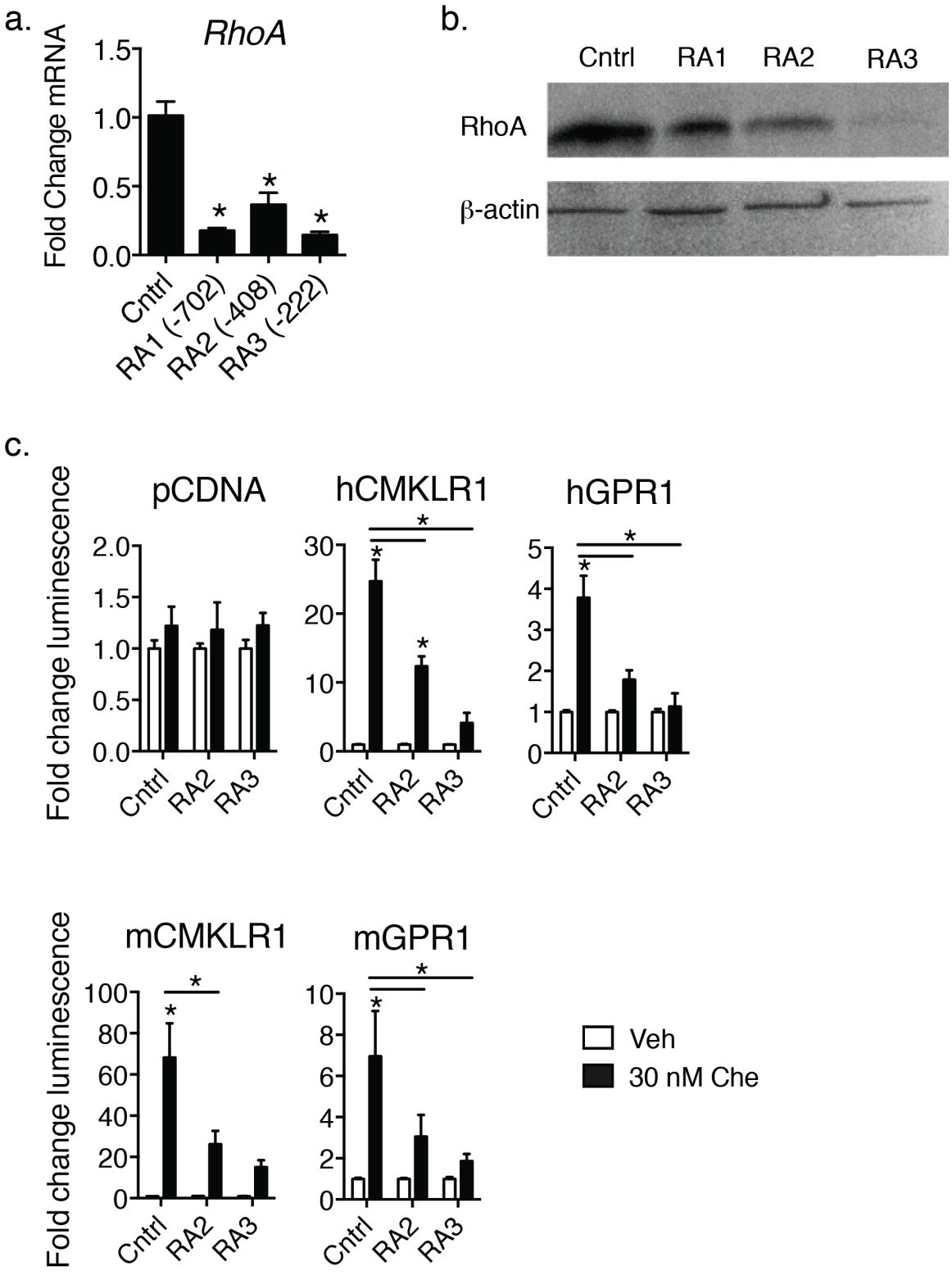
a.
RhoA
Fold Change mRNA
1.5
1.0
0.5
0.0
Cntrl
RA1 (-702)
RA2 (-408)
RA3 (-222)
b.
Cntrl
RA1
RA2
RA3
RhoA
β-actin
c.
pCDNA
hCMKLR1
hGPR1
Fold change luminescence
Cntrl
RA2
RA3
mCMKLR1
mGPR1
Veh
30 nM Che

Figure 4.6

Figure 4.7: Chemerin enhances LPA-mediated activation of SRF-RE via CMKLR1 and GPR1 in a RhoA/ROCK and $G\alpha_{i/o}$-dependent manner

HEK293A cells were transfected with SRF-RE and either the control vector pCDNA, or one of the chemerin receptors human (h) or mouse (m) CMKLR1 or GPR1. Cells were treated with vehicle (veh), 30 nM chemerin (Che), 10 μM LPA or a combination of 30 nM Che and 10 μM LPA (Both) for 4 hours (a) or pre-treated for 2 hours with 50 ng/ml pertussis toxin (PTX, $G\alpha_{i/o}$ inhibitor) (b), 1.5 μg/ml C3 transferase (C3T, RhoA inhibitor), or 30 μM Y27632 (Y27, ROCK inhibitor) (c) prior to treatment with 30 nM Che. Luminescence/β-galactosidase activity was determined and expressed relative to no LPA. N=3-6 (a), N=3 (b, c). One-way ANOVA *$p<0.05$ vs. veh (a), or two-way ANOVA vs. veh or as indicated (b & c).

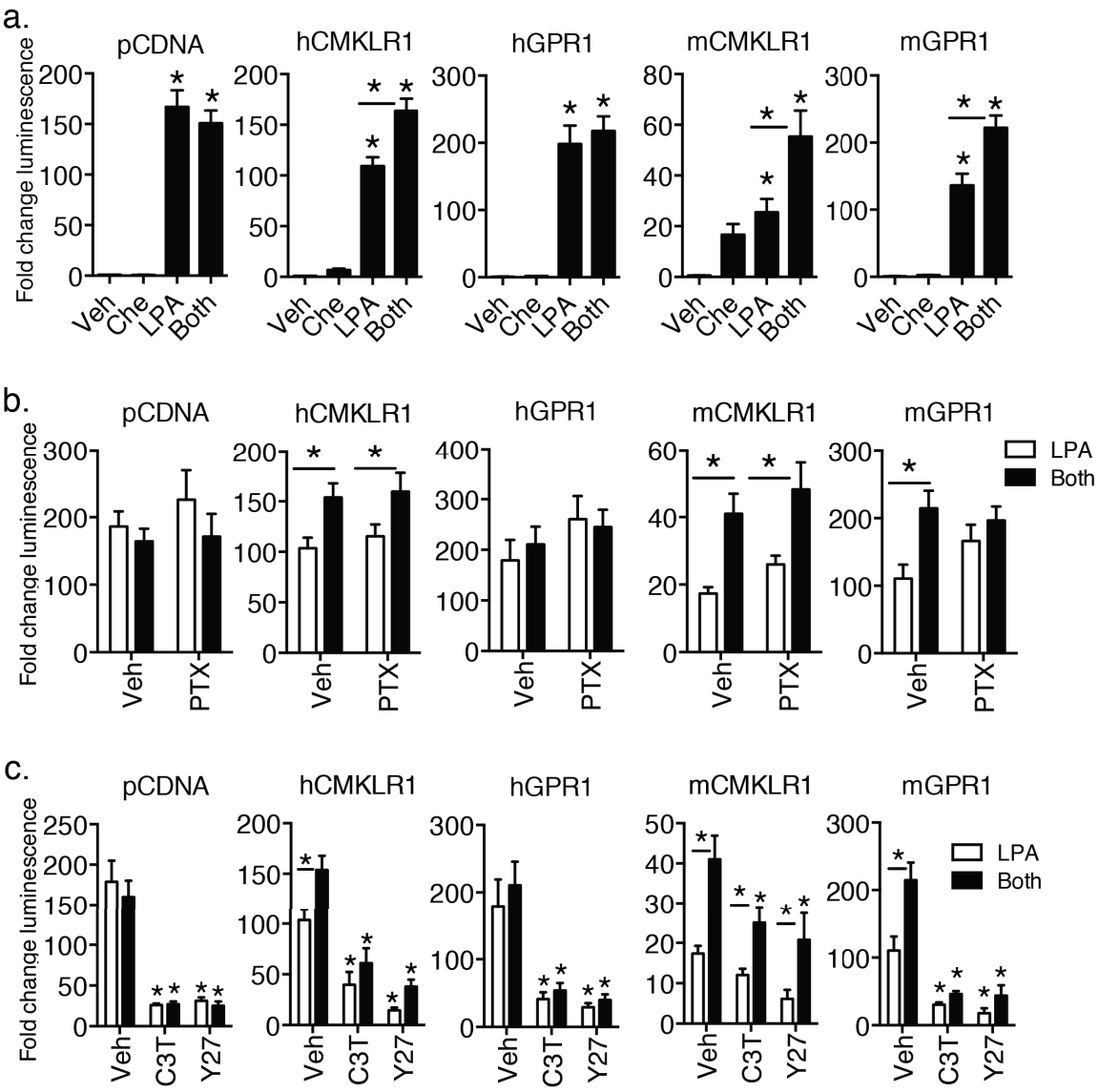
a.
pCDNA
hCMKLR1
hGPR1
mCMKLR1
mGPR1
Fold change luminescence
Veh
Che
LPA
Both
b.
PTX
LPA
Both
c.
C3T
Y27

Figure 4.7

Figure 4.8: LPA does not directly activate chemerin receptors

Quantitative PCR was used to determine the mRNA expression levels of LPA receptors (LPAR) 1, 2, 3, 5, and 6 in HEK293A cells, normalized to GAPDH and expressed relative to LPAR1 N=3 (a). HEK293A cells were transfected with SRF-RE and either the control vector pCDNA, or one of the chemerin receptors human (h) or mouse (m) CMKLR1 or GPR1. Cells were treated with 10 μM lysophosphatidic acid (LPA) or a combination of 30 nM chemerin and 10 μM LPA (Both) for 4 hours without (veh) or with 2 hour pre-treatment using the LPAR1 and LPAR3 antagonist Ki16425 (Ki1) (30 μM) prior to treatment with 30 nM chemerin. N=5 (b). HTLA tango cells were transfected with either pCDNA, or one of the chemerin receptor-tl-ta fusion proteins and treated with vehicle (veh), 30 nM chemerin (Che), 10 μM LPA, or 30 nM chemerin and 10 μM LPA together (Both) for 24 hours. Luminescence/β-galactosidase activity was determined and expressed relative to no LPA (b) or veh (c). One-way ANOVA *$p<0.05$ as indicated (a), vs. veh (c) or two-way ANOVA *$p<0.05$ vs. veh or as indicated (b).

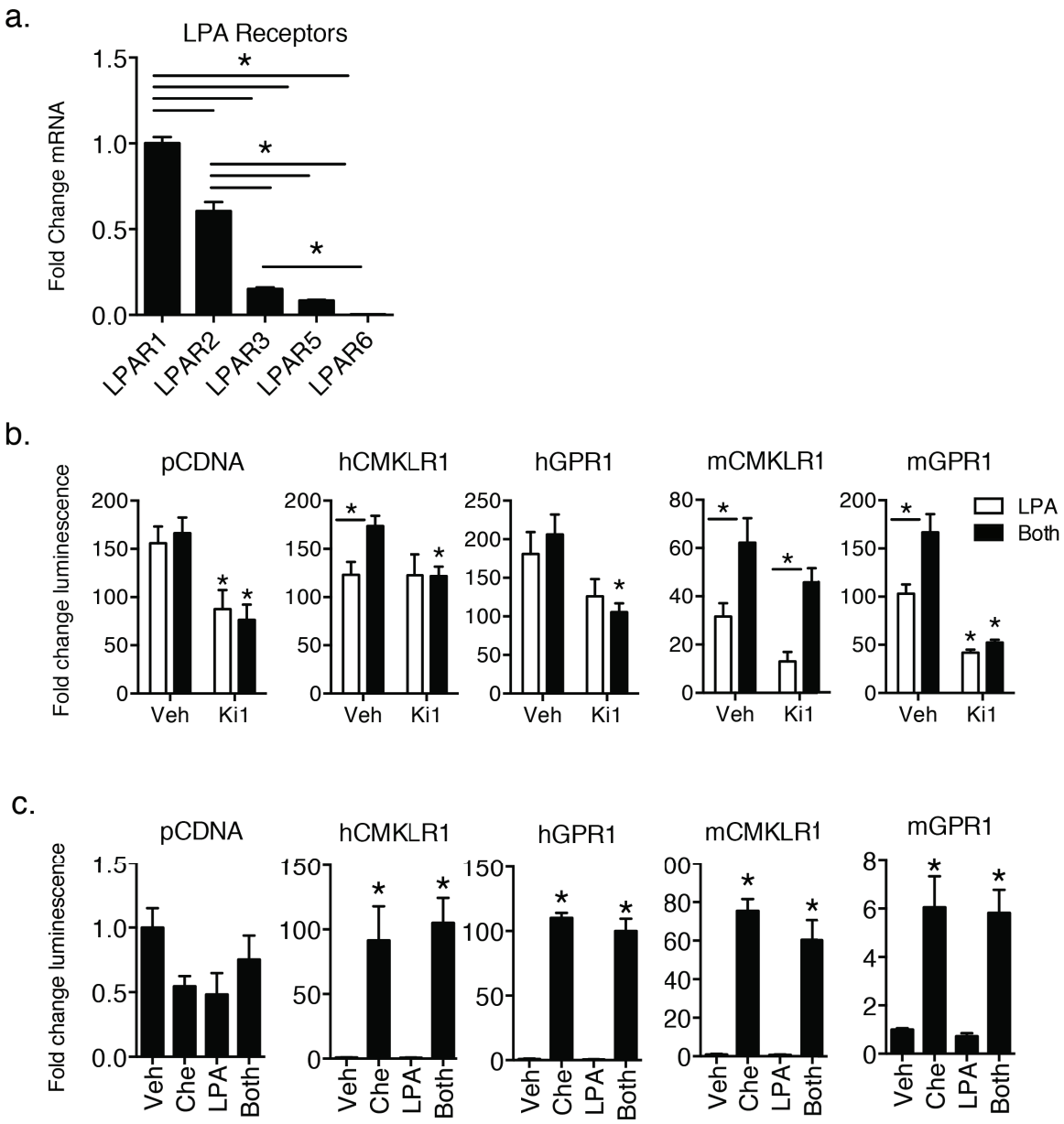
a.
LPA Receptors
Fold Change mRNA
1.5
1.0
0.5
0.0
*
*
*
LPAR1
LPAR2
LPAR3
LPAR5
LPAR6
b.
pCDNA
hCMKLR1
hGPR1
mCMKLR1
mGPR1
Fold change luminescence
LPA
Both
Veh
Ki1
c.
pCDNA
hCMKLR1
hGPR1
mCMKLR1
mGPR1
Fold change luminescence
Veh
Che
LPA
Both

Figure 4.8

Figure 4.9: Chemerin activates the MAPK/ERK-dependent SRE via CMKLR1 but does not enhance LPA-mediated SRE activation

HEK293A-SRE cells were treated with 10% FBS and 100 ng/ml epidermal growth factor (FBS/EGF) for the indicated times. N=2 replicates from a single experiment (a). To determine the sensitivity of the SRF-RE to extracellular stimuli or active rho GTPases HEK293A-SRE cells were transfected with either the pCDNA empty vector control (veh and FBS/EGF) or a constitutively active (CA) rho GTPase: Rac, CDC42, or RhoA and treated as indicated for 4 hours. N=3 replicates from a single experiment (b). HEK293A-SRE cells transfected with either the control vector pCDNA, or one of the chemerin receptors human (h) or mouse (m) CMKLR1 or GPR1 were treated with vehicle (veh), 30 nM chemerin (Che) (c), 10 μM LPA or 30 nM chemerin in combination with 10 μM LPA (both) (d) for 4 hours. N= 3-4. One-way ANOVA *$p<0.05$ vs. 4 hours (a), veh (b). T-test *$p<0.05$ vs. veh or LPA (c & d).

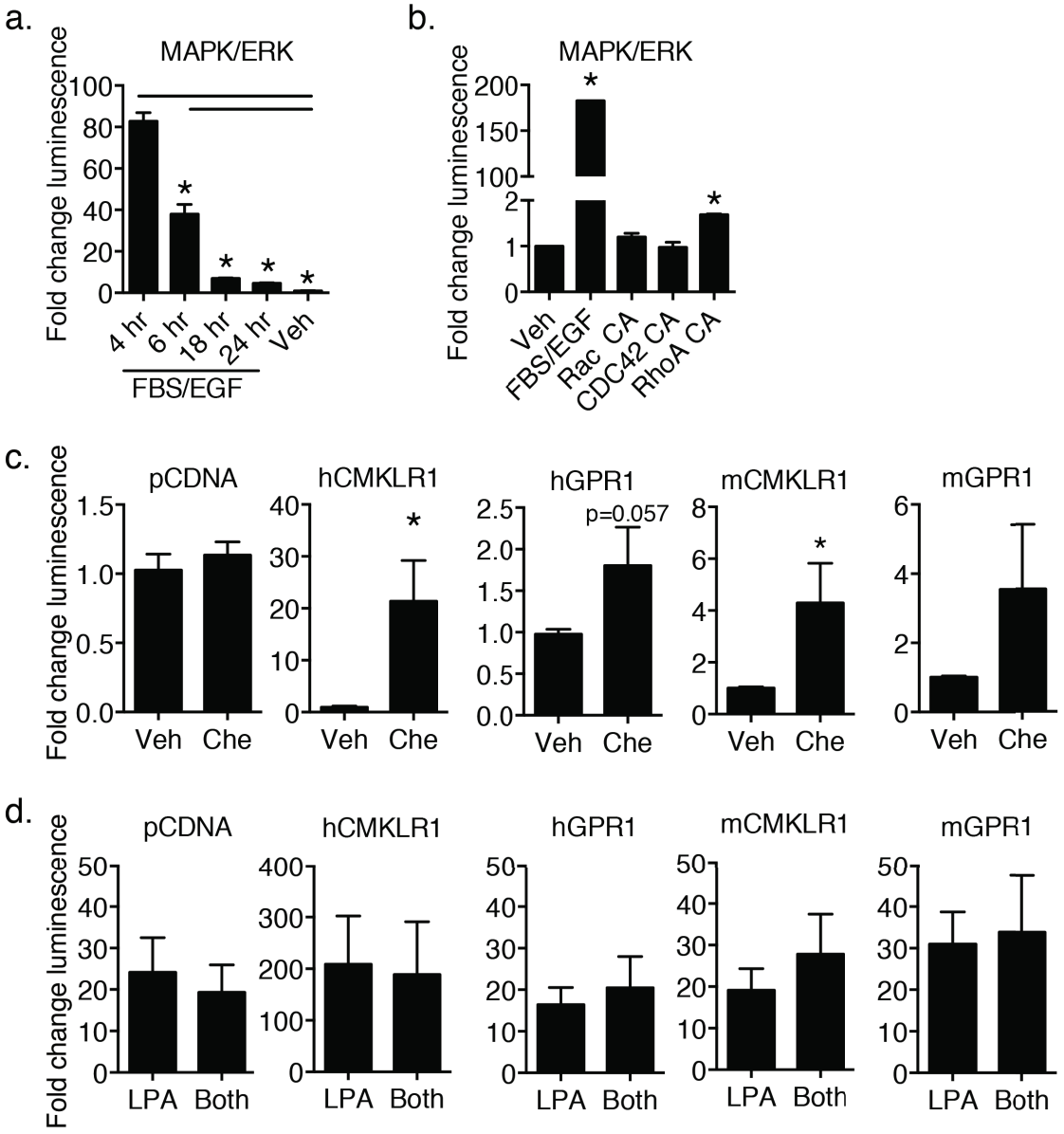
a.
MAPK/ERK
Fold change luminescence
100
80
60
40
20
0
*
*
*
*
4 hr
6 hr
18 hr
24 hr
Veh
FBS/EGF
b.
MAPK/ERK
Fold change luminescence
200
150
100
2
1
0
*
*
Veh
FBS/EGF
Rac CA
CDC42 CA
RhoA CA
c.
Fold change luminescence
pCDNA
hCMKLR1
hGPR1
mCMKLR1
mGPR1
p=0.057
Veh
Che
d.
Fold change luminescence
pCDNA
hCMKLR1
hGPR1
mCMKLR1
mGPR1
LPA
Both

Figure 4.9

Figure 4.10: MAPK-dependence of chemerin-mediated SRF-RE activation

HEK293A cells were transfected with SRF-RE and either the control vector pCDNA, or one of the chemerin receptors human (h) or mouse (m) CMKLR1 or GPR1. Cells were pre-treated for 2 hours with vehicle (Veh), 10 μM U0126 (U012, MEK1/2 inhibitor), or 10 μM SB203580 (SB20, p38 inhibitor) prior to 4 hour treatment with 30 nM chemerin (Che) (a), 10 μM LPA or 30 nM chemerin in combination with 10 μM LPA (both) (b). Luminescence/β-galactosidase activity was determined and expressed relative to no chemerin. N=3. One-way (a) or two-way (b) ANOVA *$p<0.05$ vs. veh + Che (a), or veh (b) unless otherwise indicated.

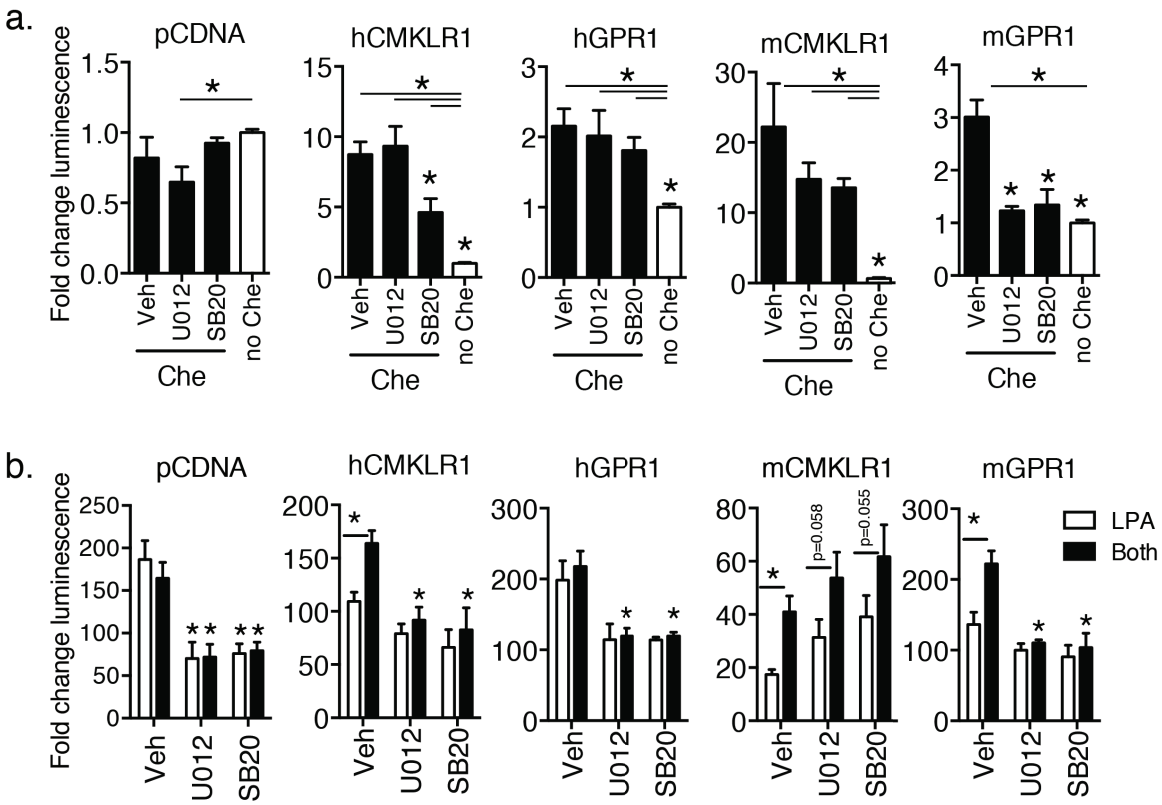
a.
pCDNA
hCMKLR1
hGPR1
mCMKLR1
mGPR1
Fold change luminescence
Veh
U012
SB20
no Che
Che
b.
LPA
Both
p=0.058
p=0.055

Figure 4.10

Figure 4.11: Chemerin increases *EGR1* and *FOS* expression in HEK293A-CMKLR1 cells

To determine optimal treatment times for SRF target-gene expression, HEK293A-CMKLR1 cells were treated with vehicle (veh) or 10 μM LPA for the indicated times and the mRNA levels of *EGR1, JUNB, FOS, SRF, VCL,* and *TPM1* were determined N=2 (a). HEK293A-CMKLR1 cells were treated with veh, 30 nM chemerin (30 Che), 100 nM chemerin (100 Che) (b), or 10 μM LPA alone or in combination with 30 nM chemerin (30/LPA) or 100 nM chemerin (100/LPA) (c) for 0.5 hours (*EGR1, JUNB, FOS*) or 4 hours (*SRF, VCL, TPM1*). N=5. All gene expression was normalized to GAPDH and expressed relative to veh. Two-way ANOVA *$p<0.05$ vs. veh (a) or One-way ANOVA vs. veh (b) or LPA (c).

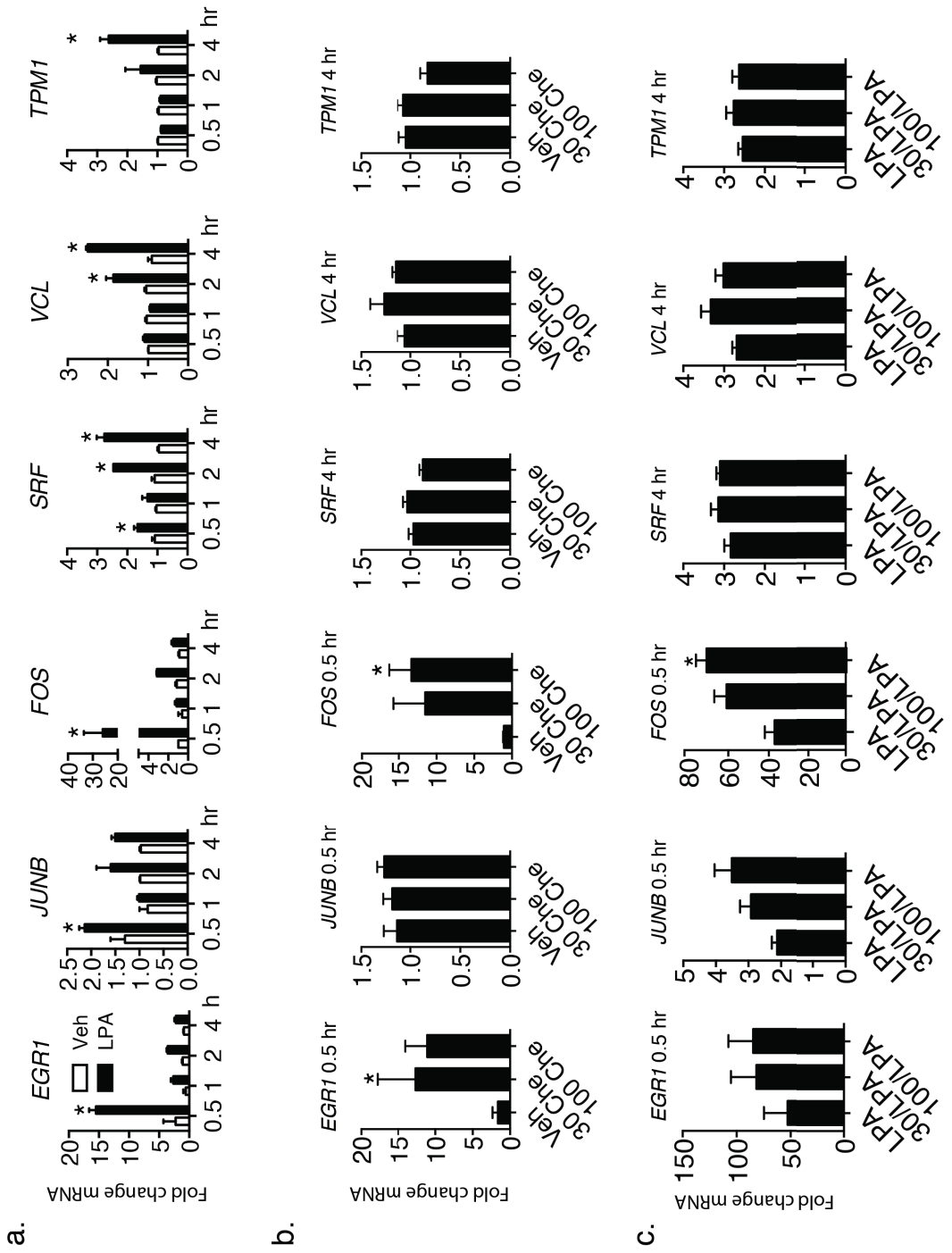
a.
b.
c.
EGR1
JUNB
FOS
SRF
VCL
TPM1
Veh
LPA
Fold change mRNA
0.5 1 2 4 h
EGR1 0.5 hr
JUNB 0.5 hr
FOS 0.5 hr
SRF 4 hr
VCL 4 hr
TPM1 4 hr
Veh
30 Che
100 Che
LPA
30/LPA
100/LPA
0.5 1 2 4 hr

Figure 4.11

Figure 4.12: AGS cells express *GPR1* and LPA receptors

The mRNA expression of chemerin, *CMKLR1*, *GPR1* (a) and the lysophosphatidic acid (LPA) receptors (*LPAR*)- 1, 2, 3, 5, and 6 (b) was measured in AGS gastric carcinoma cells. N=3. AGS cells were treated with vehicle (veh) or 10 μM LPA for various lengths of time as indicated and the mRNA levels of *EGR1, JUNB, FOS, SRF VCL* and *TPM1* were determined by quantitative PCR analysis N=5 (c). All gene expression was normalized to GAPDH and expressed relative to veh. One-way ANOVA *$p<0.05$ as indicated (a & b) or two-way ANOVA vs. veh (c).

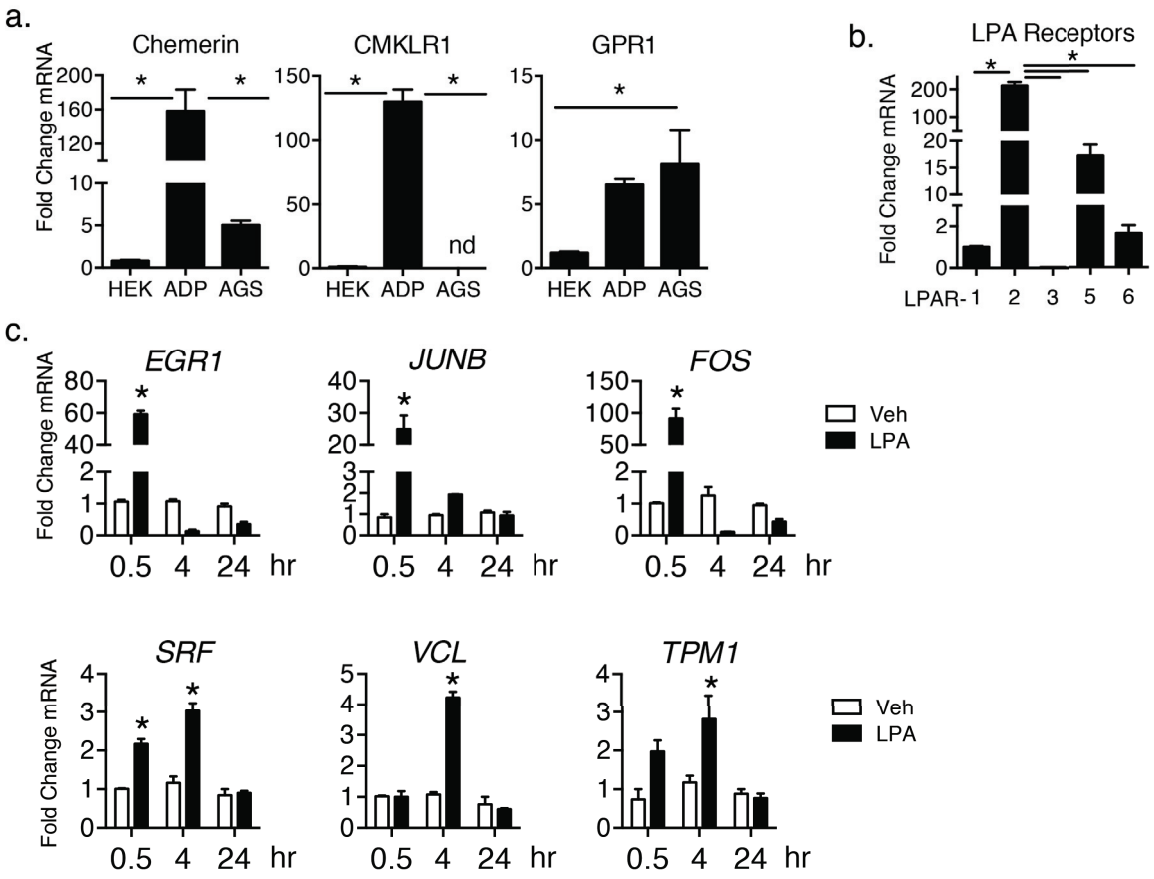
a.
Chemerin
CMKLR1
GPR1
Fold Change mRNA
HEK ADP AGS
nd
b.
LPA Receptors
LPAR- 1 2 3 5 6
c.
EGR1
JUNB
FOS
SRF
VCL
TPM1
0.5 4 24 hr
Veh
LPA

Figure 4.12

Figure 4.13: Chemerin increases *VCL* expression in AGS cells

AGS gastric carcinoma cells were treated with increasing doses of chemerin (Che) as indicated (a), or with vehicle (veh), 10 μM lysophosphatidic acid (LPA) alone or in combination with 30 nM chemerin (Both) (b) for 0.5 hours (*EGR1, JUNB, FOS*) or 4 hours (*SRF, VCL, TPM1*). N=5. All gene expression was normalized to GAPDH and expressed relative to veh. One-way ANOVA *$p<0.05$ vs. 0 nM Che (a) or vs. veh (b).

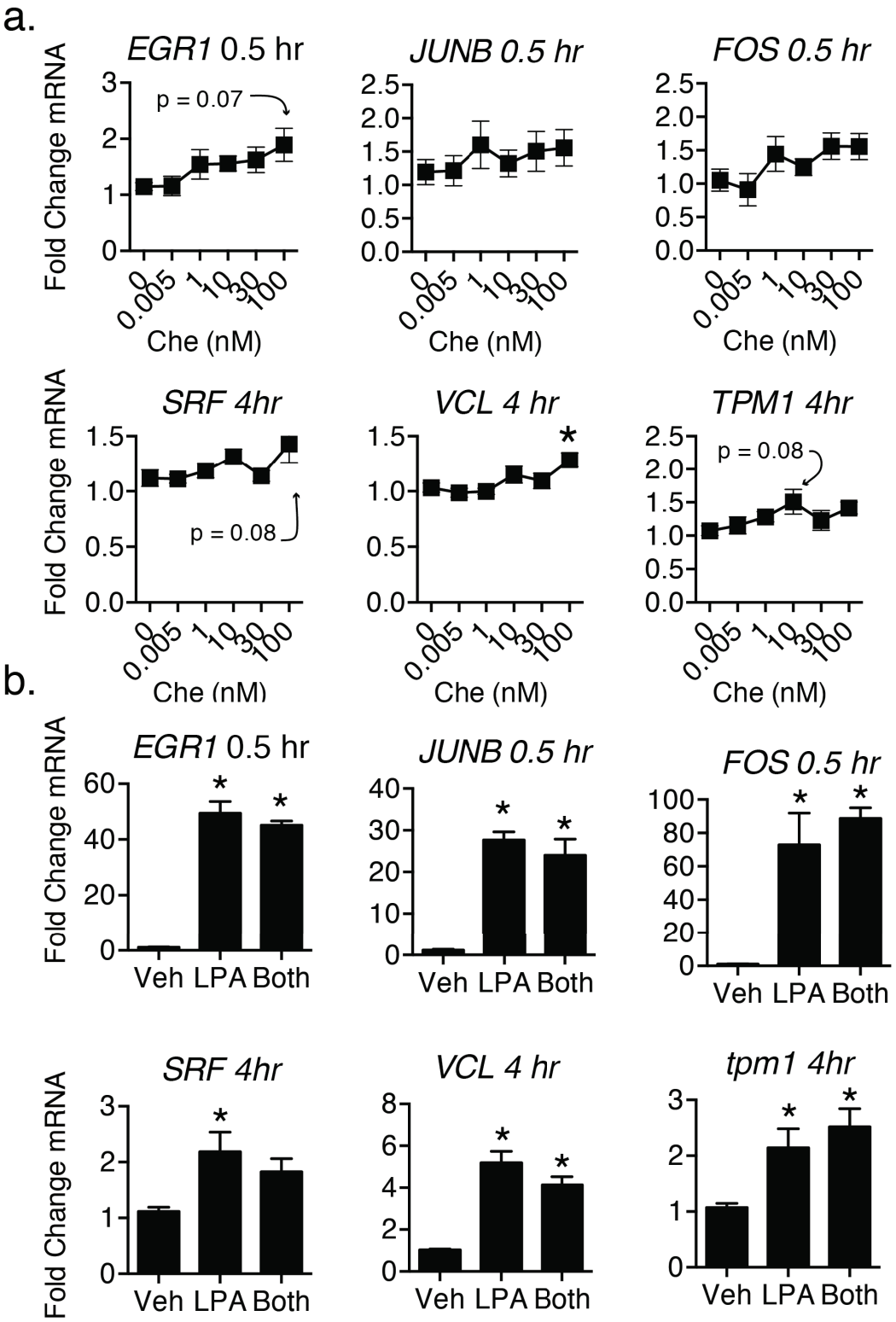
a.
EGR1 0.5 hr
JUNB 0.5 hr
FOS 0.5 hr
SRF 4hr
VCL 4 hr
TPM1 4hr
Fold Change mRNA
p = 0.07
p = 0.08
Che (nM)
0
0.005
1
10
30
100
b.
Veh
LPA
Both
tpm1 4hr

Figure 4.13

Figure 4.14: Chemerin does not alter proliferation of HEK293A-CMKLR1 or AGS cells

To determine the effect of chemerin signaling on cell proliferation HE293A-CMKLR1 (a) or AGS gastric carcinoma cells (b) were treated with increasing doses of chemerin or with 10 μM lysophosphatidic acid (LPA) alone or in combination with 30 nM chemerin (both). N=6-9 (a) and N=3-6 (b). One-way ANOVA *$p<0.05$ vs. 0 nM chemerin.

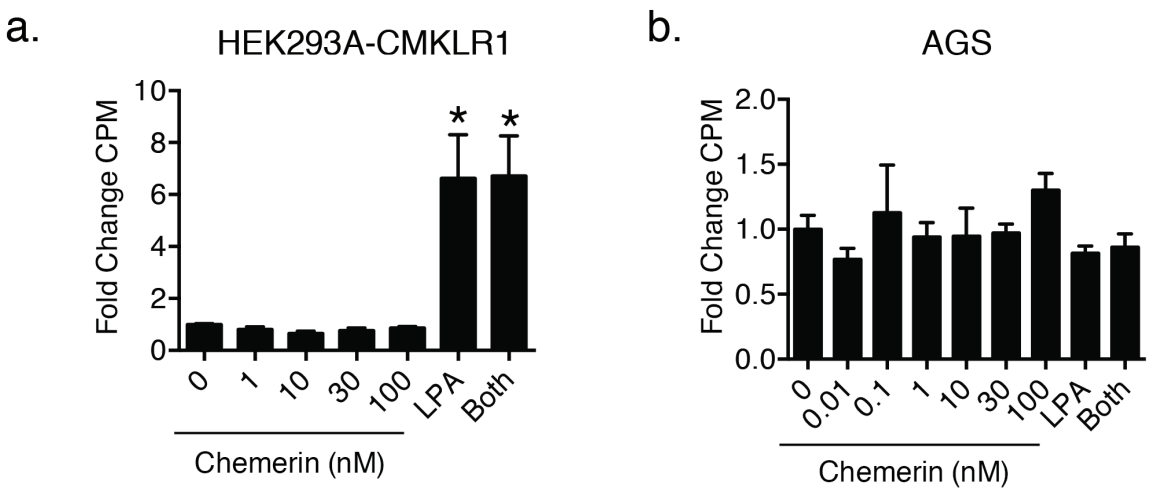
a.
HEK293A-CMKLR1
Fold Change CPM
10
8
6
4
2
0
*
*
0
1
10
30
100
LPA
Both
Chemerin (nM)
b.
AGS
Fold Change CPM
2.0
1.5
1.0
0.5
0.0
0
0.01
0.1
1
10
30
100
LPA
Both
Chemerin (nM)

Figure 4.14

Figure 4.15: Chemerin-induced chemotaxis of L1.2 lymphocytes requires $G\alpha_{i/o}$, ROCK, and p38 MAPK.

To determine the impact of chemerin signaling on chemotaxis, murine pre-B lymphocytes L1.2 stably transfected with hCMKLR1 were migrated to increasing doses of chemerin for 4 hours. (a). L1.2-hCMKLR1 cells were pre-treated for 2 hours with either the ROCK inhibitor Y27632 (b), the $G\alpha_{i/o}$ inhibitor pertussis toxin (PTX) (c), the MEK1/2 inhibitor U0126 (d), or the p38 MAPK inhibitor SB203580 (e) at the doses indicated prior to migration to 1 nM chemerin. N=6 from 3 independent experiments. One-way ANOVA vs. veh (a) or veh + Che (b, c, d, e).

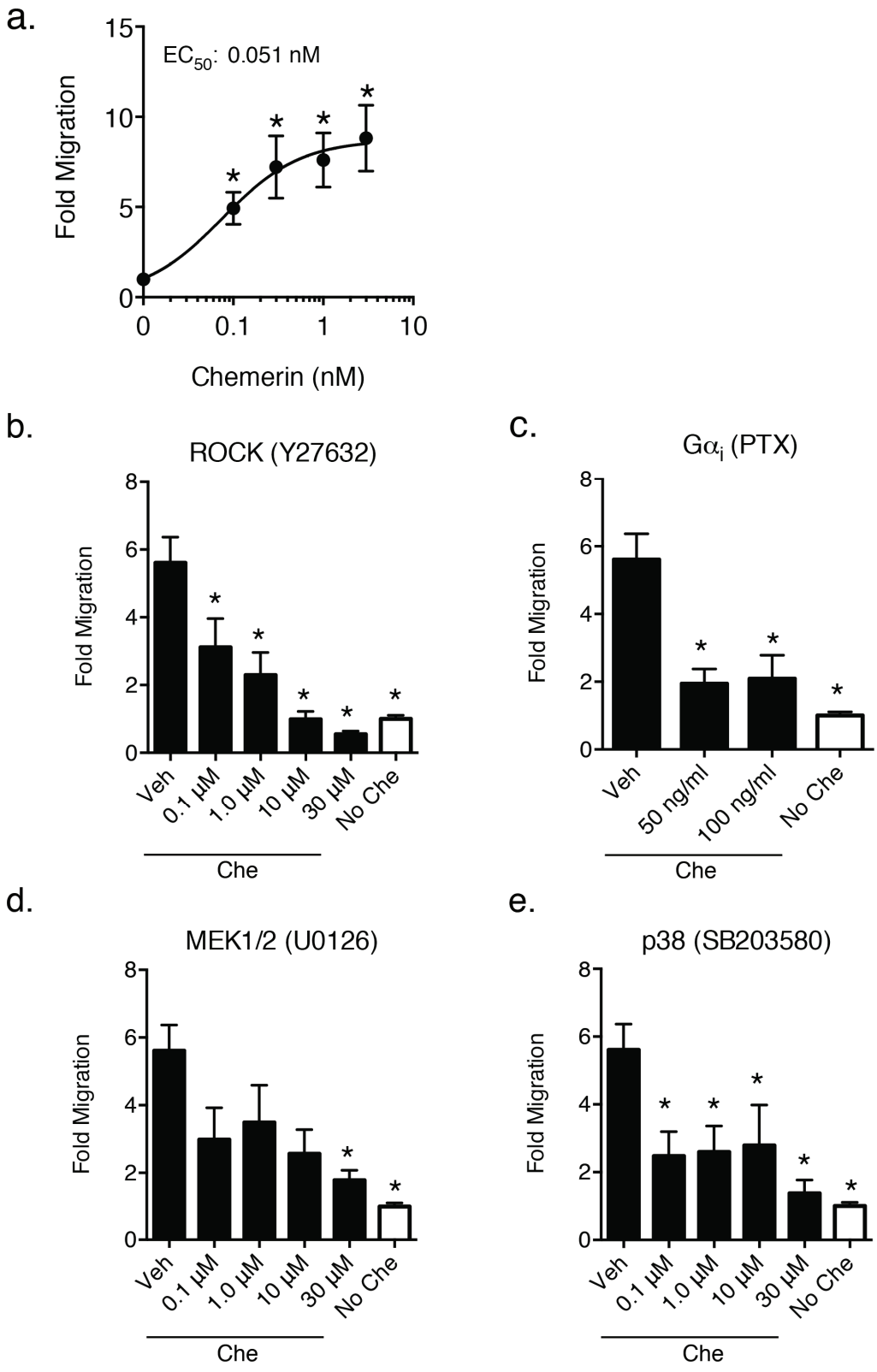
a.
EC50: 0.051 nM
Fold Migration
Chemerin (nM)
b.
ROCK (Y27632)
Fold Migration
Veh
0.1 µM
1.0 µM
10 µM
30 µM
No Che
Che
c.
Gαi (PTX)
Fold Migration
Veh
50 ng/ml
100 ng/ml
No Che
Che
d.
MEK1/2 (U0126)
Fold Migration
Veh
0.1 µM
1.0 µM
10 µM
30 µM
No Che
Che
e.
p38 (SB203580)
Fold Migration
Veh
0.1 µM
1.0 µM
10 µM
30 µM
No Che
Che

Figure 4.15

Figure 4.16: Chemerin-induced chemotaxis of AGS cells requires $G\alpha_{i/o}$, ROCK, and p38 MAPK.

To determine the impact of chemerin signaling on chemotaxis, AGS gastric carcinoma cells were migrated to increasing doses of chemerin for 24 hours. The number of cells migrated were quantified by counting five independent fields at 40x magnification (a). AGS cells were pre-treated for 15 minutes with either the ROCK inhibitor Y27632 (10 μM, Y27), the $G\alpha_{i/o}$ inhibitor pertussis toxin (100 ng/ml, PTX), the MEK1/2 inhibitor U0126 (10 μM, U0), or the p38 MAPK inhibitor SB203580 (10 μM, SB) prior to migration to 0.005 nM chemerin or vehicle (veh) (b). AGS cells were treated with 0.005 nM chemerin, 10 μM LPA, or both for 24 hours (c). Fold change migration is expressed relative to veh. N=3. One-way ANOVA *$p<0.05$ vs. 0 nM chemerin (b, f) or two-way ANOVA vs. veh (d).

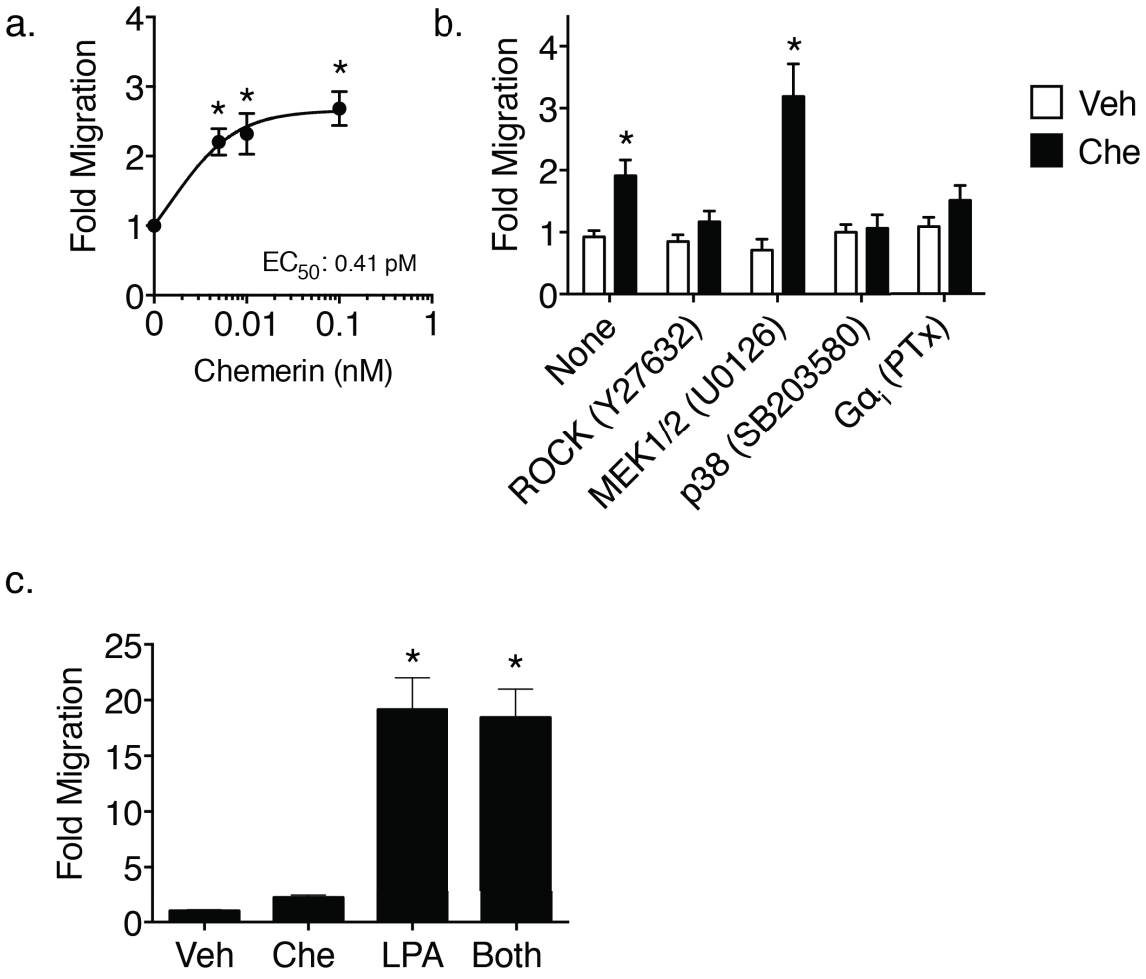
a.
Fold Migration
4
3
2
1
0
0
0.01
0.1
1
Chemerin (nM)
EC50: 0.41 pM
*
*
*
b.
Fold Migration
4
3
2
1
0
*
*
Veh
Che
None
ROCK (Y27632)
MEK1/2 (U0126)
p38 (SB203580)
Gαi (PTx)
c.
Fold Migration
25
20
15
10
5
0
*
*
Veh
Che
LPA
Both

Figure 4.16

Figure 4.17: The chemerin receptors CMKLR1 signal through RhoA and MAPK pathways to regulate SRF activation and migration

Proposed model of human (h) and mouse (m) CMKLR1 and GPR1 signal transduction. **Abbreviations**: calcium: Ca^{2+}, extracellular regulated kinase-1/2: ERK, myocardin-related transcription factor: MRTF, p38 mitogen-activated protein kinase: p38, ras homolog gene family member A: RHOA, rho-associated protein kinase: ROCK, serum response factor: SRF, serum response factor response element: SRF-RE.

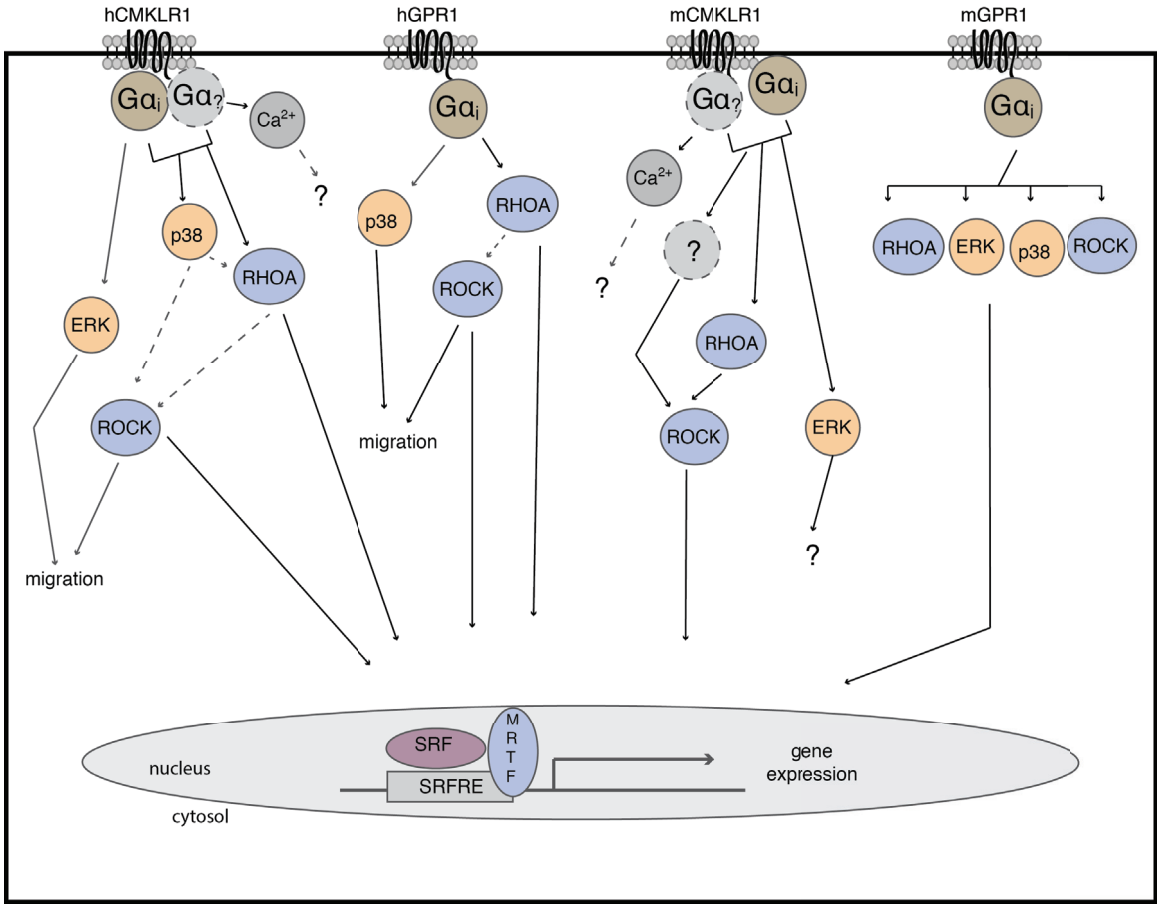
hCMKLR1
hGPR1
mCMKLR1
mGPR1
Gαi
Gα?
Ca2+
?
p38
RHOA
ERK
ROCK
migration
RHOA
ERK
p38
ROCK
nucleus
cytosol
SRF
SRFRE
MRTF
gene expression

Figure 4.17

4.7 Tables

Table 4.1: Quantitative PCR (qPCR) primers

Gene	Sequence 5' to 3'		Accession
CMKLR1	Fw	AAGGGGAGGAGAAATAGAGTCCAC	NM_001142343
	Rv	TGGCTTCCAAGGGGGATAAGTC	
EGR1	Fw	TGACCGCAGAGTCTTTTCCT	NM_001964
	Rv	TGGGTTGGTCATGCTCACTA	
FOS	Fw	TACTACCACTCACCCGCAGA	NM_005252
	Rv	CGTGGGAATGAAGTTGGCAC	
GAPDH	Fw	GAACCATGAGAAGTATGACAACAGC	NM_001256799
	Rv	AGGCAGGGATGATGTTCTGG	
GPR1	Fw	CCTTTGGCATCTGGCTGTGCAA	NM_005279
	Rv	GCCGATGAGATAAGACAGGATGG	
JUNB	Fw	TTGTCAAAGCCCTGGACGAT	NM_002229
	Rv	TTGGTGTAAACGGGAGGTGG	
RHOA	Fw	TTCCCAGAGGTGTATGTGCC	NM_001664
	Rv	TCAGGGCTGTCGATGGAAAA	
SRF	Fw	ACGACCTTCAGCAAGAGGAA	NM_003131
	Rv	AAGCCAGTGGCACTCATTCT	
TPM1	Fw	CAGAAGGCAAATGTGCCGAG	NM_000366
	Rv	TCAGCTTGTCGGAAAGGACC	
VCL	Fw	ATCTCAGGGTCTGGATGTGC	NM_003373
	Rv	GCACCTCGAATCTGCTCTTC	

Table 4.2: Summary of SRF-RE results

Vehicle vs. Chemerin (4 hours):						
	Fold *	**$G\alpha_{i/o}$** (PTX)	**RhoA** (C3T)	**ROCK** (Y27632)	**ERK1/2** (U0126)	**p38** (SB203580)
pCDNA	0.9[b]	no effect	no effect	no effect	partial	no effect
hCMK	6.7	partial	C3T-partial RA2-partial RA3-blocked	blocked	no effect	partial
hGPR1	1.7	blocked	C3T-blocked RA2-partial RA3-blocked	blocked	no effect	no effect
mCMK	16.7	partial	C3T-blocked RA2-blocked RA3-no effect	blocked	no effect	no effect
mGPR1	2.6	blocked	C3T-blocked RA2-blocked RA3-blocked	blocked	blocked	blocked
LPA vs. Both (4 hours):						
	Fold $	**$G\alpha_{i}$** (PTX)	**RhoA** (C3T)	**ROCK** (Y27632)	**ERK1/2** (U0126)	**p38** (SB203580)
pCDNA	0.9[b]	no effect	blocked	blocked	blocked	blocked
hCMK	1.5	no effect	blocked	blocked	blocked	blocked
hGPR1	1.2[b]	no effect	reduced	reduced	reduced	reduced
mCMK	2.2	no effect	partial	partial	no effect	no effect
mGPR1	1.9	blocked	blocked	blocked	blocked	blocked

* Fold change 30 nM chemerin vs. vehicle

$ Fold change LPA vs. Both

b Not significant

Chapter 5: *Gpr1* is an Active Chemerin Receptor Influencing Glucose Homeostasis in Obese Mice

5.1 Rationale and Objectives

The previous results chapters demonstrate that GPR1 is an active chemerin receptor contributing to the signal transduction and function of chemerin. As mentioned previously there have been no reports of GPR1 function in mammals. As such, the mammalian function of GPR1 is essentially unknown. Given that chemerin is an adipose-derived signaling protein (adipokine) that regulates adipocyte differentiation and function, immune function, metabolism and glucose homeostasis, the objectives of this study were to characterize *in vivo* tissue *Gpr1* expression and the metabolic effects of *Gpr1* loss. Herein we demonstrate that *Gpr1* is expressed within metabolically active tissues and report for the first time the generation and metabolic phenotyping of the *Gpr1*-null mouse. Moreover we report the novel finding that GPR1 plays a functional role in glucose homeostasis during obesity.

The figures and text presented in this chapter have been reproduced with copyright permission (Appendix I) from the article (321). Muruganandan Shanmugam, Helen Dranse, and Nichole McMullen assisted with *in vivo* tests, qPCR, and Tango assays, respectively.

5.2 Introduction

Chemerin, also known as retinoic acid receptor responder (tazarotene induced) 2, is a hormone-like protein that is secreted by the liver and WAT as well as at localized sites of inflammation (4,203). Circulating chemerin levels increase with chronic inflammatory diseases and are significantly elevated with obesity. These increases are positively correlated with deleterious elevations in levels of proinflammatory adipokines,

inflammatory markers and insulin resistance, and increased risk for the development and severity of comorbidities such as metabolic syndrome, and T2D (160,164,194).

A growing number of *in vitro* and *in vivo* studies support chemerin as a regulator of immune function, adipose tissue function and glucose homeostasis (154). In the immune system, chemerin acts as a potent chemoattractant for macrophages, immature dendritic cells, and natural killer cells (170,187,207,209). In adipocytes, chemerin and its cognate GPCR CMKLR1 promote adipocyte differentiation and influence mature adipocyte metabolic function (4,228). Chemerin secretion from WAT is increased in obesity. This increase is often but not always associated with an increase in WAT chemerin mRNA expression and/or altered *Cmklr1* expression in a variety of peripheral tissues including skeletal muscle, liver, and WAT. These changes are thought to contribute to the development and/or pathogenesis of obesity: however, the nature of this relationship remains unclear. It is widely accepted that chemerin and CMKLR1 also play a role in glucose homeostasis: however, investigations into the exact nature of this role have provided conflicting results. Notably, *Cmklr1* knockout (KO) mice have been shown to exhibit both normal and glucose intolerant phenotypes; while, chemerin knockout KO mice develop impaired insulin secretion and glucose intolerance (158,220,336,337). By contrast, several models of obese mice demonstrate exacerbated glucose intolerance with chemerin treatment (221,237). Moreover, *in vitro* studies using 3T3-L1 adipocytes show both increased and decreased glucose uptake with chemerin treatment (232,238). Collectively, these studies illustrate the complexity of chemerin function and suggest that the nature of chemerin function in glucose homeostasis is both context-specific and highly regulated.

To date, the majority of known chemerin functions have been attributed to the activation of CMKLR1 in target cells and tissues. However, this fails to fully explain the complexity of observed chemerin activities in obesity and glucose homeostasis. In 2008, GPR1, the closest phylogenetic relative of CMKLR1 in the family of chemoattractant receptors (338,339), was identified to both bind and become activated by recombinant chemerin (179). To date, chemerin is the only known ligand for GPR1. As such GPR1 may contribute to chemerin function; however the role of GPR1 as a chemerin receptor has not been explored. Consequently, aside from a few reports implicating GPR1 as a

low-efficiency HIV co-receptor (338-341), the mammalian function of this highly conserved receptor remains unknown.

5.3 Materials and Methods

5.3.1 Chemerin Receptor Tango Assay

See section 3.3.5.

5.3.2 Animals

All protocols were conducted in accordance with the Canadian Council on Animal Care guidelines and approved by the Dalhousie University Committee on Laboratory Animals. Animals were maintained at 25 ^{o}C on a 12h light: 12h darkness cycle with access to food and water and allowed to feed *ad libitum*. Wild-type *Gpr1* +/+ (WT), heterozygous *Gpr1* +/- (HET), and knockout *Gpr1* -/- (KO) male littermates used in these studies were generated as described in Fig. 2 by HET x HET mating and verified by polymerase chain reaction (PCR)-based genotyping using primers spanning endogenous or transgenic regions of genomic DNA (Table 5.1). Two groups of *Gpr1* WT, HET, and KO mice (six to eight animals per genotype per group) were individually housed at 5 weeks of age. At 7 weeks of age, one group was placed on a low-fat diet (LFD) and the other on a high fat diet (HFD) composed of 10 and 60% kcal from fat, respectively (Research Diets; New Brunswick, NJ, USA; D12450B and D12492). Animals were killed using an overdose (90 mg/kg) of pentobarbital sodium injected intraperitoneally (i.p.) followed by exsanguination.

5.3.3 Tissue and RNA Isolation

Tissues were collected, snap frozen in liquid nitrogen and stored at -80 ^{o}C until processed. RNA was isolated using TRIZOL (Life Technologies; Burlington, ON) or Direct-zol 96-RNA (Zymo Research; Irvine, CA, USA) according to the manufacturer's

protocol. Adipocyte and SVF were isolated from epididymal WAT as described previously (342).

5.3.4 Reverse Transcription and Quantitative PCR

Reverse transcription was used to generate cDNA from 0.5 μg of isolated RNA. Exon-spanning qPCR primers were designed using the Primer3 algorithm (Table 5.2). Gene expression was measured using the Brilliant III Ultrafast qPCR master mix (Agilent; Mississauga, ON, Canada) or Roche FastStart SYBR Green Master (Roche; Laval, QC) according to the manufacturers instructions. Relative gene expression was calculated using the ΔΔCt method (317) with cyclophilin A (*CycA*) as the reference gene.

5.3.5 Body Composition

Total, fat, and lean masses were quantified in anesthetized mice using dual-energy X-ray absorptiometry as described previously using a GE Lunar Piximus2 bone densitometer (220). Organ weights were measured from excised tissues.

5.3.6 Activity and Indirect Calorimetry

Activity, food consumption, and indirect calorimetry were measured in Panlab Physiocages (Panlab Harvard Apparatus; Barcelona, Spain). Data were collected for 24 h following 24 h acclimatization and analyzed using the Metabolism software (Panlab Harvard Apparatus).

5.3.7 Glucose Homeostasis

Glucose tolerance test (GTT) and insulin sensitivity test (IST) were carried out on conscious WT, HET, and KO mice at 6-7 weeks of age and following 7, 13, 19, and 23 (GTT) or 6, 12, 18, and 22 (IST) weeks of feeding with either a LFD or a HFD as described previously (221). Tissue glucose uptake during a GTT was performed as

described previously (221). Briefly, mice were fasted overnight (GTT, glucose uptake) or for 6 hours (IST) prior to injection with 2 mg/g D-glucose (for GTT), 2 mg/g D-glucose containing 10 μCi 2-[1,2-^{3}H(N)] deoxy-D-glucose (PerkinElmer; Waltham, MA) (for glucose uptake) or 0.75 U/kg human insulin (Roche, Laval, QC) (for IST). Blood glucose concentration was monitored from the saphenous vein using a Freestyle light glucometer.

5.3.8 Blood Chemistry

Blood collected from the saphenous vein of conscious mice, was clotted for 2 hours for serum collection. ELISAs were performed according to the manufacturer's instructions to determine serum levels of total insulin (Crystal Chem; Downers Grove, IL, USA; cat# 90080) and chemerin (R&D Systems; Minneapolis, ME; DY2325) from undiluted and one in 1000 serum dilution, respectively.

5.3.9 Adipocyte Colony Formation Assay

Isolation, culture, and adipocyte differentiation of bone marrow-derived mesenchymal stem cells was achieved as described previously (181,228). Briefly, bone marrow was isolated from excised tibia of mice following 24 weeks of feeding on the LFD or HFD and plated in duplicate at 1x10^{7} cells per 100 mm tissue culture dishes in 10 mL αMEM containing 1% L-glutamine and 10% FBS. After 72 hours, non-adherent hematopoietic cells were removed from all plates. The adherent mesenchymal cells were subjected to the adipocyte colony formation assay as follows. For adipocyte differentiation, the cells were treated for 2 days with adipogenic medium (αMEM supplemented with 1mM rosiglitazone, 5 mg/mL insulin, 0.1 μM dexamethasone, 50 μg/mL ascorbic acid, 60 μM indomethacin, and 10% NCS) followed by 2 days with maintenance medium (αMEM containing 5 mg/mL insulin, 10% NCS) for a total of three cycles, beyond which they were kept in maintenance medium until 20 days. For fibroblast colony formation, adherent mesenchymal cells were maintained in growth medium (αMEM containing 1% L-glutamine and 10% FBS) until 20 days. Adipocyte and fibroblast colonies were stained with oil-red O or crystal violet, respectively and the number of colonies per plate was

counted for each mouse. Adipocyte colony numbers were divided by fibroblast colonies to assess adipogenic potential of the mesenchymal stem cell population.

5.3.10 Histology

Freshly isolated tissues were fixed for 48 hours (liver) or 2 weeks (WAT) in 10% neutral buffered formalin, washed twice for 24 hours in 70% ethanol and embedded in paraffin prior to sectioning (4 μm) and hematoxylin and eosin staining. Image J was used to quantify % adipocyte area in liver. Adiposoft macro for Image J was used to quantify adipocyte size in WAT, as described (343).

5.3.11 Pancreatic Insulin Content

Following exsanguination, 50 to 100 mg of pancreas was rapidly excised from mice, placed in 5 ml ice-cold acid-ethanol (1.5% HCl in 70% EtOH), and stored at -20 ^{o}C. Frozen tissue was homogenized, incubated overnight at -20 ^{o}C, and then centrifuged at 2000 x g for 15 minutes at 4 ^{o}C. The aequeous solution was neutralized with an equal volume of 1 M Tris (pH 7.5). Insulin concentration in the resulting extract was determined using an insulin ELISA (Crystal Chem; Downers Grove, IL, USA; cat# 90080).

5.3.12 Protein Multiplex

Serum samples were collected from the saphenous vein at 9:00 or 21:00 of mice allowed to consume food *ad libitum* or following 18 hours (light) or 6 hours (dark) of fasting and clotted for 30-45 minutes at room temperature. Serum was collected by centrifugation at 1000 x g for 15 minutes at 4 ^{o}C, cleared of remaining precipitate by centrifugation at 10000 x g for 10 minutes at 4 ^{o}C, and stored at -80 ^{o}C. The serum concentration of circulating diabetes/feeding signal proteins was determined using the Bio-Plex Pro Mouse Diabetes 8-plex Assay (Biorad; Mississauga, ON, Canada, cat# 171-F7001M) on a Bio-Plex 200 system.

5.3.13 Statistical Analyses

All data are expressed as mean ± SEM. Comparisons were performed using a repeated measures, one- or two-way ANOVA, or two-tailed t-test, where appropriate with Fisher's LSD multiple comparisons test.

5.4 Results

5.4.1 GPR1 is an Active Chemerin Receptor

We used a Tango bioassay (179) to measure CMKLR1 or GPR1 activation in HTLA cells following treatment with increasing doses of chemerin (Fig. 5.1a). Chemerin activated CMKLR1 and GPR1 with a similar efficacy, reaching a maximal response (Emax) of 265.3 ± 182.2 and 185.6 ± 26.5 fold change above vehicle, respectively. Moreover, chemerin activated GPR1 with significantly higher potency (EC_{50} 18.2 ± 2.9 nM) than CMKLR1 (EC_{50} 54.6 ± 30.7 nM) demonstrating not only that chemerin activates GPR1, but also that GPR1 is a highly sensitive chemerin receptor.

5.4.2 *Gpr1* mRNA is Expressed in WAT and Skeletal Muscle

To compare the relative abundance of *Cmklr1* and *Gpr1*, the mRNA levels were measured in a panel of C57BL/6 mouse tissues (Fig. 5.1b). Consistent with previous results (4), *Cmklr1* expression was predominant in WAT and the lung, but it was also present at lower levels in heart, liver, kidney, spleen, thymus, skeletal muscle, brain, and BAT. Similar to *Cmklr1*, *Gpr1* expression was highest in the WAT and low in heart, liver, kidney, spleen, and thymus. *Gpr1* was also abundant in other metabolically active tissues including skeletal muscle, brain, and BAT. Further characterization of individual hind limb muscles demonstrated that *Cmklr1* and *Gpr1* mRNA expression was 2- to 3-fold higher in the soleus muscle compared with the gastrocnemius muscle and tibialis anterior muscles (Fig. 5.1c). This expression pattern was inversely related to the relative

expression of myosin heavy polypeptide 1 (*Myh1*), which marks the difference in fiber type found in these muscles. Chemerin mRNA was also expressed in all three muscles, following a similar pattern as *Glut4*, the primary transporter for insulin-stimulated glucose uptake in skeletal muscles.

WAT is comprised of adipocytes, which store excess energy as lipid, and a heterogeneous population of stromal vascular cells including leukocytes, adipose stem cells, endothelial cells, smooth muscle cells, and pericytes, which contribute to normal WAT maintenance and function. Consistent with our previous results (4), chemerin and *Cmklr1* mRNA were abundant in adipocytes and SVF cells (Fig. 5.1d). By contrast, *Gpr1* mRNA expression was more than 90-fold higher in SVF than in adipocytes. Differential expression of the adipocyte (leptin (*Lep)*) and SVF (tumor necrosis factor alpha (*Tnfα (Tnf)*) markers confirmed effective fraction separation. Based on this initial characterization of *Gpr1* expression and the established function of chemerin in metabolism, we proposed that GPR1 plays a role in glucose homeostasis and WAT differentiation or function.

5.4.3 *Gpr1* Loss Does Not Alter Adipose Tissue Development or Weight Gain on a HFD

To investigate the *in vivo* function of GPR1, mice lacking *Gpr1* expression in all tissues were generated using a retroviral gene trap strategy for the targeted replacement of the *Gpr1* coding sequence (CDS) with a β-galactosidase neomycin resistance fusion gene (*βgeo*) (Fig. 5.2a). Confirmation of targeted allele generation and genotyping was performed using PCR (Fig. 5.2b). Loss of *Gpr1* and gain of *βGeo* mRNA transcript expression in KO mice was confirmed using qPCR in multiple tissues of WT and *Gpr1* KO mice to show loss of *Gpr1* and gain of *βGeo* mRNA (Fig. 5.2c). Newborn and adult *Gpr1* HET and KO mice were grossly indistinguishable and had similar body mass from WT littermates when monitored from birth until 30 weeks of age (Fig. 5.2d). HET breeding crosses generated offspring exhibiting the expected Mendelian distribution and frequency of WT and KO alleles and no sexual bias (Table 5.3).

To determine whether GPR1 contributes to metabolic function, *Gpr1* WT, HET, and KO mice were placed on either a LFD or a HFD for 24 weeks. *Gpr1* mRNA levels were unchanged in WAT and gastrocnemius muscle and were significantly reduced in SOL of mice consuming HFD for 24 weeks when compared with LFD (Fig. 5.3a). As changes in either chemerin or CMKLR1 levels contribute to altered energy and glucose homeostasis, total circulating chemerin as well as *Cmklr1* and chemerin mRNA expression were measured using ELISA and qPCR, respectively (Fig. 5.3b-e). Consistent with previous reports (156,162,221), serum chemerin concentration increased by more than 2-fold following 24 weeks of feeding with a HFD compared with LFD but did not differ with respect to genotype on either diet (Fig. 5.3b). Similarly, *Gpr1* loss did not result in altered chemerin (Fig. 5.3c) expression in the liver, WAT, or soleus muscle in mice fed on either the LFD or HFD. However, chemerin mRNA levels were significantly reduced in both *Gpr1* HET and KO gastrocnemius muscle of HFD-fed mice. *Cmklr1* expression was reduced in the *Gpr1* KO liver in mice fed on a HFD and HET soleus muscle in mice fed on a LFD and was unchanged with either diet in WAT and gastrocnemius muscle (Fig. 5.3d). In the brain, *Gpr1* loss resulted in increased chemerin mRNA expression in the hypothalamus, as well as decreased cortex and hypothalamic *Cmklr1* expression (Fig. 5.3e).

To determine whether GPR1 plays a role in growth and WAT development we assessed body composition by dual-energy X-ray absorptiometry (Fig. 5.4). Mice consuming a HFD had significantly higher fat mass and accelerated body weight gain (Fig. 5.4a and b) compared with those fed on a LFD; however, no differences were observed in body, fat, or lean mass between the genotypes in mice fed on either diet. Measurement of major organ mass following 24 weeks of feeding with either a LFD or a HFD revealed a significant increase in gastrocnemius muscle, soleus muscle, perirenal WAT, and subcutaneous WAT tissue mass (Table 5.4) in mice consuming a HFD irrespective of the genotype. Similarly, liver and spleen mass were significantly elevated with the HFD in WT and KO mice, while pancreas and BAT mass were only elevated in HFD-fed WT and KO mice, respectively. No significant differences were observed between the genotypes within any particular tissue. Consistent with the absence of genotype-driven differences in WAT mass, adipocyte differentiation of mesenchymal

stem cells isolated from HET and KO mice was indistinguishable from that of WT mice (Fig. 5.5) when examined visually with respect to colony morphology (Fig. 5.5a). Quantification of the adipocyte colony to fibroblast colony ratio, an indicator of adipogenic potential of the isolated mesenchymal stem cells, showed a significant increase in HET adipocyte formation in mice consuming the LFD when compared with WT (Fig. 5.5b). Similarly, quantification of total lipid content using oil red-O showed significantly increased lipid content in adipocytes derived from both HET and KO mice when compared with WT mice consuming the LFD (Fig. 5.5c).

5.4.4 *Gpr1* Loss is Associated with Decreased Dark-Cycle Food Consumption in Mice Consuming the HFD

Given the expression of *Gpr1* in the metabolically active tissues skeletal muscle, WAT and brain, we assessed the impact of *Gpr1* loss on metabolic homeostasis by measuring activity, energy expenditure (Fig. 5.6) and food consumption (Fig. 5.7) using metabolic cages. For all genotypes, HFD-fed mice were significantly more active than LFD during the dark cycle (Fig. 5.6a). Energy expenditure was similar for all genotypes (Fig. 5.6b). *Gpr1* WT, HET and KO mice had similar total, light and dark cycle food consumption on LFD (Fig. 5.7a). WT mice consuming a HFD had comparable total calorie consumption to LFD counterparts. By contrast, *Gpr1* KO and HET mice consumed significantly fewer HFD-derived calories (30% and 20% reduction, respectively) than LFD-fed mice of the same genotype. Moreover, total HFD consumption was significantly lower in KO mice than in WT mice. Both *Gpr1* HET and KO mice also consumed significantly less total food than WT mice during the dark cycle (Fig. 5.7a). While WT mice on a HFD had a significant increase in meal frequency (Fig. 5.7b) and meal size (Fig. 5.7c) during the dark cycle, this was not observed for *Gpr1* HET or KO mice. Examination of food consumed throughout the 24-hour light/darkness cycle revealed significantly reduced food consumption of KO and HET mice when compared with WT as early as 1 hour following the initiation of darkness at 19:00 and persisting until 23:00.

To assess the role of *Gpr1* in central and systemic feeding regulation we measured the mRNA expression of key feeding signals in the brain and used a multiplex ELISA to quantify the circulating levels of endocrine factors with established effects on feeding and energy homeostasis (Fig. 5.8) in WT and KO mice consuming the HFD for 20 weeks. Serum samples were collected in both the fasting and fed state at 9:00 and 21:00 to assess hormone levels during both the light and darkness phase (Fig. 5.8a). Circulating levels of insulin, glucagon, GLP-1, leptin and plasminogen activator inhibitor-1 (PAI-1) were similar between WT and KO mice at all time points examined. By contrast, circulating levels of the anorexigenic signals resistin and GIP were significantly reduced in KO mice when compared with WT during the fasted/light and fed/dark states, respectively. Additionally, circulating levels of the orexigenic signal ghrelin were significantly elevated in KO mice when compared with WT in the fasted/light state. Expression of the hypothalamic appetite modulating hormones neuropeptide (*Npy*), agouti-related peptide (*AgRP*) and proopiomelanocortin (*Pomc*) were unchanged in the hypothalamus with *Gpr1* loss (Fig. 5.8b).

5.4.5 *Gpr1* Deletion is Associated with Exacerbated Glucose Intolerance Following Prolonged HFD Consumption

To determine whether GPR1 plays a role in glucose homeostasis, fasting glucose, IST, and GTT were conducted in *Gpr1* WT, HET and KO mice consuming either LFD or HFD (Fig. 5.9). No difference was detected between the genotypes with respect to fasting glucose before diet initiation or following up to 24 weeks of feeding with either a LFD or a HFD (Fig. 5.9a). Similarly, a single bolus of insulin produced a comparable decline in blood glucose for *Gpr1* WT, HET and KO mice (Fig. 5.9b). Consistent with the development of insulin resistance, HFD consumption resulted in a smaller insulin-stimulated reduction in blood glucose than LFD; however, no overall genotypic effect was detected. *Gpr1* loss had no significant impact on glucose tolerance at baseline or following 24 weeks of feeding with a LFD. WT mice became glucose intolerant following 24 weeks of feeding with a HFD, with peak blood glucose at 15 minutes following glucose injection approximately 20% higher than that observed in the LFD

group. By contrast, both *Gpr1* HET and KO mice exhibited significantly exacerbated glucose intolerance following 24 weeks of feeding with a HFD (Fig. 5.9c), compared with WT mice on the same diet. Glucose intolerance was more severe in KO mice, with an average approximate increase in blood glucose levels of 10% when compared with WT mice as early as 15 minutes following the glucose bolus. By 120 minutes following glucose administration, blood glucose levels of KO mice were 33% higher than WT mice. Intermediate between WT and KO, blood glucose concentration increased more slowly in *Gpr1* HET mice when compared with KO mice, becoming significantly higher than WT only at 90 and 120 minutes following the glucose injection and reaching an average of 40% increase above the levels for WT mice at 120 minutes. Upon pyruvate administration for assessment of hepatic gluconeogenesis, blood glucose levels were significantly elevated for both *Gpr1* WT and KO mice following 20 weeks of feeding with a HFD. Blood glucose levels in WT mice peaked after 30-45 minutes and declined back to baseline over the course of the experiment. While blood glucose levels rose and declined at a rate similar to that in WT mice, peak blood glucose was delayed to 90 minutes with *Gpr1* loss. Consistent with this delay, blood glucose levels were significantly higher in KO mice than in WT mice at 60, 90, 120, and 180 minutes (Fig. 5.10a). No differences in the mRNA levels for the gluconeogenic enzymes phosphoenolpyruvte carboxylase (*Pepck (Pck1)*) or glucose-6-phosphatase (*G6pc*) were observed between the genotypes (Fig. 5.10b). To determine whether the elevations in blood glucose levels observed in the GTT and PTT were associated with a decrease in basal or insulin-stimulated glucose uptake we performed tissue glucose uptake experiments in WT and *Gpr1* KO mice after 20 weeks of feeding with a HFD. Glucose uptake was unchanged with *Gpr1* loss in the key tissues responsible for peripheral glucose uptake: gastrocnemius muscle, soleus, and WAT (Fig. 5.10c). By contrast, pancreatic glucose uptake was significantly increased in KO mice when compared with WT.

To determine whether the observed glucose intolerance on the HFD was a consequence of altered pancreatic insulin secretion, *Gpr1* mRNA expression in the pancreas as well as pancreatic insulin content and circulating insulin levels were measured (Fig. 5.11). *Gpr1* mRNA expression in the pancreas was similar to that in the

brain, gastrocnemius muscle, and WAT and was significantly lower than that in soleus muscle (Fig. 5.11a). Total pancreatic insulin content was unchanged with *Gpr1* loss in HFD-fed mice (Fig. 5.11b) and fasting serum insulin levels were similar between the genotypes in mice consuming the LFD (Fig. 5.11c). Consistent with the development of insulin resistance, fasting serum insulin levels were significantly elevated in WT mice consuming the HFD compared with LFD-fed mice. By contrast, *Gpr1* KO mice exhibited more than 50% lower fasting serum insulin levels than WT mice fed on the HFD (Fig. 5.11c). Moreover, glucose-stimulated serum insulin levels (Fig. 5.11d) and area under the insulin curve (AUC) (Fig. 5.11e) were lower in KO mice compared with WT and HET mice for both the LFD and HFD; however, this trend was significant only at the 45 minutes time point of the HFD.

5.4.6 Liver and Adipose Tissue Morphology, Inflammation, and Markers of Insulin Resistance are Unchanged with *Gpr1* Loss

Liver steatosis, adipocyte hypertrophy, and inflammation are common features of obesity contributing to the development of glucose intolerance. *Gpr1* WT, HET and KO mice fed on a LFD had minimal lipid deposition in the liver and all developed similar hepatic steatosis in response to the HFD (Fig. 5.12a and b). Although liver steatosis is commonly associated with inflammation, hepatic mRNA expression of the proinflammatory cytokines *TNFα* and *Il6* did not reveal any differences in liver inflammation on either diet or with *Gpr1* loss (Fig. 5.12c). Similarly, WAT histology demonstrated an increase in crown-like structures indicative of infiltrating macrophages and dead adipocytes (344) with a HFD but did not display any gross morphological differences between the genotypes on either diet (Fig. 5.13a). There was no difference between the genotypes in *TNFα* or the macrophage marker macrophage antigen-1 (*Mac1 (Mph1)*) mRNA expression in WAT on either diet (Fig. 5.13b). Frequency analysis of the adipocyte size showed that *Gpr1* HET and KO mice had a similar distribution of adipocyte sizes to WT mice fed on both the LFD and the HFD (Fig. 5.13c). Taken together these data indicate that *Gpr1* loss does not alter liver/WAT morphology or inflammation in lean or obese mice.

In peripheral tissues, insulin activation of the insulin receptor (INSR) promotes GLUT4-mediated glucose uptake and lowering of blood glucose levels. Insulin resistance and impaired peripheral tissue glucose uptake are common features of obesity-associated glucose intolerance. Consistent with the development of insulin resistance, *Glut4* mRNA expression in WAT was 50% lower in mice fed on a HFD compared with mice consuming a LFD; however, compared with WT mice, *Gpr1* HET and KO mice did not have altered *Glut4* mRNA expression in any of the tissues examined on either diet (Fig. 5.14a). By contrast, while *InsR* mRNA expression showed no change with a HFD in the examined tissues and no difference with *Gpr1* loss in WAT or soleus muscle, there was a significant decrease in *InsR* mRNA expression in the gastrocnemius muscle of *Gpr1* KO mice fed on a HFD (Fig. 5.14b).

5.5 Discussion

The goal of this study was to examine the contribution of GPR1 to the biological effects of chemerin by evaluating the phenotype of *Gpr1* KO mice. We have shown that *Gpr1* mRNA expression predominates in skeletal muscle and WAT, and is highest in the SVF of WAT. While *Gpr1* KO mice consumed significantly less food, their total activity and energy expenditure were not different from WT. Consistent with this, *Gpr1* KO mice had normal body weight, adipose development and tissue inflammation. However, loss of *Gpr1* resulted in exacerbation of HFD-induced glucose intolerance, elevated blood glucose following a pyruvate challenge, and reduced glucose-stimulated circulating insulin in obese mice. As such, this study provides the first empirical evidence supporting a mammalian function for GPR1 as a modifier of glucose homeostasis during obesity.

The varied population of adipose stem cells and leukocytes within the SVF supports WAT differentiation and expansion and connect energy homeostasis with immunity and inflammation (345). Although *Gpr1* mRNA was reported previously in adipocytes (182), we report here for the first time that *Gpr1* mRNA expression was markedly higher in the SVF than in adipocytes. As such, the relative importance of chemerin signaling through GPR1 may be greatest in the SVF where GPR1 may contribute to immune function and/or WAT development. There is, however, no evidence

for *Gpr1* expression in endothelial cells, lymphocytes, or leukocytes (205,346,347). Additionally, peripheral tissue inflammation, and WAT mass were largely unaffected by *Gpr1* loss, suggesting that the function of GPR1 within the SVF is likely not in modulation of inflammation or adipose tissue development, both established chemerin functions (157,181,228,314). With respect to precursor cell differentiation, *Gpr1* loss did increase adipocyte colony formation and total lipid content in differentiated adipocytes derived from mice consuming the LFD suggesting a potential role for *Gpr1* in lipid storage in MSC-derived adipocytes. These *in vitro* results were not recapitulated in mice consuming the HFD or *in vivo* where adipocyte size was unaffected by *Gpr1* loss. Taken together, these studies suggest that GPR1 does not contribute to WAT inflammation during obesity, lipid storage, or adipogenesis; however, we cannot rule out the possibility that GPR1 plays a specialized role in chemerin-mediated immune or WAT function or in MSC-derived adipocytes at other body sites.

In this study we found that both *Gpr1* HET and KO mice fed on the HFD consumed significantly less food than WT counterparts, largely as a consequence of reduced dark cycle meal frequency and size. While *Gpr1* mRNA was expressed in the hypothalamus, we observed no change in the hypothalamic mRNA expression of the key feeding hormones *NPY*, *AgRP*, and *POMC*. Paradoxically, several orexigenic signals were activated with *Gpr1* loss. Notably; circulating levels of resistin and ghrelin were both altered in the fasted/light state in a manner that would be predicted to increase food consumption. Additionally, we observed an increase in hypothalamic chemerin mRNA levels coincident with a decrease in *Cmklr1* expression for *Gpr1* KO mice. Thus, while our data suggest that *Gpr1* may influence circadian appetite regulation during HFD consumption, it is also possible that the altered chemerin/*Cmklr1* expression could have contributed to decreased food consumption. Investigations on a possible role for chemerin and CMKLR1 in feeding regulation are limited and have thus far provided conflicting results. *Cmklr1* KO but not chemerin KO mice consume less food than WT mice despite unaltered levels of the feeding genes *NPY* and *AgRP* (158,220). Likewise, peripheral but not central chemerin injection reduces food consumption in association with a decrease in *AgRP* expression (348,349). To date, the only reported *Gpr1* mRNA expression in humans is in the brain (350); however, no studies have investigated a role

for chemerin, CMKLR1, or GPR1 in feeding in humans. While the mechanism and implications of GPR1-mediated feeding modulation remains unclear, these findings reiterate the need for further studies on the role that chemerin and its receptors play in the regulation of feeding and energy balance.

Insulin regulates glucose homeostasis by balancing glucose uptake in peripheral tissues with *de novo* hepatic glucose production via gluconeogenesis. In obesity, insulin resistance and insulin-deficiency are associated with reduced glucose uptake and increased gluconeogenesis. In severe cases, this can lead to pancreatic stress and a decline in insulin secretion, further exacerbating glucose intolerance. *Gpr1* loss resulted in a detrimental exacerbation of glucose intolerance with obesity. Interestingly, in obese mice *Gpr1* loss was also associated with severely elevated blood glucose levels following a pyruvate challenge. Similar rates of glucose accumulation and disposal in the PTT suggest that the elevated blood glucose levels in *Gpr1* KO mice do not reflect alterations in either gluconeogenesis or glucose uptake, respectively. Consistent with this, we observed no change in key gluconeogenic enzymes or the quantity of glucose taken up into peripheral tissues 60 minutes following a glucose challenge with *Gpr1* loss. These data are, however consistent with a delay in glucose disposal, which could arise as a consequence of insulin resistance in peripheral tissues (WAT, liver, and skeletal muscle) and/or impairment in GSIS. Clinical, *in vivo,* and *in vitro* studies suggest a potential role for the chemerin axis in insulin resistance (154). We found no evidence of altered adipose or liver tissue inflammation or lipid deposition, common features of obesity-associated insulin resistance, suggesting that these are not likely contributing to the observed phenotype. With respect to a potential role for *Gpr1* in skeletal muscle function, we demonstrate expression of chemerin, *Gpr1*, and *Cmklr1* within the hind limb, suggesting that muscle may be both a source and target of chemerin signaling through CMKLR1 and GPR1. Similar expression has been shown previously in mouse gastrocnemius muscle (221). Coincident with the HFD glucose intolerance, gastrocnemius muscle *InsR* mRNA levels were elevated in WT mice. This increase was observed to a lesser extent in both HET and KO mice, suggesting that failure to up regulate *InsR* expression in skeletal muscle with a HFD may contribute to exacerbated insulin resistance in KO mice. A similar pattern of *InsR* expression was observed previously in *Cmklr1* KO mice, which

also exhibit glucose intolerance (220). *Gpr1* loss could also be contributing to dysfunctional skeletal muscle metabolism through alteration of the chemerin axis as we show decreased *Cmklr1* and chemerin mRNA expression in KO soleus and gastrocnemius muscle respectively. These changes were not sufficient to alter circulating chemerin levels, but could contribute to local changes in chemerin secretion in the muscle.

Previous studies have implicated chemerin as a positive regulator of pancreatic insulin secretion (158). In this study, *Gpr1* loss was associated with reduced GSIS in the context of the HFD. Furthermore, *Gpr1* KO mice had lower fasting insulin levels after chronic feeding of the HFD. Given that no difference was observed for pancreatic insulin content, it is most likely that *Gpr1* KO mice are deficient in glucose-evoked pancreatic insulin release rather than in insulin synthesis or β-cell development. Interestingly, KO mice had significantly lower circulating levels of the incretin hormone GIP, which normally functions to increase GSIS (351), suggesting that this system may be impaired in *Gpr1* KO mice. While *Gpr1* KO mice exhibited higher peak glucose levels in the GTT and PTT, the rate at which glucose was cleared from the blood did not differ between genotypes. Taken together, these data suggest that *Gpr1* KO mice exhibit a delayed glucose uptake response to the elevated blood glucose levels produced in these tests. As there were no obvious differences in insulin sensitivity between genotypes, this may have been a consequence of the combined effects of reduced insulin release, or changes in INSR signaling and decreased skeletal muscle *Insr* expression. While the precise mechanism remains to be elucidated, it is clear that the effects of *Gpr1* loss on pancreatic insulin release and glucose uptake are contextual and become apparent only in the presence of obesity and insulin resistance.

It is well established that following secretion chemerin is cleaved by a variety of proteases to generate chemerin peptides with varying degrees of activity (174,176,352). The finding that certain isoforms may be selectively elevated in localized sites of inflammation, suggests that the nature of chemerin function in a given disease state probably depends upon the profile of chemerin isoforms present (175). It is unknown as to which chemerin isoforms are elevated in obesity; however, it is possible that GPR1 function is essential in obese but not lean mice because it serves as a functional receptor

for isoforms that predominate in obesity. Alternatively, Huang *et al.* postulated that *Cmklr1* and *Gpr1* might have diverged subsequent to a gene duplication event (338) suggesting the possibility of some redundancy in receptor functions. Given that *Cmklr1* and chemerin expression were altered in skeletal muscles in *Gpr1* KO mice, we cannot rule out the possibility that changes in chemerin activation of *Cmklr1* in the *Gpr1* KO mice compensated for the loss of GPR1 function. As such, metabolic evaluation of *Gpr1/Cmklr1* double knockout mice could provide further insight into the role that these receptors play in regulating chemerin function.

In summary, we report for the first time the generation and metabolic phenotyping of mice lacking the active chemerin receptor GPR1. This study provides further support that a functional chemerin system is required for the maintenance of healthy glucose homeostasis during obesity. Loss of *Gpr1 in vivo* alters food consumption and results in glucose intolerance in obese mice. In humans, elevations in circulating chemerin correlate with obesity, inflammation, and diabetes risk; however, no studies to date have examined human GPR1 expression or function in any detail. Given that mouse GPR1 shares 47% amino acid identity with human GPR1, consideration of GPR1 as a functional chemerin receptor in WAT, skeletal muscle, satiety, and glucose homeostasis in future studies using both mice and humans could help clarify the complex role chemerin plays in metabolic function.

5.6 Figures

Figure 5.1: GPR1 is an active chemerin receptor and is expressed in metabolically active tissues

GPR1- or CMKLR1-tTA fusion receptors were expressed in HTLA cells to assess receptor activation following treatment with increasing doses of recombinant human chemerin. The resulting luminescent signal was expressed as fold change luminescence relative to 0 nM chemerin treatment, N= 13-28 (a). *Gpr1* and *Cmklr1* mRNA expression was measured by qPCR analysis in the indicated tissues from 8-12 week old mice and expressed relative to heart, N= 6 (b). *Gpr1*, *Cmklr1*, chemerin, *Glut4* and myosin heavy polypeptide 1 (*Myh1*) mRNA levels were measured by qPCR analysis in isolated Tibialis anterior (TA), soleus (SOL) and gastrocnemius muscle (GA) muscles from male and female mice and expressed relative to TA, N= 5-7 (c). *Gpr1*, *Cmklr1*, chemerin, leptin and tumor necrosis factor alpha (*TNFα)* mRNA expression were determined by qPCR analysis in adipocyte (Adp) and stromal vascular fraction (SVF) cells isolated from WAT, N= 5-6. Results are expressed relative to Adp (d). All tissues were collected from wild-type mice 10-12 weeks old. One-way ANOVA (c) t-test (d) *$p<0.05$ as indicated.

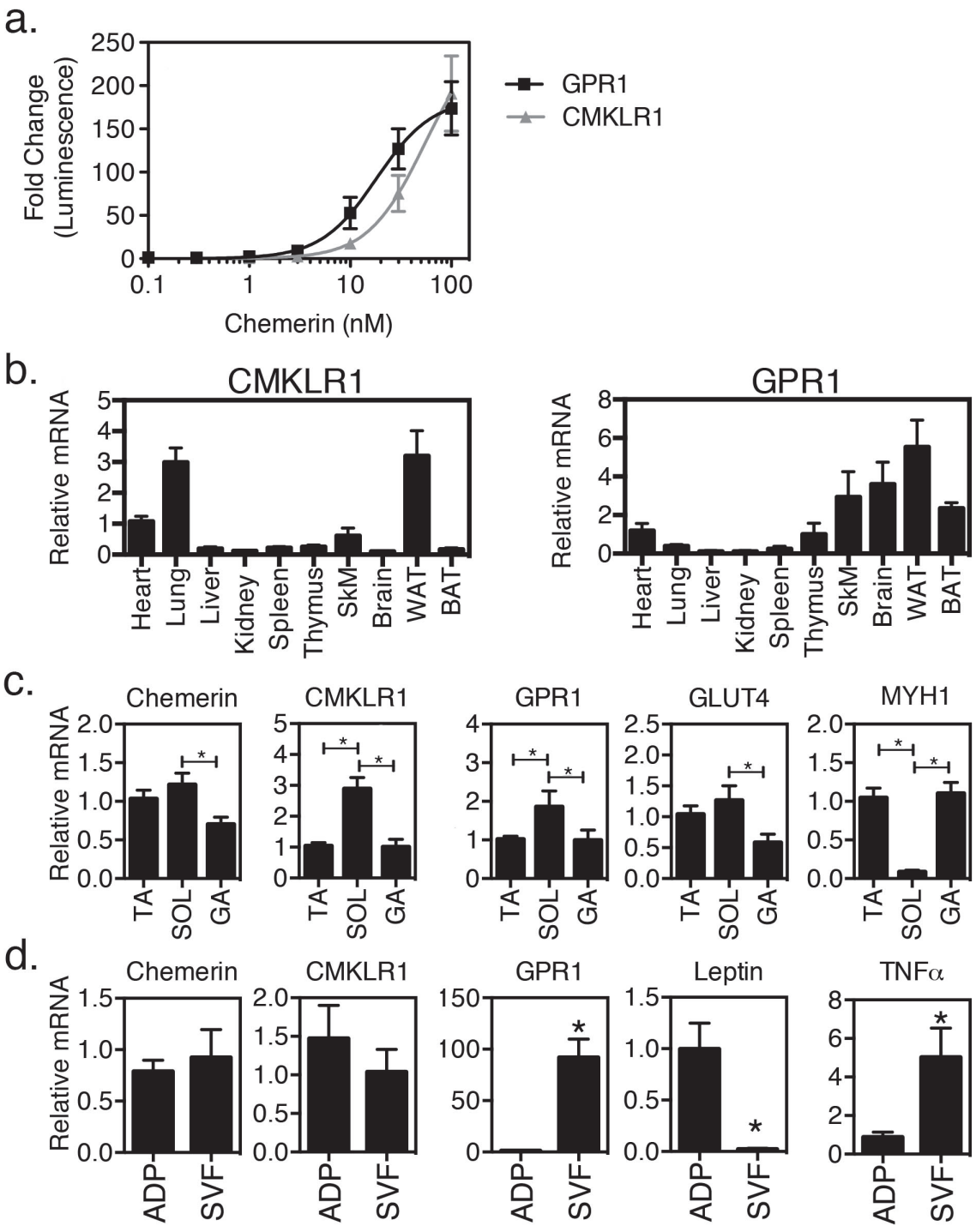
a.
Fold Change (Luminescence)
250
200
150
100
50
0
0.1
1
10
100
Chemerin (nM)
GPR1
CMKLR1
b.
CMKLR1
Relative mRNA
Heart
Lung
Liver
Kidney
Spleen
Thymus
SkM
Brain
WAT
BAT
GPR1
c.
Chemerin
CMKLR1
GPR1
GLUT4
MYH1
TA
SOL
GA
d.
Chemerin
CMKLR1
GPR1
Leptin
TNFα
ADP
SVF

Figure 5.1

Figure 5.2: *Gpr1* null mouse model generation and confirmation of gene deletion

Heterozygous *Gpr1* +/- (HET) mice on a C57BL/6 background were generated at the Texas Institute of Genomic Medicine using a retroviral gene trap strategy for the targeted disruption of the *Gpr1* allele. Schematic representation of the endogenous wild-type *Gpr1* allele or the targeted allele containing the viral long terminal repeats (LTR) used for target sequence insertion, the splice acceptor (SA) required for alternative splicing of the targeted transcript, a β-galactosidase neomycin resistance fusion gene (*βgeo*) and a polyadenylation sequence (pA) (a). Transcripts produced from the endogenous allele contain all 3 *Gpr1* exons (represented by numbered grey boxes), including exon 3, which contains the complete *Gpr1* coding sequence. As a consequence of the SA in the targeted allele, the target mRNA transcript contains only exon 1, *βGeo*, and a polyadenylated tale ($AAAA_n$). Confirmation of targeted allele generation and genotyping was performed using a PCR assay. Arrows indicate the position of *Gpr1* genotyping primers: a forward primer (Ef) located 5' to the insertion site together with a combination of reverse primers located in the endogenous (Er) sequence 3' to the insertion site and the long terminal repeat (LTR) of the targeted (Tr) sequence. To determine the genotype of mice from Het x Het breeding pairs, PCR products generated using ear clip DNA and the genotyping primers were resolved by DNA gel electrophoresis with size approximation using a 1-kb+ ladder. The arrow indicates Endogenous (E) and transgenic (T) product sizes (b). Loss of *Gpr1* and gain of *βGeo* mRNA transcript expression in KO mice was confirmed using quantitative real-time PCR (qPCR) in gastrocnemius muscle (GA), soleus (SOL), epididymal white adipose tissue (WAT), brown adipose tissue (BAT) and brain of wild-type (WT) and *Gpr1* homozygous knockout (KO) mice to show loss (not detected: nd) of *Gpr1* and gain of *βGeo* mRNA in WT and KO mice, respectively (c). Results are expressed relative to GA, N=3-4. Total body mass was measured at birth and at 30 weeks of age for WT, heterozygous (HET), and KO mice generated from HET x HET crosses (d).

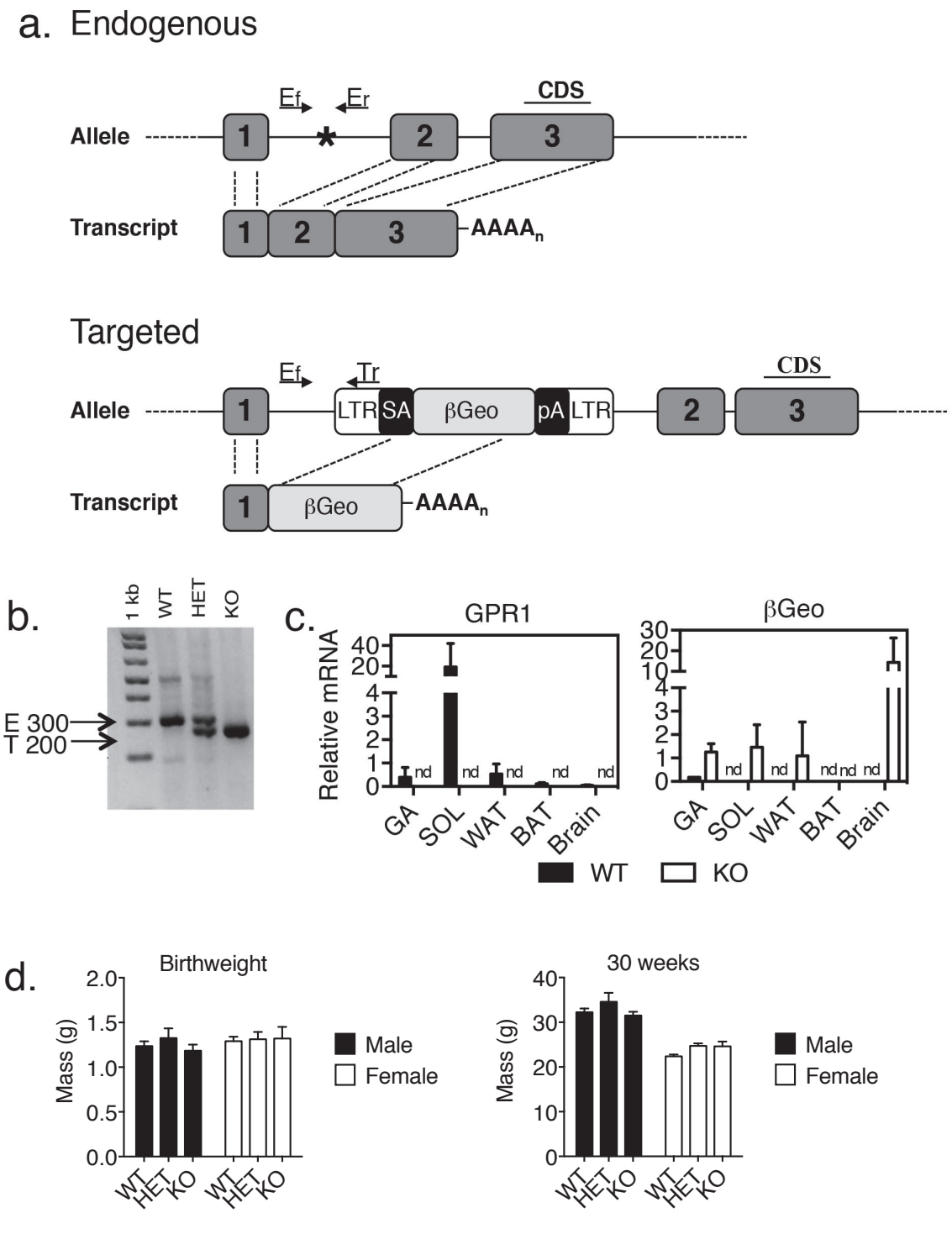
a. Endogenous
Ef
Er
CDS
Allele
1
2
3
Transcript
AAAAn
Targeted
Tr
LTR
SA
βGeo
pA
b.
1 kb
WT
HET
KO
E 300
T 200
c.
GPR1
βGeo
Relative mRNA
nd
GA
SOL
WAT
BAT
Brain
WT
KO
d.
Birthweight
30 weeks
Mass (g)
Male
Female

Figure 5.2

Figure 5.3: Chemerin and *Cmklr1* expression with *Gpr1* loss

Gpr1 mRNA expression was measured in epididymal white adipose tissue (WAT), gastrocnemius muscle (GA) and soleus (SOL) muscles from wild-type (WT) mice (a) N=4-7. Results are expressed relative to low-fat diet (LFD) WAT. * $p<0.05$ vs. LFD, # $p<0.05$ vs. WAT and GA. Total circulating chemerin concentration in serum samples was determined using a mouse chemerin ELISA, N=5-8 * $p<0.05$ vs. LFD (b). Chemerin (c) and *Cmklr1* (d) mRNA expression were measured using qPCR analysis in liver, WAT, GA and SOL muscles, and brown adipose tissue (BAT) N=5-8. Results are expressed relative to LFD WT. All samples were from *Gpr1* (WT), heterozygous (HET), or homozygous knockout (KO) mice following 24 weeks of either LFD or high-fat (HFD) diet as indicated. One-way ANOVA*$p<0.05$ vs. WT within diet, or # $p<0.05$ vs. LFD. Chemerin, *Cmklr1*, and *Gpr1* mRNA expression was measured in whole brain, cortex, and hypothalamus isolated from 30 week old WT and KO mice consuming LFD (e) N=4. Results are expressed relative to WT whole brain. Two-way ANOVA *$p<0.05$ vs. WT within tissue.

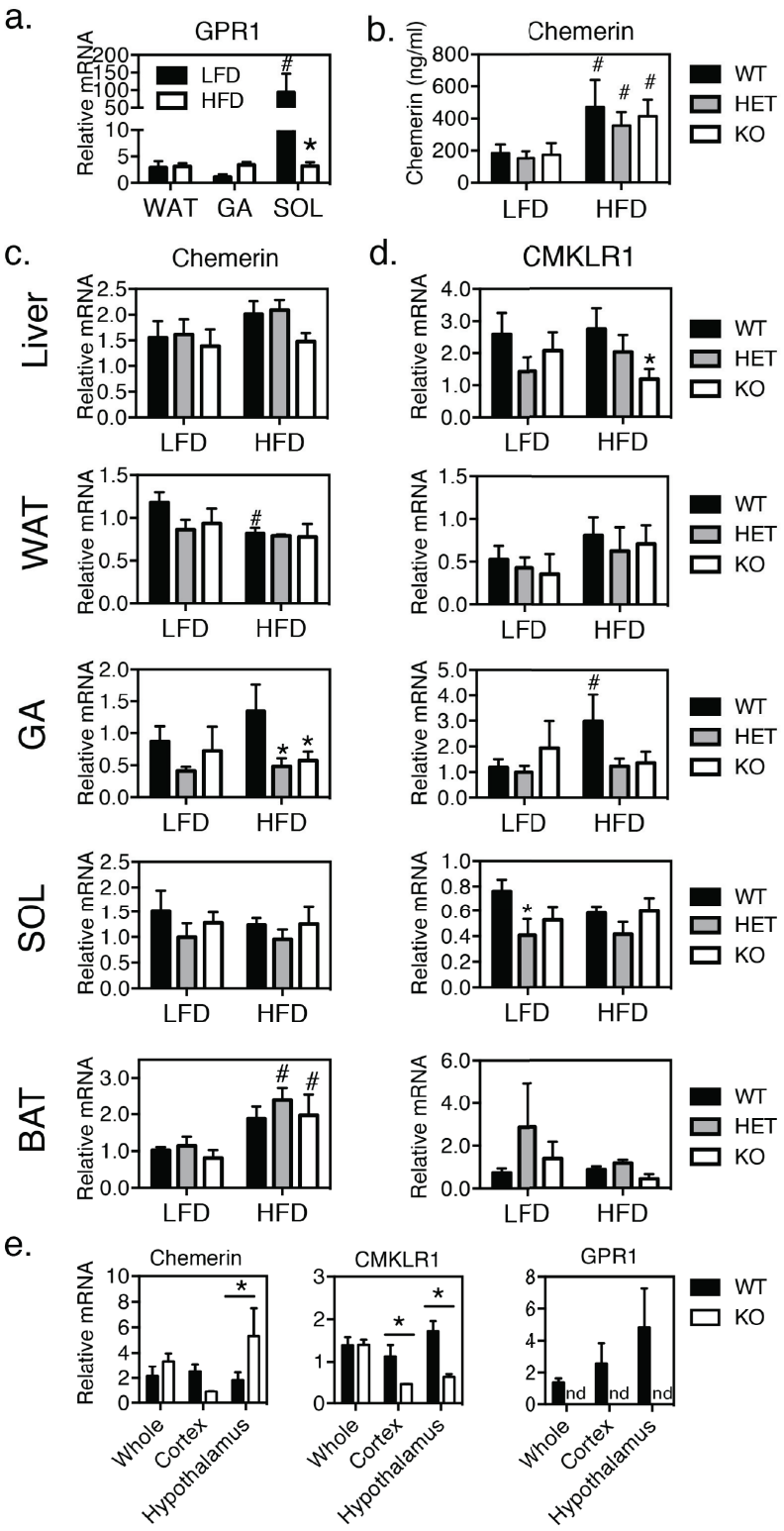
a.
GPR1
Relative mRNA
LFD
HFD
WAT GA SOL
b.
Chemerin
Chemerin (ng/ml)
WT
HET
KO
LFD HFD
c.
Chemerin
d.
CMKLR1
Liver
WAT
GA
SOL
BAT
Relative mRNA
e.
Chemerin
CMKLR1
GPR1
nd
Whole
Cortex
Hypothalamus

Figure 5.3

Figure 5.4: *Gpr1* KO mice have normal body weight and fat mass

Total body mass was measured for 24 weeks in *Gpr1* wild-type (WT), heterozygous (HET), or homozygous knockout (KO) mice consuming either a low-fat diet (LFD) or high fat diet (HFD) beginning at 7 weeks of age (a). Dual energy x-ray absorptiometry was used to calculate mass of total fat (white bars) and lean (dark bars) tissues at 6 weeks of age prior to diet initiation (Baseline pooled LFD and HFD before diet initiation, N= 10-15) and following 24 weeks of either LFD or HFD (N=6-8) (b). One-way (b) repeated measures (a) ANOVA *$p<0.05$ vs. WT within diet.

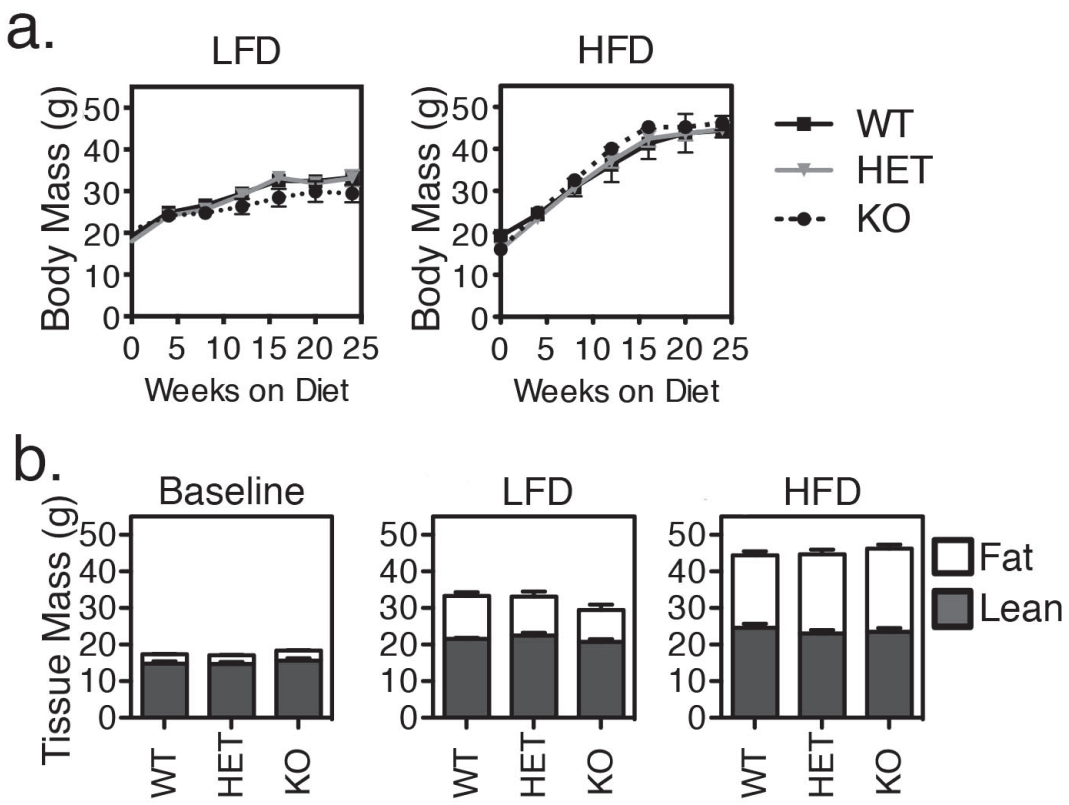
a.
LFD
HFD
Body Mass (g)
0
10
20
30
40
50
0 5 10 15 20 25
Weeks on Diet
WT
HET
KO
b.
Baseline
LFD
HFD
Tissue Mass (g)
WT
HET
KO
Fat
Lean

Figure 5.4

Figure 5.5: Adipocyte differentiation of mesenchymal stem cells isolated from *Gpr1* HET and KO mice is similar to that of WT mice

Mesenchymal stem cells freshly isolated from wild-type (WT), heterozygous (HET), and homozygous knockout (KO) mice consuming the low-fat diet (LFD) or high-fat diet (HFD) for 24 weeks were grown with an adipogenic cocktail for 20 days to induce adipocyte differentiation. Representative images of Oil Red-O stained lipid droplets (a), quantification of adipocyte colonies (N=4 LFD, N=8 HFD) are represented as a ratio of adipocyte:fibroblast colonies per plate (b) and oil red-O staining (N=2 LFD, N=8 HFD) (c). Two-way ANOVA *$p<0.05$ vs. WT within diet, #$p<0.05$ vs. LFD within genotype.

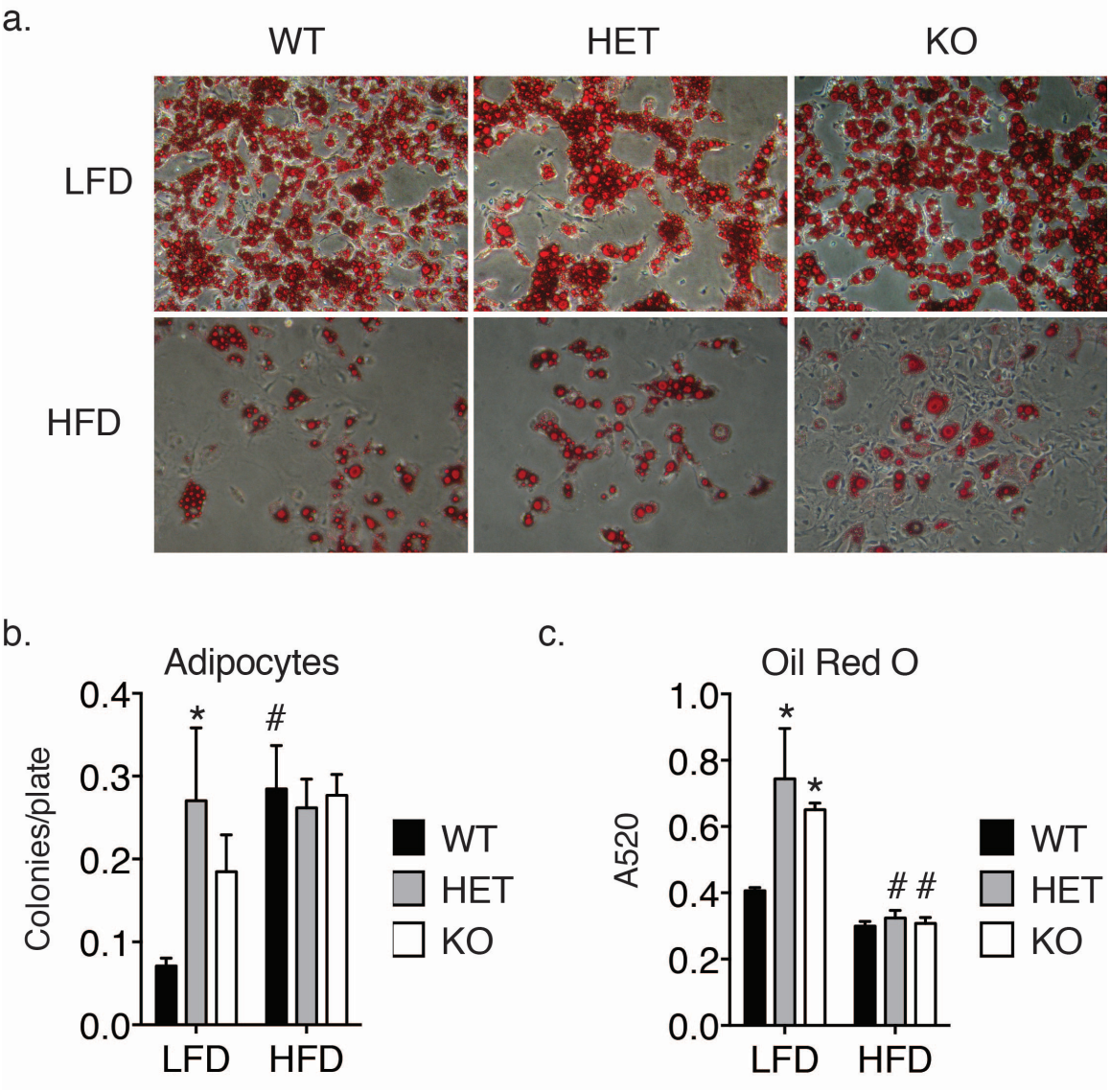
a.
WT
HET
KO
LFD
HFD
b.
Adipocytes
Colonies/plate
0.4
0.3
0.2
0.1
0.0
*
#
LFD
HFD
WT
HET
KO
c.
Oil Red O
A520
1.0
0.8
0.6
0.4
0.2
0.0
*
*
# #
LFD
HFD
WT
HET
KO

Figure 5.5

Figure 5.6: *Gpr1* loss does not alter energy homeostasis

Metabolic cages were used to measure locomotor activity (a), and VO_2 consumption/ CO_2 generation for calculation of energy expenditure (b). Metabolic cage measurements were taken automatically every 2 minutes over a 24-hour light/ dark cycle in wild-type (WT), heterozygous (HET), or homozygous knockout (KO) mice following 24 weeks of either low fat (LFD) or high fat (HFD) diet, as indicated. Two-way repeated measures ANOVA *$p<0.05$ vs. WT within light cycle.

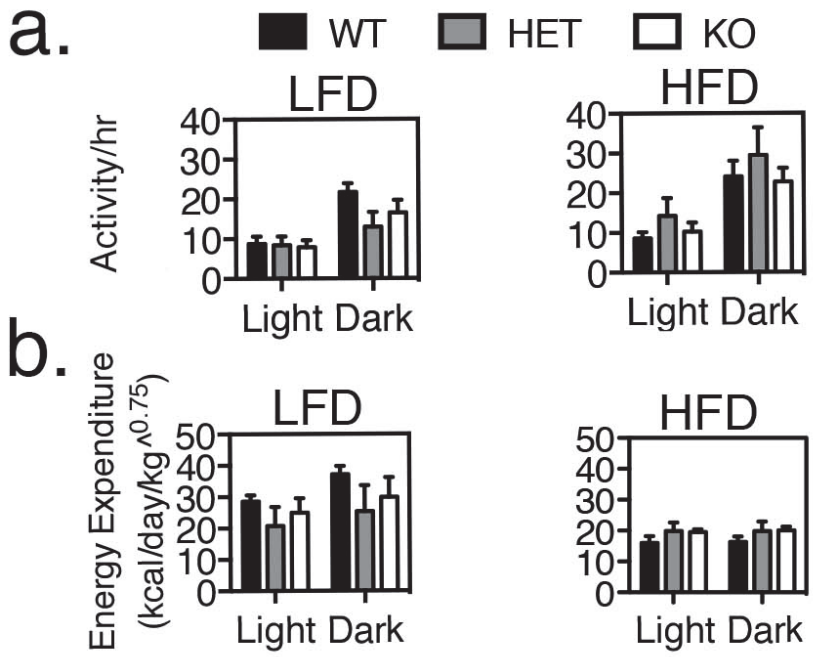
a.
WT
HET
KO
LFD
HFD
Activity/hr
40
30
20
10
0
Light Dark
b.
Energy Expenditure
(kcal/day/kg^0.75)
50
40
30
20
10
0
Light Dark

Figure 5.6

Figure 5.7: *Gpr1* loss is associated with decreased dark-cycle feeding

Metabolic cages were used to measure food consumption. Metabolic cage measurements were taken automatically every 2 minutes over a 24-hour light/ dark cycle in wild-type (WT), heterozygous (HET) or homozygous knockout (KO) mice following 24 weeks of either low fat (LFD) or high fat diet (HFD), as indicated. Data are represented as total Kcal consumed per kg body weight (a), meals per hour (b) meal size (c) or food consumed per hour normalized to mouse mass (g) (d). Darkness began at 19:00. Two-way repeated measures ANOVA *$p<0.05$ vs. WT within light cycle (a, b, c), or relative to KO (*) or HET (ϕ) (d), N=6-8.

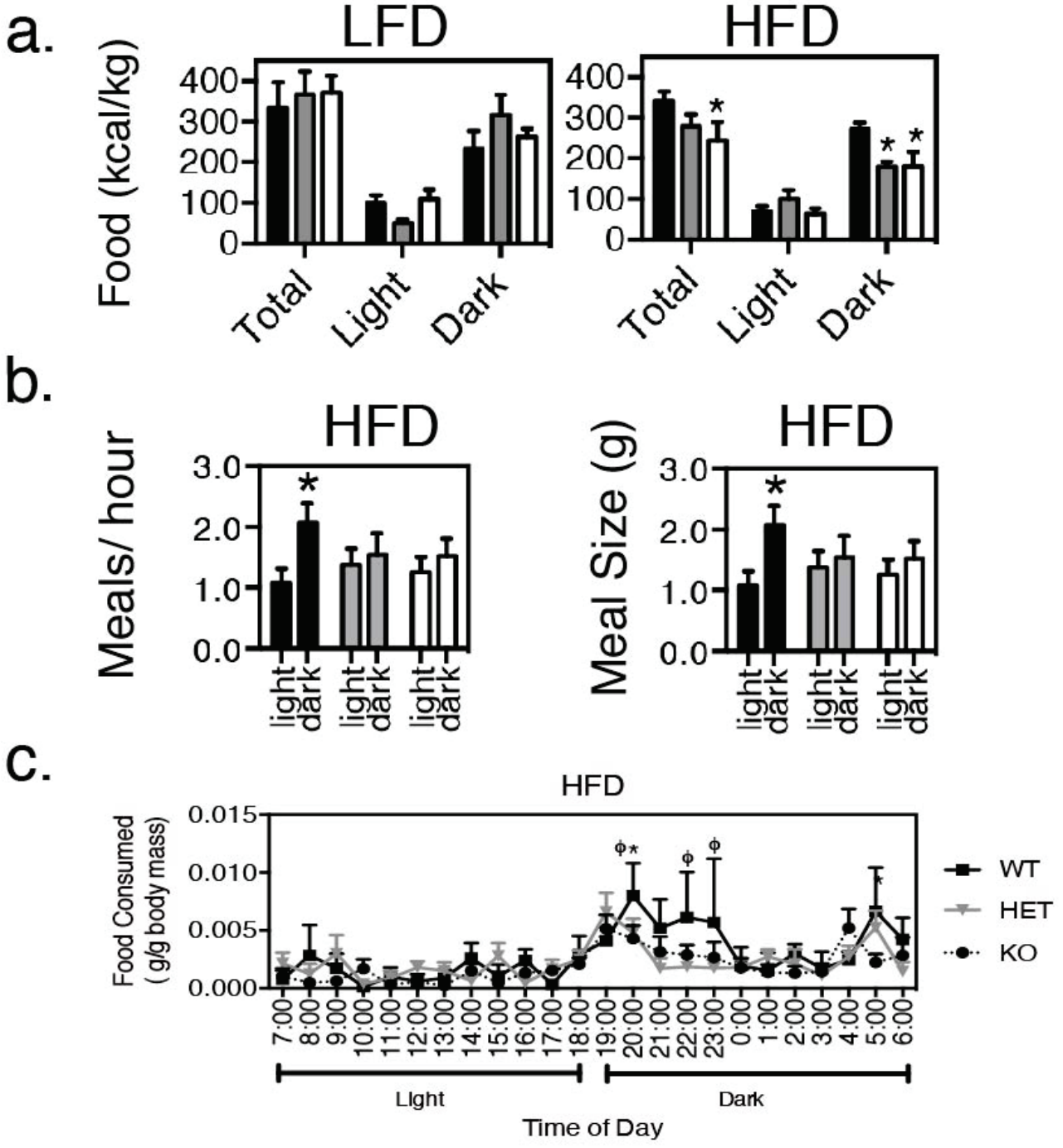
a.
LFD
HFD
Food (kcal/kg)
400
300
200
100
0
Total
Light
Dark
b.
HFD
HFD
Meals/ hour
Meal Size (g)
3.0
2.0
1.0
0.0
light
dark
c.
HFD
Food Consumed
(g/g body mass)
0.015
0.010
0.005
0.000
WT
HET
KO
7:00
8:00
9:00
10:00
11:00
12:00
13:00
14:00
15:00
16:00
17:00
18:00
19:00
20:00
21:00
22:00
23:00
0:00
1:00
2:00
3:00
4:00
5:00
6:00
Light
Dark
Time of Day

Figure 5.7

Figure 5.8: *Gpr1* loss is associated with increased orexigenic signals

A protein multiplex assay was used to determine serum levels of key diabetes/feeding signals in wild-type (WT) (black bars) and homozygous knockout (KO) (white bars) mice following 20-weeks of feeding with the high-fat diet (HFD) during light/dark and fed/fasted states, as indicated, N=5-7 (a). Neuropeptide Y *(NPY),* agouti-related peptide *(AgRP),* and proopiomelanocortin *(POMC)* mRNA levels were measured in the whole brain, cerebral cortex, and hypothalamus of adult mice. Data are expressed relative to whole brain. One-way ANOVA *$p<0.05$ vs. WT within feeding/light condition (a) or whole brain (b).

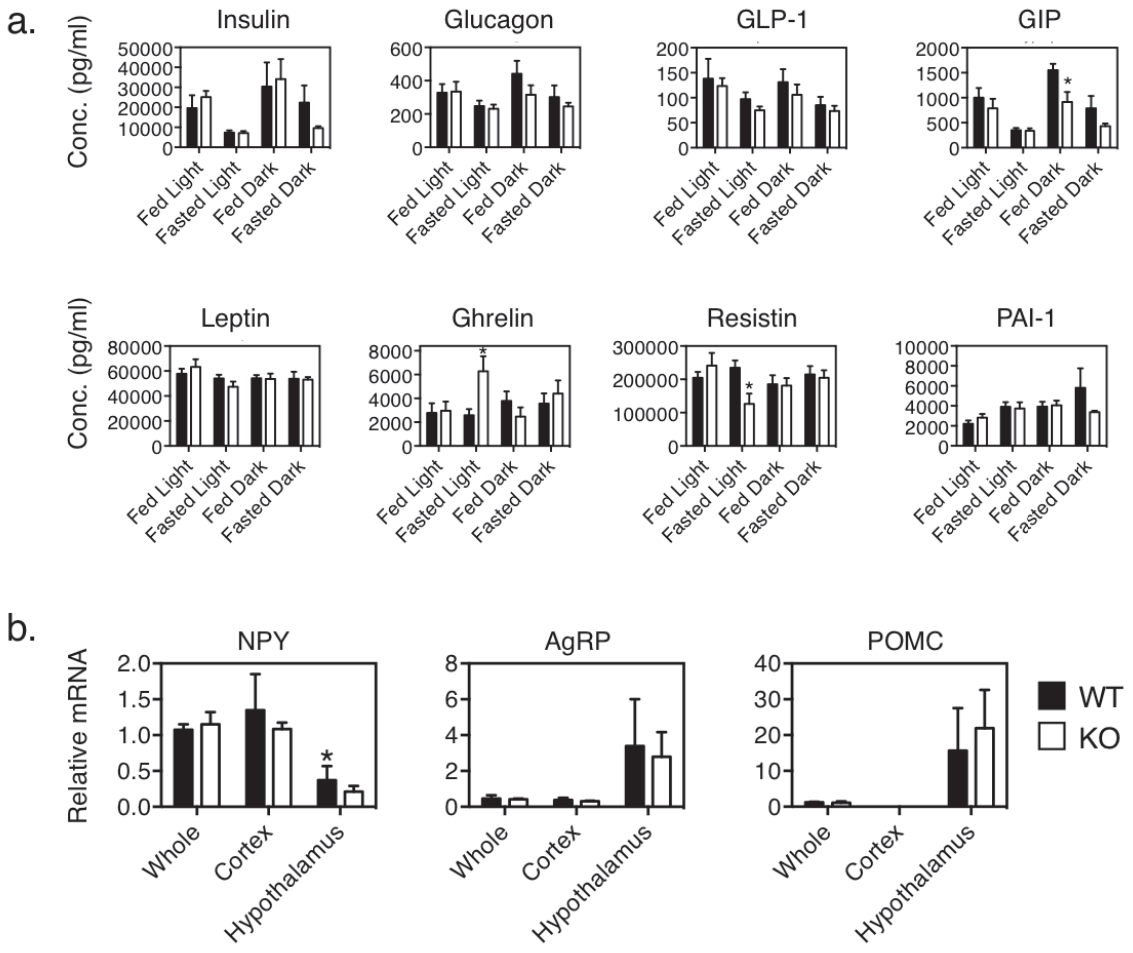
a.
Insulin
Glucagon
GLP-1
GIP
Leptin
Ghrelin
Resistin
PAI-1
Conc. (pg/ml)
Fed Light
Fasted Light
Fed Dark
Fasted Dark
b.
NPY
AgRP
POMC
Relative mRNA
Whole
Cortex
Hypothalamus
WT
KO

Figure 5.8

Figure 5.9: *Gpr1* loss exacerbates glucose intolerance in mice fed a HFD for 24 weeks

Blood glucose concentration was measured following a 5-6 hour fast (a). Insulin sensitivity (b) and glucose tolerance (c) tests were conducted following 18 hour and 6 hour fasts, respectively. Blood glucose was monitored using a Freestyle Light glucometer with saphenous vein blood prior to (time 0) and 15, 45, 90 and 120 minutes following injection of human insulin 0.75 U/Kg (b) or glucose (2 mg/g) (c). Insulin and glucose testing were done on wild-type (WT), heterozygous (HET) or homozygous knockout (KO) mice prior to diet initiation (Baseline pooled low-fat diet (LFD) and high-fat diet (HFD), N= 9-14) or following 24 weeks of either LFD or high fat HFD (N=6-8) as indicated. One-way ANOVA (a), one-way repeated measures ANOVA (b, c) * $p<0.05$ WT vs. KO or Φ $p<0.05$ WT vs. HET at the indicated time points.

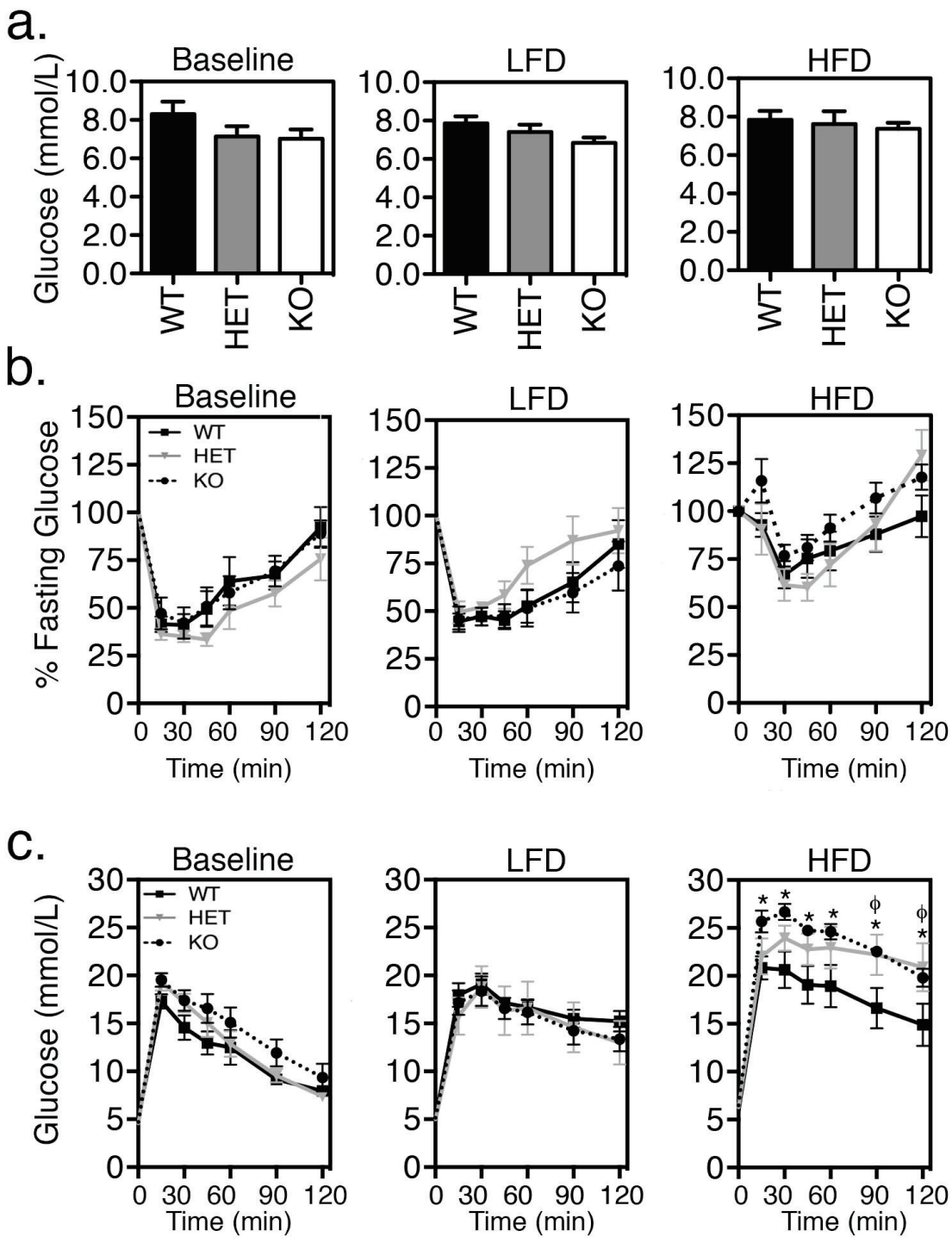
a.
Baseline
LFD
HFD
Glucose (mmol/L)
10.0
8.0
6.0
4.0
2.0
0.0
WT
HET
KO
b.
% Fasting Glucose
150
125
100
75
50
25
0
0 30 60 90 120
Time (min)
c.
Glucose (mmol/L)
30
25
20
15
10
5
0
*
ϕ

Figure 5.9

Figure 5.10: Blood glucose is elevated in *Gpr1* KO mice following pyruvate administration

Gluconeogenic capacity was assessed using a pyruvate tolerance test following a 6 hour fast in wild-type (WT) and homozygous knockout (KO) mice consuming high-fat diet (HFD) for 18 weeks. Blood glucose was monitored using a Freestyle Light glucometer with saphenous vein blood prior to (time 0) and 15, 45, 90 and 120 minutes following injection of pyruvate (2 mg/g) N= 6-7 (a). To assess liver gluconeogenesis, liver *phosphoenolpyruvte carboxylase* (*Pepck*) and *glucose-6-phosphatase (G6pc)* mRNA levels from WT, heterozygous (HET) or KO mice consuming either low-fat diet (LFD) or HFD for 24 weeks were examined by qPCR analysis, N=5-6 (b). Results are expressed relative to LFD WT within tissue. *In vivo* tissue glucose uptake was measured in WT and KO mice consuming HFD for 20 weeks at 60 minutes following injection of tritiated 2-deoxy glucose (c). One-way repeated measures (a) or two-way (b, c) ANOVA *$p<0.05$ vs. WT within diet/tissue.

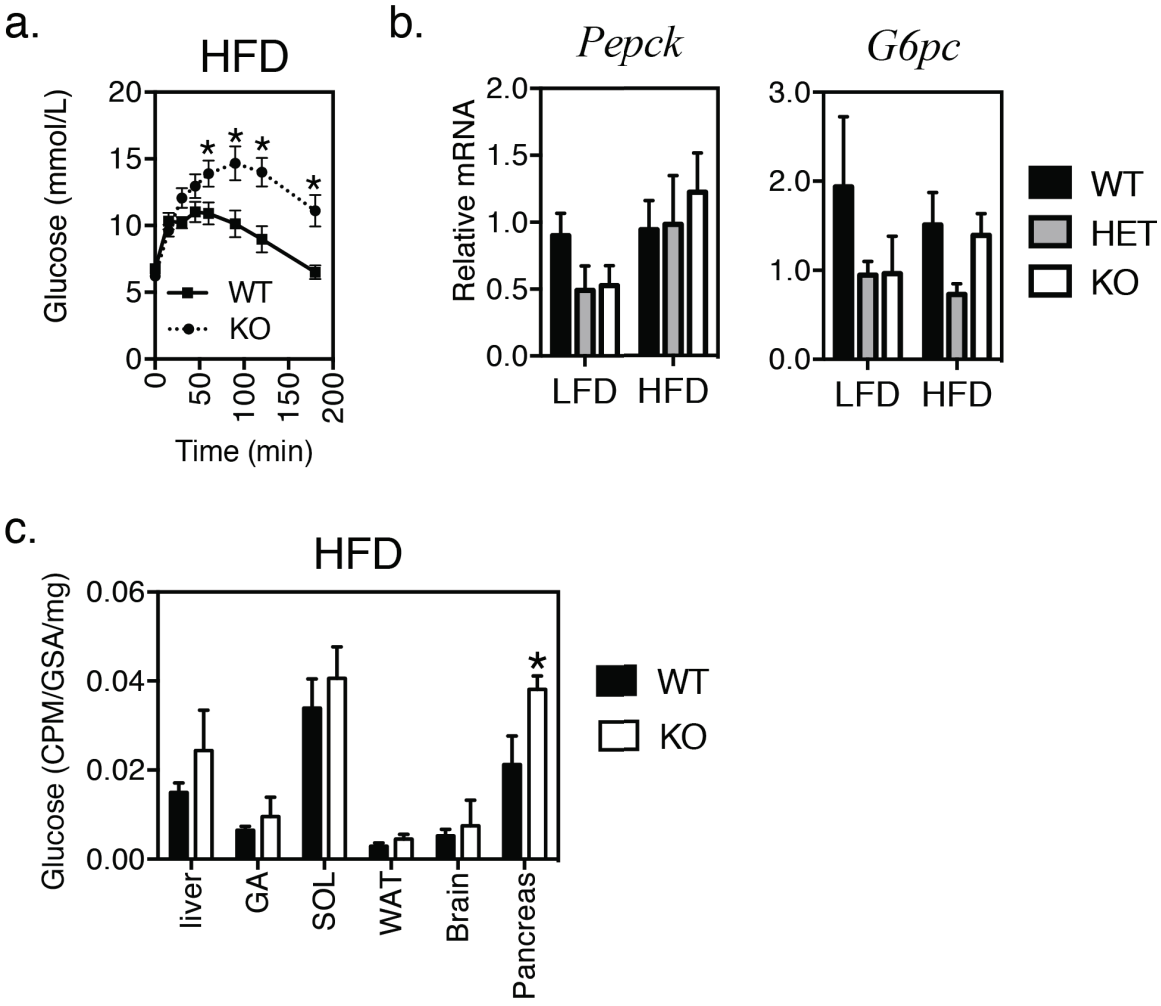
a.
HFD
Glucose (mmol/L)
Time (min)
WT
KO
b.
Pepck
G6pc
Relative mRNA
LFD
HFD
WT
HET
KO
c.
HFD
Glucose (CPM/GSA/mg)
liver
GA
SOL
WAT
Brain
Pancreas
WT
KO

Figure 5.10

Figure 5.11: Insulin secretion is reduced in obese *Gpr1* KO mice

Gpr1 mRNA expression was measured in epididymal white adipose tissue (WAT), gastrocnemius muscle (GA) and soleus (SOL) muscles, brain and pancreas from 30 week-old wild-type (WT) mice (a). Results are expressed relative to WAT. One-way ANOVA * $p<0.05$ vs. SOL N=4. Total pancreatic insulin was extracted from WT and homozygous knockout (KO) mice following 20 weeks of HFD and quantified by ELISA N=4-7 (b). Serum insulin concentration during the glucose tolerance test (GTT) was measured in the fasting state prior to (c) and at 15, 45, 90 and 120 minutes (d) following glucose injection using a mouse insulin ELISA. *$p<0.05$ vs. WT, one-way (c, e) and repeated measures (d) ANOVA N=6-8 (d). Area under the curve (AUC) for insulin was calculated using Prism6 software.

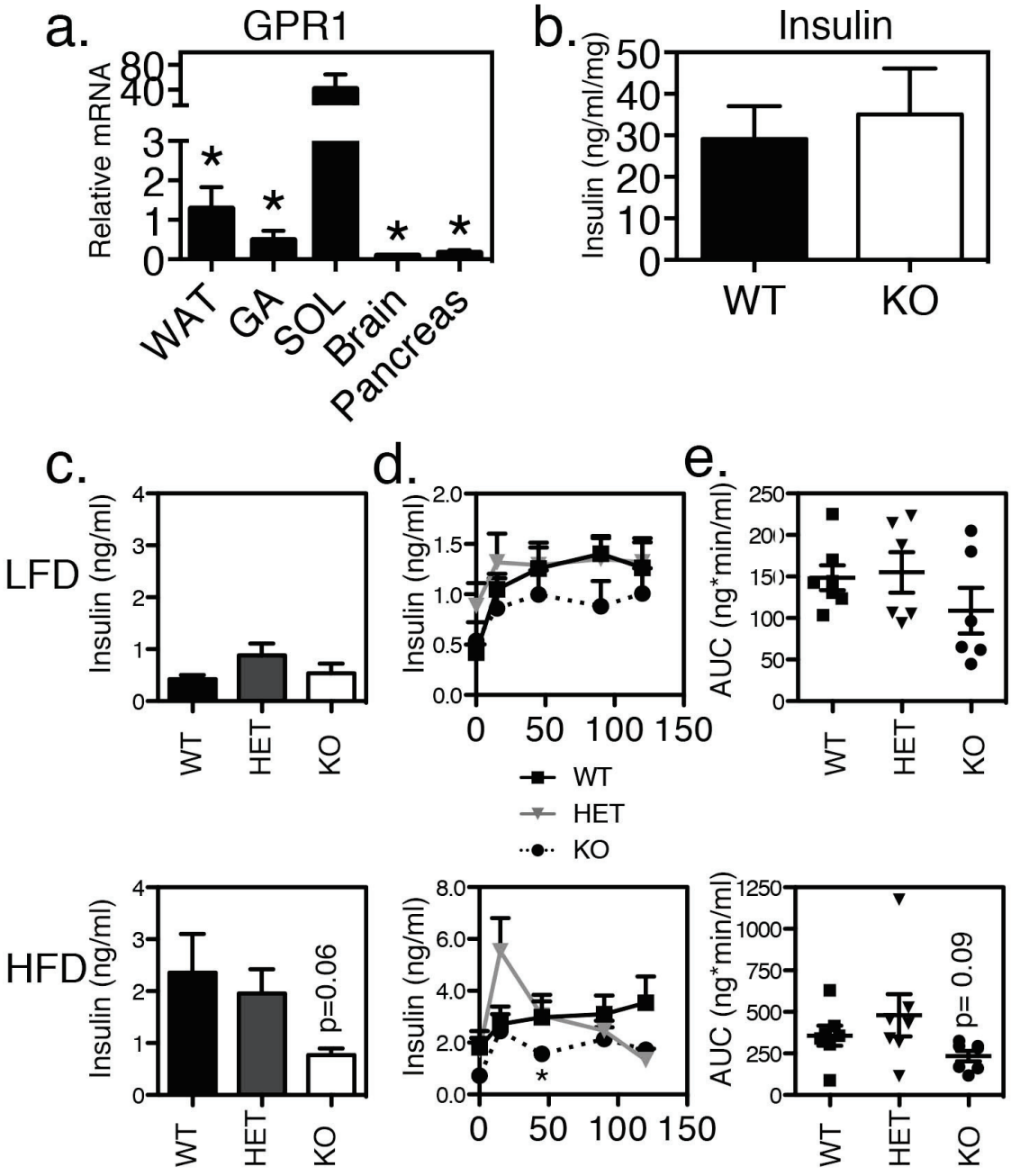
a.
GPR1
Relative mRNA
80
40
3
2
1
0
*
*
*
*
WAT
GA
SOL
Brain
Pancreas
b.
Insulin
Insulin (ng/ml/mg)
50
40
30
20
10
0
WT
KO
c.
LFD
Insulin (ng/ml)
4
3
2
1
0
WT
HET
KO
d.
Insulin (ng/ml)
2.0
1.5
1.0
0.5
0.0
0
50
100
150
WT
HET
KO
e.
AUC (ng*min/ml)
250
200
150
100
50
0
WT
HET
KO
HFD
Insulin (ng/ml)
4
3
2
1
0
p=0.06
WT
HET
KO
Insulin (ng/ml)
8.0
6.0
4.0
2.0
0.0
*
0
50
100
150
AUC (ng*min/ml)
1250
1000
750
500
250
0
p= 0.09
WT
HET
KO

Figure 5.11

Figure 5.12: *Gpr1* loss is not associated with altered liver steatosis

Hematoxylin and eosin staining of liver from wild-type (WT), heterozygous (HET) or homozygous knockout (KO) mice consuming either low-fat (LFD) or high-fat (HFD) for 24 weeks. Representative images of liver (a) were used for quantification of % adipocyte area using Image J software, N=6 (b). Scale bar represents 200 μm. Liver *TNFα* and macrophage antigen-1 (*Mac1*) mRNA levels were examined by qPCR analysis, N=5-6 (c). Results are expressed relative to WT LFD. One-way ANOVA $p<0.05$ vs. WT within diet.

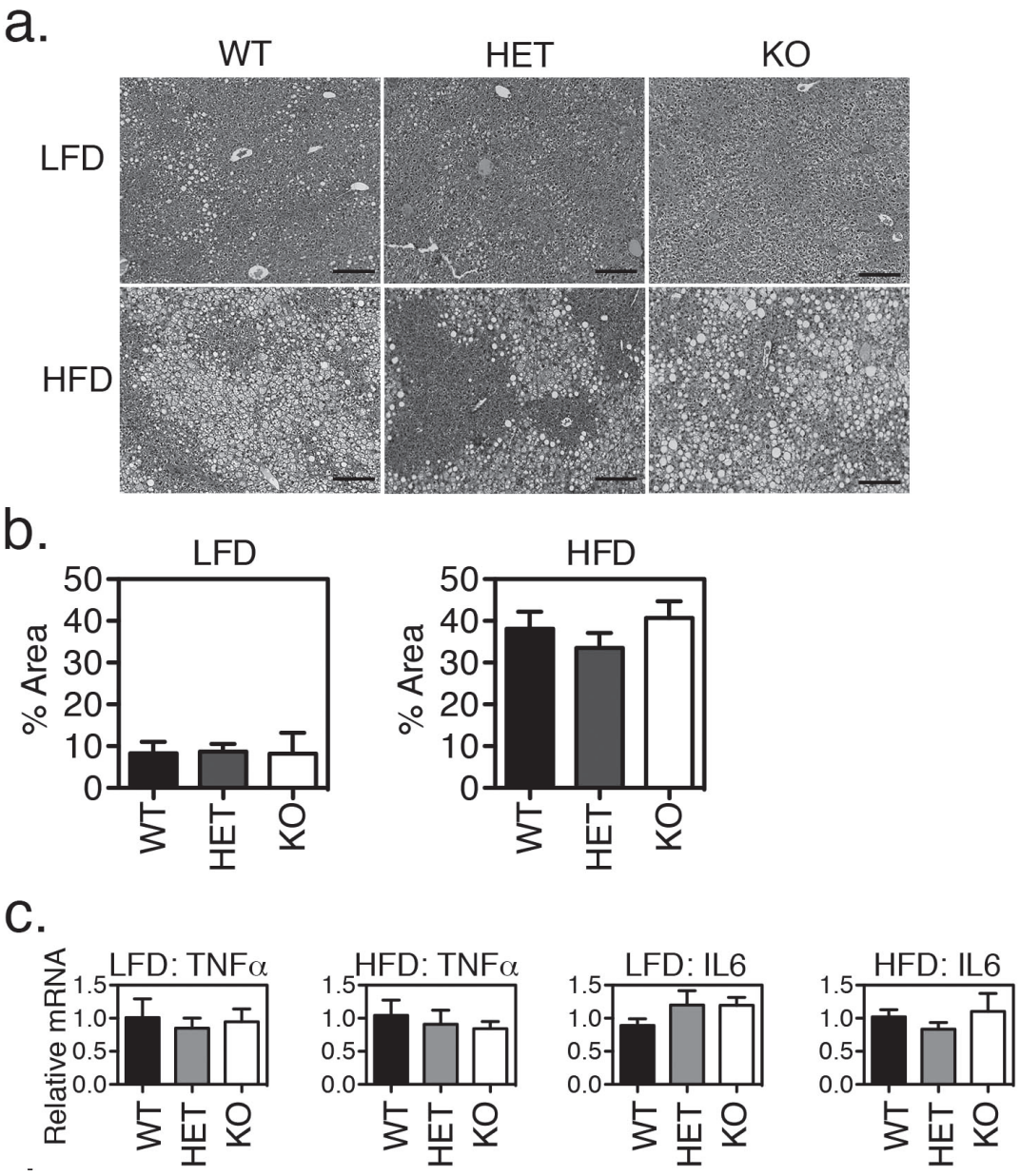
a.
WT
HET
KO
LFD
HFD
b.
LFD
HFD
% Area
50
40
30
20
10
0
WT
HET
KO
c.
Relative mRNA
LFD: TNFα
HFD: TNFα
LFD: IL6
HFD: IL6
1.5
1.0
0.5
0.0
WT
HET
KO

Figure 5.12

Figure 5.13: Adipocyte size and inflammation are unchanged with *Gpr1* loss

Hematoxylin and eosin staining of white adipose tissue (WAT) isolated from wild-type (WT), heterozygous (HET) or homozygous knockout (KO) mice consuming either low-fat diet (LFD) or high-fat diet (HFD) for 24 weeks. Representative images of stained adipose tissue sections, N=3. Scale bar represents 20 μm (a). Representative adipocytes with crown-like structures are marked with *. WAT *TNFα* and *Il6* mRNA levels were examined by qPCR analysis, N= 5-6 (b) and expressed relative to WT LFD. Frequency distribution of % adipocytes was generated using cross-sectional area of adipocytes as calculated using Image J (c). Solid black bars: WT, Grey bars: HET, White bars: KO. One-way ANOVA $p<0.05$ vs. WT within diet. Adiposoft macro for Image J was used to quantify adipocyte area (c).

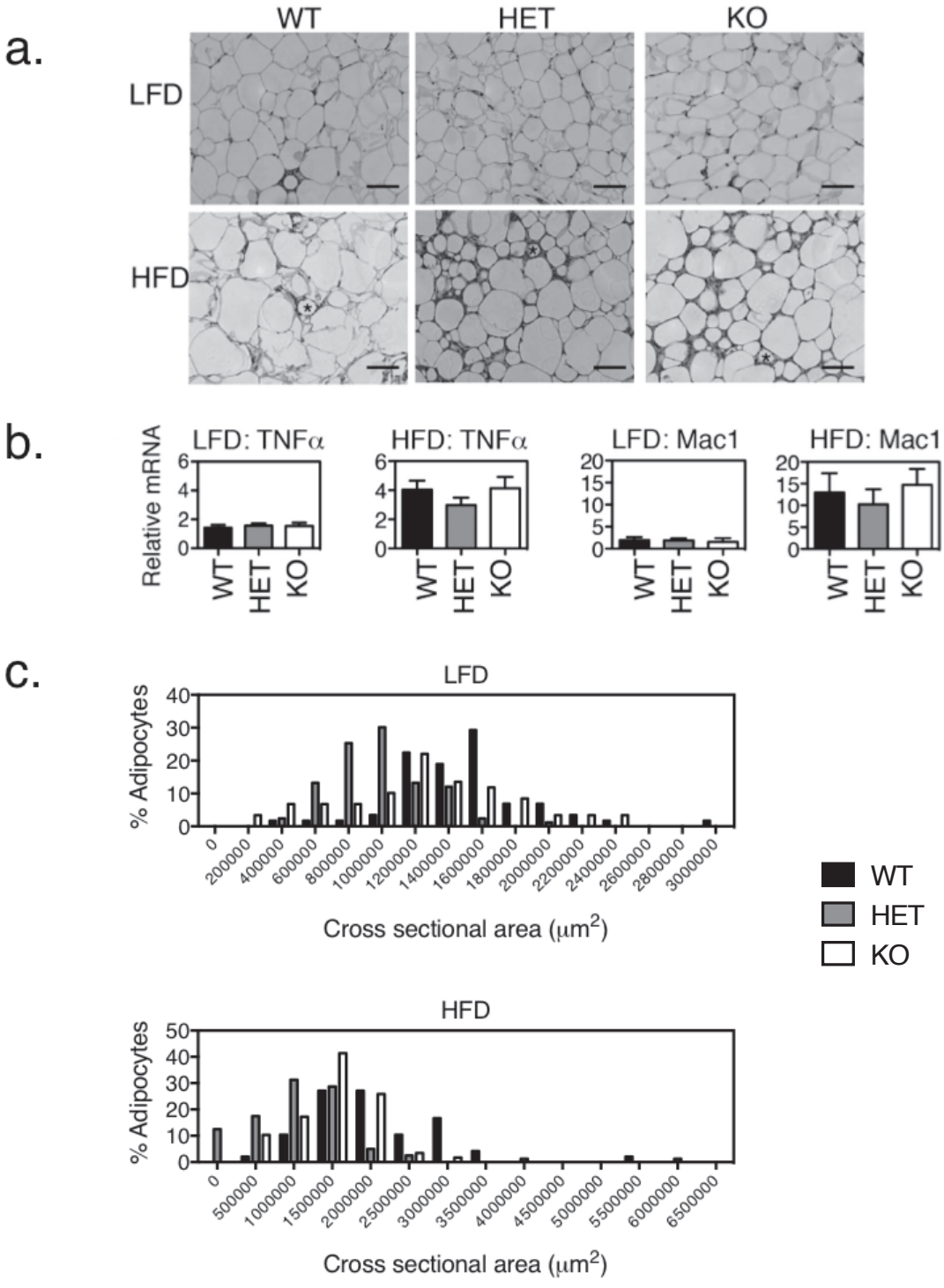
a.
WT
HET
KO
LFD
HFD
b.
LFD: TNFα
HFD: TNFα
LFD: Mac1
HFD: Mac1
Relative mRNA
WT
HET
KO
c.
LFD
% Adipocytes
Cross sectional area (μm2)
HFD
WT
HET
KO

Figure 5.13

Figure 5.14: Insulin receptor expression is reduced in *Gpr1* KO mice fed a HFD for 24 weeks

Glucose transporter 4 (*Glut4*) (a) and insulin receptor (*InsR*) (b) mRNA expression was measured by qPCR analysis in epididymal white adipose tissue (WAT), gastrocnemius muscle (GA) and soleus (SOL) muscles of wild-type (WT), heterozygous (HET) or homozygous knockout (KO) mice following 24 weeks of either low-fat diet (LFD) or high-fat diet (HFD), as indicated. Results are expressed relative to LFD WT. One-way ANOVA *$p<0.05$ vs. WT within diet, N=5-7.

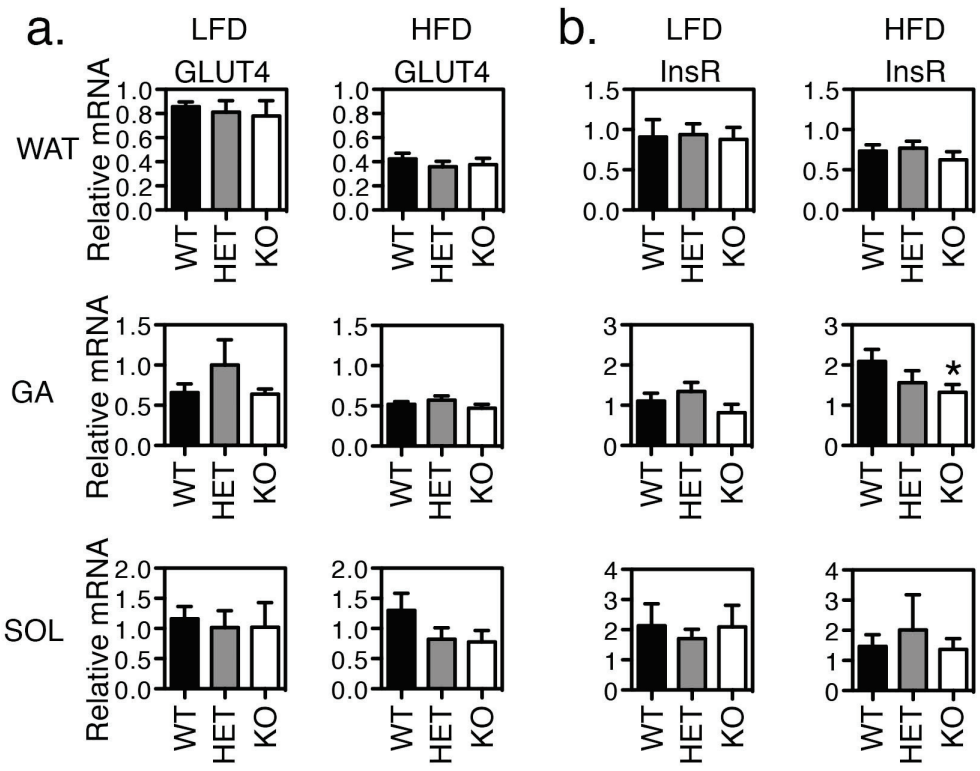
a.
LFD
HFD
GLUT4
GLUT4
b.
LFD
HFD
InsR
InsR
WAT
GA
SOL
Relative mRNA
WT
HET
KO
*

Figure 5.14

5.7 Tables

Table 5.1: Genotyping primers

Gene	Sequence 5' to 3'	Accession
***Gpr1* Genotyping Primers**		
Endogenous (Ef)	Fw CGTGGAGCATATGAAACTCAAGG	NM_146250
Endogenous (Er)	Rv TGTTCTCTTCTTCCACCTTGTGG	NM_146250
Targeted (Tr)	Rv AAATGGCGTTACTTAAGCTAGCTTGC	EU676801

Table 5.2: Quantitative PCR (qPCR) primers

Gene	Sequence 5' to 3'	Accession
qPCR Primers		
Chemerin	Fw TACAGGTGGCTCTGGAGGAGTTC	NM_027852
	Rv CTTCTCCCGTTTGGTTTGATTG	
Cmklr1	Fw GCTTTGGCTACTTTGTGGACTT	NM_008153
	Rv CAGTGTTCACGGTCTTCTTCATCTTG	
Gpr1	Fw GTCTCCCAGCTTCCCCGCTG	NM_146250
	Rv CAAGCTGTCGTGGTGTTTGA	
Glut4	Fw ACTCTTGCCACACAGGCTCT	NM_009204
	Rv AATGGAGACTGATGCGCTCT	
Myh1	Fw CTTCAACCACCACATGTTCG	NM_030679
	Rv AGGTTTGGGCTTTTGGAAGT	
Tnfα	Fw CCCTCACACTCAGATCATCTTCT	NM_013693
	Rv GCTACGACGTGGGCTACAG	
Il6	Fw TAGTCCTTCCTACCCCAATTTCC	NM_031168
	Rv TTGGTCCTTAGCCACTCCTTC	
Lep	Fw GAGACCCCTGTGTCGGTTC	NM_008493
	Rv CTGCGTGTGTGAAATGTCATTG	
InsR	Fw CCTGTACCCTGGAGAGGTGT	NM_010568
	Rv CGGATGACTGTGAGATTTGG	
βGeo	Fw GTCTCCCAGCTTCCCCGCTG	NM_146250
	Rv ACAGTATCGGCCTCAGGAA	EU676801
Cyca	Fw GAGCTGTTTGCAGACAAAGTTC	NM_008907
	Rv CCCTGGCACATGAATCCTGG	
Pepck	Fw AAGCATTCAACGCCAGGTTC	NM_011044
	Rv GGGCGAGTCTGTCAGTTCAAT	
G6pc	Fw CAGTGGTCGGAGACTGGTTC	NM_001289856
	Rv GTCCAGGACCCACCAATACG	

Table 5.3: Mendelian distribution and frequency of *Gpr1* WT and KO alleles from HET x HET breeding pairs

Litters total	11
Animals total	74
Animals per litter	6.8
Male animals	37
Female Animals	37
WT animals	20
HET animals	35
KO animals	18

% Male animals	50
% Female animals	50
% WT animals	27
% HET animals	47
% KO animals	24

Table 5.4: Anatomical parameters of *Gpr1* WT, HET and KO littermates fed LFD or HFD for 24 weeks

	LFD			HFD		
Weight (g)	WT	HET	KO	WT	HET	KO
Whole Body	34.16±1.42	36.52±2.01	32.44±2.84	45.23±3.09[a]	43.6±1.50[a]	47.62±1.78[a]
Liver	1.72±0.15	1.77±0.15	1.65±0.242	2.63±0.31[a]	2.10±0.28	2.62±0.24[a]
GA	0.23±0.03	0.25±0.02	0.21±0.03	0.34±0.02[a]	0.33±0.02[a]	0.37±0.01[a]
Pancreas	0.25±0.02	0.30±0.03	0.31±0.04	0.41±0.06[a]	0.40±0.06	0.34±0.05
Spleen	0.09±0.01	0.09±0.01	0.09±0.01	0.14±0.02[a]	0.11±0.02	0.12±0.01[a]
PR WAT	0.80±0.10	0.83±0.10	0.57±0.13	2.14±0.15[a]	2.09±0.17[a]	2.47±0.22[a]
EP WAT	1.86±0.16	1.773±0.22	1.22±0.41	1.84±0.35	1.87±0.24	1.98±0.16
SC WAT	0.95±0.09	1.04±0.15	0.6±0.21	2.13±0.14[a]	2.37±0.10[a]	2.45±0.16[a]
BAT	0.31±0.03	0.29±0.04	0.27±0.06	0.32±0.04	0.31±0.03	0.41±0.05[a]

Values are mean ± SEM n=6-9. [a] $P<0.05$ vs. LFD of the same genotype. Abbreviations: White adipose tissue (WAT), Brown adipose tissue (BAT), low-fat diet (LFD), High-fat diet (HFD), Gastrocnemius (GA), Perirenal (PR), Epididymal (EP), Subcutaneous (SC)

Chapter 6: General Discussion and Conclusions

Sections 6.4 (Therapeutic Strategies and Clinical Utility) and 6.5 (Remaining Questions and Recommendations for Future Studies) and 6.6 (Perspectives and Concluding Remarks) presented in this chapter are reproduced with copyright permission (Appendix I) from the review article (154). This review article was written in equal partnership with Helen Dranse. The majority of this text was included in chapter 2. For clarity of the thesis minor editorial changes were made from the original.

Obesity is characterized by excess accumulation of adipose tissue and a chronic state of systemic inflammation. Over 60% of Canadians are overweight or obese, and are consequently at increased risk for a number of comorbidities, including heart disease, T2D, and cancer. In addition to resulting in poor individual health, disability, and loss of work, this increased illness susceptibility in obese individuals results in increased need for medical care and places economic burden on the health care system. In addition to storing energy as fat, adipose tissue is an endocrine organ that secretes a collection of biologically active proteins called adipokines. The secretion and function of these hormone-like proteins becomes dysfunctional in obesity and contributes to pathological changes in metabolism, inflammation, and energy homeostasis and ultimately influences the development and severity of obesity comorbidities.

In 2007 the Sinal lab identified chemerin as a novel adipokine that promotes the development of adipocytes from precursor cells and modulates various aspects of mature adipocyte metabolism (4). Chemerin also contributes to glucose homeostasis and immune cell recruitment in both lean and obese rodents and humans (162,220,221). To date, these functions have been solely attributed to chemerin activation of the GPCR CMKLR1. Chemerin also binds very strongly to another GPCR, GPR1 (179). While GPR1 plays a critical role in nutrient sensing in yeast, essentially nothing is known about the function or signaling of GPR1 in mammals. I hypothesized that GPR1 contributes to the biological function of chemerin in energy homeostasis and metabolism. Thus, this thesis focuses on determining if GPR1 is an active signaling receptor for chemerin and to what extent GPR1 plays a role in regulating chemerin biology. My overall goals were to: elucidate the signal transduction mechanisms of GPR1 in comparison to CMKLR1; determine if, like CMKLR1, GPR1 supports chemerin-mediated chemotaxis; and examine the role of GPR1 in normal and obese energy and glucose homeostasis.

Herein, chemerin activated arrestin recruitment to GPR1 with higher potency than CMKLR1, and this activation resulted in both overlapping and unique signaling cascades. Both chemerin receptors signaled through the Rho family of small GTPases, a novel chemerin signaling pathway, with particular relevance to chemerin-mediated chemotaxis of immune cells. In adipose tissue, *Cmklr1* was highly expressed in the lipid-filled adipocytes. In contrast, *Gpr1* expression was predominant in the adipose SVF, a

collection of non-adipocyte support cells, which include fibroblasts, stem cells, immune cells, and vasculature. *Gpr1* was also expressed in skeletal muscle, pancreas and brain. My studies using *Gpr1* knockout mice demonstrated that GPR1 was required for supporting pancreatic insulin secretion and glucose homeostasis during obesity. These results demonstrate for the first time that GPR1 is an active chemerin signaling receptor, and suggest a role for GPR1 in metabolic homeostasis. Together, these experiments enhance our understanding of how chemerin activity is regulated at the level of the chemerin receptors, and provide valuable insight into the function of GPR1 in normal health and obesity. Chemerin levels are elevated in obesity and associated with increased risk for inflammation, metabolic syndrome, and T2D suggesting that chemerin and its receptors could be a novel therapeutic target for treatment or prevention of obesity-related diseases. The following sections discuss how the findings presented herein contribute to our current understanding of chemerin biology in obesity and T2D pathogenesis.

6.1 Chemerin, CMKLR1, and GPR1 in Insulin Resistance

There is controversy regarding the role of chemerin in peripheral tissue insulin sensitivity. The well-established elevations in circulating chemerin in humans have been positively correlated with insulin resistance (199,240,353). To date, basic science studies examining mechanisms of chemerin interaction with glucose uptake have failed to produce a unified consensus on the precise role of chemerin in glucose homeostasis through its actions on adipose tissue, skeletal muscle, and liver. For example, chemerin treatment of 3T3-L1 adipocytes resulted in both increased (238) and decreased (232) insulin-stimulated glucose uptake. Chemerin treatment of human skeletal muscle cells reduced insulin sensitivity and impaired glucose uptake (239). Very little has been done with respect to examining the direct actions of chemerin on hepatocyte insulin sensitivity; however, decreased liver glucose uptake and impaired insulin suppression of hepatic glucose production were demonstrated *in vivo* using acute chemerin treatment and chemerin knockout, respectively (158,221). While these studies are consistent with a role for chemerin in hepatic insulin resistance, one

clinical study reported that serum chemerin levels were unchanged in patients who had impaired fasting glucose that had not yet progressed to T2D (199), suggesting that hepatic insulin resistance precedes elevated circulating chemerin and that increases in chemerin secretion may be more likely to contribute during later stages of insulin resistance or β-cell failure. We showed that glucose uptake in skeletal muscle, adipose tissue, and liver is unchanged following chemerin injection or loss of CMKLR1 or GPR1 in lean, normoglycaemic mice (221,321). In chapter two, we propose that these results are suggestive of a tissue- and context-specific role for chemerin in peripheral tissue insulin resistance in the liver, skeletal muscle and adipose tissue. This is consistent with other adipokines like IL-6 and leptin, which exhibit dose-dependent and context-specific effects on insulin sensitivity (354,355). For example, IL-6 elevations in chronic disease states are believed to result in insulin resistance, while acute exercise-induced increases improve insulin sensitivity (355). As such, employing multiple cellular and *in vivo* models of normal and obese glucose uptake will likely be required to clarify the subtleties of chemerin function in insulin sensitivity and resistance.

The mechanisms governing chemerin function in insulin sensitivity also remain unclear. Our studies using obese CMKLR1 and GPR1 knockout mice suggest that loss of chemerin signaling may contribute to insulin resistance through down regulation of insulin receptor expression (220,321). In human skeletal muscle cells chemerin activation of ERK and p38 increased insulin resistance through NFκB activation, inhibitory IRS serine phosphorylation, and reduced insulin-mediated AKT activation (239). Our findings of chemerin signaling through RhoA/ROCK may also be relevant to chemerin function in insulin resistance. Loss of ROCK activation in adipocytes and skeletal muscle cells has been implicated in inhibitory serine phosphorylation of IRS and insulin resistance *in vivo* and ROCK activity appears to be impaired in insulin resistant humans (356,357). Moreover, MAPK-dependent insulin signaling has been demonstrated to result in SRF activation and contribute to essential insulin-regulated gene expression, specifically FOS expression (74). As such investigations of the potential role for chemerin-mediated RhoA/ROCK/SRF

signaling in peripheral tissue insulin resistance may provide further insight into mechanisms of chemerin function for promotion or inhibition of glucose uptake.

6.2 Chemerin, CMKLR1, and GPR1 in the Pancreas

β-cell insulin secretion plays a critical role in distinguishing those obese individuals who progress from insulin resistance to T2D from those who do not. Elevated chemerin levels are positively correlated with increased circulating insulin in obese diabetic individuals, suggesting that chemerin may play a role in β-cell insulin secretion; however, the scarcity of studies examining chemerin levels throughout the various stages of diabetes development and the correlative nature of human clinical studies prohibit any determination of whether this relationship is reactive or causative. Herein we propose that the chemerin signaling axis is required to support β-cell function and insulin secretion in obesity. We showed that chemerin, CMKLR1, and GPR1 mRNA are expressed in the pancreas (321). Consistent with this, Takahashi *et al*. showed chemerin, CMKLR1, and GPR1 protein localization in the pancreatic islet (158). Unlike insulin resistance, the basic science literature examining the impact of chemerin signaling on insulin secretion strongly suggests that chemerin signaling is required for normal insulin secretion. For example, despite having normal islet morphology and insulin content, chemerin knockout mice have impaired glucose stimulated insulin secretion *in vivo* and in isolated islet cultures (158). Interestingly, this deficit was also present with KCl-induced insulin secretion suggesting that the β-cell insulin secretory capacity was impaired in chemerin knockout mice. Similar to our finding that obese GPR1 KO mice failed to sustain insulin secretion following glucose injection, glucose-stimulated insulin levels tended to be normal immediately following glucose injection but lower in HFD-fed chemerin KO mice around 30 minutes (158). Additionally, CMKLR1-KO mice also exhibited reduced glucose-stimulated circulating insulin under both LFD and HFD conditions when compared with WT (220). Together, these findings suggest that chemerin, CMKLR1, and GPR1 are each required for β-cell insulin secretion, especially in the

context of the increased insulin demand that occurs with obesity and insulin resistance. As such, chemerin joins the ever-growing list of adipokines that have direct roles in mediating β-cell insulin secretion.

The two established phases of insulin secretion depend upon dynamic changes in the actin cytoskeleton. The first phase of rapid (10 minutes) insulin secretion requires actin depolymerization to permit membrane-docked vesicle exocytosis, while the prolonged insulin secretion of the second phase requires actin/myosin fiber formation (48). The molecular mechanisms regulating these features of insulin secretion are only beginning to come to light. Inhibition or knockdown of the RhoA/ROCK effector protein cofilin was recently shown to result in impaired F-actin remodeling and reduced second phase insulin secretion from Min6 pancreatic β-cells (358), while acute inhibition of RhoA and ROCK appears to enhance glucose stimulated insulin secretion of rat β-cells and Min6 cells in 3D culture (359,360). Additionally, RhoA and ROCK are required for insulin gene expression (361). As such it appears that chemerin signaling through RhoA/ROCK could contribute to β-cell function and insulin secretion. Given the above studies, chemerin signaling could be predicted to both increase and decrease second-phase insulin secretion. Thorough experimental examination of the role of chemerin, CMKLR1, and GPR1 signaling in β-cell insulin granule exocytosis and actin dynamics will be required to determine how acute and chronic chemerin treatments influence insulin secretion of healthy, pre-diabetic, and diabetic β-cells.

6.3 Models for Chemerin, CMKLR1, and GPR1 Function in Obesity and Glucose Homeostasis

As discussed in chapter 2 circulating chemerin levels in humans are positively correlated with BMI, MetS, T2D, and a number of inflammatory, lipid, and metabolic derangements that occur with obesity. The mechanisms that regulate circulating chemerin levels are poorly understood and little is known about the anatomical location of chemerin, CMKLR1, and GPR1 expression or the factors that contribute to changes in

their abundance in humans. Two independent studies have reported that variation in the chemerin gene *RARRES2* is heritable (229,362). Genome-wide association studies have identified numerous SNPs within the *RARRES2*, *CMKLR1*, and *GPR1* gene loci as well as copy number variations in *RARRES* and *GPR1* (363). While no clinical significance is known or SNPs in *CMKLR1* or *GPR1*, the minor allele *RARRES2* SNPs rs17173608, rs10278590, and rs7806429 are significantly associated with lower visceral adipose tissue mass in lean individuals (362,364). This suggests that genetic variation in *RARRES2* may contribute to regional fat distribution in humans. These SNPs were not associated with insulin sensitivity or secretion; however, visceral adipose tissue mass is a key determinant of T2D risk (365) suggesting a possible link between visceral adipose tissue-derived chemerin and T2D. SNPs in as many as 45 different genes have been identified to associate with plasma chemerin levels (229,234). One of these, rs10282458 was also associated with BMI and MetS, while another set of 4 unique SNPs in the *EDIL3* gene were associated with angiogenesis suggesting that genetic variation in the regulation of chemerin expression may contribute to obesity and its comorbidities (229,234). Future studies are needed to examine the clinical significance of many of the identified SNPs in *RARRES2*, *CMKLR1*, *GPR1,* and associated genes specifically with respect to the potential impact of this genetic variation on adiposity, metabolism, and glucose homeostasis.

Despite limited understanding of the genetic regulation of chemerin expression, it is clear that circulating chemerin levels are significantly elevated in obesity and correlate with diabetes development. Moreover, chemerin treatment of obese mice lowers serum insulin levels and exacerbates glucose intolerance (161,221) suggesting that inhibition of chemerin signaling could result in metabolic improvements during obesity. Paradoxically, CMKLR1, GPR1, and chemerin are required for glucose homeostasis during obesity, with loss of each resulting in impaired insulin secretion and glucose intolerance (158,220,321). This begs the question whether chemerin function is disrupted in obesity, not solely as a consequence of the rising chemerin levels, but through a change in chemerin function. One possibility is that, like the dose dependence of leptin and apelin, chemerin actions on the β-cell, for example, may follow a U-shaped pattern where high doses produce the opposite effect of low doses. Additionally, while leptin treatment had

no effect on circulating chemerin levels in people, adiponectin treatment of hepatocytes *in vitro* significantly increased chemerin secretion suggesting that other adipokines may influence chemerin levels (366). We also proposed that chemerin has the ability to synergize with other extracellular stimuli, a property that could differentially contribute to insulin resistance and β-cell function depending on the network of other cytokines, lipids, and metabolic mediators present. Moreover, it is well established that numerous chemerin isoforms exist and the anatomical localization of these isoforms has been predicted to change with different disease states suggesting that obesity may be associated with a unique balance in chemerin isoforms providing another possible mechanism for the apparent paradox. We also show that GPR1 loss results in changes in the circulating levels of the metabolic regulators GIP and resistin, suggesting that in addition to direct chemerin actions on tissues central to obesity and glucose homeostasis, chemerin may indirectly influence adiposity and glucose handling through modulation of other endocrine mediators of metabolism. Future studies examining the signal transduction and functional consequences of CMKR1 and GPR1 activation by these isoforms, alone, in combination or in the presence/absence of other metabolic and inflammatory mediators therefore has the potential to further increase our understanding of the potential differences between chemerin function in healthy and obese individuals.

Similar to chemerin, leptin and leptin receptor loss in mice results in insulin resistance and diabetes leading many early investigations to speculate that leptin replacement would have therapeutic benefit in obesity and diabetes (85). This hope was hampered by the subsequent discovery that leptin levels were not low but substantially elevated in obesity and associated with a state of leptin resistance (367). Similar to leptin, chemerin levels are lowest in states of energy deprivation and elevated with feeding or adiposity suggesting that chemerin may also serve as an indicator of energy status (368). Like the knockout mouse models where chemerin function is diminished or lost, chronically elevated chemerin levels may result in an effective state of chemerin functional loss through desensitization or chemerin resistance. While no mechanisms for this have been reported or investigated several studies, including our own support internalization and desensitization of chemerin receptor signaling with high doses or prolonged treatment (4,180,185,205,261,369). In this theory of chemerin function,

chemerin may normally act as a required indicator of inflammation and adipose tissue energy status through the adipo-insular axis, providing support that is required for adaptation to the increased metabolic demands of obesity. In obesity; however, this beneficial function may be lost as a consequence of impaired chemerin sensitivity or function resulting in exacerbated obesity and diabetes.

6.4 Therapeutic Strategies and Clinical Utility

Targeting chemerin function may be a therapeutic strategy of value for treating inflammation, insulin resistance and obesity-associated comorbidities. The viability of chemerin, CMKLR1, and GPR1 knockout mice suggests that inhibiting chemerin function has low risk of developmental effects. However, it is important to note that tissue culture, animal model, and human data suggest that in addition to contributing negatively to metabolic and inflammatory dysregulation, chemerin is essential for normal metabolism and immune function. Thus, while inhibition of chemerin-mediated chemotaxis and pro- inflammatory cytokine production might have therapeutic utility for reducing inflammation in obesity and numerous other chronic inflammatory conditions, therapeutics of this nature must be used with caution. Blockade of chemerin signaling might impair the innate immune response to infection and possibly even cancer. For example, down-regulation of chemerin expression in hepatocellular (370) and squamous cell (371) carcinoma is negatively correlated with tumour size and is associated with a poorer prognosis (370). Similarly, while inhibition of chemerin signaling appears to be an attractive approach for improving insulin resistance and glucose handling in obesity and diabetes, both tissue culture and animal studies suggest that complete removal of chemerin signaling can be detrimental to glucose homeostasis and adipose tissue function (4,220). Given the contextual nature of chemerin signaling, it is also possible that chemerin/CMKLR1/GPR1 targeting drugs may demonstrate efficacy in the context of metabolic disease but not in healthy individuals. Altogether the diversity of clinical and basic science chemerin studies suggest that chemerin-targeted therapeutics must focus on restoring the balance to normal chemerin activity, rather than removing it altogether. As

such, the ideal therapeutic would target dysregulated or pathologic chemerin signaling, while preserving or promoting essential chemerin function.

Specific modulation of chemerin signaling of this nature might be achieved through both small molecule and protein-based biomolecular (biologics) approaches targeted towards modulation of chemerin regulation (secretion, processing, receptors). For example, specific protease inhibitors might have utility in altering the ratio of inactive to active chemerin isoforms. Selective modulation of CMKLR1, GPR1, or CCRL2 through highly specific soluble molecules (agonists, antagonists, or partial agonists), synthetic chemerin analogues, mutant chemerin peptides (214,249), and humanized antibodies specific for neutralization of chemerin isoforms or receptors might provide the necessary flexibility for directing chemerin function. Ideally, methods such as these would permit selective inhibition of deleterious alterations in chemerin function while preserving protective chemerin signals. Targeted therapeutics of this nature could reduce neutrophil and monocyte recruitment in established inflammatory settings, reduce impairment in glucose uptake and insulin sensitivity, and potentially contribute to improved tissue function.

While pharmacological agents targeting chemerin activity and function are a future prospect, measurement of circulating, chemerin levels (total and bioactive) has current potential clinical utility as an early biomarker for metabolic and inflammatory diseases. As evidence of this, a recent clinical study reported that, when assessed as a surrogate early measure for insulin sensitivity, circulating chemerin concentration was more predictive than measures of insulin resistance and leptin in a population lacking clinical signs of metabolic syndrome (199). Similarly, using 240 ng/ml as a cut -off chemerin concentration, Stejskal *et al*. were able to predict metabolic syndrome diagnosis with 75% sensitivity and 67% specificity (165). Moreover, circulating chemerin concentrations can be further exacerbated by and predictive of cardiovascular complications (163) and inflammation (CRP) in overweight and obese children and adults independent of age, sex, and BMI (162,194,198). This close association with CRP levels, which is used as an early diagnostic tool and marker of severity in many inflammatory conditions, suggests that measurement of circulating chemerin levels may also have clinical utility as a biomarker in inflammatory conditions beyond obesity.

6.5 Remaining Questions and Recommendations for Future Studies

In order to fully understand the role of chemerin in human health and disease, and to modulate levels of chemerin bioactivity for the treatment and/or prevention of metabolic and inflammatory diseases, a number of key research questions remain to be answered. A combination of basic science and clinical studies will be required to determine:

1. In metabolic and inflammatory diseases, do dysregulated chemerin levels serve a pathogenic or protective role? What is the precise mechanism for chemerin in specific disease processes?
2. Under what conditions is chemerin pro- versus anti-inflammatory? Pro- versus anti-diabetic?
3. Does desensitization occur with chronic or high-doses of chemerin? Are chemerin levels in obese patients similar to those that might be required for desensitization? Does chemerin function follow a U-shaped curve like leptin and apelin?
4. How does chemerin signaling and function interact with other cytokines, lipids, and hormones? Does this interaction change with obesity?
5. How do the differing signal transduction pathways of CMKLR1, and GPR1 contribute to chemerin function? Do these roles change in different cell types, or with different chemerin isoforms?
6. Which chemerin isoforms are generated under pathological conditions? To what extent do these isoforms have different signaling and functional properties?
7. What is the role of chemerin in the CNS, particularly with relevance to food intake and energy balance?
8. How do drugs commonly prescribed for treatment of metabolic and inflammatory disorders affect chemerin processing, signaling, and biological function?

6.6 Perspectives and Concluding Remarks

Experimental and clinical investigations support the importance of chemerin in normal physiology and pathobiology of inflammation and metabolic disorders. Most notably, loss of chemerin signaling disrupts adipose tissue and glucose homeostasis. Moreover, adipose derived elevations in circulating chemerin are associated with numerous inflammatory and metabolic perturbations in obese patients and may serve as a biomarker for disease development and progression. Similar to many other adipokines (199,233,246,248), functional chemerin regulation is only one component of a complex multifactorial network of changes that occur with obesity. Future studies need to address the changes that occur in expression, secretion, localization, and bioactivity of chemerin, both alone and in the context of other inflammatory mediators and adipokines. It will be interesting to see, as more studies are conducted, whether chemerin plays a role in additional physiological processes. For example, a number of studies have identified potential roles for chemerin signaling in systemic processes including bone metabolism (181), food intake (220), gestational metabolism (372), arthritis (166,183,184,210), renal failure (190), and cancer (206,373), as well as exhibiting antibacterial activity (211). Investigations of this nature will be instrumental in determining the contribution of chemerin as a pathogenic or protective adipokine in numerous disease contexts, particularly inflammation and metabolism. While the first treatment for obesity and related diseases will always remain lifestyle adjustment through exercise and nutrition, elucidating chemerin dynamics is an exciting and growing field of research with chemerin representing a promising and novel therapeutic target for the treatment of obesity and associated disorders.

References

1. WHO. (2014) Obesity and Overweight: Fact Sheet Number 311. in *WHO Fact Sheets*, World Health Organization: http://www.who.int/mediacentre/factsheets/fs311/en/

2. Lamers, D., Famulla, S., Wronkowitz, N., Hartwig, S., Lehr, S., Ouwens, D. M., Eckardt, K., Kaufman, J. M., Ryden, M., Muller, S., Hanisch, F. G., Ruige, J., Arner, P., Sell, H., and Eckel, J. (2011) Dipeptidyl peptidase 4 is a novel adipokine potentially linking obesity to the metabolic syndrome. *Diabetes* **60**, 1917-1925

3. Wozniak, S. E., Gee, L. L., Wachtel, M. S., and Frezza, E. E. (2009) Adipose tissue: the new endocrine organ? A review article. *Digestive diseases and sciences* **54**, 1847-1856

4. Goralski, K. B., McCarthy, T. C., Hanniman, E. A., Zabel, B. A., Butcher, E. C., Parlee, S. D., Muruganandan, S., and Sinal, C. J. (2007) Chemerin, a novel adipokine that regulates adipogenesis and adipocyte metabolism. *The Journal of biological chemistry* **282**, 28175-28188

5. International_Diabetes_Federation. (2013) *IDF Diabetes Atlas*, 6th edition ed., International Diabetes Federation

6. Canadian Diabetes Association Clinical Practice Guidelines Expert, C., Booth, G., and Cheng, A. Y. (2013) Canadian Diabetes Association 2013 clinical practice guidelines for the prevention and management of diabetes in Canada. Methods. *Canadian journal of diabetes* **37 Suppl 1**, S4-7

7. Pelletier, C., Dai, S., Roberts, K. C., Bienek, A., Onysko, J., and Pelletier, L. (2012) Report summary. Diabetes in Canada: facts and figures from a public health perspective. *Chronic diseases and injuries in Canada* **33**, 53-54

8. Ashcroft, F. M., and Rorsman, P. (2012) Diabetes mellitus and the beta cell: the last ten years. *Cell* **148**, 1160-1171

9. Roden, M., and Bernroider, E. (2003) Hepatic glucose metabolism in humans--its role in health and disease. *Best practice & research. Clinical endocrinology & metabolism* **17**, 365-383

10. American Diabetes, A. (2012) Diagnosis and classification of diabetes mellitus. *Diabetes care* **35 Suppl 1**, S64-71

11. Heilig, C. W., Concepcion, L. A., Riser, B. L., Freytag, S. O., Zhu, M., and Cortes, P. (1995) Overexpression of glucose transporters in rat mesangial cells cultured in a normal glucose milieu mimics the diabetic phenotype. *The Journal of clinical investigation* **96**, 1802-1814

12. Kaiser, N., Sasson, S., Feener, E. P., Boukobza-Vardi, N., Higashi, S., Moller, D. E., Davidheiser, S., Przybylski, R. J., and King, G. L. (1993) Differential regulation of glucose transport and transporters by glucose in vascular endothelial and smooth muscle cells. *Diabetes* **42**, 80-89

13. Aronson, D. (2008) Hyperglycemia and the pathobiology of diabetic complications. *Advances in cardiology* **45**, 1-16

14. Brownlee, M. (2005) The pathobiology of diabetic complications: a unifying mechanism. *Diabetes* **54**, 1615-1625

15. Nukada, H. (2014) Ischemia and diabetic neuropathy. *Handbook of clinical neurology* **126**, 469-487

16. Ahsan, H. (2014) Diabetic retinopathy - Biomolecules and multiple pathophysiology. *Diabetes & metabolic syndrome*

17. Sheen, Y. J., and Sheu, W. H. (2014) Risks of rapid decline renal function in patients with type 2 diabetes. *World journal of diabetes* **5**, 835-846

18. Gilbert, M. P. (2015) Screening and Treatment by the Primary Care Provider of Common Diabetes Complications. *The Medical clinics of North America* **99**, 201-219

19. McCarthy, M. I. (2010) Genomics, type 2 diabetes, and obesity. *The New England journal of medicine* **363**, 2339-2350

20. Bonnefond, A., Froguel, P., and Vaxillaire, M. (2010) The emerging genetics of type 2 diabetes. *Trends in molecular medicine* **16**, 407-416

21. Kivimaki, M., Hamer, M., Batty, G. D., Geddes, J. R., Tabak, A. G., Pentti, J., Virtanen, M., and Vahtera, J. (2010) Antidepressant medication use, weight gain, and risk of type 2 diabetes: a population-based study. *Diabetes care* **33**, 2611-2616

22. Mezuk, B., Eaton, W. W., Albrecht, S., and Golden, S. H. (2008) Depression and type 2 diabetes over the lifespan: a meta-analysis. *Diabetes care* **31**, 2383-2390

23. Shaw, J. E., Punjabi, N. M., Wilding, J. P., Alberti, K. G., Zimmet, P. Z., International Diabetes Federation Taskforce on, E., and Prevention. (2008) Sleep-disordered breathing and type 2 diabetes: a report from the International Diabetes Federation Taskforce on Epidemiology and Prevention. *Diabetes research and clinical practice* **81**, 2-12

24. Brook, R. D., Rajagopalan, S., Pope, C. A., 3rd, Brook, J. R., Bhatnagar, A., Diez-Roux, A. V., Holguin, F., Hong, Y., Luepker, R. V., Mittleman, M. A., Peters, A., Siscovick, D., Smith, S. C., Jr., Whitsel, L., Kaufman, J. D., American Heart Association Council on, E., Prevention, C. o. t. K. i. C. D., Council on Nutrition, P. A., and Metabolism. (2010) Particulate matter air pollution and cardiovascular disease: An update to the scientific statement from the American Heart Association. *Circulation* **121**, 2331-2378

25. Kramer, U., Herder, C., Sugiri, D., Strassburger, K., Schikowski, T., Ranft, U., and Rathmann, W. (2010) Traffic-related air pollution and incident type 2 diabetes: results from the SALIA cohort study. *Environmental health perspectives* **118**, 1273-1279

26. Mozaffarian, D., Kamineni, A., Carnethon, M., Djousse, L., Mukamal, K. J., and Siscovick, D. (2009) Lifestyle risk factors and new-onset diabetes mellitus in older adults: the cardiovascular health study. *Archives of internal medicine* **169**, 798-807

27. Hu, F. B., Manson, J. E., Stampfer, M. J., Colditz, G., Liu, S., Solomon, C. G., and Willett, W. C. (2001) Diet, lifestyle, and the risk of type 2 diabetes mellitus in women. *The New England journal of medicine* **345**, 790-797

28. Statistics_Canada. (2013) Overweight and obese adults (self-reported), 2013. Statistics Canada: http://www.statcan.gc.ca/pub/82-625-x/2013001/article/11840-eng.htm

29. Gudala, K., Bansal, D., Schifano, F., and Bhansali, A. (2013) Diabetes mellitus and risk of dementia: A meta-analysis of prospective observational studies. *Journal of diabetes investigation* **4**, 640-650

30. Shikata, K., Ninomiya, T., and Kiyohara, Y. (2013) Diabetes mellitus and cancer risk: review of the epidemiological evidence. *Cancer science* **104**, 9-14

31. Tirosh, A., Shai, I., Afek, A., Dubnov-Raz, G., Ayalon, N., Gordon, B., Derazne, E., Tzur, D., Shamis, A., Vinker, S., and Rudich, A. (2011) Adolescent BMI trajectory and risk of diabetes versus coronary disease. *The New England journal of medicine* **364**, 1315-1325

32. Mokdad, A. H., Bowman, B. A., Ford, E. S., Vinicor, F., Marks, J. S., and Koplan, J. P. (2001) The continuing epidemics of obesity and diabetes in the United States. *JAMA : the journal of the American Medical Association* **286**, 1195-1200

33. Gastaldelli, A. (2011) Role of beta-cell dysfunction, ectopic fat accumulation and insulin resistance in the pathogenesis of type 2 diabetes mellitus. *Diabetes research and clinical practice* **93 Suppl 1**, S60-65

34. Cnop, M., Foufelle, F., and Velloso, L. A. (2012) Endoplasmic reticulum stress, obesity and diabetes. *Trends in molecular medicine* **18**, 59-68

35. Osborn, O., and Olefsky, J. M. (2012) The cellular and signaling networks linking the immune system and metabolism in disease. *Nature medicine* **18**, 363-374

36. Cantley, J. (2014) The control of insulin secretion by adipokines: current evidence for adipocyte-beta cell endocrine signalling in metabolic homeostasis. *Mammalian genome : official journal of the International Mammalian Genome Society* **25**, 442-454

37. Kwon, H., and Pessin, J. E. (2013) Adipokines mediate inflammation and insulin resistance. *Frontiers in endocrinology* **4**, 1-13

38. Leto, D., and Saltiel, A. R. (2012) Regulation of glucose transport by insulin: traffic control of GLUT4. *Nature reviews. Molecular cell biology* **13**, 383-396

39. Hoffman, N. J., and Elmendorf, J. S. (2011) Signaling, cytoskeletal and membrane mechanisms regulating GLUT4 exocytosis. *Trends in endocrinology and metabolism: TEM* **22**, 110-116

40. Xiong, W., Jordens, I., Gonzalez, E., and McGraw, T. E. (2010) GLUT4 is sorted to vesicles whose accumulation beneath and insertion into the plasma membrane are differentially regulated by insulin and selectively affected by insulin resistance. *Molecular biology of the cell* **21**, 1375-1386

41. Leavens, K. F., and Birnbaum, M. J. (2011) Insulin signaling to hepatic lipid metabolism in health and disease. *Critical reviews in biochemistry and molecular biology* **46**, 200-215

42. Matsuzaka, T., and Shimano, H. (2013) Insulin-dependent and -independent regulation of sterol regulatory element-binding protein-1c. *Journal of diabetes investigation* **4**, 411-412

43. Timmerman, K. L., Lee, J. L., Dreyer, H. C., Dhanani, S., Glynn, E. L., Fry, C. S., Drummond, M. J., Sheffield-Moore, M., Rasmussen, B. B., and Volpi, E. (2010) Insulin stimulates human skeletal muscle protein synthesis via an indirect mechanism involving endothelial-dependent vasodilation and mammalian target of rapamycin complex 1 signaling. *The Journal of clinical endocrinology and metabolism* **95**, 3848-3857

44. Chen, Q., Li, N., Zhu, W., Li, W., Tang, S., Yu, W., Gao, T., Zhang, J., and Li, J. (2011) Insulin alleviates degradation of skeletal muscle protein by inhibiting the ubiquitin-proteasome system in septic rats. *Journal of inflammation* **8**, 1-8

45. Andersson, S. A., Pedersen, M. G., Vikman, J., and Eliasson, L. (2011) Glucose-dependent docking and SNARE protein-mediated exocytosis in mouse pancreatic alpha-cell. *Pflugers Archiv : European journal of physiology* **462**, 443-454

46. Le Marchand, S. J., and Piston, D. W. (2010) Glucose suppression of glucagon secretion: metabolic and calcium responses from alpha-cells in intact mouse pancreatic islets. *The Journal of biological chemistry* **285**, 14389-14398

47. MacDonald, P. E., and Rorsman, P. (2006) Oscillations, intercellular coupling, and insulin secretion in pancreatic beta cells. *PLoS biology* **4**, e49

48. Seino, S., Shibasaki, T., and Minami, K. (2011) Dynamics of insulin secretion and the clinical implications for obesity and diabetes. *The Journal of clinical investigation* **121**, 2118-2125

49. McCulloch, L. J., van de Bunt, M., Braun, M., Frayn, K. N., Clark, A., and Gloyn, A. L. (2011) GLUT2 (SLC2A2) is not the principal glucose transporter in human pancreatic beta cells: implications for understanding genetic association signals at this locus. *Molecular genetics and metabolism* **104**, 648-653

50. Hulse, R. E., Ralat, L. A., and Wei-Jen, T. (2009) Structure, function, and regulation of insulin-degrading enzyme. *Vitamins and hormones* **80**, 635-648

51. Duvillie, B. (2013) Vascularization of the pancreas: an evolving role from embryogenesis to adulthood. *Diabetes* **62**, 4004-4005

52. Kjems, L. L., Holst, J. J., Volund, A., and Madsbad, S. (2003) The influence of GLP-1 on glucose-stimulated insulin secretion: effects on beta-cell sensitivity in type 2 and nondiabetic subjects. *Diabetes* **52**, 380-386

53. Orskov, C. (1992) Glucagon-like peptide-1, a new hormone of the entero-insular axis. *Diabetologia* **35**, 701-711

54. Drucker, D. J. (2006) The biology of incretin hormones. *Cell metabolism* **3**, 153-165

55. Moens, K., Heimberg, H., Flamez, D., Huypens, P., Quartier, E., Ling, Z., Pipeleers, D., Gremlich, S., Thorens, B., and Schuit, F. (1996) Expression and functional activity of glucagon, glucagon-like peptide I, and glucose-dependent insulinotropic peptide receptors in rat pancreatic islet cells. *Diabetes* **45**, 257-261

56. Edwards, C. M., Todd, J. F., Mahmoudi, M., Wang, Z., Wang, R. M., Ghatei, M. A., and Bloom, S. R. (1999) Glucagon-like peptide 1 has a physiological role in the control of postprandial glucose in humans: studies with the antagonist exendin 9-39. *Diabetes* **48**, 86-93

57. Schirra, J., Nicolaus, M., Roggel, R., Katschinski, M., Storr, M., Woerle, H. J., and Goke, B. (2006) Endogenous glucagon-like peptide 1 controls endocrine pancreatic secretion and antro-pyloro-duodenal motility in humans. *Gut* **55**, 243-251

58. Schirra, J., Sturm, K., Leicht, P., Arnold, R., Goke, B., and Katschinski, M. (1998) Exendin(9-39)amide is an antagonist of glucagon-like peptide-1(7-36)amide in humans. *The Journal of clinical investigation* **101**, 1421-1430

59. Holz, G. G. (2004) Epac: A new cAMP-binding protein in support of glucagon-like peptide-1 receptor-mediated signal transduction in the pancreatic beta-cell. *Diabetes* **53**, 5-13

60. Wang, X., Cahill, C. M., Pineyro, M. A., Zhou, J., Doyle, M. E., and Egan, J. M. (1999) Glucagon-like peptide-1 regulates the beta cell transcription factor, PDX-1, in insulinoma cells. *Endocrinology* **140**, 4904-4907

61. Kieffer, T. J., McIntosh, C. H., and Pederson, R. A. (1995) Degradation of glucose-dependent insulinotropic polypeptide and truncated glucagon-like peptide 1 in vitro and in vivo by dipeptidyl peptidase IV. *Endocrinology* **136**, 3585-3596

62. Harbeck, M. C., Louie, D. C., Howland, J., Wolf, B. A., and Rothenberg, P. L. (1996) Expression of insulin receptor mRNA and insulin receptor substrate 1 in pancreatic islet beta-cells. *Diabetes* **45**, 711-717

63. Lee, J., and Pilch, P. F. (1994) The insulin receptor: structure, function, and signaling. *The American journal of physiology* **266**, C319-334

64. Rui, L., Yuan, M., Frantz, D., Shoelson, S., and White, M. F. (2002) SOCS-1 and SOCS-3 block insulin signaling by ubiquitin-mediated degradation of IRS1 and IRS2. *The Journal of biological chemistry* **277**, 42394-42398

65. Zeigerer, A., McBrayer, M. K., and McGraw, T. E. (2004) Insulin stimulation of GLUT4 exocytosis, but not its inhibition of endocytosis, is dependent on RabGAP AS160. *Molecular biology of the cell* **15**, 4406-4415

66. Gonzalez, E., and McGraw, T. E. (2006) Insulin signaling diverges into Akt-dependent and -independent signals to regulate the recruitment/docking and the fusion of GLUT4 vesicles to the plasma membrane. *Molecular biology of the cell* **17**, 4484-4493

67. Chen, X. W., Leto, D., Chiang, S. H., Wang, Q., and Saltiel, A. R. (2007) Activation of RalA is required for insulin-stimulated Glut4 trafficking to the plasma membrane via the exocyst and the motor protein Myo1c. *Developmental cell* **13**, 391-404

68. Kimura, A., Baumann, C. A., Chiang, S. H., and Saltiel, A. R. (2001) The sorbin homology domain: a motif for the targeting of proteins to lipid rafts. *Proceedings of the National Academy of Sciences of the United States of America* **98**, 9098-9103

69. Liu, J., Deyoung, S. M., Zhang, M., Dold, L. H., and Saltiel, A. R. (2005) The stomatin/prohibitin/flotillin/HflK/C domain of flotillin-1 contains distinct sequences that direct plasma membrane localization and protein interactions in 3T3-L1 adipocytes. *The Journal of biological chemistry* **280**, 16125-16134

70. Chiang, S. H., Hou, J. C., Hwang, J., Pessin, J. E., and Saltiel, A. R. (2002) Cloning and functional characterization of related TC10 isoforms, a subfamily of Rho proteins involved in insulin-stimulated glucose transport. *The Journal of biological chemistry* **277**, 13067-13073

71. Watson, R. T., Shigematsu, S., Chiang, S. H., Mora, S., Kanzaki, M., Macara, I. G., Saltiel, A. R., and Pessin, J. E. (2001) Lipid raft microdomain compartmentalization of TC10 is required for insulin signaling and GLUT4 translocation. *The Journal of cell biology* **154**, 829-840

72. Inoue, M., Chang, L., Hwang, J., Chiang, S. H., and Saltiel, A. R. (2003) The exocyst complex is required for targeting of Glut4 to the plasma membrane by insulin. *Nature* **422**, 629-633

73. Moore, M. C., Coate, K. C., Winnick, J. J., An, Z., and Cherrington, A. D. (2012) Regulation of hepatic glucose uptake and storage in vivo. *Advances in nutrition* **3**, 286-294

74. Sutherland, C. O. B., RM.;Granner, DK.;. (2000) Insulin Action Gene Regulation. in *Madame Curie Biosciences Database (Internet)*, Landes Bioscience, Austin Tx

75. Skolnik, E. Y., Batzer, A., Li, N., Lee, C. H., Lowenstein, E., Mohammadi, M., Margolis, B., and Schlessinger, J. (1993) The function of GRB2 in linking the insulin receptor to Ras signaling pathways. *Science* **260**, 1953-1955

76. Dadke, S., Kusari, J., and Chernoff, J. (2000) Down-regulation of insulin signaling by protein-tyrosine phosphatase 1B is mediated by an N-terminal binding region. *The Journal of biological chemistry* **275**, 23642-23647

77. Saltiel, A. R., and Kahn, C. R. (2001) Insulin signalling and the regulation of glucose and lipid metabolism. *Nature* **414**, 799-806

78. Di Guglielmo, G. M., Drake, P. G., Baass, P. C., Authier, F., Posner, B. I., and Bergeron, J. J. (1998) Insulin receptor internalization and signalling. *Molecular and cellular biochemistry* **182**, 59-63

79. Fagerholm, S., Ortegren, U., Karlsson, M., Ruishalme, I., and Stralfors, P. (2009) Rapid insulin-dependent endocytosis of the insulin receptor by caveolae in primary adipocytes. *PloS one* **4**, e5985

80. Kublaoui, B., Lee, J., and Pilch, P. F. (1995) Dynamics of signaling during insulin-stimulated endocytosis of its receptor in adipocytes. *The Journal of biological chemistry* **270**, 59-65

81. Emanuelli, B., Peraldi, P., Filloux, C., Chavey, C., Freidinger, K., Hilton, D. J., Hotamisligil, G. S., and Van Obberghen, E. (2001) SOCS-3 inhibits insulin signaling and is up-regulated in response to tumor necrosis factor-alpha in the adipose tissue of obese mice. *The Journal of biological chemistry* **276**, 47944-47949

82. Wick, K. R., Werner, E. D., Langlais, P., Ramos, F. J., Dong, L. Q., Shoelson, S. E., and Liu, F. (2003) Grb10 inhibits insulin-stimulated insulin receptor substrate (IRS)-phosphatidylinositol 3-kinase/Akt signaling pathway by disrupting the association of IRS-1/IRS-2 with the insulin receptor. *The Journal of biological chemistry* **278**, 8460-8467

83. Kahn, S. E., Prigeon, R. L., McCulloch, D. K., Boyko, E. J., Bergman, R. N., Schwartz, M. W., Neifing, J. L., Ward, W. K., Beard, J. C., Palmer, J. P., and et al. (1993) Quantification of the relationship between insulin sensitivity and beta-cell function in human subjects. Evidence for a hyperbolic function. *Diabetes* **42**, 1663-1672

84. Kieffer, T. J., Heller, R. S., and Habener, J. F. (1996) Leptin receptors expressed on pancreatic beta-cells. *Biochemical and biophysical research communications* **224**, 522-527

85. Denroche, H. C., Huynh, F. K., and Kieffer, T. J. (2012) The role of leptin in glucose homeostasis. *Journal of diabetes investigation* **3**, 115-129

86. Gautron, L., and Elmquist, J. K. (2011) Sixteen years and counting: an update on leptin in energy balance. *The Journal of clinical investigation* **121**, 2087-2093

87. Shoelson, S. E., Lee, J., and Goldfine, A. B. (2006) Inflammation and insulin resistance. *The Journal of clinical investigation* **116**, 1793-1801

88. Qatanani, M., and Lazar, M. A. (2007) Mechanisms of obesity-associated insulin resistance: many choices on the menu. *Genes & development* **21**, 1443-1455

89. Samuel, V. T., and Shulman, G. I. (2012) Mechanisms for insulin resistance: common threads and missing links. *Cell* **148**, 852-871

90. Snel, M., Jonker, J. T., Schoones, J., Lamb, H., de Roos, A., Pijl, H., Smit, J. W., Meinders, A. E., and Jazet, I. M. (2012) Ectopic fat and insulin resistance: pathophysiology and effect of diet and lifestyle interventions. *International journal of endocrinology* **2012**, 983814

91. Yamauchi, T., Kamon, J., Minokoshi, Y., Ito, Y., Waki, H., Uchida, S., Yamashita, S., Noda, M., Kita, S., Ueki, K., Eto, K., Akanuma, Y., Froguel, P., Foufelle, F., Ferre, P., Carling, D., Kimura, S., Nagai, R., Kahn, B. B., and Kadowaki, T. (2002) Adiponectin stimulates glucose utilization and fatty-acid oxidation by activating AMP-activated protein kinase. *Nature medicine* **8**, 1288-1295

92. Li, S., Shin, H. J., Ding, E. L., and van Dam, R. M. (2009) Adiponectin levels and risk of type 2 diabetes: a systematic review and meta-analysis. *JAMA : the journal of the American Medical Association* **302**, 179-188

93. Maeda, N., Shimomura, I., Kishida, K., Nishizawa, H., Matsuda, M., Nagaretani, H., Furuyama, N., Kondo, H., Takahashi, M., Arita, Y., Komuro, R., Ouchi, N., Kihara, S., Tochino, Y., Okutomi, K., Horie, M., Takeda, S., Aoyama, T., Funahashi, T., and Matsuzawa, Y. (2002) Diet-induced insulin resistance in mice lacking adiponectin/ACRP30. *Nature medicine* **8**, 731-737

94. Kim, J. Y., van de Wall, E., Laplante, M., Azzara, A., Trujillo, M. E., Hofmann, S. M., Schraw, T., Durand, J. L., Li, H., Li, G., Jelicks, L. A., Mehler, M. F., Hui, D. Y., Deshaies, Y., Shulman, G. I., Schwartz, G. J., and Scherer, P. E. (2007) Obesity-associated improvements in metabolic profile through expansion of adipose tissue. *The Journal of clinical investigation* **117**, 2621-2637

95. Tschritter, O., Fritsche, A., Thamer, C., Haap, M., Shirkavand, F., Rahe, S., Staiger, H., Maerker, E., Haring, H., and Stumvoll, M. (2003) Plasma adiponectin concentrations predict insulin sensitivity of both glucose and lipid metabolism. *Diabetes* **52**, 239-243

96. Abbasi, F., Chu, J. W., Lamendola, C., McLaughlin, T., Hayden, J., Reaven, G. M., and Reaven, P. D. (2004) Discrimination between obesity and insulin resistance in the relationship with adiponectin. *Diabetes* **53**, 585-590

97. Schaffler, A., Neumeier, M., Herfarth, H., Furst, A., Scholmerich, J., and Buchler, C. (2005) Genomic structure of human omentin, a new adipocytokine expressed in omental adipose tissue. *Biochimica et biophysica acta* **1732**, 96-102

98. Tan, B. K., Adya, R., Farhatullah, S., Chen, J., Lehnert, H., and Randeva, H. S. (2010) Metformin treatment may increase omentin-1 levels in women with polycystic ovary syndrome. *Diabetes* **59**, 3023-3031

99. Yang, R. Z., Lee, M. J., Hu, H., Pray, J., Wu, H. B., Hansen, B. C., Shuldiner, A. R., Fried, S. K., McLenithan, J. C., and Gong, D. W. (2006) Identification of omentin as a novel depot-specific adipokine in human adipose tissue: possible role in modulating insulin action. *American journal of physiology. Endocrinology and metabolism* **290**, E1253-1261

100. de Souza Batista, C. M., Yang, R. Z., Lee, M. J., Glynn, N. M., Yu, D. Z., Pray, J., Ndubuizu, K., Patil, S., Schwartz, A., Kligman, M., Fried, S. K., Gong, D. W., Shuldiner, A. R., Pollin, T. I., and McLenithan, J. C. (2007) Omentin plasma levels and gene expression are decreased in obesity. *Diabetes* **56**, 1655-1661

101. Grodsky, G. M., Karam, J. H., Pavlatos, F. C., and Forsham, P. H. (1963) Reduction by phenformin of excessive insulin levels after glucose loading in obese and diabetic subjects. *Metabolism: clinical and experimental* **12**, 278-286

102. Karam, J. H., Grodsky, G. M., and Forsham, P. H. (1963) Excessive insulin response to glucose in obese subjects as measured by immunochemical assay. *Diabetes* **12**, 197-204

103. Weir, G. C., and Bonner-Weir, S. (2004) Five stages of evolving beta-cell dysfunction during progression to diabetes. *Diabetes* **53 Suppl 3**, S16-21

104. Polonsky, K. S., Given, B. D., Hirsch, L., Shapiro, E. T., Tillil, H., Beebe, C., Galloway, J. A., Frank, B. H., Karrison, T., and Van Cauter, E. (1988) Quantitative study of insulin secretion and clearance in normal and obese subjects. *The Journal of clinical investigation* **81**, 435-441

105. Butler, A. E., Janson, J., Bonner-Weir, S., Ritzel, R., Rizza, R. A., and Butler, P. C. (2003) Beta-cell deficit and increased beta-cell apoptosis in humans with type 2 diabetes. *Diabetes* **52**, 102-110

106. Kloppel, G., Lohr, M., Habich, K., Oberholzer, M., and Heitz, P. U. (1985) Islet pathology and the pathogenesis of type 1 and type 2 diabetes mellitus revisited. *Survey and synthesis of pathology research* **4**, 110-125

107. Maclean, N., and Ogilvie, R. F. (1955) Quantitative estimation of the pancreatic islet tissue in diabetic subjects. *Diabetes* **4**, 367-376

108. Yoon, K. H., Ko, S. H., Cho, J. H., Lee, J. M., Ahn, Y. B., Song, K. H., Yoo, S. J., Kang, M. I., Cha, B. Y., Lee, K. W., Son, H. Y., Kang, S. K., Kim, H. S., Lee, I. K., and Bonner-Weir, S. (2003) Selective beta-cell loss and alpha-cell expansion in patients with type 2 diabetes mellitus in Korea. *The Journal of clinical endocrinology and metabolism* **88**, 2300-2308

109. Melloul, D., Marshak, S., and Cerasi, E. (2002) Regulation of insulin gene transcription. *Diabetologia* **45**, 309-326

110. Prentki, M., and Nolan, C. J. (2006) Islet beta cell failure in type 2 diabetes. *The Journal of clinical investigation* **116**, 1802-1812

111. Weyer, C., Bogardus, C., Mott, D. M., and Pratley, R. E. (1999) The natural history of insulin secretory dysfunction and insulin resistance in the pathogenesis of type 2 diabetes mellitus. *The Journal of clinical investigation* **104**, 787-794

112. Leahy, J. L. (2005) Pathogenesis of type 2 diabetes mellitus. *Archives of medical research* **36**, 197-209

113. Considine, R. V., Sinha, M. K., Heiman, M. L., Kriauciunas, A., Stephens, T. W., Nyce, M. R., Ohannesian, J. P., Marco, C. C., McKee, L. J., Bauer, T. L., and et al. (1996) Serum immunoreactive-leptin concentrations in normal-weight and obese humans. *The New England journal of medicine* **334**, 292-295

114. Emilsson, V., Liu, Y. L., Cawthorne, M. A., Morton, N. M., and Davenport, M. (1997) Expression of the functional leptin receptor mRNA in pancreatic islets and direct inhibitory action of leptin on insulin secretion. *Diabetes* **46**, 313-316

115. Kulkarni, R. N., Wang, Z. L., Wang, R. M., Hurley, J. D., Smith, D. M., Ghatei, M. A., Withers, D. J., Gardiner, J. V., Bailey, C. J., and Bloom, S. R. (1997) Leptin rapidly suppresses insulin release from insulinoma cells, rat and human islets and, in vivo, in mice. *The Journal of clinical investigation* **100**, 2729-2736

116. Brown, J. E., Thomas, S., Digby, J. E., and Dunmore, S. J. (2002) Glucose induces and leptin decreases expression of uncoupling protein-2 mRNA in human islets. *FEBS letters* **513**, 189-192

117. Niswender, K. D., and Magnuson, M. A. (2007) Obesity and the beta cell: lessons from leptin. *The Journal of clinical investigation* **117**, 2753-2756

118. Rakatzi, I., Mueller, H., Ritzeler, O., Tennagels, N., and Eckel, J. (2004) Adiponectin counteracts cytokine- and fatty acid-induced apoptosis in the pancreatic beta-cell line INS-1. *Diabetologia* **47**, 249-258

119. Dunmore, S. J., and Brown, J. E. (2013) The role of adipokines in beta-cell failure of type 2 diabetes. *The Journal of endocrinology* **216**, T37-45

120. Arita, Y., Kihara, S., Ouchi, N., Takahashi, M., Maeda, K., Miyagawa, J., Hotta, K., Shimomura, I., Nakamura, T., Miyaoka, K., Kuriyama, H., Nishida, M., Yamashita, S., Okubo, K., Matsubara, K., Muraguchi, M., Ohmoto, Y., Funahashi, T., and Matsuzawa, Y. (1999) Paradoxical decrease of an adipose-specific protein, adiponectin, in obesity. *Biochemical and biophysical research communications* **257**, 79-83

121. Jin, H., Jiang, B., Tang, J., Lu, W., Wang, W., Zhou, L., Shang, W., Li, F., Ma, Q., Yang, Y., and Chen, M. (2008) Serum visfatin concentrations in obese adolescents and its correlation with age and high-density lipoprotein cholesterol. *Diabetes research and clinical practice* **79**, 412-418

122. Kharroubi, I., Rasschaert, J., Eizirik, D. L., and Cnop, M. (2003) Expression of adiponectin receptors in pancreatic beta cells. *Biochemical and biophysical research communications* **312**, 1118-1122

123. Winzell, M. S., Nogueiras, R., Dieguez, C., and Ahren, B. (2004) Dual action of adiponectin on insulin secretion in insulin-resistant mice. *Biochemical and biophysical research communications* **321**, 154-160

124. Staiger, K., Stefan, N., Staiger, H., Brendel, M. D., Brandhorst, D., Bretzel, R. G., Machicao, F., Kellerer, M., Stumvoll, M., Fritsche, A., and Haring, H. U. (2005) Adiponectin is functionally active in human islets but does not affect insulin secretory function or beta-cell lipoapoptosis. *The Journal of clinical endocrinology and metabolism* **90**, 6707-6713

125. Chang, Y. H., Chang, D. M., Lin, K. C., Shin, S. J., and Lee, Y. J. (2011) Visfatin in overweight/obesity, type 2 diabetes mellitus, insulin resistance, metabolic syndrome and cardiovascular diseases: a meta-analysis and systemic review. *Diabetes/metabolism research and reviews* **27**, 515-527

126. Brown, J. E., Onyango, D. J., Ramanjaneya, M., Conner, A. C., Patel, S. T., Dunmore, S. J., and Randeva, H. S. (2010) Visfatin regulates insulin secretion, insulin receptor signalling and mRNA expression of diabetes-related genes in mouse pancreatic beta-cells. *Journal of molecular endocrinology* **44**, 171-178

127. Riva, M., Nitert, M. D., Voss, U., Sathanoori, R., Lindqvist, A., Ling, C., and Wierup, N. (2011) Nesfatin-1 stimulates glucagon and insulin secretion and beta cell NUCB2 is reduced in human type 2 diabetic subjects. *Cell and tissue research* **346**, 393-405

128. Wu, L. E., Samocha-Bonet, D., Whitworth, P. T., Fazakerley, D. J., Turner, N., Biden, T. J., James, D. E., and Cantley, J. (2014) Identification of fatty acid binding protein 4 as an adipokine that regulates insulin secretion during obesity. *Molecular metabolism* **3**, 465-473

129. Zhao, Y., Ma, X., Wang, Q., Zhou, Y., Zhang, Y., Wu, L., Ji, H., Qin, G., Lu, J., Bi, Y., and Ning, G. (2015) Nesfatin-1 correlates with hypertension in overweight or obese Han Chinese population. *Clinical and experimental hypertension* **37**, 51-56

130. Hotamisligil, G. S., Arner, P., Caro, J. F., Atkinson, R. L., and Spiegelman, B. M. (1995) Increased adipose tissue expression of tumor necrosis factor-alpha in human obesity and insulin resistance. *The Journal of clinical investigation* **95**, 2409-2415

131. Hotamisligil, G. S., Shargill, N. S., and Spiegelman, B. M. (1993) Adipose expression of tumor necrosis factor-alpha: direct role in obesity-linked insulin resistance. *Science* **259**, 87-91

132. Weisberg, S. P., McCann, D., Desai, M., Rosenbaum, M., Leibel, R. L., and Ferrante, A. W., Jr. (2003) Obesity is associated with macrophage accumulation in adipose tissue. *The Journal of clinical investigation* **112**, 1796-1808

133. Vozarova, B., Weyer, C., Hanson, K., Tataranni, P. A., Bogardus, C., and Pratley, R. E. (2001) Circulating interleukin-6 in relation to adiposity, insulin action, and insulin secretion. *Obesity research* **9**, 414-417

134. Kwon, B., Yu, K. Y., Ni, J., Yu, G. L., Jang, I. K., Kim, Y. J., Xing, L., Liu, D., Wang, S. X., and Kwon, B. S. (1999) Identification of a novel activation-inducible protein of the tumor necrosis factor receptor superfamily and its ligand. *The Journal of biological chemistry* **274**, 6056-6061

135. Zhang, S., and Kim, K. H. (1995) TNF-alpha inhibits glucose-induced insulin secretion in a pancreatic beta-cell line (INS-1). *FEBS letters* **377**, 237-239

136. Vozarova de Courten, B., Degawa-Yamauchi, M., Considine, R. V., and Tataranni, P. A. (2004) High serum resistin is associated with an increase in adiposity but not a worsening of insulin resistance in Pima Indians. *Diabetes* **53**, 1279-1284

137. Nieva-Vazquez, A., Perez-Fuentes, R., Torres-Rasgado, E., Lopez-Lopez, J. G., and Romero, J. R. (2014) Serum resistin levels are associated with adiposity and insulin sensitivity in obese Hispanic subjects. *Metabolic syndrome and related disorders* **12**, 143-148

138. Nakata, M., Okada, T., Ozawa, K., and Yada, T. (2007) Resistin induces insulin resistance in pancreatic islets to impair glucose-induced insulin release. *Biochemical and biophysical research communications* **353**, 1046-1051

139. Al-Salam, S., Rashed, H., and Adeghate, E. (2011) Diabetes mellitus is associated with an increased expression of resistin in human pancreatic islet cells. *Islets* **3**, 246-249

140. Nagaev, I., Bokarewa, M., Tarkowski, A., and Smith, U. (2006) Human resistin is a systemic immune-derived proinflammatory cytokine targeting both leukocytes and adipocytes. *PloS one* **1**, e31

141. Schwartz, D. R., and Lazar, M. A. (2011) Human resistin: found in translation from mouse to man. *Trends in endocrinology and metabolism: TEM* **22**, 259-265

142. Boucher, J., Masri, B., Daviaud, D., Gesta, S., Guigne, C., Mazzucotelli, A., Castan-Laurell, I., Tack, I., Knibiehler, B., Carpene, C., Audigier, Y., Saulnier-Blache, J. S., and Valet, P. (2005) Apelin, a newly identified adipokine up-regulated by insulin and obesity. *Endocrinology* **146**, 1764-1771

143. Dray, C., Knauf, C., Daviaud, D., Waget, A., Boucher, J., Buleon, M., Cani, P. D., Attane, C., Guigne, C., Carpene, C., Burcelin, R., Castan-Laurell, I., and Valet, P. (2008) Apelin stimulates glucose utilization in normal and obese insulin-resistant mice. *Cell metabolism* **8**, 437-445

144. Guo, L., Li, Q., Wang, W., Yu, P., Pan, H., Li, P., Sun, Y., and Zhang, J. (2009) Apelin inhibits insulin secretion in pancreatic beta-cells by activation of PI3-kinase-phosphodiesterase 3B. *Endocrine research* **34**, 142-154

145. Sorhede Winzell, M., Magnusson, C., and Ahren, B. (2005) The apj receptor is expressed in pancreatic islets and its ligand, apelin, inhibits insulin secretion in mice. *Regulatory peptides* **131**, 12-17

146. Ringstrom, C., Nitert, M. D., Bennet, H., Fex, M., Valet, P., Rehfeld, J. F., Friis-Hansen, L., and Wierup, N. (2010) Apelin is a novel islet peptide. *Regulatory peptides* **162**, 44-51

147. Ortis, F., Miani, M., Colli, M. L., Cunha, D. A., Gurzov, E. N., Allagnat, F., Chariot, A., and Eizirik, D. L. (2012) Differential usage of NF-kappaB activating signals by IL-1beta and TNF-alpha in pancreatic beta cells. *FEBS letters* **586**, 984-989

148. Ortis, F., Pirot, P., Naamane, N., Kreins, A. Y., Rasschaert, J., Moore, F., Theatre, E., Verhaeghe, C., Magnusson, N. E., Chariot, A., Orntoft, T. F., and Eizirik, D. L. (2008) Induction of nuclear factor-kappaB and its downstream genes by TNF-alpha and IL-1beta has a pro-apoptotic role in pancreatic beta cells. *Diabetologia* **51**, 1213-1225

149. Wijesekara, N., Krishnamurthy, M., Bhattacharjee, A., Suhail, A., Sweeney, G., and Wheeler, M. B. (2010) Adiponectin-induced ERK and Akt phosphorylation protects against pancreatic beta cell apoptosis and increases insulin gene expression and secretion. *The Journal of biological chemistry* **285**, 33623-33631

150. Wente, W., Efanov, A. M., Brenner, M., Kharitonenkov, A., Koster, A., Sandusky, G. E., Sewing, S., Treinies, I., Zitzer, H., and Gromada, J. (2006) Fibroblast growth factor-21 improves pancreatic beta-cell function and survival by activation of extracellular signal-regulated kinase 1/2 and Akt signaling pathways. *Diabetes* **55**, 2470-2478

151. Okuya, S., Tanabe, K., Tanizawa, Y., and Oka, Y. (2001) Leptin increases the viability of isolated rat pancreatic islets by suppressing apoptosis. *Endocrinology* **142**, 4827-4830

152. Holland, W. L., Miller, R. A., Wang, Z. V., Sun, K., Barth, B. M., Bui, H. H., Davis, K. E., Bikman, B. T., Halberg, N., Rutkowski, J. M., Wade, M. R., Tenorio, V. M., Kuo, M. S., Brozinick, J. T., Zhang, B. B., Birnbaum, M. J., Summers, S. A., and Scherer, P. E. (2011) Receptor-mediated activation of ceramidase activity initiates the pleiotropic actions of adiponectin. *Nature medicine* **17**, 55-63

153. Brown, J. E., Conner, A. C., Digby, J. E., Ward, K. L., Ramanjaneya, M., Randeva, H. S., and Dunmore, S. J. (2010) Regulation of beta-cell viability and gene expression by distinct agonist fragments of adiponectin. *Peptides* **31**, 944-949

154. Rourke, J. L., Dranse, H. J., and Sinal, C. J. (2013) Towards an integrative approach to understanding the role of chemerin in human health and disease. *Obesity reviews : an official journal of the International Association for the Study of Obesity* **14**, 245-262

155. Nagpal, S., Patel, S., Jacobe, H., DiSepio, D., Ghosn, C., Malhotra, M., Teng, M., Duvic, M., and Chandraratna, R. A. (1997) Tazarotene-induced gene 2 (TIG2), a novel retinoid-responsive gene in skin. *The Journal of investigative dermatology* **109**, 91-95

156. Bozaoglu, K., Bolton, K., McMillan, J., Zimmet, P., Jowett, J., Collier, G., Walder, K., and Segal, D. (2007) Chemerin is a novel adipokine associated with obesity and metabolic syndrome. *Endocrinology* **148**, 4687-4694

157. Issa, M. E., Muruganandan, S., Ernst, M. C., Parlee, S. D., Zabel, B. A., Butcher, E. C., Sinal, C. J., and Goralski, K. B. (2012) Chemokine-like receptor 1 regulates skeletal muscle cell myogenesis. *American journal of physiology. Cell physiology* **302**, C1621-1631

158. Takahashi, M., Okimura, Y., Iguchi, G., Nishizawa, H., Yamamoto, M., Suda, K., Kitazawa, R., Fujimoto, W., Takahashi, K., Zolotaryov, F. N., Hong, K. S., Kiyonari, H., Abe, T., Kaji, H., Kitazawa, S., Kasuga, M., Chihara, K., and Takahashi, Y. (2011) Chemerin regulates beta-cell function in mice. *Scientific reports* **1**, 1-10

159. Parlee, S. D., Ernst, M. C., Muruganandan, S., Sinal, C. J., and Goralski, K. B. (2010) Serum chemerin levels vary with time of day and are modified by obesity and tumor necrosis factor-{alpha}. *Endocrinology* **151**, 2590-2602

160. Tan, B. K., Chen, J., Farhatullah, S., Adya, R., Kaur, J., Heutling, D., Lewandowski, K. C., O'Hare, J. P., Lehnert, H., and Randeva, H. S. (2009) Insulin and metformin regulate circulating and adipose tissue chemerin. *Diabetes* **58**, 1971-1977

161. Bozaoglu, K., Segal, D., Shields, K. A., Cummings, N., Curran, J. E., Comuzzie, A. G., Mahaney, M. C., Rainwater, D. L., VandeBerg, J. L., MacCluer, J. W., Collier, G., Blangero, J., Walder, K., and Jowett, J. B. (2009) Chemerin is associated with metabolic syndrome phenotypes in a Mexican-American population. *The Journal of clinical endocrinology and metabolism* **94**, 3085-3088

162. Chakaroun, R., Raschpichler, M., Kloting, N., Oberbach, A., Flehmig, G., Kern, M., Schon, M. R., Shang, E., Lohmann, T., Dressler, M., Fasshauer, M., Stumvoll, M., and Bluher, M. (2012) Effects of weight loss and exercise on chemerin serum concentrations and adipose tissue expression in human obesity. *Metabolism: clinical and experimental* **61**, 706-714

163. Dong, B., Ji, W., and Zhang, Y. (2011) Elevated serum chemerin levels are associated with the presence of coronary artery disease in patients with metabolic syndrome. *Intern Med* **50**, 1093-1097

164. Lehrke, M., Becker, A., Greif, M., Stark, R., Laubender, R. P., von Ziegler, F., Lebherz, C., Tittus, J., Reiser, M., Becker, C., Goke, B., Leber, A. W., Parhofer, K. G., and Broedl, U. C. (2009) Chemerin is associated with markers of inflammation and components of the metabolic syndrome but does not predict coronary atherosclerosis. *European journal of endocrinology / European Federation of Endocrine Societies* **161**, 339-344

165. Stejskal, D., Karpisek, M., Hanulova, Z., and Svestak, M. (2008) Chemerin is an independent marker of the metabolic syndrome in a Caucasian population--a pilot study. *Biomedical papers of the Medical Faculty of the University Palacky, Olomouc, Czechoslovakia* **152**, 217-221

166. Huang, K., Du, G., Li, L., Liang, H., and Zhang, B. (2012) Association of chemerin levels in synovial fluid with the severity of knee osteoarthritis. *Biomarkers : biochemical indicators of exposure, response, and susceptibility to chemicals* **17**, 16-20

167. Weigert, J., Neumeier, M., Wanninger, J., Filarsky, M., Bauer, S., Wiest, R., Farkas, S., Scherer, M. N., Schaffler, A., Aslanidis, C., Scholmerich, J., and Buechler, C. (2010) Systemic chemerin is related to inflammation rather than obesity in type 2 diabetes. *Clinical endocrinology* **72**, 342-348

168. Yamamoto, T., Qureshi, A. R., Anderstam, B., Heimburger, O., Barany, P., Lindholm, B., Stenvinkel, P., and Axelsson, J. (2010) Clinical importance of an elevated circulating chemerin level in incident dialysis patients. *Nephrology, dialysis, transplantation : official publication of the European Dialysis and Transplant Association - European Renal Association* **25**, 4017-4023

169. Yang, M., Yang, G., Dong, J., Liu, Y., Zong, H., Liu, H., Boden, G., and Li, L. (2010) Elevated plasma levels of chemerin in newly diagnosed type 2 diabetes mellitus with hypertension. *Journal of investigative medicine : the official publication of the American Federation for Clinical Research* **58**, 883-886

170. Wittamer, V., Franssen, J. D., Vulcano, M., Mirjolet, J. F., Le Poul, E., Migeotte, I., Brezillon, S., Tyldesley, R., Blanpain, C., Detheux, M., Mantovani, A., Sozzani, S., Vassart, G., Parmentier, M., and Communi, D. (2003) Specific recruitment of antigen-presenting cells by chemerin, a novel processed ligand from human inflammatory fluids. *The Journal of experimental medicine* **198**, 977-985

171. Du, X. Y., Zabel, B. A., Myles, T., Allen, S. J., Handel, T. M., Lee, P. P., Butcher, E. C., and Leung, L. L. (2009) Regulation of chemerin bioactivity by plasma carboxypeptidase N, carboxypeptidase B (activated thrombin-activable fibrinolysis inhibitor), and platelets. *The Journal of biological chemistry* **284**, 751-758

172. Meder, W., Wendland, M., Busmann, A., Kutzleb, C., Spodsberg, N., John, H., Richter, R., Schleuder, D., Meyer, M., and Forssmann, W. G. (2003) Characterization of human circulating TIG2 as a ligand for the orphan receptor ChemR23. *FEBS letters* **555**, 495-499

173. Yamaguchi, Y., Du, X. Y., Zhao, L., Morser, J., and Leung, L. L. (2011) Proteolytic cleavage of chemerin protein is necessary for activation to the active form, Chem157S, which functions as a signaling molecule in glioblastoma. *The Journal of biological chemistry* **286**, 39510-39519

174. Zabel, B. A., Allen, S. J., Kulig, P., Allen, J. A., Cichy, J., Handel, T. M., and Butcher, E. C. (2005) Chemerin activation by serine proteases of the coagulation, fibrinolytic, and inflammatory cascades. *The Journal of biological chemistry* **280**, 34661-34666

175. Zhao, L., Yamaguchi, Y., Sharif, S., Du, X. Y., Song, J. J., Lee, D. M., Recht, L. D., Robinson, W. H., Morser, J., and Leung, L. L. (2011) Chemerin158K protein is the dominant chemerin isoform in synovial and cerebrospinal fluids but not in plasma. *The Journal of biological chemistry* **286**, 39520-39527

176. Guillabert, A., Wittamer, V., Bondue, B., Godot, V., Imbault, V., Parmentier, M., and Communi, D. (2008) Role of neutrophil proteinase 3 and mast cell chymase in chemerin proteolytic regulation. *Journal of leukocyte biology* **84**, 1530-1538

177. Kraakman, L., Lemaire, K., Ma, P., Teunissen, A. W., Donaton, M. C., Van Dijck, P., Winderickx, J., de Winde, J. H., and Thevelein, J. M. (1999) A Saccharomyces cerevisiae G-protein coupled receptor, Gpr1, is specifically required for glucose activation of the cAMP pathway during the transition to growth on glucose. *Molecular microbiology* **32**, 1002-1012

178. Lorenz, M. C., Pan, X., Harashima, T., Cardenas, M. E., Xue, Y., Hirsch, J. P., and Heitman, J. (2000) The G protein-coupled receptor gpr1 is a nutrient sensor that regulates pseudohyphal differentiation in Saccharomyces cerevisiae. *Genetics* **154**, 609-622

179. Barnea, G., Strapps, W., Herrada, G., Berman, Y., Ong, J., Kloss, B., Axel, R., and Lee, K. J. (2008) The genetic design of signaling cascades to record receptor activation. *Proceedings of the National Academy of Sciences of the United States of America* **105**, 64-69

180. Zabel, B. A., Nakae, S., Zuniga, L., Kim, J. Y., Ohyama, T., Alt, C., Pan, J., Suto, H., Soler, D., Allen, S. J., Handel, T. M., Song, C. H., Galli, S. J., and Butcher, E. C. (2008) Mast cell-expressed orphan receptor CCRL2 binds chemerin and is required for optimal induction of IgE-mediated passive cutaneous anaphylaxis. *The Journal of experimental medicine* **205**, 2207-2220

181. Muruganandan, S., Roman, A. A., and Sinal, C. J. (2010) Role of chemerin/CMKLR1 signaling in adipogenesis and osteoblastogenesis of bone marrow stem cells. *Journal of bone and mineral research : the official journal of the American Society for Bone and Mineral Research* **25**, 222-234

182. Regard, J. B., Sato, I. T., and Coughlin, S. R. (2008) Anatomical profiling of G protein-coupled receptor expression. *Cell* **135**, 561-571

183. Berg, V., Sveinbjornsson, B., Bendiksen, S., Brox, J., Meknas, K., and Figenschau, Y. (2010) Human articular chondrocytes express ChemR23 and chemerin; ChemR23 promotes inflammatory signalling upon binding the ligand chemerin(21-157). *Arthritis research & therapy* **12**, R228

184. Kaneko, K., Miyabe, Y., Takayasu, A., Fukuda, S., Miyabe, C., Ebisawa, M., Yokoyama, W., Watanabe, K., Imai, T., Muramoto, K., Terashima, Y., Sugihara, T., Matsushima, K., Miyasaka, N., and Nanki, T. (2011) Chemerin activates fibroblast-like synoviocytes in patients with rheumatoid arthritis. *Arthritis research & therapy* **13**, R158

185. Kaur, J., Adya, R., Tan, B. K., Chen, J., and Randeva, H. S. (2010) Identification of chemerin receptor (ChemR23) in human endothelial cells: chemerin-induced endothelial angiogenesis. *Biochemical and biophysical research communications* **391**, 1762-1768

186. Roh, S. G., Song, S. H., Choi, K. C., Katoh, K., Wittamer, V., Parmentier, M., and Sasaki, S. (2007) Chemerin--a new adipokine that modulates adipogenesis via its own receptor. *Biochemical and biophysical research communications* **362**, 1013-1018

187. Hart, R., and Greaves, D. R. (2010) Chemerin contributes to inflammation by promoting macrophage adhesion to VCAM-1 and fibronectin through clustering of VLA-4 and VLA-5. *J Immunol* **185**, 3728-3739

188. Yamawaki, H., Kameshima, S., Usui, T., Okada, M., and Hara, Y. (2012) A novel adipocytokine, chemerin exerts anti-inflammatory roles in human vascular endothelial cells. *Biochemical and biophysical research communications* **423**, 152-157

189. Pfau, D., Bachmann, A., Lossner, U., Kratzsch, J., Bluher, M., Stumvoll, M., and Fasshauer, M. (2010) Serum levels of the adipokine chemerin in relation to renal function. *Diabetes care* **33**, 171-173

190. Rutkowski, P., Sledzinski, T., Zielinska, H., Lizakowski, S., Goyke, E., Szrok-Wojtkiewicz, S., Swierczynski, J., and Rutkowski, B. (2012) Decrease of serum chemerin concentration in patients with end stage renal disease after successful kidney transplantation. *Regulatory peptides* **173**, 55-59

191. Adrych, K., Stojek, M., Smoczynski, M., Sledzinski, T., Sylwia, S. W., and Swierczynski, J. (2012) Increased serum chemerin concentration in patients with chronic pancreatitis. *Digestive and liver disease : official journal of the Italian Society of Gastroenterology and the Italian Association for the Study of the Liver* **44**, 393-397

192. Stepan, H., Philipp, A., Roth, I., Kralisch, S., Jank, A., Schaarschmidt, W., Lossner, U., Kratzsch, J., Bluher, M., Stumvoll, M., and Fasshauer, M. (2011) Serum levels of the adipokine chemerin are increased in preeclampsia during and 6 months after pregnancy. *Regulatory peptides* **168**, 69-72

193. Kukla, M., Zwirska-Korczala, K., Gabriel, A., Waluga, M., Warakomska, I., Szczygiel, B., Berdowska, A., Mazur, W., Wozniak-Grygiel, E., and Kryczka, W. (2010) Chemerin, vaspin and insulin resistance in chronic hepatitis C. *Journal of viral hepatitis* **17**, 661-667

194. Sell, H., Divoux, A., Poitou, C., Basdevant, A., Bouillot, J. L., Bedossa, P., Tordjman, J., Eckel, J., and Clement, K. (2010) Chemerin correlates with markers for fatty liver in morbidly obese patients and strongly decreases after weight loss induced by bariatric surgery. *The Journal of clinical endocrinology and metabolism* **95**, 2892-2896

195. Yilmaz, Y., Kurt, R., Gurdal, A., Alahdab, Y. O., Yonal, O., Senates, E., Polat, N., Eren, F., Imeryuz, N., and Oflaz, H. (2011) Circulating vaspin levels and epicardial adipose tissue thickness are associated with impaired coronary flow reserve in patients with nonalcoholic fatty liver disease. *Atherosclerosis* **217**, 125-129

196. Yilmaz, Y., Yonal, O., Kurt, R., Alahdab, Y. O., Eren, F., Ozdogan, O., Celikel, C. A., Imeryuz, N., Kalayci, C., and Avsar, E. (2011) Serum levels of omentin, chemerin and adipsin in patients with biopsy-proven nonalcoholic fatty liver disease. *Scandinavian journal of gastroenterology* **46**, 91-97

197. Feng, X., Li, P., Zhou, C., Jia, X., and Kang, J. (2012) Elevated levels of serum chemerin in patients with obstructive sleep apnea syndrome. *Biomarkers : biochemical indicators of exposure, response, and susceptibility to chemicals* **17**, 248-253

198. Landgraf, K., Friebe, D., Ullrich, T., Kratzsch, J., Dittrich, K., Herberth, G., Adams, V., Kiess, W., Erbs, S., and Korner, A. (2012) Chemerin as a mediator between obesity and vascular inflammation in children. *The Journal of clinical endocrinology and metabolism* **97**, E556-564

199. Tonjes, A., Fasshauer, M., Kratzsch, J., Stumvoll, M., and Bluher, M. (2010) Adipokine pattern in subjects with impaired fasting glucose and impaired glucose tolerance in comparison to normal glucose tolerance and diabetes. *PloS one* **5**, e13911

200. De Palma, G., Castellano, G., Del Prete, A., Sozzani, S., Fiore, N., Loverre, A., Parmentier, M., Gesualdo, L., Grandaliano, G., and Schena, F. P. (2011) The possible role of ChemR23/Chemerin axis in the recruitment of dendritic cells in lupus nephritis. *Kidney international* **79**, 1228-1235

201. Maheshwari, A., Kurundkar, A. R., Shaik, S. S., Kelly, D. R., Hartman, Y., Zhang, W., Dimmitt, R., Saeed, S., Randolph, D. A., Aprahamian, C., Datta, G., and Ohls, R. K. (2009) Epithelial cells in fetal intestine produce chemerin to recruit macrophages. *American journal of physiology. Gastrointestinal and liver physiology* **297**, G1-G10

202. Albanesi, C., Scarponi, C., Bosisio, D., Sozzani, S., and Girolomoni, G. (2010) Immune functions and recruitment of plasmacytoid dendritic cells in psoriasis. *Autoimmunity* **43**, 215-219

203. Albanesi, C., Scarponi, C., Pallotta, S., Daniele, R., Bosisio, D., Madonna, S., Fortugno, P., Gonzalvo-Feo, S., Franssen, J. D., Parmentier, M., De Pita, O., Girolomoni, G., and Sozzani, S. (2009) Chemerin expression marks early psoriatic skin lesions and correlates with plasmacytoid dendritic cell recruitment. *The Journal of experimental medicine* **206**, 249-258

204. Lande, R., Gafa, V., Serafini, B., Giacomini, E., Visconti, A., Remoli, M. E., Severa, M., Parmentier, M., Ristori, G., Salvetti, M., Aloisi, F., and Coccia, E. M. (2008) Plasmacytoid dendritic cells in multiple sclerosis: intracerebral recruitment and impaired maturation in response to interferon-beta. *Journal of neuropathology and experimental neurology* **67**, 388-401

205. Monnier, J., Lewen, S., O'Hara, E., Huang, K., Tu, H., Butcher, E. C., and Zabel, B. A. (2012) Expression, regulation, and function of atypical chemerin receptor CCRL2 on endothelial cells. *J Immunol* **189**, 956-967

206. Pachynski, R. K., Zabel, B. A., Kohrt, H. E., Tejeda, N. M., Monnier, J., Swanson, C. D., Holzer, A. K., Gentles, A. J., Sperinde, G. V., Edalati, A., Hadeiba, H. A., Alizadeh, A. A., and Butcher, E. C. (2012) The chemoattractant chemerin suppresses melanoma by recruiting natural killer cell antitumor defenses. *The Journal of experimental medicine* **209**, 1427-1435

207. Parolini, S., Santoro, A., Marcenaro, E., Luini, W., Massardi, L., Facchetti, F., Communi, D., Parmentier, M., Majorana, A., Sironi, M., Tabellini, G., Moretta, A., and Sozzani, S. (2007) The role of chemerin in the colocalization of NK and dendritic cell subsets into inflamed tissues. *Blood* **109**, 3625-3632

208. Vermi, W., Lonardi, S., Morassi, M., Rossini, C., Tardanico, R., Venturini, M., Sala, R., Tincani, A., Poliani, P. L., Calzavara-Pinton, P. G., Cerroni, L., Santoro, A., and Facchetti, F. (2009) Cutaneous distribution of plasmacytoid dendritic cells in lupus erythematosus. Selective tropism at the site of epithelial apoptotic damage. *Immunobiology* **214**, 877-886

209. Vermi, W., Riboldi, E., Wittamer, V., Gentili, F., Luini, W., Marrelli, S., Vecchi, A., Franssen, J. D., Communi, D., Massardi, L., Sironi, M., Mantovani, A., Parmentier, M., Facchetti, F., and Sozzani, S. (2005) Role of ChemR23 in directing the migration of myeloid and plasmacytoid dendritic cells to lymphoid organs and inflamed skin. *The Journal of experimental medicine* **201**, 509-515

210. Eisinger, K., Bauer, S., Schaffler, A., Walter, R., Neumann, E., Buechler, C., Muller-Ladner, U., and Frommer, K. W. (2012) Chemerin induces CCL2 and TLR4 in synovial fibroblasts of patients with rheumatoid arthritis and osteoarthritis. *Experimental and molecular pathology* **92**, 90-96

211. Kulig, P., Zabel, B. A., Dubin, G., Allen, S. J., Ohyama, T., Potempa, J., Handel, T. M., Butcher, E. C., and Cichy, J. (2007) Staphylococcus aureus-derived staphopain B, a potent cysteine protease activator of plasma chemerin. *J Immunol* **178**, 3713-3720

212. Wittamer, V., Bondue, B., Guillabert, A., Vassart, G., Parmentier, M., and Communi, D. (2005) Neutrophil-mediated maturation of chemerin: a link between innate and adaptive immunity. *J Immunol* **175**, 487-493

213. Graham, K. L., Zabel, B. A., Loghavi, S., Zuniga, L. A., Ho, P. P., Sobel, R. A., and Butcher, E. C. (2009) Chemokine-like receptor-1 expression by central nervous system-infiltrating leukocytes and involvement in a model of autoimmune demyelinating disease. *J Immunol* **183**, 6717-6723

214. Cash, J. L., Hart, R., Russ, A., Dixon, J. P., Colledge, W. H., Doran, J., Hendrick, A. G., Carlton, M. B., and Greaves, D. R. (2008) Synthetic chemerin-derived peptides suppress inflammation through ChemR23. *The Journal of experimental medicine* **205**, 767-775

215. Luangsay, S., Wittamer, V., Bondue, B., De Henau, O., Rouger, L., Brait, M., Franssen, J. D., de Nadai, P., Huaux, F., and Parmentier, M. (2009) Mouse ChemR23 is expressed in dendritic cell subsets and macrophages, and mediates an anti-inflammatory activity of chemerin in a lung disease model. *J Immunol* **183**, 6489-6499

216. Bondue, B., Vosters, O., de Nadai, P., Glineur, S., De Henau, O., Luangsay, S., Van Gool, F., Communi, D., De Vuyst, P., Desmecht, D., and Parmentier, M. (2011) ChemR23 dampens lung inflammation and enhances anti-viral immunity in a mouse model of acute viral pneumonia. *PLoS pathogens* **7**, e1002358

217. Bondue, B., De Henau, O., Luangsay, S., Devosse, T., de Nadai, P., Springael, J. Y., Parmentier, M., and Vosters, O. (2012) The chemerin/ChemR23 system does not affect the pro-inflammatory response of mouse and human macrophages ex vivo. *PloS one* **7**, e40043

218. Arita, M., Bianchini, F., Aliberti, J., Sher, A., Chiang, N., Hong, S., Yang, R., Petasis, N. A., and Serhan, C. N. (2005) Stereochemical assignment, antiinflammatory properties, and receptor for the omega-3 lipid mediator resolvin E1. *The Journal of experimental medicine* **201**, 713-722

219. Arita, M., Ohira, T., Sun, Y. P., Elangovan, S., Chiang, N., and Serhan, C. N. (2007) Resolvin E1 selectively interacts with leukotriene B4 receptor BLT1 and ChemR23 to regulate inflammation. *J Immunol* **178**, 3912-3917

220. Ernst, M. C., Haidl, I. D., Zuniga, L. A., Dranse, H. J., Rourke, J. L., Zabel, B. A., Butcher, E. C., and Sinal, C. J. (2012) Disruption of the chemokine-like receptor-1 (CMKLR1) gene is associated with reduced adiposity and glucose intolerance. *Endocrinology* **153**, 672-682

221. Ernst, M. C., Issa, M., Goralski, K. B., and Sinal, C. J. (2010) Chemerin exacerbates glucose intolerance in mouse models of obesity and diabetes. *Endocrinology* **151**, 1998-2007

222. Yoo, H. J., Choi, H. Y., Yang, S. J., Kim, H. Y., Seo, J. A., Kim, S. G., Kim, N. H., Choi, K. M., Choi, D. S., and Baik, S. H. (2012) Circulating chemerin level is independently correlated with arterial stiffness. *Journal of atherosclerosis and thrombosis* **19**, 59-66; discussion 67-58

223. Shin, H. Y., Lee, D. C., Chu, S. H., Jeon, J. Y., Lee, M. K., Im, J. A., and Lee, J. W. (2012) Chemerin levels are positively correlated with abdominal visceral fat accumulation. *Clinical endocrinology* **77**, 47-50

224. Ress, C., Tschoner, A., Engl, J., Klaus, A., Tilg, H., Ebenbichler, C. F., Patsch, J. R., and Kaser, S. (2010) Effect of bariatric surgery on circulating chemerin levels. *European journal of clinical investigation* **40**, 277-280

225. Bluher, M., Rudich, A., Kloting, N., Golan, R., Henkin, Y., Rubin, E., Schwarzfuchs, D., Gepner, Y., Stampfer, M. J., Fiedler, M., Thiery, J., Stumvoll, M., and Shai, I. (2012) Two patterns of adipokine and other biomarker dynamics in a long-term weight loss intervention. *Diabetes care* **35**, 342-349

226. Saremi, A., Shavandi, N., Parastesh, M., and Daneshmand, H. (2010) Twelve-week aerobic training decreases chemerin level and improves cardiometabolic risk factors in overweight and obese men. *Asian journal of sports medicine* **1**, 151-158

227. Ernst, M. C., and Sinal, C. J. (2010) Chemerin: at the crossroads of inflammation and obesity. *Trends in endocrinology and metabolism: TEM* **21**, 660-667

228. Muruganandan, S., Parlee, S. D., Rourke, J. L., Ernst, M. C., Goralski, K. B., and Sinal, C. J. (2011) Chemerin, a novel peroxisome proliferator-activated receptor gamma (PPARgamma) target gene that promotes mesenchymal stem cell adipogenesis. *The Journal of biological chemistry* **286**, 23982-23995

229. Bozaoglu, K., Curran, J. E., Stocker, C. J., Zaibi, M. S., Segal, D., Konstantopoulos, N., Morrison, S., Carless, M., Dyer, T. D., Cole, S. A., Goring, H. H., Moses, E. K., Walder, K., Cawthorne, M. A., Blangero, J., and Jowett, J. B. (2010) Chemerin, a novel adipokine in the regulation of angiogenesis. *The Journal of clinical endocrinology and metabolism* **95**, 2476-2485

230. Lumeng, C. N., and Saltiel, A. R. (2011) Inflammatory links between obesity and metabolic disease. *The Journal of clinical investigation* **121**, 2111-2117

231. Bauer, S., Wanninger, J., Schmidhofer, S., Weigert, J., Neumeier, M., Dorn, C., Hellerbrand, C., Zimara, N., Schaffler, A., Aslanidis, C., and Buechler, C. (2011) Sterol regulatory element-binding protein 2 (SREBP2) activation after excess triglyceride storage induces chemerin in hypertrophic adipocytes. *Endocrinology* **152**, 26-35

232. Kralisch, S., Weise, S., Sommer, G., Lipfert, J., Lossner, U., Bluher, M., Stumvoll, M., and Fasshauer, M. (2009) Interleukin-1beta induces the novel adipokine chemerin in adipocytes in vitro. *Regulatory peptides* **154**, 102-106

233. Chu, S. H., Lee, M. K., Ahn, K. Y., Im, J. A., Park, M. S., Lee, D. C., Jeon, J. Y., and Lee, J. W. (2012) Chemerin and adiponectin contribute reciprocally to metabolic syndrome. *PloS one* **7**, e34710

234. Min, J. L., Nicholson, G., Halgrimsdottir, I., Almstrup, K., Petri, A., Barrett, A., Travers, M., Rayner, N. W., Magi, R., Pettersson, F. H., Broxholme, J., Neville, M. J., Wills, Q. F., Cheeseman, J., Allen, M., Holmes, C. C., Spector, T. D., Fleckner, J., McCarthy, M. I., Karpe, F., Lindgren, C. M., and Zondervan, K. T. (2012) Coexpression network analysis in abdominal and gluteal adipose tissue reveals regulatory genetic loci for metabolic syndrome and related phenotypes. *PLoS genetics* **8**, e1002505

235. Yan, Q., Zhang, Y., Hong, J., Gu, W., Dai, M., Shi, J., Zhai, Y., Wang, W., Li, X., and Ning, G. (2012) The association of serum chemerin level with risk of coronary artery disease in Chinese adults. *Endocrine* **41**, 281-288

236. Hah, Y. J., Kim, N. K., Kim, M. K., Kim, H. S., Hur, S. H., Yoon, H. J., Kim, Y. N., and Park, K. G. (2011) Relationship between Chemerin Levels and Cardiometabolic Parameters and Degree of Coronary Stenosis in Korean Patients with Coronary Artery Disease. *Diabetes & metabolism journal* **35**, 248-254

237. Becker, M., Rabe, K., Lebherz, C., Zugwurst, J., Goke, B., Parhofer, K. G., Lehrke, M., and Broedl, U. C. (2010) Expression of human chemerin induces insulin resistance in the skeletal muscle but does not affect weight, lipid levels, and atherosclerosis in LDL receptor knockout mice on high-fat diet. *Diabetes* **59**, 2898-2903

238. Takahashi, M., Takahashi, Y., Takahashi, K., Zolotaryov, F. N., Hong, K. S., Kitazawa, R., Iida, K., Okimura, Y., Kaji, H., Kitazawa, S., Kasuga, M., and Chihara, K. (2008) Chemerin enhances insulin signaling and potentiates insulin-stimulated glucose uptake in 3T3-L1 adipocytes. *FEBS letters* **582**, 573-578

239. Sell, H., Laurencikiene, J., Taube, A., Eckardt, K., Cramer, A., Horrighs, A., Arner, P., and Eckel, J. (2009) Chemerin is a novel adipocyte-derived factor inducing insulin resistance in primary human skeletal muscle cells. *Diabetes* **58**, 2731-2740

240. Ouwens, D. M., Bekaert, M., Lapauw, B., Van Nieuwenhove, Y., Lehr, S., Hartwig, S., Calders, P., Kaufman, J. M., Sell, H., Eckel, J., and Ruige, J. B. (2012) Chemerin as biomarker for insulin sensitivity in males without typical characteristics of metabolic syndrome. *Archives of physiology and biochemistry* **118**, 135-138

241. Rabe, K., Lehrke, M., Parhofer, K. G., and Broedl, U. C. (2008) Adipokines and insulin resistance. *Mol Med* **14**, 741-751

242. Wilson, P. W., D'Agostino, R. B., Parise, H., Sullivan, L., and Meigs, J. B. (2005) Metabolic syndrome as a precursor of cardiovascular disease and type 2 diabetes mellitus. *Circulation* **112**, 3066-3072

243. Zakareia, F. A. (2012) Correlation of peripheral arterial blood flow with plasma chemerin and VEGF in diabetic peripheral vascular disease. *Biomarkers in medicine* **6**, 81-87

244. Xiaotao, L., Xiaoxia, Z., Yue, X., and Liye, W. (2012) Serum chemerin levels are associated with the presence and extent of coronary artery disease. *Coronary artery disease* **23**, 412-416

245. Gao, X., Mi, S., Zhang, F., Gong, F., Lai, Y., Gao, F., Zhang, X., Wang, L., and Tao, H. (2011) Association of chemerin mRNA expression in human epicardial adipose tissue with coronary atherosclerosis. *Cardiovascular diabetology* **10**, 87

246. Spiroglou, S. G., Kostopoulos, C. G., Varakis, J. N., and Papadaki, H. H. (2010) Adipokines in periaortic and epicardial adipose tissue: differential expression and relation to atherosclerosis. *Journal of atherosclerosis and thrombosis* **17**, 115-130

247. Ren, R. Z., Zhang, X., Xu, J., Zhang, H. Q., Yu, C. X., Cao, M. F., Gao, L., Guan, Q. B., and Zhao, J. J. (2012) Chronic ethanol consumption increases the levels of chemerin in the serum and adipose tissue of humans and rats. *Acta pharmacologica Sinica* **33**, 652-659

248. Alfadda, A. A., Sallam, R. M., Chishti, M. A., Moustafa, A. S., Fatma, S., Alomaim, W. S., Al-Naami, M. Y., Bassas, A. F., Chrousos, G. P., and Jo, H. (2012) Differential patterns of serum concentration and adipose tissue expression of chemerin in obesity: adipose depot specificity and gender dimorphism. *Molecules and cells* **33**, 591-596

249. Shimamura, K., Matsuda, M., Miyamoto, Y., Yoshimoto, R., Seo, T., and Tokita, S. (2009) Identification of a stable chemerin analog with potent activity toward ChemR23. *Peptides* **30**, 1529-1538

250. Hu, W., Yu, Q., Zhang, J., and Liu, D. (2012) Rosiglitazone ameliorates diabetic nephropathy by reducing the expression of Chemerin and ChemR23 in the kidney of streptozotocin-induced diabetic rats. *Inflammation* **35**, 1287-1293

251. Pei, L., Yang, J., Du, J., Liu, H., Ao, N., and Zhang, Y. (2012) Downregulation of chemerin and alleviation of endoplasmic reticulum stress by metformin in adipose tissue of rats. *Diabetes research and clinical practice* **97**, 267-275

252. Zabel, B. A., Silverio, A. M., and Butcher, E. C. (2005) Chemokine-like receptor 1 expression and chemerin-directed chemotaxis distinguish plasmacytoid from myeloid dendritic cells in human blood. *J Immunol* **174**, 244-251

253. Zhao, R. J., and Wang, H. (2011) Chemerin/ChemR23 signaling axis is involved in the endothelial protection by K(ATP) channel opener iptakalim. *Acta pharmacologica Sinica* **32**, 573-580

254. Nakajima, H., Nakajima, K., Nagano, Y., Yamamoto, M., Tarutani, M., Takahashi, M., Takahashi, Y., and Sano, S. (2010) Circulating level of chemerin is upregulated in psoriasis. *Journal of dermatological science* **60**, 45-47

255. Hu, W., and Feng, P. (2011) Elevated serum chemerin concentrations are associated with renal dysfunction in type 2 diabetic patients. *Diabetes research and clinical practice* **91**, 159-163

256. Pfau, D., Stepan, H., Kratzsch, J., Verlohren, M., Verlohren, H. J., Drynda, K., Lossner, U., Bluher, M., Stumvoll, M., and Fasshauer, M. (2010) Circulating levels of the adipokine chemerin in gestational diabetes mellitus. *Hormone research in paediatrics* **74**, 56-61

257. Verrijn Stuart, A. A., Schipper, H. S., Tasdelen, I., Egan, D. A., Prakken, B. J., Kalkhoven, E., and de Jager, W. (2012) Altered plasma adipokine levels and in vitro adipocyte differentiation in pediatric type 1 diabetes. *The Journal of clinical endocrinology and metabolism* **97**, 463-472

258. Kukla, M., Mazur, W., Buldak, R. J., and Zwirska-Korczala, K. (2011) Potential role of leptin, adiponectin and three novel adipokines--visfatin, chemerin and vaspin--in chronic hepatitis. *Mol Med* **17**, 1397-1410

259. Duan, D. M., Niu, J. M., Lei, Q., Lin, X. H., and Chen, X. (2012) Serum levels of the adipokine chemerin in preeclampsia. *Journal of perinatal medicine* **40**, 121-127

260. Weigert, J., Obermeier, F., Neumeier, M., Wanninger, J., Filarsky, M., Bauer, S., Aslanidis, C., Rogler, G., Ott, C., Schaffler, A., Scholmerich, J., and Buechler, C. (2010) Circulating levels of chemerin and adiponectin are higher in ulcerative colitis and chemerin is elevated in Crohn's disease. *Inflammatory bowel diseases* **16**, 630-637

261. Li, L., Huang, C., Zhang, X., Wang, J., Ma, P., Liu, Y., Xiao, T., Zabel, B. A., and Zhang, J. V. (2014) Chemerin-derived peptide C-20 suppressed gonadal steroidogenesis. *Am J Reprod Immunol* **71**, 265-277

262. Garland, S. L. (2013) Are GPCRs still a source of new targets? *Journal of biomolecular screening* **18**, 947-966

263. Lappano, R., and Maggiolini, M. (2011) G protein-coupled receptors: novel targets for drug discovery in cancer. *Nature reviews. Drug discovery* **10**, 47-60

264. Siehler, S. (2007) G12/13-dependent signaling of G-protein-coupled receptors: disease context and impact on drug discovery. *Expert opinion on drug discovery* **2**, 1591-1604

265. Tatsumi, E., Yamanaka, H., Kobayashi, K., Yagi, H., Sakagami, M., and Noguchi, K. (2015) RhoA/ROCK pathway mediates p38 MAPK activation and morphological changes downstream of P2Y12/13 receptors in spinal microglia in neuropathic pain. *Glia* **63**, 216-228

266. Rovati, G. E., Capra, V., and Neubig, R. R. (2007) The highly conserved DRY motif of class A G protein-coupled receptors: beyond the ground state. *Molecular pharmacology* **71**, 959-964

267. Cohen, G. B., Yang, T., Robinson, P. R., and Oprian, D. D. (1993) Constitutive activation of opsin: influence of charge at position 134 and size at position 296. *Biochemistry* **32**, 6111-6115

268. Alewijnse, A. E., Timmerman, H., Jacobs, E. H., Smit, M. J., Roovers, E., Cotecchia, S., and Leurs, R. (2000) The effect of mutations in the DRY motif on the constitutive activity and structural instability of the histamine H(2) receptor. *Molecular pharmacology* **57**, 890-898

269. Capra, V., Veltri, A., Foglia, C., Crimaldi, L., Habib, A., Parenti, M., and Rovati, G. E. (2004) Mutational analysis of the highly conserved ERY motif of the thromboxane A2 receptor: alternative role in G protein-coupled receptor signaling. *Molecular pharmacology* **66**, 880-889

270. Sgourakis, N. G., Bagos, P. G., and Hamodrakas, S. J. (2005) Prediction of the coupling specificity of GPCRs to four families of G-proteins using hidden Markov models and artificial neural networks. *Bioinformatics* **21**, 4101-4106

271. Sgourakis, N. G., Bagos, P. G., Papasaikas, P. K., and Hamodrakas, S. J. (2005) A method for the prediction of GPCRs coupling specificity to G-proteins using refined profile Hidden Markov Models. *BMC bioinformatics* **6**, 1-12

272. Oakley, R. H., Laporte, S. A., Holt, J. A., Caron, M. G., and Barak, L. S. (2000) Differential affinities of visual arrestin, beta arrestin1, and beta arrestin2 for G protein-coupled receptors delineate two major classes of receptors. *The Journal of biological chemistry* **275**, 17201-17210

273. Wong, S. K. (2003) G protein selectivity is regulated by multiple intracellular regions of GPCRs. *Neuro-Signals* **12**, 1-12

274. Ferre, S., Casado, V., Devi, L. A., Filizola, M., Jockers, R., Lohse, M. J., Milligan, G., Pin, J. P., and Guitart, X. (2014) G protein-coupled receptor oligomerization revisited: functional and pharmacological perspectives. *Pharmacological reviews* **66**, 413-434

275. de Poorter, C., Baertsoen, K., Lannoy, V., Parmentier, M., and Springael, J. Y. (2013) Consequences of ChemR23 heteromerization with the chemokine receptors CXCR4 and CCR7. *PloS one* **8**, e58075

276. Ferguson, S. S., Downey, W. E., 3rd, Colapietro, A. M., Barak, L. S., Menard, L., and Caron, M. G. (1996) Role of beta-arrestin in mediating agonist-promoted G protein-coupled receptor internalization. *Science* **271**, 363-366

277. Seasholtz, T. M., Majumdar, M., and Brown, J. H. (1999) Rho as a Mediator of G Protein-Coupled Receptor Signaling. *Mol. Pharmacol.* **55**, 949-956

278. Whitehead, I. P., Zohn, I. E., and Der, C. J. (2001) Rho GTPase-dependent transformation by G protein-coupled receptors. *Oncogene* **20**, 1547-1555

279. Seasholtz, T. M., Majumdar, M., and Brown, J. H. (1999) Rho as a mediator of G protein-coupled receptor signaling. *Molecular pharmacology* **55**, 949-956

280. Zarubin, T., and Han, J. (2005) Activation and signaling of the p38 MAP kinase pathway. *Cell research* **15**, 11-18

281. Miano, J. M. (2003) Serum response factor: toggling between disparate programs of gene expression. *Journal of molecular and cellular cardiology* **35**, 577-593

282. Lee, S. M., Vasishtha, M., and Prywes, R. (2010) Activation and repression of cellular immediate early genes by serum response factor cofactors. *The Journal of biological chemistry* **285**, 22036-22049

283. Mao, J., Yuan, H., Xie, W., Simon, M. I., and Wu, D. (1998) Specific involvement of G proteins in regulation of serum response factor-mediated gene transcription by different receptors. *The Journal of biological chemistry* **273**, 27118-27123

284. Vickers, E. R., Kasza, A., Kurnaz, I. A., Seifert, A., Zeef, L. A., O'Donnell, A., Hayes, A., and Sharrocks, A. D. (2004) Ternary complex factor-serum response factor complex-regulated gene activity is required for cellular proliferation and inhibition of apoptotic cell death. *Molecular and cellular biology* **24**, 10340-10351

285. Wang, Z., Wang, D. Z., Hockemeyer, D., McAnally, J., Nordheim, A., and Olson, E. N. (2004) Myocardin and ternary complex factors compete for SRF to control smooth muscle gene expression. *Nature* **428**, 185-189

286. Li, S., Czubryt, M. P., McAnally, J., Bassel-Duby, R., Richardson, J. A., Wiebel, F. F., Nordheim, A., and Olson, E. N. (2005) Requirement for serum response factor for skeletal muscle growth and maturation revealed by tissue-specific gene deletion in mice. *Proceedings of the National Academy of Sciences of the United States of America* **102**, 1082-1087

287. Pipes, G. C., Creemers, E. E., and Olson, E. N. (2006) The myocardin family of transcriptional coactivators: versatile regulators of cell growth, migration, and myogenesis. *Genes & development* **20**, 1545-1556

288. Olson, E. N., and Nordheim, A. (2010) Linking actin dynamics and gene transcription to drive cellular motile functions. *Nature reviews. Molecular cell biology* **11**, 353-365

289. Miano, J. M. (2010) Role of serum response factor in the pathogenesis of disease. *Laboratory investigation; a journal of technical methods and pathology* **90**, 1274-1284

290. Medjkane, S., Perez-Sanchez, C., Gaggioli, C., Sahai, E., and Treisman, R. (2009) Myocardin-related transcription factors and SRF are required for cytoskeletal dynamics and experimental metastasis. *Nature cell biology* **11**, 257-268

291. Choi, H. N., Kim, K. R., Lee, J. H., Park, H. S., Jang, K. Y., Chung, M. J., Hwang, S. E., Yu, H. C., and Moon, W. S. (2009) Serum response factor enhances liver metastasis of colorectal carcinoma via alteration of the E-cadherin/beta-catenin complex. *Oncology reports* **21**, 57-63

292. Park, M. Y., Kim, K. R., Park, H. S., Park, B. H., Choi, H. N., Jang, K. Y., Chung, M. J., Kang, M. J., Lee, D. G., and Moon, W. S. (2007) Expression of the serum response factor in hepatocellular carcinoma: implications for epithelial-mesenchymal transition. *International journal of oncology* **31**, 1309-1315

293. Iwahara, T., Akagi, T., Shishido, T., and Hanafusa, H. (2003) CrkII induces serum response factor activation and cellular transformation through its function in Rho activation. *Oncogene* **22**, 5946-5957

294. Pellegrini, L., Tan, S., and Richmond, T. J. (1995) Structure of serum response factor core bound to DNA. *Nature* **376**, 490-498

295. Treisman, R. (1986) Identification of a protein-binding site that mediates transcriptional response of the c-fos gene to serum factors. *Cell* **46**, 567-574

296. Selvaraj, A., and Prywes, R. (2004) Expression profiling of serum inducible genes identifies a subset of SRF target genes that are MKL dependent. *BMC molecular biology* **5**, 1-15

297. Sun, Q., Chen, G., Streb, J. W., Long, X., Yang, Y., Stoeckert, C. J., Jr., and Miano, J. M. (2006) Defining the mammalian CArGome. *Genome research* **16**, 197-207

298. Cooper, S. J., Trinklein, N. D., Nguyen, L., and Myers, R. M. (2007) Serum response factor binding sites differ in three human cell types. *Genome research* **17**, 136-144

299. Posern, G., and Treisman, R. (2006) Actin' together: serum response factor, its cofactors and the link to signal transduction. *Trends in cell biology* **16**, 588-596

300. Buchwalter, G., Gross, C., and Wasylyk, B. (2004) Ets ternary complex transcription factors. *Gene* **324**, 1-14

301. Miralles, F., Posern, G., Zaromytidou, A. I., and Treisman, R. (2003) Actin dynamics control SRF activity by regulation of its coactivator MAL. *Cell* **113**, 329-342

302. Cotton, M., and Claing, A. (2009) G protein-coupled receptors stimulation and the control of cell migration. *Cellular signalling* **21**, 1045-1053

303. Sotiropoulos, A., Gineitis, D., Copeland, J., and Treisman, R. (1999) Signal-regulated activation of serum response factor is mediated by changes in actin dynamics. *Cell* **98**, 159-169

304. Guettler, S., Vartiainen, M. K., Miralles, F., Larijani, B., and Treisman, R. (2008) RPEL motifs link the serum response factor cofactor MAL but not myocardin to Rho signaling via actin binding. *Molecular and cellular biology* **28**, 732-742

305. Treisman, R. (1994) Ternary complex factors: growth factor regulated transcriptional activators. *Current opinion in genetics & development* **4**, 96-101

306. Cen, B., Selvaraj, A., Burgess, R. C., Hitzler, J. K., Ma, Z., Morris, S. W., and Prywes, R. (2003) Megakaryoblastic leukemia 1, a potent transcriptional coactivator for serum response factor (SRF), is required for serum induction of SRF target genes. *Molecular and cellular biology* **23**, 6597-6608

307. Li, S., Wang, D. Z., Wang, Z., Richardson, J. A., and Olson, E. N. (2003) The serum response factor coactivator myocardin is required for vascular smooth muscle development. *Proceedings of the National Academy of Sciences of the United States of America* **100**, 9366-9370

308. Wang, Z., Wang, D. Z., Pipes, G. C., and Olson, E. N. (2003) Myocardin is a master regulator of smooth muscle gene expression. *Proceedings of the National Academy of Sciences of the United States of America* **100**, 7129-7134

309. Yoshida, T., Sinha, S., Dandre, F., Wamhoff, B. R., Hoofnagle, M. H., Kremer, B. E., Wang, D. Z., Olson, E. N., and Owens, G. K. (2003) Myocardin is a key regulator of CArG-dependent transcription of multiple smooth muscle marker genes. *Circulation research* **92**, 856-864

310. Zaromytidou, A. I., Miralles, F., and Treisman, R. (2006) MAL and ternary complex factor use different mechanisms to contact a common surface on the serum response factor DNA-binding domain. *Molecular and cellular biology* **26**, 4134-4148

311. Murai, K., and Treisman, R. (2002) Interaction of serum response factor (SRF) with the Elk-1 B box inhibits RhoA-actin signaling to SRF and potentiates transcriptional activation by Elk-1. *Molecular and cellular biology* **22**, 7083-7092

312. Schmitz, A. A., Govek, E. E., Bottner, B., and Van Aelst, L. (2000) Rho GTPases: signaling, migration, and invasion. *Experimental cell research* **261**, 1-12

313. Yang, H., Li, F., Kong, X., Yuan, X., Wang, W., Huang, R., Li, T., Geng, M., Wu, G., and Yin, Y. (2012) Chemerin regulates proliferation and differentiation of myoblast cells via ERK1/2 and mTOR signaling pathways. *Cytokine* **60**, 646-652

314. Muruganandan, S., Dranse, H. J., Rourke, J. L., McMullen, N. M., and Sinal, C. J. (2013) Chemerin Neutralization Blocks Hematopoietic Stem Cell Osteoclastogenesis. *Stem Cells* **10**, 2172-2182

315. Ragu, C., Elain, G., Mylonas, E., Ottolenghi, C., Cagnard, N., Daegelen, D., Passegue, E., Vainchenker, W., Bernard, O. A., and Penard-Lacronique, V. (2010) The transcription factor Srf regulates hematopoietic stem cell adhesion. *Blood* **116**, 4464-4473

316. McBeath, R., Pirone, D. M., Nelson, C. M., Bhadriraju, K., and Chen, C. S. (2004) Cell shape, cytoskeletal tension, and RhoA regulate stem cell lineage commitment. *Developmental cell* **6**, 483-495

317. Livak, K. J., and Schmittgen, T. D. (2001) Analysis of relative gene expression data using real-time quantitative PCR and the 2(-Delta Delta C(T)) Method. *Methods* **25**, 402-408

318. Xiang, S. Y., Dusaban, S. S., and Brown, J. H. (2013) Lysophospholipid receptor activation of RhoA and lipid signaling pathways. *Biochimica et biophysica acta* **1831**, 213-222

319. Atwood, B. K., Lopez, J., Wager-Miller, J., Mackie, K., and Straiker, A. (2011) Expression of G protein-coupled receptors and related proteins in HEK293, AtT20, BV2, and N18 cell lines as revealed by microarray analysis. *BMC genomics* **12**, 1-14

320. Chun, J. (2013) *Lysophospholipid Receptors: Signaling and Biochemistry*, John Wiley & Sons

321. Rourke, J. L., Muruganandan, S., Dranse, H. J., McMullen, N. M., and Sinal, C. J. (2014) Gpr1 is an active chemerin receptor influencing glucose homeostasis in obese mice. *The Journal of endocrinology* **222**, 201-215

322. Wang, C., Wu, W. K., Liu, X., To, K. F., Chen, G. G., Yu, J., and Ng, E. K. (2014) Increased serum chemerin level promotes cellular invasiveness in gastric cancer: a clinical and experimental study. *Peptides* **51**, 131-138

323. Gonzalvo-Feo, S., Del Prete, A., Pruenster, M., Salvi, V., Wang, L., Sironi, M., Bierschenk, S., Sperandio, M., Vecchi, A., and Sozzani, S. (2014) Endothelial cell-derived chemerin promotes dendritic cell transmigration. *J Immunol* **192**, 2366-2373

324. Bondue, B., Wittamer, V., and Parmentier, M. (2011) Chemerin and its receptors in leukocyte trafficking, inflammation and metabolism. *Cytokine & growth factor reviews* **22**, 331-338

325. Lin, M. T., Lin, B. R., Chang, C. C., Chu, C. Y., Su, H. J., Chen, S. T., Jeng, Y. M., and Kuo, M. L. (2007) IL-6 induces AGS gastric cancer cell invasion via activation of the c-Src/RhoA/ROCK signaling pathway. *International journal of cancer. Journal international du cancer* **120**, 2600-2608

326. Murray, D., Horgan, G., Macmathuna, P., and Doran, P. (2008) NET1-mediated RhoA activation facilitates lysophosphatidic acid-induced cell migration and invasion in gastric cancer. *British journal of cancer* **99**, 1322-1329

327. Noble, P. J., Wilde, G., White, M. R., Pennington, S. R., Dockray, G. J., and Varro, A. (2003) Stimulation of gastrin-CCKB receptor promotes migration of gastric AGS cells via multiple paracrine pathways. *American journal of physiology. Gastrointestinal and liver physiology* **284**, G75-84

328. Yamin, R., and Morgan, K. G. (2012) Deciphering actin cytoskeletal function in the contractile vascular smooth muscle cell. *The Journal of physiology* **590**, 4145-4154

329. Ono, S. (2010) Dynamic regulation of sarcomeric actin filaments in striated muscle. *Cytoskeleton* **67**, 677-692

330. Nobusue, H., Onishi, N., Shimizu, T., Sugihara, E., Oki, Y., Sumikawa, Y., Chiyoda, T., Akashi, K., Saya, H., and Kano, K. (2014) Regulation of MKL1 via actin cytoskeleton dynamics drives adipocyte differentiation. *Nature communications* **5**, 3368

331. Lobato, N. S., Neves, K. B., Filgueira, F. P., Fortes, Z. B., Carvalho, M. H., Webb, R. C., Oliveira, A. M., and Tostes, R. C. (2012) The adipokine chemerin augments vascular reactivity to contractile stimuli via activation of the MEK-ERK1/2 pathway. *Life sciences* **91**, 600-606

332. Reverchon, M., Cornuau, M., Rame, C., Guerif, F., Royere, D., and Dupont, J. (2012) Chemerin inhibits IGF-1-induced progesterone and estradiol secretion in human granulosa cells. *Hum Reprod* **27**, 1790-1800

333. Gouwy, M., Schiraldi, M., Struyf, S., Van Damme, J., and Uguccioni, M. (2012) Possible mechanisms involved in chemokine synergy fine tuning the inflammatory response. *Immunology letters* **145**, 10-14

334. Gouwy, M., Struyf, S., Proost, P., and Van Damme, J. (2005) Synergy in cytokine and chemokine networks amplifies the inflammatory response. *Cytokine & growth factor reviews* **16**, 561-580

335. Gouwy, M., Struyf, S., Leutenez, L., Portner, N., Sozzani, S., and Van Damme, J. (2014) Chemokines and other GPCR ligands synergize in receptor-mediated migration of monocyte-derived immature and mature dendritic cells. *Immunobiology* **219**, 218-229

336. Rouger, L., Denis, G. R., Luangsay, S., and Parmentier, M. (2013) ChemR23 knockout mice display mild obesity but no deficit in adipocyte differentiation. *The Journal of endocrinology* **219**, 279-289

337. Gruben, N., Aparicio Vergara, M., Kloosterhuis, N. J., van der Molen, H., Stoelwinder, S., Youssef, S., de Bruin, A., Delsing, D. J., Kuivenhoven, J. A., van de Sluis, B., Hofker, M. H., and Koonen, D. P. (2014) Chemokine-like receptor 1 deficiency does not affect the development of insulin resistance and nonalcoholic Fatty liver disease in mice. *PloS one* **9**, e96345

338. Huang, J., Zhang, J., Lei, T., Chen, X., Zhang, Y., Zhou, L., Yu, A., Chen, Z., Zhou, R., and Yang, Z. (2010) Cloning of porcine chemerin, ChemR23 and GPR1 and their involvement in regulation of lipogenesis. *BMB reports* **43**, 491-498

339. Marchese, A., Cheng, R., Lee, M. C., Porter, C. A., Heiber, M., Goodman, M., George, S. R., and O'Dowd, B. F. (1994) Mapping studies of two G protein-coupled receptor genes: an amino acid difference may confer a functional variation between a human and rodent receptor. *Biochemical and biophysical research communications* **205**, 1952-1958

340. Edinger, A. L., Hoffman, T. L., Sharron, M., Lee, B., O'Dowd, B., and Doms, R. W. (1998) Use of GPR1, GPR15, and STRL33 as coreceptors by diverse human immunodeficiency virus type 1 and simian immunodeficiency virus envelope proteins. *Virology* **249**, 367-378

341. Farzan, M., Choe, H., Martin, K., Marcon, L., Hofmann, W., Karlsson, G., Sun, Y., Barrett, P., Marchand, N., Sullivan, N., Gerard, N., Gerard, C., and Sodroski, J. (1997) Two orphan seven-transmembrane segment receptors which are expressed in CD4-positive cells support simian immunodeficiency virus infection. *The Journal of experimental medicine* **186**, 405-411

342. Hausman, D. B., Park, H. J., and Hausman, G. J. (2008) Isolation and culture of preadipocytes from rodent white adipose tissue. *Methods Mol Biol* **456**, 201-219

343. Galarraga, M., Campion, J., Munoz-Barrutia, A., Boque, N., Moreno, H., Martinez, J. A., Milagro, F., and Ortiz-de-Solorzano, C. (2012) Adiposoft: automated software for the analysis of white adipose tissue cellularity in histological sections. *Journal of lipid research* **53**, 2791-2796

344. Cinti, S., Mitchell, G., Barbatelli, G., Murano, I., Ceresi, E., Faloia, E., Wang, S., Fortier, M., Greenberg, A. S., and Obin, M. S. (2005) Adipocyte death defines macrophage localization and function in adipose tissue of obese mice and humans. *Journal of lipid research* **46**, 2347-2355

345. Lolmede K, D. C., Zakaroff-Girard A, Bouloumie A. (2011) Immune cells in adipose tissue: key players in metabolic disorders. *Diabetes & metabolism journal* **4**, 283-290

346. Edinger, A. L., Mankowski, J. L., Doranz, B. J., Margulies, B. J., Lee, B., Rucker, J., Sharron, M., Hoffman, T. L., Berson, J. F., Zink, M. C., Hirsch, V. M., Clements, J. E., and Doms, R. W. (1997) CD4-independent, CCR5-dependent infection of brain capillary endothelial cells by a neurovirulent simian immunodeficiency virus strain. *Proceedings of the National Academy of Sciences of the United States of America* **94**, 14742-14747

347. Mognetti, B., Moussa, M., Croitoru, J., Menu, E., Dormont, D., Roques, P., and Chaouat, G. (2000) HIV-1 co-receptor expression on trophoblastic cells from early placentas and permissivity to infection by several HIV-1 primary isolates. *Clinical and experimental immunology* **119**, 486-492

348. Brunetti, L., Di Nisio, C., Recinella, L., Chiavaroli, A., Leone, S., Ferrante, C., Orlando, G., and Vacca, M. (2011) Effects of vaspin, chemerin and omentin-1 on feeding behavior and hypothalamic peptide gene expression in the rat. *Peptides* **32**, 1866-1871

349. Brunetti, L., Orlando, G., Ferrante, C., Recinella, L., Leone, S., Chiavaroli, A., Di Nisio, C., Shohreh, R., Manippa, F., Ricciuti, A., and Vacca, M. (2014) Peripheral chemerin administration modulates hypothalamic control of feeding. *Peptides* **51**, 115-121

350. Marchese, A., Docherty, J. M., Nguyen, T., Heiber, M., Cheng, R., Heng, H. H., Tsui, L. C., Shi, X., George, S. R., and O'Dowd, B. F. (1994) Cloning of human genes encoding novel G protein-coupled receptors. *Genomics* **23**, 609-618

351. Miyawaki, K., Yamada, Y., Yano, H., Niwa, H., Ban, N., Ihara, Y., Kubota, A., Fujimoto, S., Kajikawa, M., Kuroe, A., Tsuda, K., Hashimoto, H., Yamashita, T., Jomori, T., Tashiro, F., Miyazaki, J., and Seino, Y. (1999) Glucose intolerance caused by a defect in the entero-insular axis: a study in gastric inhibitory polypeptide receptor knockout mice. *Proceedings of the National Academy of Sciences of the United States of America* **96**, 14843-14847

352. Parlee, S. D., McNeil, J. O., Muruganandan, S., Sinal, C. J., and Goralski, K. B. (2012) Elastase and tryptase govern TNFalpha-mediated production of active chemerin by adipocytes. *PloS one* **7**, e51072

353. Kloting, N., Fasshauer, M., Dietrich, A., Kovacs, P., Schon, M. R., Kern, M., Stumvoll, M., and Bluher, M. (2010) Insulin-sensitive obesity. *American journal of physiology. Endocrinology and metabolism* **299**, E506-515

354. Morton, G. J., and Schwartz, M. W. (2011) Leptin and the central nervous system control of glucose metabolism. *Physiological reviews* **91**, 389-411

355. Sarvas, J. L., Khaper, N., and Lees, S. J. (2013) The IL-6 Paradox: Context Dependent Interplay of SOCS3 and AMPK. *Journal of diabetes & metabolism* **Suppl 13**

356. Furukawa, N., Ongusaha, P., Jahng, W. J., Araki, K., Choi, C. S., Kim, H. J., Lee, Y. H., Kaibuchi, K., Kahn, B. B., Masuzaki, H., Kim, J. K., Lee, S. W., and Kim, Y. B. (2005) Role of Rho-kinase in regulation of insulin action and glucose homeostasis. *Cell metabolism* **2**, 119-129

357. Lee, D. H., Shi, J., Jeoung, N. H., Kim, M. S., Zabolotny, J. M., Lee, S. W., White, M. F., Wei, L., and Kim, Y. B. (2009) Targeted disruption of ROCK1 causes insulin resistance in vivo. *The Journal of biological chemistry* **284**, 11776-11780

358. Uenishi, E., Shibasaki, T., Takahashi, H., Seki, C., Hamaguchi, H., Yasuda, T., Tatebe, M., Oiso, Y., Takenawa, T., and Seino, S. (2013) Actin dynamics regulated by the balance of neuronal Wiskott-Aldrich syndrome protein (N-WASP) and cofilin activities determines the biphasic response of glucose-induced insulin secretion. *The Journal of biological chemistry* **288**, 25851-25864

359. Liu, X., Yan, F., Yao, H., Chang, M., Qin, J., Li, Y., Wang, Y., and Pei, X. (2014) Involvement of RhoA/ROCK in insulin secretion of pancreatic beta-cells in 3D culture. *Cell and tissue research* **358**, 359-369

360. Hammar, E., Tomas, A., Bosco, D., and Halban, P. A. (2009) Role of the Rho-ROCK (Rho-associated kinase) signaling pathway in the regulation of pancreatic beta-cell function. *Endocrinology* **150**, 2072-2079

361. Nakamura, Y., Kaneto, H., Miyatsuka, T., Matsuoka, T. A., Matsuhisa, M., Node, K., Hori, M., and Yamasaki, Y. (2006) Marked increase of insulin gene transcription by suppression of the Rho/Rho-kinase pathway. *Biochemical and biophysical research communications* **350**, 68-73

362. Tonjes, A., Scholz, M., Breitfeld, J., Marzi, C., Grallert, H., Gross, A., Ladenvall, C., Schleinitz, D., Krause, K., Kirsten, H., Laurila, E., Kriebel, J., Thorand, B., Rathmann, W., Groop, L., Prokopenko, I., Isomaa, B., Beutner, F., Kratzsch, J., Thiery, J., Fasshauer, M., Kloting, N., Gieger, C., Bluher, M., Stumvoll, M., and Kovacs, P. (2014) Genome Wide Meta-analysis Highlights the Role of Genetic Variation in RARRES2 in the Regulation of Circulating Serum Chemerin. *PLoS genetics* **10**, e1004854

363. Shaikh, T. H., Gai, X., Perin, J. C., Glessner, J. T., Xie, H., Murphy, K., O'Hara, R., Casalunovo, T., Conlin, L. K., D'Arcy, M., Frackelton, E. C., Geiger, E. A., Haldeman-Englert, C., Imielinski, M., Kim, C. E., Medne, L., Annaiah, K., Bradfield, J. P., Dabaghyan, E., Eckert, A., Onyiah, C. C., Ostapenko, S., Otieno, F. G., Santa, E., Shaner, J. L., Skraban, R., Smith, R. M., Elia, J., Goldmuntz, E., Spinner, N. B., Zackai, E. H., Chiavacci, R. M., Grundmeier, R., Rappaport, E. F., Grant, S. F., White, P. S., and Hakonarson, H. (2009) High-resolution mapping and analysis of copy number variations in the human genome: a data resource for clinical and research applications. *Genome research* **19**, 1682-1690

364. Mussig, K., Staiger, H., Machicao, F., Thamer, C., Machann, J., Schick, F., Claussen, C. D., Stefan, N., Fritsche, A., and Haring, H. U. (2009) RARRES2, encoding the novel adipokine chemerin, is a genetic determinant of disproportionate regional body fat distribution: a comparative magnetic resonance imaging study. *Metabolism: clinical and experimental* **58**, 519-524

365. Boyko, E. J., Fujimoto, W. Y., Leonetti, D. L., and Newell-Morris, L. (2000) Visceral adiposity and risk of type 2 diabetes: a prospective study among Japanese Americans. *Diabetes care* **23**, 465-471

366. Wanninger, J., Bauer, S., Eisinger, K., Weiss, T. S., Walter, R., Hellerbrand, C., Schaffler, A., Higuchi, A., Walsh, K., and Buechler, C. (2012) Adiponectin upregulates hepatocyte CMKLR1 which is reduced in human fatty liver. *Molecular and cellular endocrinology* **349**, 248-254

367. Myers, M. G., Jr., Leibel, R. L., Seeley, R. J., and Schwartz, M. W. (2010) Obesity and leptin resistance: distinguishing cause from effect. *Trends in endocrinology and metabolism: TEM* **21**, 643-651

368. Chamberland, J. P., Berman, R. L., Aronis, K. N., and Mantzoros, C. S. (2013) Chemerin is expressed mainly in pancreas and liver, is regulated by energy deprivation, and lacks day/night variation in humans. *European journal of endocrinology / European Federation of Endocrine Societies* **169**, 453-462

369. Zhou, J. X., Liao, D., Zhang, S., Cheng, N., He, H. Q., and Ye, R. D. (2014) Chemerin C9 peptide induces receptor internalization through a clathrin-independent pathway. *Acta pharmacologica Sinica* **35**, 653-663

370. Lin, W., Chen, Y. L., Jiang, L., and Chen, J. K. (2011) Reduced expression of chemerin is associated with a poor prognosis and a lowed infiltration of both dendritic cells and natural killer cells in human hepatocellular carcinoma. *Clinical laboratory* **57**, 879-885

371. Zheng, Y., Luo, S., Wang, G., Peng, Z., Zeng, W., Tan, S., Xi, Y., and Fan, J. (2008) Downregulation of tazarotene induced gene-2 (TIG2) in skin squamous cell carcinoma. *European journal of dermatology : EJD* **18**, 638-641

372. Garces, M. F., Sanchez, E., Acosta, B. J., Angel, E., Ruiz, A. I., Rubio-Romero, J. A., Dieguez, C., Nogueiras, R., and Caminos, J. E. (2012) Expression and regulation of chemerin during rat pregnancy. *Placenta* **33**, 373-378

373. Rama, D., Esendagli, G., and Guc, D. (2011) Expression of chemokine-like receptor 1 (CMKLR1) on J744A.1 macrophages co-cultured with fibroblast and/or tumor cells: modeling the influence of microenvironment. *Cellular immunology* **271**, 134-140

Appendix A: Copyright Agreement Letters

A modified version of the following manuscript is reproduced in chapter 5.

BIOSCIENTIFICA LTD. ORDER DETAILS

Jul 10, 2014

Order Number	500888334
Order date	Jul 10, 2014
Licensed content publisher	BioScientifica Ltd.
Licensed content publication	Journal of Endocrinology
Licensed content title	Gpr1 is an active chemerin receptor influencing glucose homeostasis in obese mice
Licensed copyright line	Copyright © 2014, Society for Endocrinology
Licensed content author	Jillian L Rourke, Shanmugam Muruganandan, Helen J Dranse et al.
Licensed content date	Jun 3, 2014
Type of Use	Thesis/Dissertation
Requestor type	Author of requested content
Format	Print, Electronic
Portion	chapter/article
Rights for	Main product
Duration of use	Life of current edition
Creation of copies for the disabled	no
With minor editing privileges	yes
For distribution to	Canada
In the following language(s)	Original language of publication
With incidental promotional use	no
The lifetime unit quantity of new product	0 to 499
Specified additional information	The article in question was accepted for publication June 3 2014 in the Journal of Endocrinology. I wish to reproduce this article in full as a chapter of my PhD dissertation. The contents would appear as in the original accepted article, except for required format changes. A maximum of 3 copies of my completed thesis containing this article would be produced.
The requesting person/organization is:	Jillian Rourke, Dalhousie University
Order reference number	None
Title of your thesis / dissertation	Characterizing the role of GPR1 and CMKLR1 signalling in regulation of chemerin function
Expected completion date	Dec 2014
Expected size (number of pages)	200

Portions of the following text are reproduced in Chapter 1, Chapter 2, and Chapter 6.

JOHN WILEY AND SONS LICENSE TERMS AND CONDITIONS

Jul 10, 2014

This is a License Agreement between Jillian Rourke ("You") and John Wiley and Sons ("John Wiley and Sons") provided by Copyright Clearance Center ("CCC"). The license consists of your order details, the terms and conditions provided by John Wiley and Sons, and the payment terms and conditions.

All payments must be made in full to CCC. For payment instructions, please see information listed at the bottom of this form.

License Number	3425490809803
License date	Jul 10, 2014
Licensed content publisher	John Wiley and Sons
Licensed content publication	Obesity Reviews
Licensed content title	Towards an integrative approach to understanding the role of chemerin in human health and disease
Licensed copyright line	© 2012 The Authors. obesity reviews © 2012 International Association for the Study of Obesity
Licensed content author	J. L. Rourke,H. J. Dranse,C. J. Sinal
Licensed content date	Dec 6, 2012
Start page	245
End page	262
Type of use	Dissertation/Thesis
Requestor type	Author of this Wiley article
Format	Print and electronic
Portion	Full article
Will you be translating?	No
Title of your thesis / dissertation	Characterizing the role of GPR1 and CMKLR1 signalling in regulation of chemerin function
Expected completion date	Dec 2014
Expected size (number of pages)	200
Total	0.00 USD
Terms and Conditions	